1. Report No. FHWA/OH-2004/012	2. Government Accession No.	3. Recipient's Catalog No.
4. Title and Subtitle Accelerated Testing of Ohio SHRP Sections 390101, 390102, 390105, and 390107		**5. Report Date** December 2004 **6. Performing Organization Code**
7. Author(s) Shad M. Sargand, William Edwards		**8. Performing Organization Report No.**
9. Performing Organization Name and Address Ohio Research Institute for Transportation and the Environment (ORITE) 114 Stocker Center Ohio University Athens OH 45701-2979		**10. Work Unit No. (TRAIS)** **11. Contract or Grant No.** State Job No. 14744(0)
12. Sponsoring Agency Name and Address Ohio Department of Transportation Office of Research and Development 1980 West Broad St. Columbus OH 43223		**13. Type of Report and Period Covered** Final Report **14. Sponsoring Agency Code**

15. Supplementary Notes
Prepared in cooperation with the Ohio Department of Transportation (ODOT) and the U.S. Department of Transportation, Federal Highway Administration

16. Abstract

The Ohio SHRP Test Road was constructed to provide data for 40 sections in the LTPP SPS-1, 2, 8 and 9 experiments under specific traffic, environmental and soil conditions existing at one site in Ohio. Sensors were installed at the time of construction to continuously monitor subsurface temperature, moisture and frost in eighteen sections, and to measure dynamic strain, deflection and pressure response in thirty-three sections during controlled vehicle testing. Falling Weight Deflectometer (FWD) measurements provided additional dynamic deflection data.

Four SPS-1 sections which showed early distress on the test road were reconstructed at the Accelerated Pavement Loading Facility (APLF) in Lancaster Ohio. Response measurements in the APLF included FWD, and strain and deflection readings from sensors mounted similarly to those installed on the test road. Performance was gauged by surface rutting which was monitored periodically in the APLF as rolling wheel loads were applied at various combinations of temperature and load. This project compared response and performance on these four SPS-1 sections at the two facilities.

17. Key Words	18. Distribution Statement
Asphalt Concrete Pavement, Accelerated Pavement loading, SHRP Test Road, Long-Term Pavement Performance, Falling Weight Deflectometer, Rutting	No Restrictions. This document is available to the public through the National Technical Information Service, Springfield, Virginia 22161

19. Security Classif. (of this report)	20. Security Classif. (of this page)	21. No. of Pages	22. Price
Unclassified	Unclassified	188	

ACCELERATED TESTING OF OHIO SHRP SECTIONS 390101, 390102, 390105 and 390107

OHIO DEPARTMENT OF TRANSPORTATION

and

FEDERAL HIGHWAY ADMINISTRATION

William F. Edwards
Research Engineer
Ohio University
Athens Ohio

Shad M. Sargand
Russ Professor of Civil and Environmental Engineering
Ohio University
Athens Ohio

December 2004

TABLE OF CONTENTS

LIST OF FIGURES

LIST OF TABLES

ACKNOWLEDGEMENTS

This project could not have been completed without the assistance of several people in the pavement community. These included: Larry Shively at the Shelly Company who directed construction of the AC mixes in the APLF to match those used on the Ohio SHRP Test Road and the Shelly Company who constructed the APLF pavements, Ed Shaw at Shaw and Holter Construction Company who directed preparation the subgrade and aggregate bases in the APLF, Roger Green at ODOT who contributed much wisdom and guidance on pavement matters as the APLF testing progressed, Dwayne McKinney at ODOT who adjusted his schedule on many occasions to perform the FWD tests at the APLF facility in Lancaster, Mike Krumlauf at ORITE who assisted with all phases of testing in the APLF and kept the equipment running, Sam Khoury at ORITE who directed installation of the response sensors and collection of the measured responses, and Wally Richardson at ORITE who kept our laser profilometer running properly and developed computer software to facilitate data collection in the APLF.

ABSTRACT

The Ohio SHRP Test Road was constructed to provide data for 40 sections in the LTPP SPS-1, 2, 8 and 9 experiments under specific traffic, environmental and soil conditions existing at one site in Ohio. Sensors were installed at the time of construction to continuously monitor subsurface temperature, moisture and frost in eighteen sections, and to measure dynamic strain, deflection and pressure response in thirty-three sections during controlled vehicle testing. Falling Weight Deflectometer (FWD) measurements provided additional dynamic deflection data. Four SPS-1 sections which showed early distress on the test road were reconstructed at the Accelerated Pavement Loading Facility (APLF) in Lancaster Ohio. Response measurements in the APLF included FWD, and strain and deflection readings from sensors mounted similarly to those installed on the test road. Performance was gauged by surface rutting which was monitored periodically in the APLF as rolling wheel loads were applied at various combinations of temperature and load. This project compared response and performance on these four SPS-1 sections at the two facilities.

CHAPTER 1

INTRODUCTION

Transportation agencies continuously strive to design and construct highway pavements which are more cost effective and provide better service. Years ago, pavement performance was determined largely by observing the rate at which surface condition deteriorated and by monitoring financial expenditures required to maintain the pavement at an acceptable level of serviceability. Since these calculations could only be performed as data became available, several years were required to fully evaluate performance. Nondestructive testing (NDT) was introduced as a methodology to assess current structural condition and to estimate future structural performance through the measurement of dynamic deflection response. NDT has improved over time through the development of the Benkelman Beam, the Dynaflect, the Falling Weight Deflectometer (FWD) and, more recently, the Rolling Wheel Deflectometer which offers the potential for further advancement in NDT. The installation of strain, deflection and pressure sensors in experimental pavements like MnRoad, WesTrack, NCAT Track and the Ohio SHRP Test Road has permitted the gathering of additional information on structural response.

The Strategic Highway Research Program (SHRP) was initiated in 1987 to improve pavement performance nationwide by developing and coordinating a comprehensive material and structural research program across the country. The Long-Term Pavement Performance (LTPP) Program was a major portion of SHRP and consisted of several activities, including the Specific Pavement Studies (SPS), which were a series of experiments directed toward improving the structural performance of flexible and rigid pavements. Part of Ohio's participation in SHRP was to construct the Ohio SHRP Test Road which contained forty test sections in the SPS-1, SPS-2, SPS-8 and SPS-9 experiments. FWD measurements were obtained on successive material layers as they were completed and accepted by ODOT during construction. Thirty-three of the forty test sections were instrumented to measure dynamic strain, deflection and pressure during controlled vehicle testing, and eighteen sections were instrumented to continuously monitor moisture, temperature and frost depth in the pavement structure. A weather station was located at the site to monitor climatic conditions and a weigh-in-motion (WIM) system was installed to monitor traffic.

Response measurements on the test road consisted of FWD measurements to monitor in-situ stiffness, and controlled vehicle tests where strain gauges, LVDTs and pressure cells were monitored as trucks passed over the instrumented sections at various speeds, loads and pavement temperatures. Performance of the pavement sections was monitored periodically through the monitoring of visible distress and surface roughness as environmental conditions and traffic loading were continuously recorded at the site.

In 1997, Ohio University and Ohio State University jointly constructed an Accelerated Pavement Loading Facility (APLF) capable of testing flexible and rigid pavements over a range of controlled environmental and loading conditions. Pavements constructed in the APLF also can be instrumented to monitor dynamic response. The Ohio Department of Transportation contracted with the Ohio Research Institute for Transportation and the Environment (ORITE) at Ohio University to construct four asphalt concrete SPS-1 sections (390101, 390102, 390105 and 390107) in the APLF which, as anticipated, displayed distress quite early on the test road, and to correlate response and performance observed at the two facilities. Specific objectives listed in the proposal were, as follows:

1. Construct sections in the APLF identical to the four distressed sections on US 23.
2. Test these sections in the APLF over a range of traffic loading and environmental conditions representative of those experienced on US 23.
3. Compare the performance of the sections on US 23 with those in the APLF based on sensor response, FWD/Dynaflect measurements and observed distress.
4. Develop performance correlations between the two sites and demonstrate how accelerated testing can be used to predict the life of asphalt concrete pavements.

A large pad containing five, six-foot (1.8 m) wide by 45-foot (13.7 m) long lanes of the four distressed AC pavement sections was constructed in the APLF using A-6 subgrade soil similar to that encountered on the test road. A second section of Section 390101 was included in the pad for additional performance testing, making a total of five pavement lanes. Each of these 45-foot (13.7 m) long lanes was divided into two 22.5-foot (6.9 m) sections to accommodate a test matrix comprised of ten different combinations of load and temperature. After testing was

complete on the first pad, it was to be removed and replaced with an identical second pad. Moisture was to be added to the subgrade under the second pad and loadings repeated to determine the effect of moisture on response and rutting performance. Since rutting was rather minimal in all sections on the first pad and since sensor measurements indicated little, if any, difference in structural response as a result of the repeated loads, the same pad was used for the second set of measurements after water had been added to the APLF subgrade. The use of a single pad for all performance tests eliminated any structural differences that might have occurred between the two pads.

Response measurements in the APLF consisted of FWD readings on the various material layers during and after construction, and dynamic strain and deflection readings recorded on the pavement sections under different loads, lateral positions and temperatures. Section performance was quantified through the measurement of wheelpath rutting as repeated wheel loads were applied under specific controlled load and environmental conditions. Various combinations of load and temperature were used to assess the individual effects of each parameter. Correlations were developed to compare actual load and environmental conditions observed on the test road with response and performance observed in the APLF.

CHAPTER 2

OHIO SHRP TEST ROAD

FWD Measurements

During construction of the Ohio SHRP Test Road, FWD measurements were obtained on individual material layers within each 500-foot (152.4 m) long SPS section as they were placed and accepted by ODOT. Upon completion of the test road, a set of as-constructed FWD measurements was performed on all but two mainline sections on June 11, 1996, two months prior to being opened to traffic. Tests on all layers consisted of measurements at 50-foot (15.2 m) intervals along the centerline and right wheelpath of each section. Nominal loads of 3 to 6 kips (1.36-1.72 Mg) were used on the subgrade and unstabilized aggregate, and loads of 9 to 12 kips (4.08-5.44 Mg) were used on the stabilized base and pavement layers. Maximum deflections were normalized to a 1 kip (0.45 Mg) load to eliminate differences inherent in the applied FWD load. Average basin deflections collected on these layers are summarized in Table 2.1. The test road subgrade was completed during the summer of 1995, and the bases and pavements were constructed in the spring of 1996, providing an opportunity for moisture to migrate into the subgrade during the winter of 1995/96.

Soon after the test road was opened to traffic on August 14-15, 1996, Sections 390102, 390107 and 390101 exhibited moderate rutting of ~1/2" (13 mm) and were replaced with thicker pavement sections. Section 390105 had a sudden localized failure which required that it also be replaced in 1998. Design parameters for these four sections are shown in Table 2.2. The length of service provided by these sections was consistent with that predicted by AASHTO equations and correlated with the magnitude of average FWD normalized maximum deflections measured before the sections were opened to traffic, as follows: Section 390102 (3.34 mils/kip), Section 390107 (2.01 mils/kip), Section 390101 (1.62 mils/kip) and Section 390105 (1.37 mils/kip).

Average normalized maximum and basin deflections measured with the FWD on individual layers within each of the four distressed sections are shown in Tables A1 and A2, respectively, in Appendix A. Longitudinal deflection profiles for these sections are shown in

Table 2.1

FWD Layer Basins on Test Road and in APLF

Section	Material Layer	Avg. Pvt. Temp. (°F)	Average Normalized Deflection (mils/kip) @ R (in.)						
			0	8	12	18	24	36	60
Test Road									
390101	Subgrade		8.28	4.34	2.60	1.38	0.82	0.46	0.22
	DGAB		3.63	2.28	1.41	0.79	0.56	0.37	0.19
	AC Pvt.	78	1.62	1.34	1.14	0.87	0.65	0.39	0.18
390102	Subgrade		4.31	1.98	1.34	0.84	0.57	0.36	0.18
	DGAB		3.65	2.01	1.09	0.55	0.39	0.29	0.18
	AC Pvt.	77	3.34	2.62	2.08	1.38	0.89	0.42	0.21
390105	Subgrade		4.80	2.76	1.50	0.81	0.58	0.36	0.19
	DGAB		4.92	2.54	1.07	0.61	0.47	0.32	0.17
	ATB		1.97	1.56	1.24	0.84	0.57	0.32	0.17
	AC Pvt.	72	1.37	1.20	1.06	0.86	0.67	0.42	0.18
390107	Subgrade		5.06	2.05	1.25	0.78	0.51	0.34	0.19
	DGAB		5.44	2.28	1.02	0.60	0.45	0.31	0.17
	PATB		5.57	3.27	1.74	0.58	0.30	0.29	0.19
	AC Pvt.	77	2.01	1.61	1.33	0.95	0.67	0.37	0.18
APLF									
101E	Subgrade(*)		3.44	0.09	0.11	0.24	0.23	0.15	0.15
	DGAB(*)		4.39	1.42	1.34	0.39	0.21	0.16	0.11
	AC Pvt.	70	0.83	0.62	0.50	0.36	0.27	0.16	0.08
101W	Subgrade(*)		4.74	0.43	0.28	0.32	0.29	0.17	0.18
	DGAB(*)		3.25	1.11	1.01	0.33	0.23	0.18	0.10
	AC Pvt.	70	0.74	0.57	0.46	0.34	0.25	0.15	0.08
102	Subgrade(*)		3.40	0.35	0.61	0.45	0.31	0.23	0.11
	DGAB(*)		2.79	1.32	1.22	0.52	0.31	0.20	0.10
	AC Pvt.	70	1.20	0.87	0.64	0.40	0.26	0.13	0.07
105	Subgrade(*)		12.28	0.29	1.03	0.11	0.10	0.18	0.10
	DGAB(*)		9.40	2.30	2.33	0.18	0.10	0.15	0.09
	ATB		2.03	1.28	0.79	0.38	0.22	0.12	0.07
	AC Pvt.	70	0.69	0.53	0.44	0.32	0.25	0.14	0.07
107	Subgrade(*)		4.11	0.31	0.58	0.17	0.18	0.15	0.11
	DGAB(*)		7.14	0.69	0.85	0.15	0.17	0.16	0.11
	PATB		3.24	1.55	0.78	0.32	0.20	0.14	0.08
	AC Pvt.	70	0.97	0.68	0.51	0.34	0.24	0.13	0.07

(*) 18” Diameter Load Plate

Figures A1–A4. Of particular interest in these figures are localized areas of unusually low subgrade stiffness and areas where deflections on DGAB and PATB layers were higher than deflections on the underlying layers. These weaknesses appeared to dissipate as stiffer layers were added to the pavement structures. Average normalized maximum deflections measured on individual layers in these four SPS-1 sections during construction are summarized in Table 2.3. Average pavement temperature ranged between 72º and 78º F (22.2 and 25.6º C) during the June 1996 FWD measurements on the completed pavement structures. Moisture readings in the subgrade were not available during construction because the time-domain reflectometry probes were not activated until July 1996.

Table 2.2

Test Road Section Design Parameters

Section	Layer Thickness (in.)				Drainage
	AC	ATB	PATB	DGAB	
390101	7			8	No
390102	4			12	No
390105	4	4		4	No
390107	4		4	4	Yes

AC – Asphalt concrete DGAB – Dense-graded aggregate base
ATB – Asphalt treated base PATB – Permeable asphalt treated base

Table 2.3
Maximum Normalized FWD Layer Deflections on Test Road

Layer	Average Normalized Df1 in Section (mils/kip)			
	390101	390102	390105	390107
Subgrade	8.28	4.31	4.81	5.10
DGAB	4.24	3.86	5.00	5.54
ATB			2.08	
PATB				5.25
AC Pvt.	1.62	3.34	1.37	2.01

Average normalized FWD deflection basins measured with a nominal 9-kip (4.08 Mg) load in June 1996, and the corresponding layer moduli backcalculated with MODULUS 5.1 are

shown in Table 2.4. The MODULUS 5.1 calculations indicated that the modulus of the A-4, A-6 and A-7-6 subgrade ranged from 8,000 to 13,000 psi (55.2-89.6 MPa) in the four distressed sections, with Section 390102 having the weakest subgrade. Calculations using ELSYM5 and the FWD Df6 deflection at R = 36" showed subgrade moduli to range from 18,000 - 20,000 psi (124.1-137.9 MPa), with Sections 390102 and 390105 having the weakest subgrade. Better backcalculation results were obtained on Section 390105 when the AC pavement and asphalt treated base were combined into a single layer.

Table 2.4
As-Constructed FWD Measurements and Backcalculated Moduli on Test Road

Section	Avg. Pvt. Temp. (°F)	Average Normalized Deflection (mils/kip) @ R (in.)							Layer Moduli Backcalculated from MODULUS 5.1 (ksi)				
		0	8	12	18	24	36	60	AC	ATB	PATB	DGAB	Subgrade
Test Road 6/11/96													
390101	78	1.62	1.34	1.14	0.87	0.65	0.39	0.18	389	-	-	26	12
390102	77	3.34	2.62	2.08	1.38	0.89	0.42	0.21	457	-	-	12	8
390105	72	1.37	1.20	1.06	0.86	0.67	0.42	0.18	544		-	21	12
390107	77	2.01	1.61	1.33	0.95	0.67	0.37	0.18	330	-	120	21	13

Controlled Vehicle Response

Just prior to the opening of the test road to traffic, a series of controlled vehicle tests were run on August 6, 1996 to measure dynamic strain, deflection and pressure on six instrumented AC test sections and five instrumented PCC test sections as single and tandem-axle dump trucks ran a response matrix consisting of two loads, four speeds and two temperatures (morning and afternoon). This response instrumentation was located outside the 500-foot (152.4 m) long SPS sections. Sections 390102, 390105 and 390107 were included in this initial series of tests, but Section 390101 was not tested. Typically, three to five replicate runs were made for each cell in the matrix, with the exception of creep speed where one run was often used because of the extensive amount of memory required to store the data. During these tests, the truck drivers attempted to straddle a line of response sensors embedded in the right wheelpath between the right rear dual tires at the prescribed loads and speeds. Megadac data acquisition systems were used to continuously monitor response during the entire loading/unloading cycle. Only one series of response data obtained with the single-axle dump truck at one load and one temperature,

LVDTs referenced about twelve feet below the pavement surface and Dynatest PAST-II AC strain gauges mounted longitudinally at the bottom of the AC stabilized layers in the right wheel path were used for this study. An analysis of the effects of load, tandem-axles, pavement temperature and other variables affecting response was beyond the scope of this research project.

Figure 2.1 shows load geometry of the single-axle dump truck used in this series of tests. The distance between the line of sensors and the outside edge of the rear dual tires was recorded after each pass of the test truck at two locations along the sensor array and combined to determine the average lateral offset distance of tires on the right side of the truck with respect to the sensors. Figures 2.2 and 2.3 show typical strain and deflection traces with average peak responses measured for each matrix cell being shown in Table 2.5. The data in Table 2.5 represent 38 runs on the three sections where lateral offsets of between +0.32 and +1.03 feet (9.8 and 31.4 cm) indicated that the front tire passed over the sensors and the rear dual tires either passed over or straddled the sensors. Deflections are shown as total deformation referenced to a depth of about twelve feet below the pavement surface.

Pavement temperature was determined from thermocouples mounted at depths of 1.0, 2.0, 3.5, 5.5 and 8.5 in. (2.5, 5.1, 8.9, 14.0, and 21.6 cm) below the pavement surface in Section 390102. Differences in pavement temperature between sections resulted mainly from differences in the thickness of AC materials. Because the responses of all sections were monitored during each pass of the trucks, any changes in temperature over time were similar for all sections.

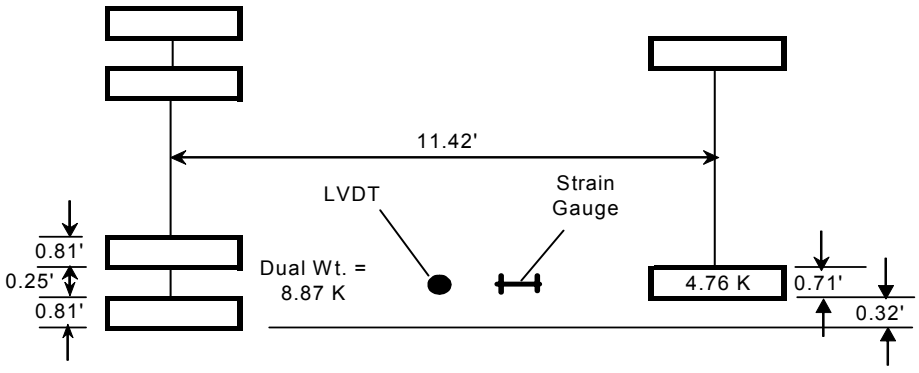

Figure 2.1 – Single-Axle Truck Weight and Geometry

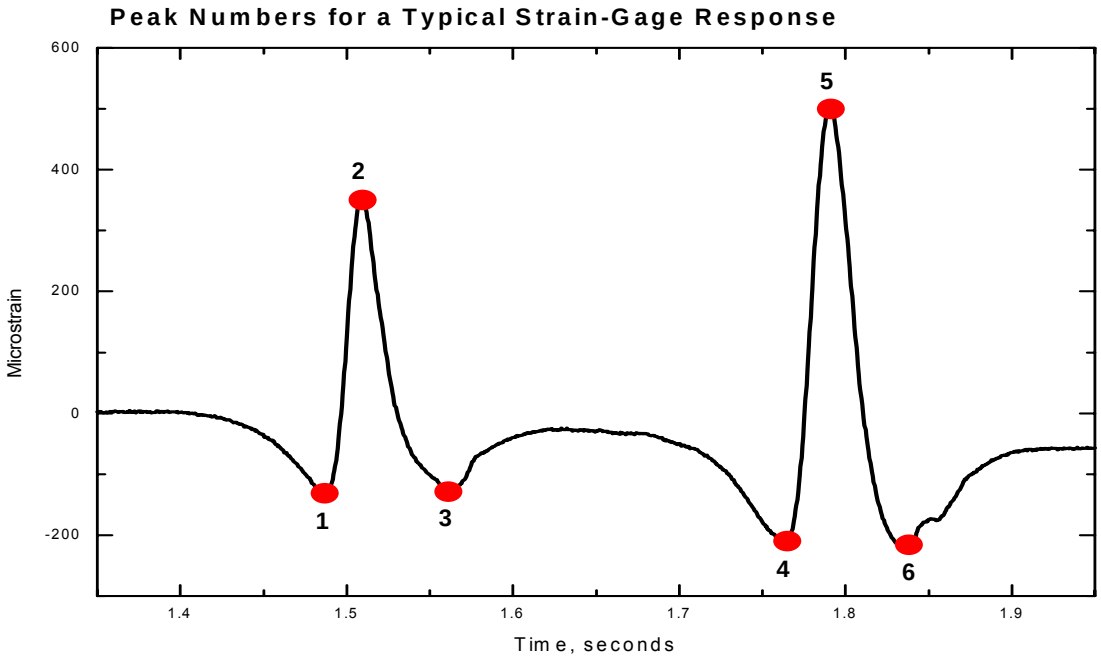

Figure 2.2 – Typical Dynatest Strain Gauge Response Trace

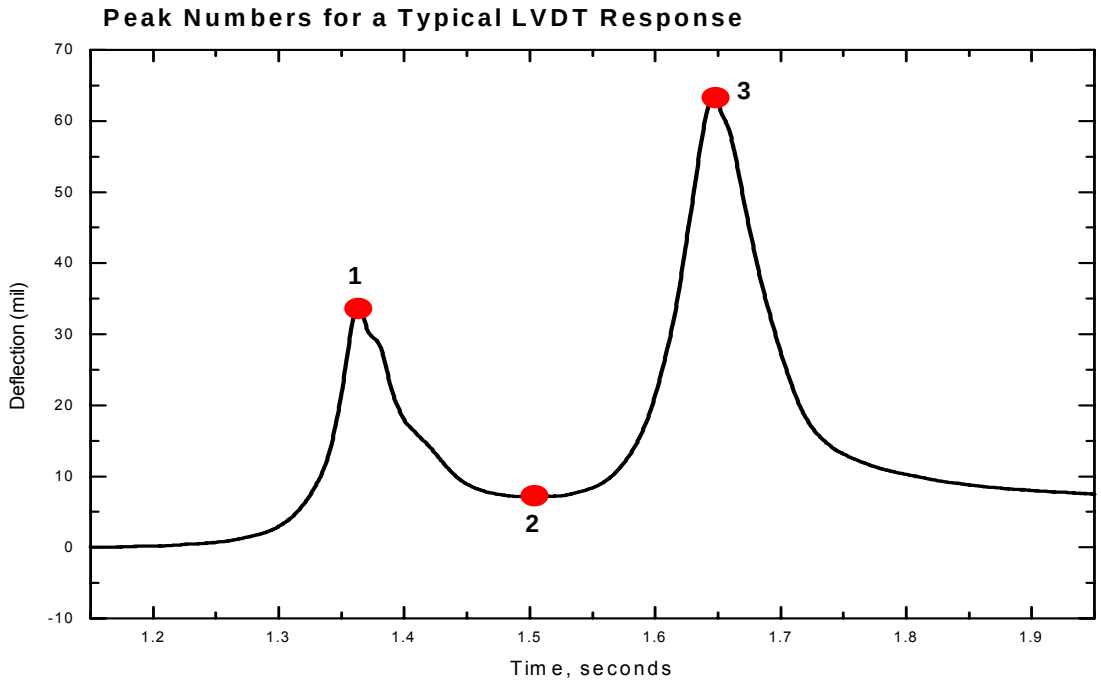

Figure 2.3 – Typical LVDT Response Trace

Table 2.5

Dynamic Sensor Responses on Test Road

Section No. Sensors	Avg. Truck Speed (mph)	Avg. Pvt. Temp. (°F)	No. of Runs	Avg. Lateral Offset (ft.)	Average Total and Normalized Longitudinal Strain @ Peak							Average Total and Normalized Deflection @ Peak Referenced to 12' (mils)		
					Z (in.)	1	2 (Single tire)	3	4	5 (Dual tires)	6	1 (Single tire)	2	3 (Dual tires)
390102 2 LVDTs 1 Gauge (Z = 4")	3.4	114	1	+0.71	4	-391	1506	-175	-291	1627	-126	56.4	4.2	78.7
	29.0		5	+0.86	4	-321	1161	-144	-302	1457	-148	41.4	2.8	72.2
	39.4		3	+0.78	4	-374	1245	-143	-330	1665	-155	43.7	3.1	76.2
	49.7		3	+0.94	4	-335	1030	-94	-356	1637	-185	41.2	2.4	63.8
390105 2 LVDTs 2 Gauges (Z = 4") 1 Gauge (Z = 8")	4.7	104	1	+0.92	4	-122	259	-31	-105	377	-37	42.1	9.0	75.3
					8	-237	456	-189	-358	725	-289			
	27.7		5	+0.82	4	-96	124	-18	-69	182	-11	36.0	7.5	69.6
					8	-143	338	-139	-233	493	-213			
	39.3		4	+0.79	4	-88	136	-10	-50	189	-10	35.0	6.9	62.1
					8	-151	302	-102	-180	436	-158			
	49.3		4	+0.71	4	-73	149	-3	-43	205	-2	31.6	6.2	66.8
					8	-155	325	-101	-206	460	-167			
390107 2 LVDTs 2 Gauges (Z = 4")	3.5	104	1	+0.85	4	-314	1060	-155	-196	1285	-124	78.3	4.2	127.3
	29.7		3	+0.75	4	-184	626	-75	-67	889	-31	65.5	8.8	116.2
	39.3		4	+0.73	4	-147	606	-52	-53	892	-42	67.2	8.5	117.0
	49.3		4	+0.91	4	-108	533	-54	-59	775	-31	63.5	7.6	117.5

Figures 2.4, 2.5 and 2.6 show maximum strain (Fig. 2.2 - Peaks 2, 5) and maximum deflection (Fig. 2.3 - Peaks 1, 3) responses in Section 390102, 390105 and 390107, respectively, as the single-axle dump truck passed over the sensors at different speeds. Each data point represents the average output from one to five redundant runs and the corresponding best-fit lines show the effect of truck speed on longitudinal strain and deflection. Light lines show best-fit trends for individual sensors while bold lines show the best-fit trend for the average of two redundant sensors. Data points for the averages are not shown. Responses under the single front tire are shown as dashed lines, while responses under the rear dual tires are shown as solid lines. In Sections 390102, one longitudinal strain gauge was available to measure strain at Z = 4 in. (10.2 cm), and two redundant LVDTs were available to measure deflection referenced to about twelve feet below the pavement surface. In Section 390105, two redundant longitudinal strain gauges were available to measure strain at Z = 4 in. (10.2 cm), one gauge was available to measure longitudinal strain at Z = 8 in. (20.3 cm), and two redundant LVDTs were available to measure deflection referenced to about 12 feet (3.66 m) below the pavement surface. In Section 390107, two redundant longitudinal strain gauges were available to measure strain at Z = 4 in. (10.2 cm), and two redundant LVDTs were available to measure deflection referenced to about twelve feet below the pavement surface.

Best-fit curves for speed vs. strain and deflection were quite similar in shape for the three sections, with variation between redundant sensors being highest on Section 390107. While there does not appear to be any particular reason why sensor variations differed in the three sections other than random chance, it is interesting that the variation between redundant strain and deflection sensors were both highest in Section 390107, which contained coarse PATB material which was observed to be rather unstable during construction. Figures 2.7 and 2.8 show the correlation between redundant strain gauges and LVDTs in each of the three sections tested. Only one longitudinal strain gauge provided valid data in Section 390102 and at Z = 8 in. (20.3 cm), in Section 390105. While the agreement between redundant sensors in Sections 390102 and 390105 was reasonable, the discrepancies for strain and deflection in Section 390107 seem to be greater than expected.

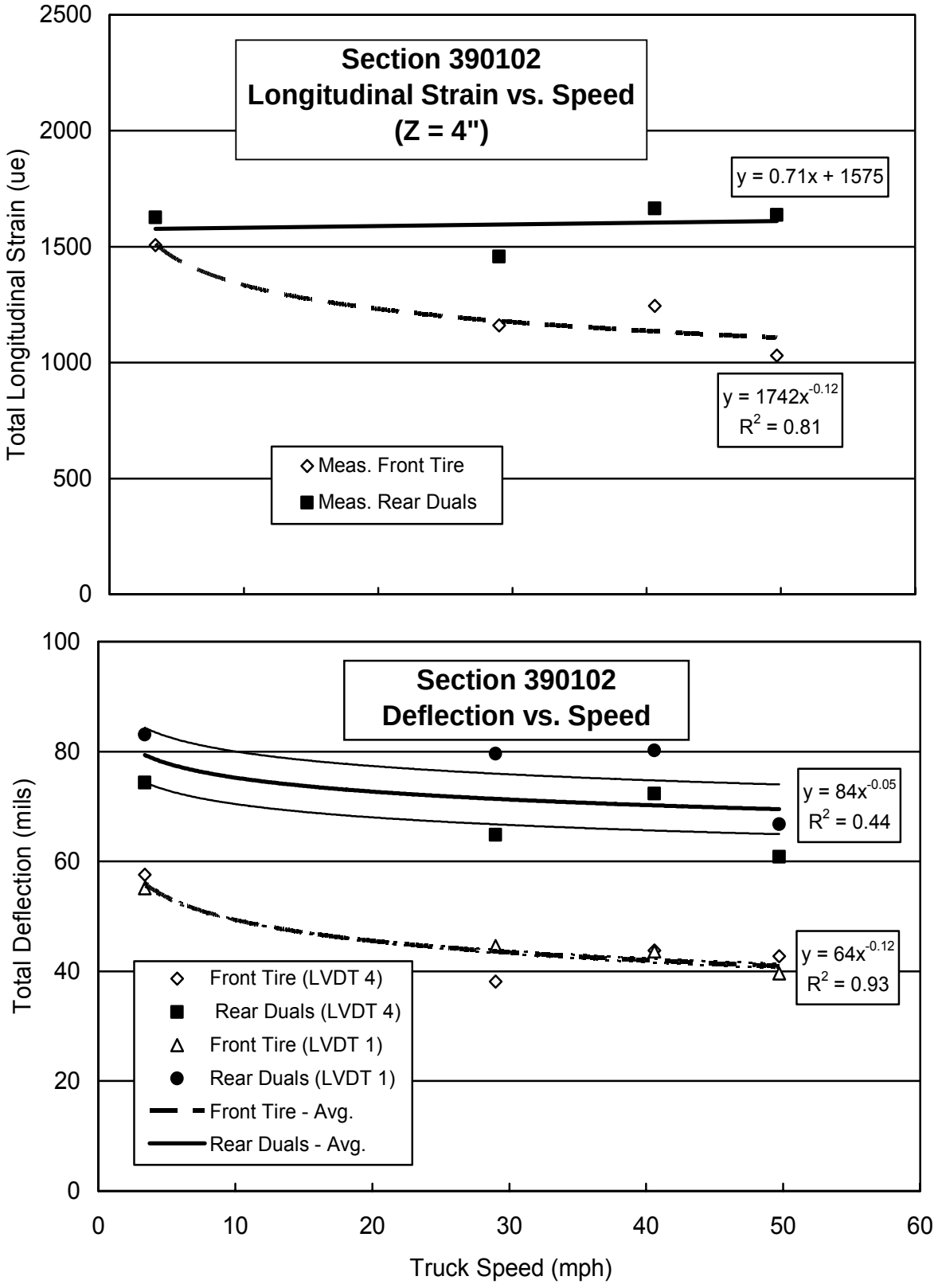

Figure 2.4 – Strain and Deflection Response vs. Speed on Test Road Section 390102

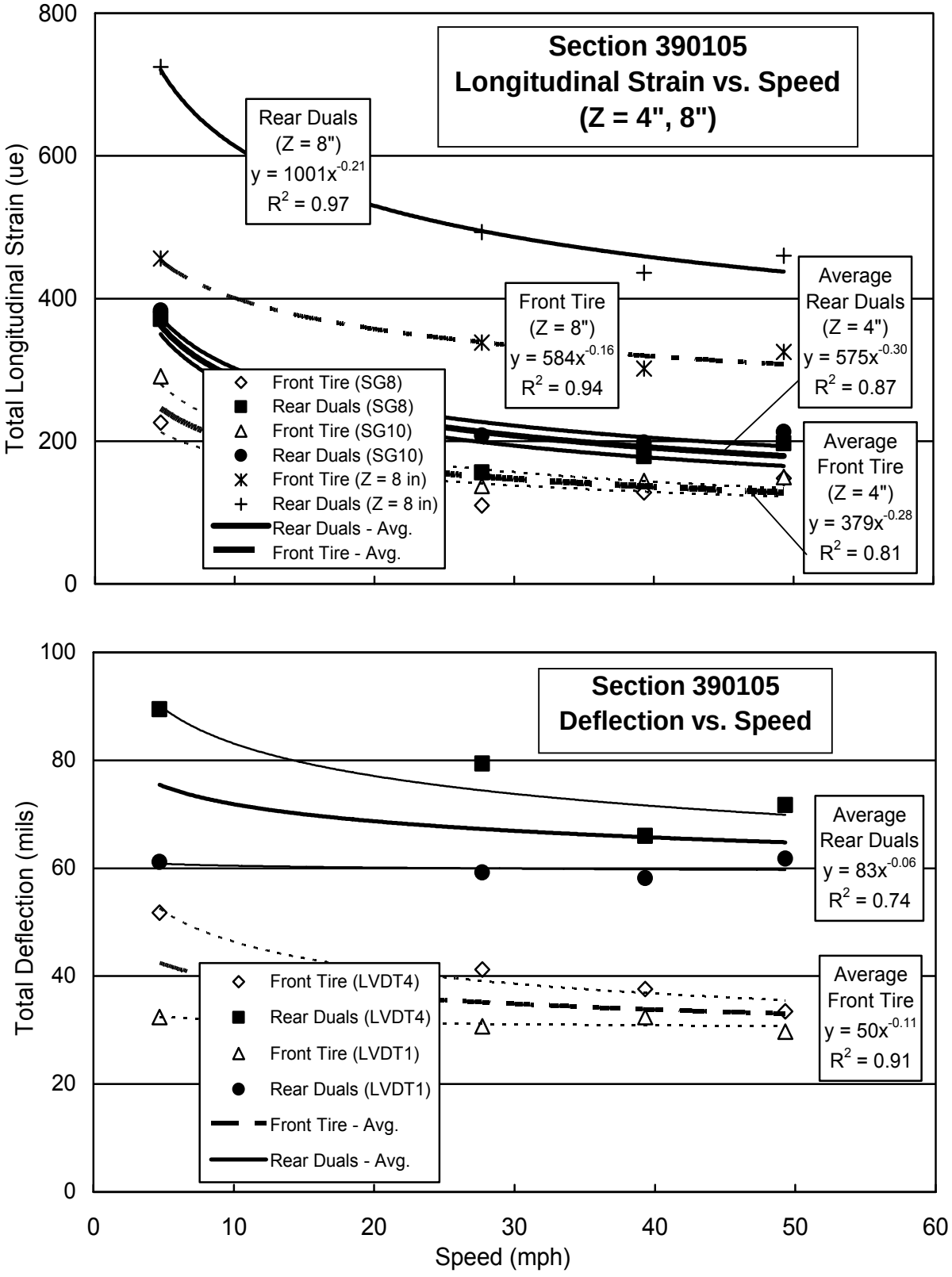

Figure 2.5 – Strain and Deflection Response vs. Speed on Test Road Section 390105

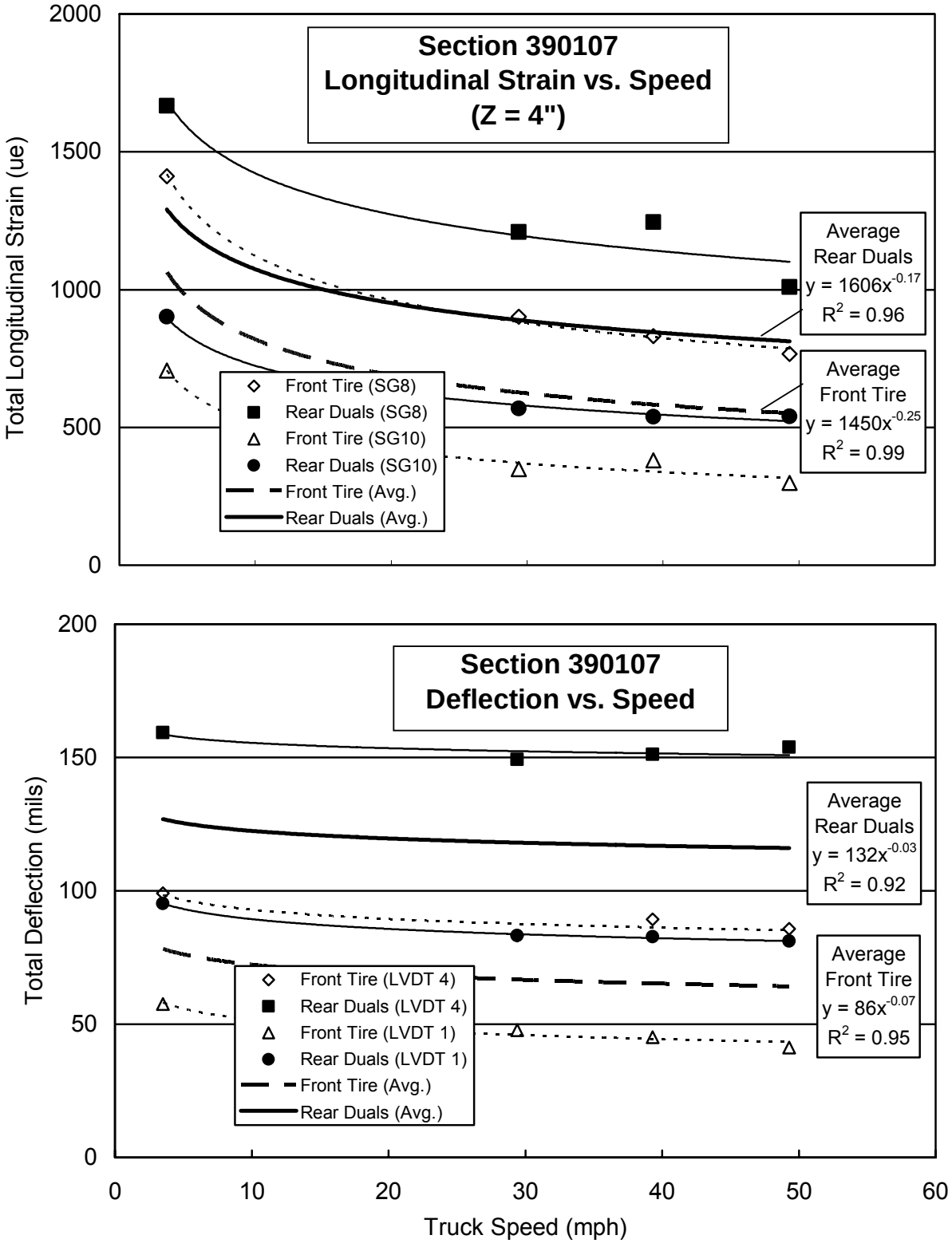

Figure 2.6 – Strain and Deflection Response vs. Speed on Test Road Section 390107

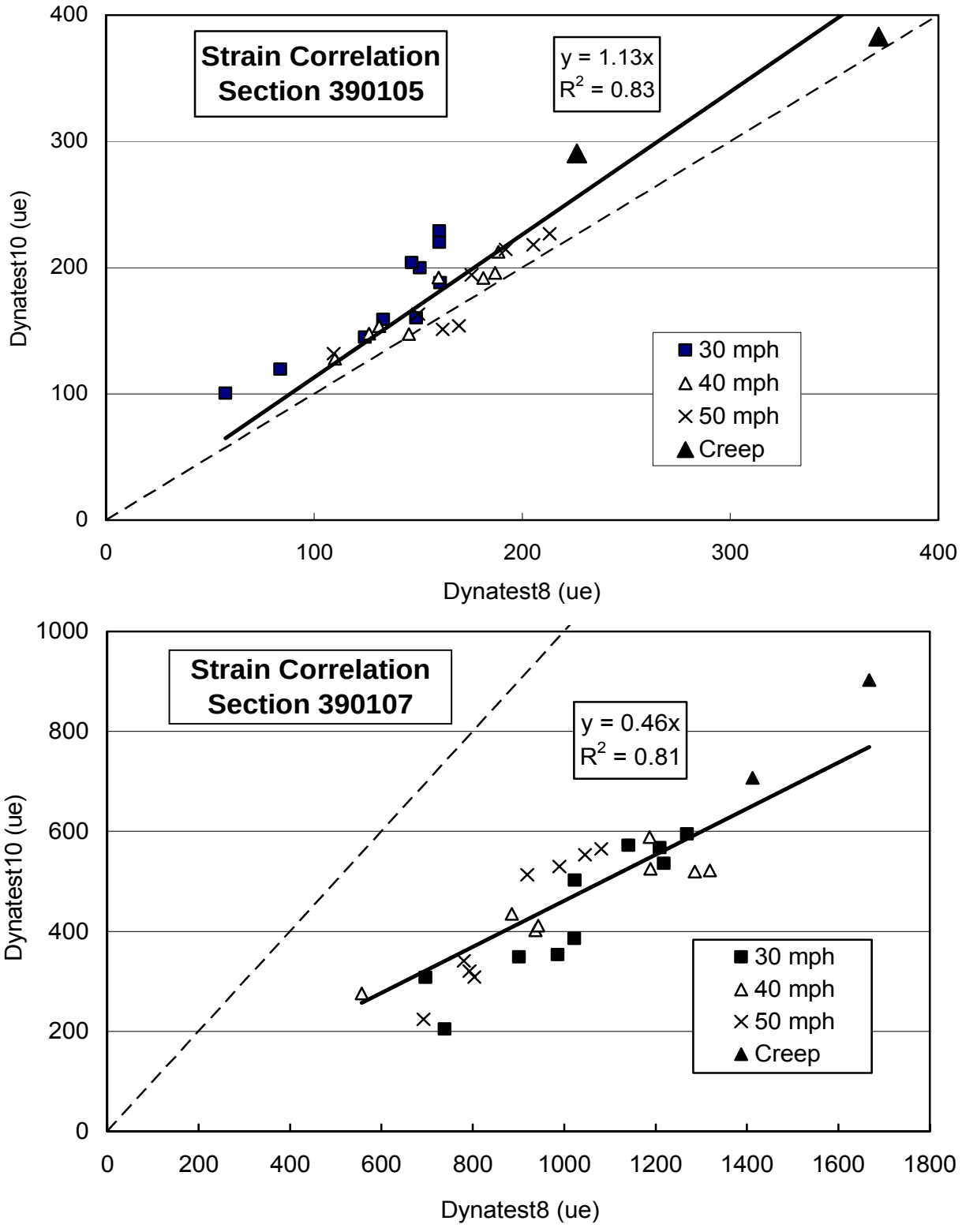

Figure 2.7 – Correlation of Redundant Strain Gauges on Test Road

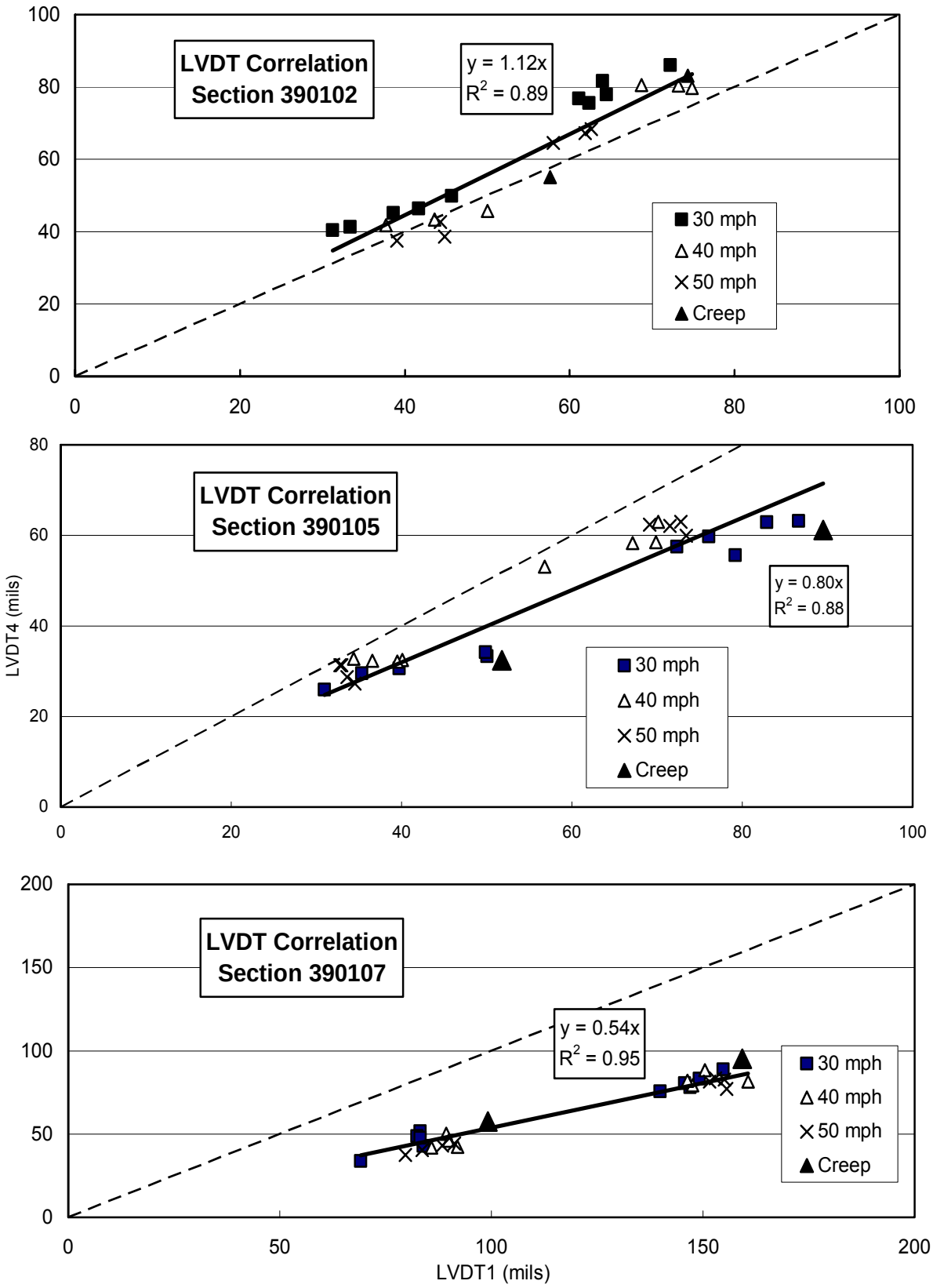

Figure 2.8 – Correlation of Redundant LVDTs on Test Road

In addition to summarizing peak responses, Table 2.5 shows other information regarding the number of sensors providing valid data, average pavement temperature, average truck speed measured on the sensor traces, number of runs within each speed category, and the average lateral offset for those runs. Because the three test sections were monitored concurrently as the test trucks traveled the length of the project on each run, temperature conditions were similar in all sections during each run. Some differences in subgrade stiffness were likely between sections due to normal variations in material properties and moisture along the project length.

Deflections measured during the controlled vehicle tests, even at 50 mph (80 k/hr), were much larger than deflections measured with the FWD and, while Section 390105 remained the stiffest of the three sections in both series of tests, the relative stiffness of Sections 390102 and 390107 was different for the two series of tests. Total maximum deflections on the four sections ranged from 12.3 – 30.1 mils (0.31-0.76 mm) with the FWD, 31.6 – 78.3 mils (0.80-1.99 mm) under the single truck tire, and 62.1 – 127.3 mils (1.58-3.23) under the dual truck tires. These higher vehicle responses and the change in relative section stiffness between 390102 and 390107 was largely due to higher pavement temperature and higher subgrade moisture during the controlled vehicle tests, with some possible minor effects from differences in stiffness between the 500-foot (152.4 m) long SPS sections and the instrumented sections outside the SPS sections. In other tests on the Ohio SHRP Test Road, deflections measured with the FWD agreed quite well with deflections measured with pavement LVDTs at the same time under the FWD plate, indicating that FWD and LVDT measurements are comparable.

Temperature Conditions

Hourly temperatures measured with thermistors to a depth of 8.5 in. (21.6 cm) in Section 390102 during the FWD tests on 6/11/96 and during the controlled vehicle tests on 8/6/96 are shown in Figure 2.9. Temperatures were not being collected yet in the other sections when these tests were being performed. Because of differences in testing methodology, the procedures for calculating average pavement temperature were slightly different for the two types of measurements. For the FWD, which required less than 30 minutes per section, sections were tested sequentially and average temperature consisted of interpolating between hourly temperatures during the time each section was tested, and over the thickness of asphalt stabilized

materials in the section. On 6/11/96, testing started at 9:19 on Section 390105, 10:47 on Section 390102, 11:09 on Section 390107 and 11:30 on Section 390101. During the controlled vehicle tests, all sections were monitored simultaneously as the trucks traveled the length of the project on each run. Therefore, the two-hour test period (16:30 to 18:30) was the same for all sections and the only difference in average temperature between sections resulted from the thickness of asphalt stabilized material in the section. Average pavement temperatures calculated during the FWD and vehicle tests are shown in Tables 2.4 and 2.5.

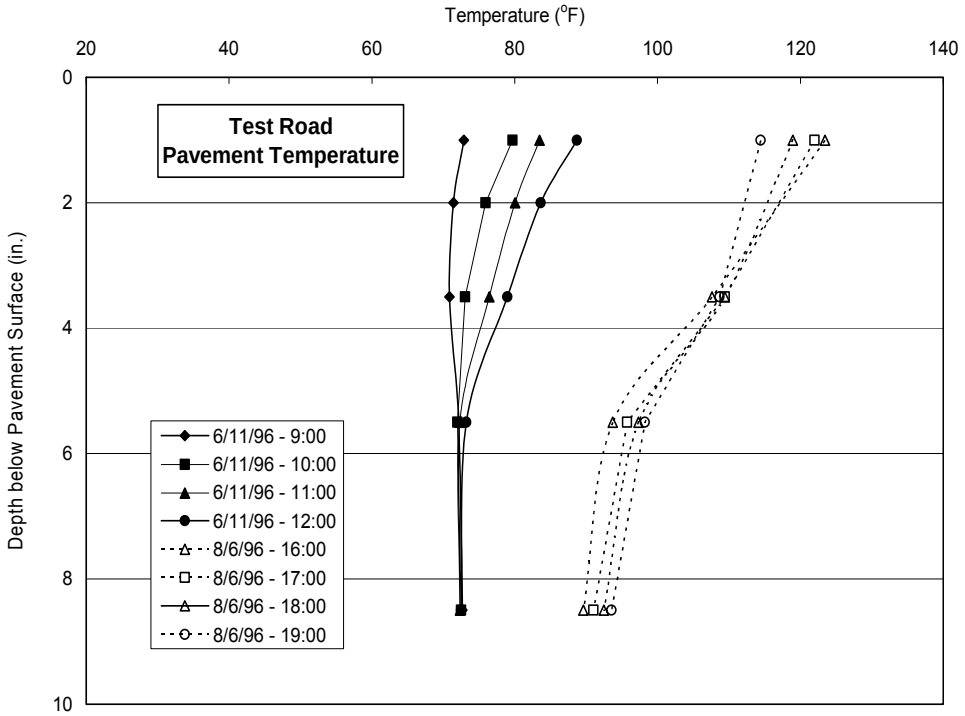

Figure 2.9 – Pavement Temperatures on Test Road

Subgrade Moisture Conditions

Subsurface moisture was measured with time-domain reflectometry (TDR) probes placed at various depths below the pavement surface in eighteen sections. These probes measured volumetric moisture in percent. Figures 2.10 and 2.11 show moisture plots over the time the TDRs remained in service on Sections 390101 and 390102, and Figure 2.12 shows moisture measured over a two year period in Section 390108. Section 390107, which contained no

environmental instrumentation, was located between Sections 390101 and 390102. Section 390105, which also contained no environmental instrumentation, was adjacent to Section 390108. The initial TDR readings were taken on July 25-26, 1996 which was after the FWD measurements in June and before the controlled vehicle tests in August. The July 1996 moisture profiles are shown as heavy lines in Figures 2.10 – 2.12 to differentiate them from subsequent profiles, which were added to illustrate the relative stability of profile shape over time after the pavement sections were in place. The initial profile in Section 390101 was somewhat different than the later profiles with a generally linear shape and higher moisture.

Based upon the relative consistency of the moisture profiles after July 1996, it would be easy to assume that subgrade moisture during the FWD tests in June 1996 was about the same as it was in July and August of 1996. Rainfall records from the on-site weather station indicate, however, that approximately five inches (12.7 cm) of precipitation fell during this two-month period of time, as shown in Figure 2.13. Therefore, based upon these precipitation data, it is likely that subgrade moisture increased during the two-month period between the June FWD and the August controlled vehicle tests.

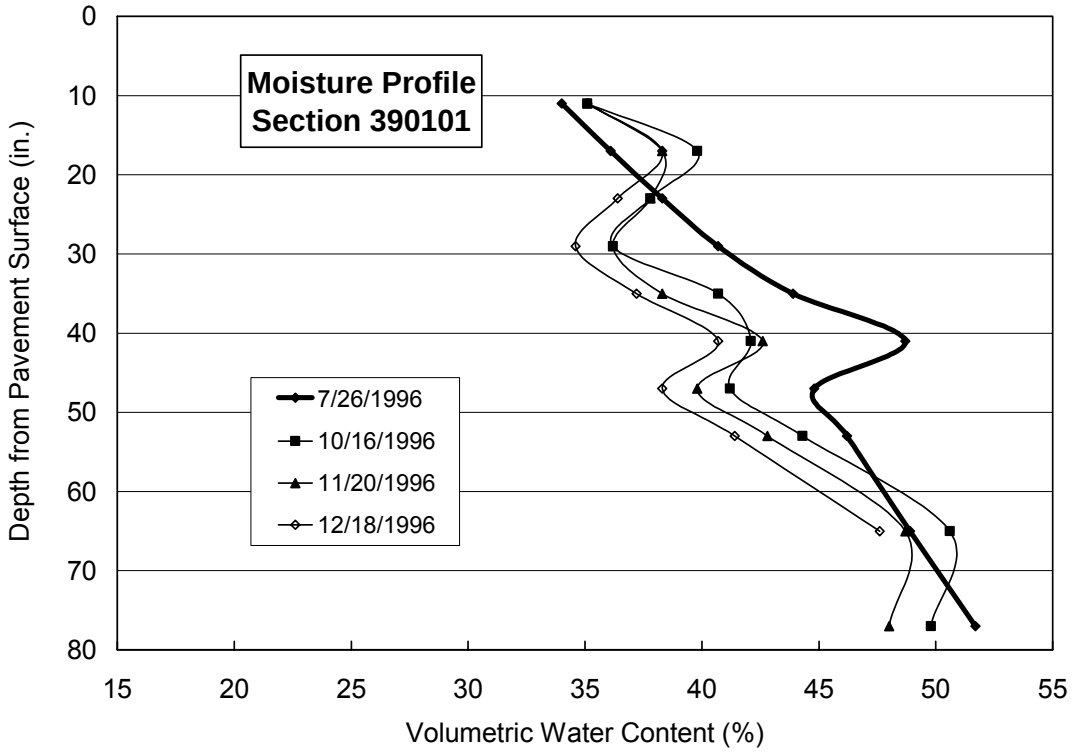

Figure 2.10 – Subgrade Moisture in Section 390101

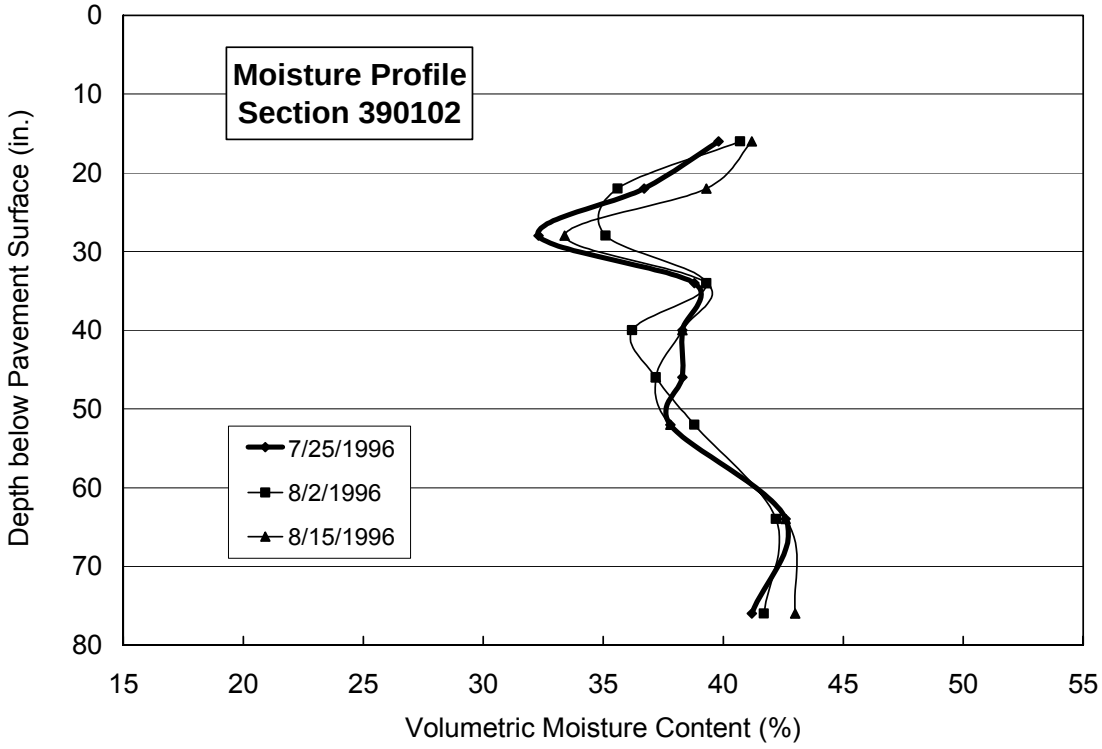

Figure 2.11 – Subgrade Moisture in Section 390102

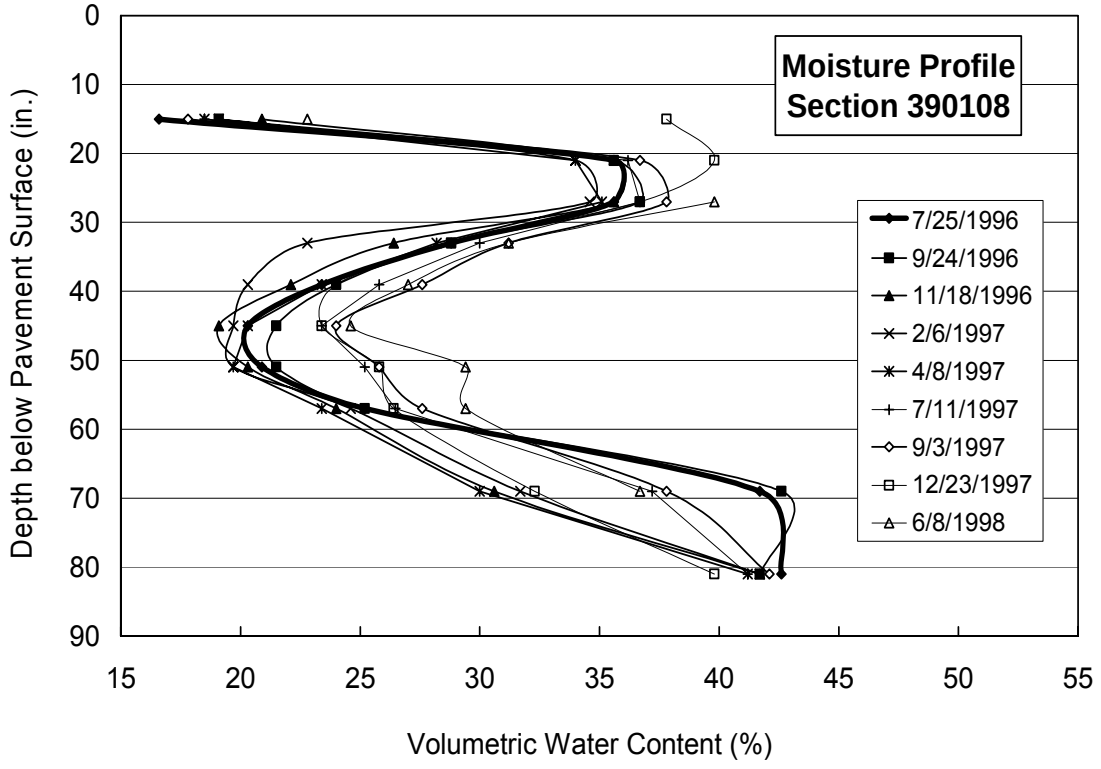

Figure 2.12 – Subgrade Moisture in Section 390108

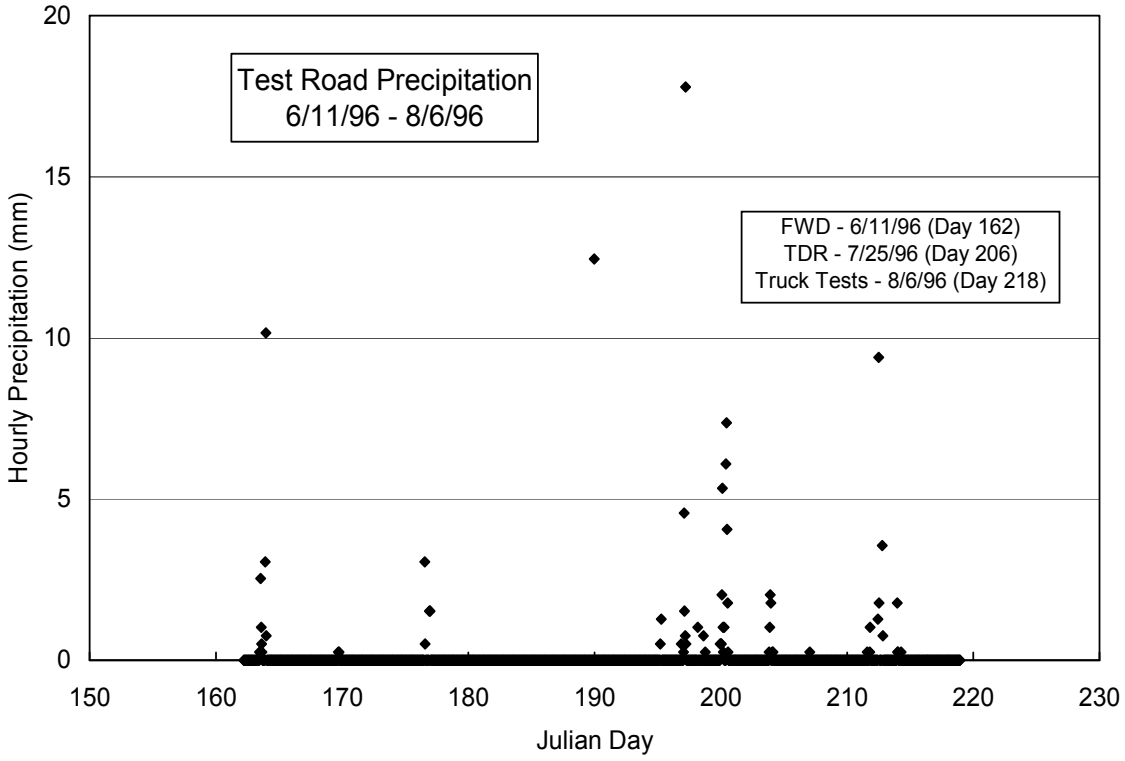

Figure 2.13 – Rainfall on Test Road during FWD and Controlled Vehicle Testing

Material Properties

Cores of the various stabilized materials were removed from a sampling section located just outside the SPS section limits and tested in the laboratory in accordance with SHRP protocol. Figure 2.14 shows the effect of temperature on the resilient modulus of asphalt stabilized materials on the test road. The relative stiffness of these materials looks reasonable with ATB being the stiffest of the four materials, followed by the Type 2 leveling mix which had a slightly higher modulus than the Type 1 surface mix, and PATB being the weakest material. It was essentially impossible to obtain intact cores of PATB. Usually, the PATB cores would come out in pieces, which were recompacted without reheating in the laboratory prior to testing.

Figure 2.15 shows resilient moduli of the dense graded aggregate base as a function of deviator stress and Figure 2.16 shows resilient moduli of the A-7-6 subgrade in Section 390107 as a function of moisture and deviator stress.

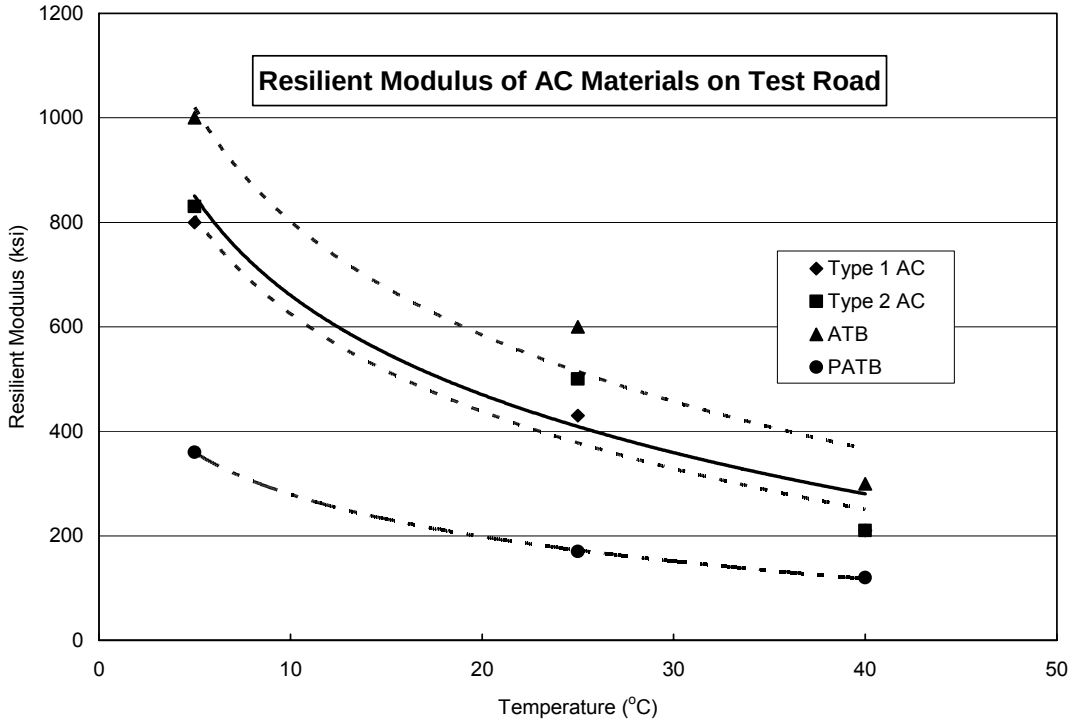

Figure 2.14 – Resilient Moduli of AC Materials on Test Road

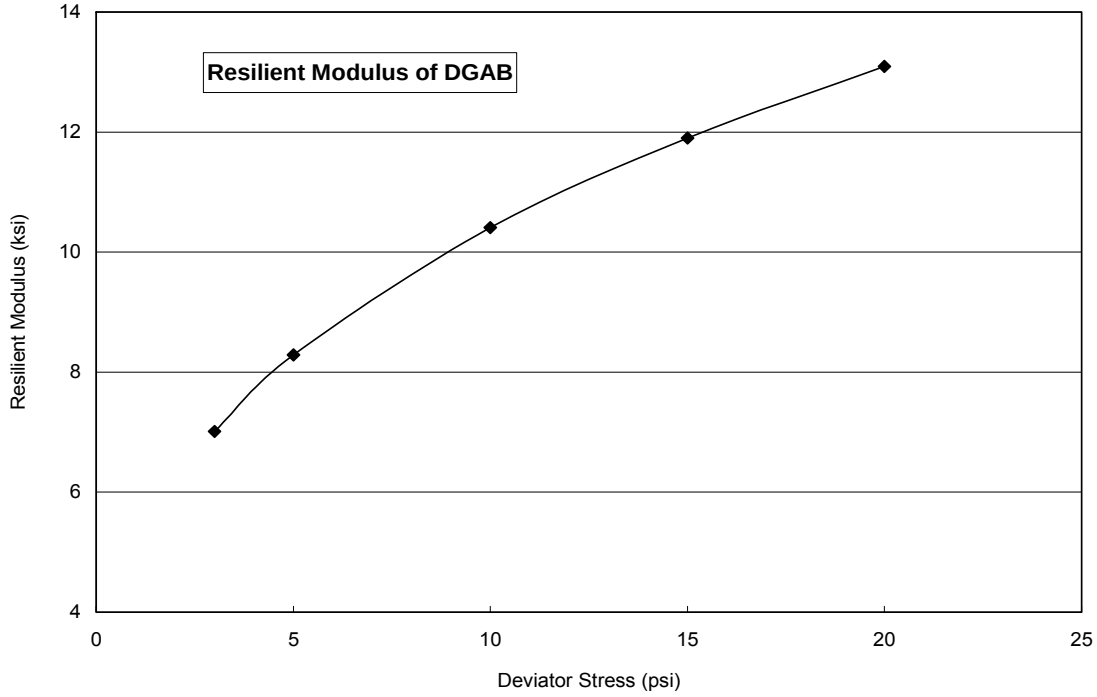

Figure 2.15 – Resilient Moduli of Dense Graded Aggregate Base on Test Road

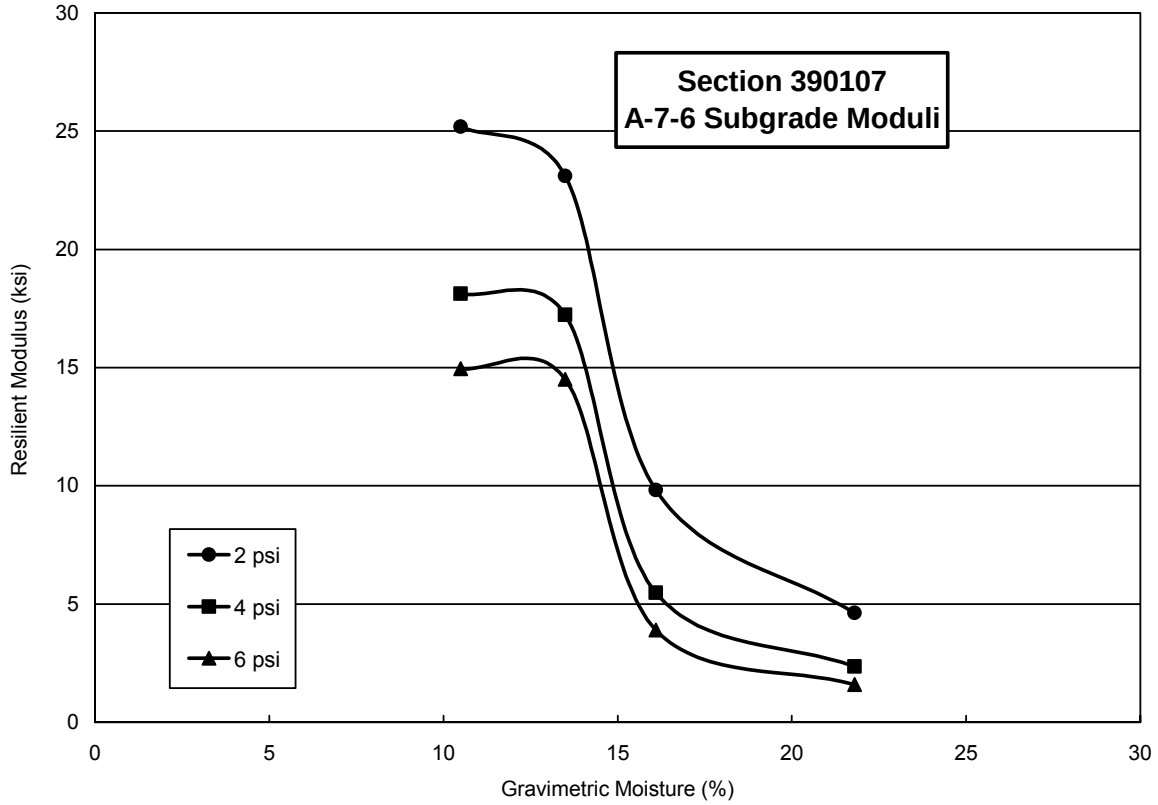

Figure 2.16 – Subgrade Moduli on Test Road

Performance

The test road was functionally complete and opened to mainline traffic on August 14, 1996. Within a few days, noticeable ruts, approximately ½ in. (13 mm) deep, were detected in Sections 390102 and 390107, and there was concern these sections might deteriorate rapidly over the upcoming Labor Day weekend. Fortunately, no problems arose during the weekend, but there was considerable doubt that the sections would remain intact over the winter months. The prospect of having to perform emergency repairs on a major highway in the winter prompted the consideration of some type of immediate remedial action. After some deliberation, it was decided to remove the 4-inch thick AC pavement layer and some base material from both sections and replace these materials with a thicker layer of temporary AC pavement to get them through the winter. The lanes were closed on September 3, 1996 to complete this work. A total removal of the temporary pavement and replacement with more robust supplemental sections of interest to the state was planned for 1997. While the distress in Sections 390102 and 390107

occurred somewhat earlier than expected using ODOT design parameters and assumed subgrade conditions, AASHTO equations did forecast these sections to be the first to fail.

During the rehabilitation of Section 390107, a portion of the underdrains originally installed to drain the pavement were observed to be not connected to outlet pipes, thus making the section partially drained and partially undrained. Shortly after placement of the temporary pavement in Sections 390102 and 390107, and reopening of the southbound lanes on September 11, 1996, moderate rutting began to develop in Section 390101. To avoid a midwinter or early spring failure in this section and to preserve the integrity of dynamic response sensors in the thinner AC sections for the 1997 controlled vehicle tests, the SPS-1 and SPS-9 experiments were closed to traffic again on December 3, 1996, and not re-opened until November 11, 1997, after the performance of additional controlled vehicle tests and replacement of the distressed sections.

During the winter of 1996-97, plans were prepared for removal of the three distressed SPS-1 sections and installation of heavier sections similar to those in SPS-9 because SHRP had no follow-up plans for distressed sections in the SPS-1 and SPS-2 experiments. Replacement of the two SPS-8 AC sections was included in the same contract because of premature distress caused by earlier response testing performed for FHWA.

Visual observations of the three distressed SPS-1 sections indicated moderate to severe rutting throughout, with localized areas also exhibiting wheel path cracking. Because it was not possible visually to determine the specific causes of the distress, ODOT personnel and ORITE staff and students conducted a forensic investigation to more clearly define the failure mechanism in Section 390101. Results of the forensic study showed the following:

- Essentially all of the rutting could be attributed to the base and subgrade, with no consolidation or instability being observed in the AC layer.
- Debonding of the Type 1 and Type 2 layers was observed in the most severely distressed areas. ODOT did not require the AC lifts to be tacked during construction.
- Subgrade moisture was considerably higher than anticipated throughout the section.

Judging by the nature and timing of distress in the other two sections, their modes of failure were likely to be very similar.

A sudden and rather dramatic failure occurred at Station 2+30 in Section 390105. Within a few hours after the distress was first reported to ODOT by passing motorists on May 29, 1998, considerable AC material from an area approximately 20 feet (6.1 m) long and covering the right half of the driving lane had been removed by traffic and scattered along the side of the road. The two lifts of AC pavement had debonded from the ATB and from each other over a 3-foot wide by 6-foot long (0.9-1.8 m) oval at the center of the failed area. The ATB was also broken and in danger of being removed at that point. Away from the most distressed area, debonding was still evident, but less severe. Heavy rainfall the previous day likely precipitated the failure.

Over the next few days, an ODOT maintenance crew shut the driving lane down in Section 390105 only, removed the severely debonded AC over a 6-foot wide by 40-foot long (1.8-12.2 m) area in the right side of the lane, and patched it with hot mix AC. Severe rutting was noted in other areas of the section and in the instrumented area immediately preceding the section. Consequently, other portions of the section were expected to fail in a short period of time. FWD and Dynaflect measurements obtained three weeks prior to this failure confirmed the area between Stations 2+00 and 2+50 to be particularly weak in the right wheelpath, with mid-lane measurements showing good uniformity throughout the entire section length.

CHAPTER 3

ACCELERATED PAVEMENT LOADING FACILITY

General

The Accelerated Pavement Loading Facility (APLF) consists of an enclosed reinforced concrete test pit 38 feet (11.6 m) wide by 45 feet (13.7 m) long by 8 feet (2.4 m) deep. Air temperature can be maintained between +10º F (12º C) and +130º F (54º C), and water can be added to subgrade beneath the test pavements. The four sections being studied in this project were reconstructed to the extent possible adjacent to each other in six-foot (1.8 m) wide lanes, as shown in Figures 3.1 and 3.2. Two lanes of Section 390101, identified as 101E and 101W, were constructed for performance testing. Approximately six feet (1.8 m) of A-6 subgrade placed over one foot (0.3 m) of #57 aggregate in the test pit at the time the facility was constructed remained intact at the time the SPS sections were placed in the facility. Aggregate for the pavement and bases was hauled from the same Marion, Ohio source used on the test road, and essentially the same AC mix designs were used for the pavement and stabilized base layers. Sections constructed on the original APLF subgrade were referred to as Pad A. A second pad, constructed identical to the first pad but with water added to the subgrade, was to be identified as Pad B.

FWD Measurements – Pad A

On May 9, 2002, the FWD was used to measure stiffness at four positions along each 45-foot long completed lane after air temperature in the facility had been maintained at 70º F (21º C) for several days. While pavement temperatures were not available at that time, an infrared thermometer used to monitor temperature of the pavement surface remained at 70º F (21º C) for the duration of the testing. On this basis, temperature of the pavement sections was assumed to be a uniform 70º F (21º C). Data in Table 3.1 show average normalized deflections generated by nominal 5 kip (2.3 Mg) loads on the subgrade and DGAB, and nominal 9 kip (4.1 Mg) loads on the stabilized layers. Average deflection basins and backcalculated layer moduli are shown in Table 3.2, while Figure 3.3 shows a comparison of average maximum normalized FWD deflections measured at the two sites. The relative stiffness of the four test sections was identical at the two sites, but deflection on the test road was two to three times higher than at the APLF.

Figure 3.1 – Photograph of APLF Test Pad

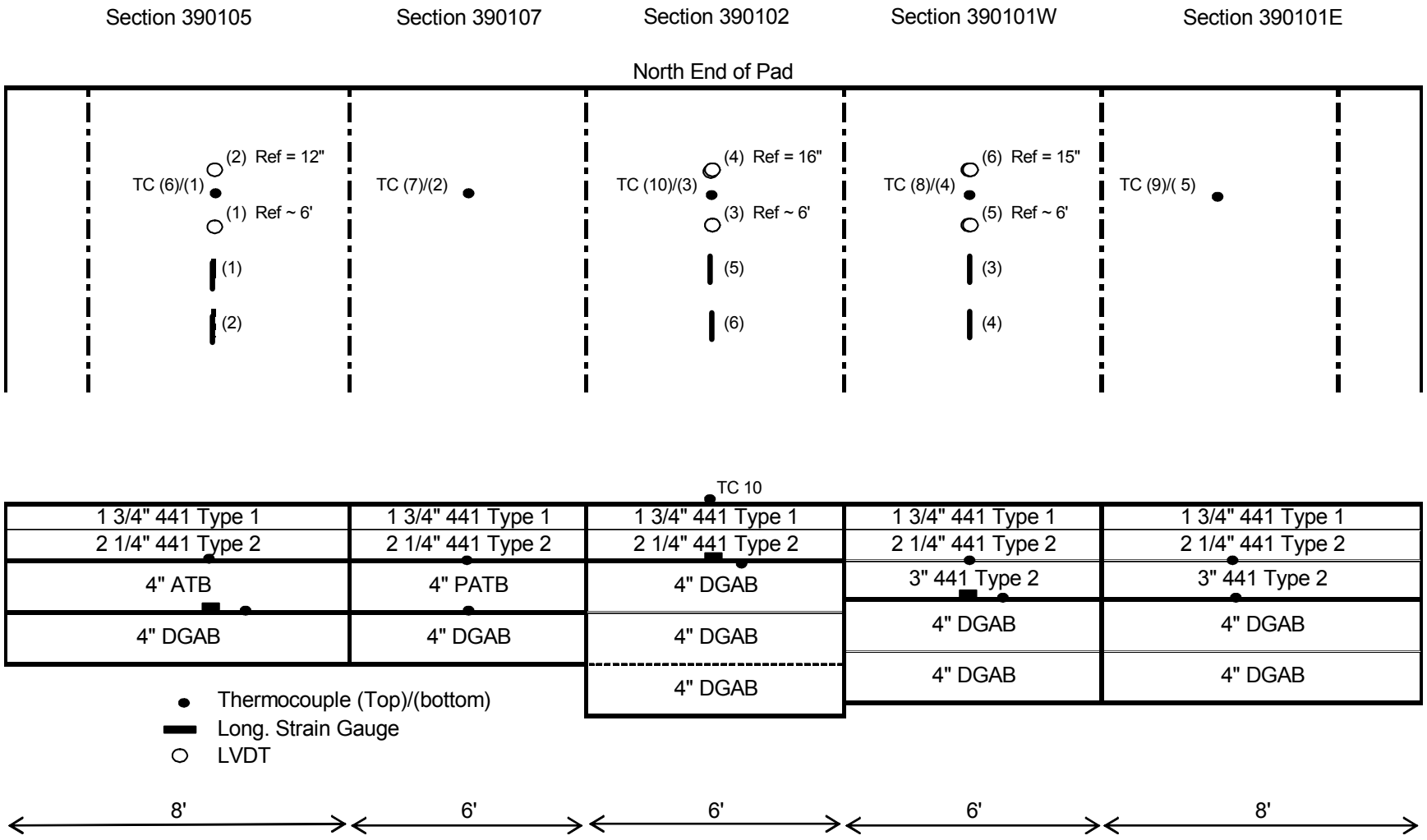

Figure 3.2 – Schematic Drawing of APLF Test Pad

Table 3.1

Summary of FWD Normalized Maximum Layer Deflections in APLF– Pad A

Section	Layer	Normalized FWD Df1 (mils/kip)		
		US 23	APLF	
		11.8" Plate	11.8" Plate	18" Plate
101E	Subgrade	8.28	7.09	3.26*
	8” DGAB	4.24		4.39
	3” Type 2	-	2.21	
	7” AC	1.63	0.83	
101W	Subgrade	8.28		4.71
	8” DGAB	4.24		3.25
	3” Type 2	-	1.88	
	7” AC	1.63	0.74	
102	Subgrade	4.31		3.81
	12" DGAB	3.86	3.51	3.23*
	4”AC	3.36	1.20	
105	Subgrade	4.81		19.20
	4” DGAB	5.00		9.22
	4” ATB	2.08	2.04	
	4” AC	1.39	0.69	
107	Subgrade	5.10		4.10
	4” DGAB	5.54		5.68
	4” PATB	5.25	3.25	
	4” AC	2.01	0.98	
* Avg. at same locations where 11.8" plate used.				

Table 3.2

FWD Basin Measurements and Backcalculated Moduli in APLF – Pad A

Section	Avg. Pvt. Temp. (°F)	Average Normalized Deflection (mils/kip) @ R (in.)							Layer Moduli Backcalculated from MODULUS 5.1 (ksi)				
		0	8	12	18	24	36	60	AC	ATB	PATB	DGAB	Subgrade
APLF 5/9/02													
101E	70	0.83	0.62	0.50	0.36	0.27	0.16	0.08	436	-	-	68	30
101W	70	0.74	0.57	0.46	0.34	0.25	0.15	0.08	561	-	-	73	30
102	70	1.20	0.87	0.64	0.40	0.26	0.13	0.07	769	-	-	35	31
105	70	0.69	0.53	0.44	0.32	0.25	0.14	0.07	519			113	32
107	70	0.97	0.68	0.51	0.34	0.24	0.13	0.07	453	-	120	66	33

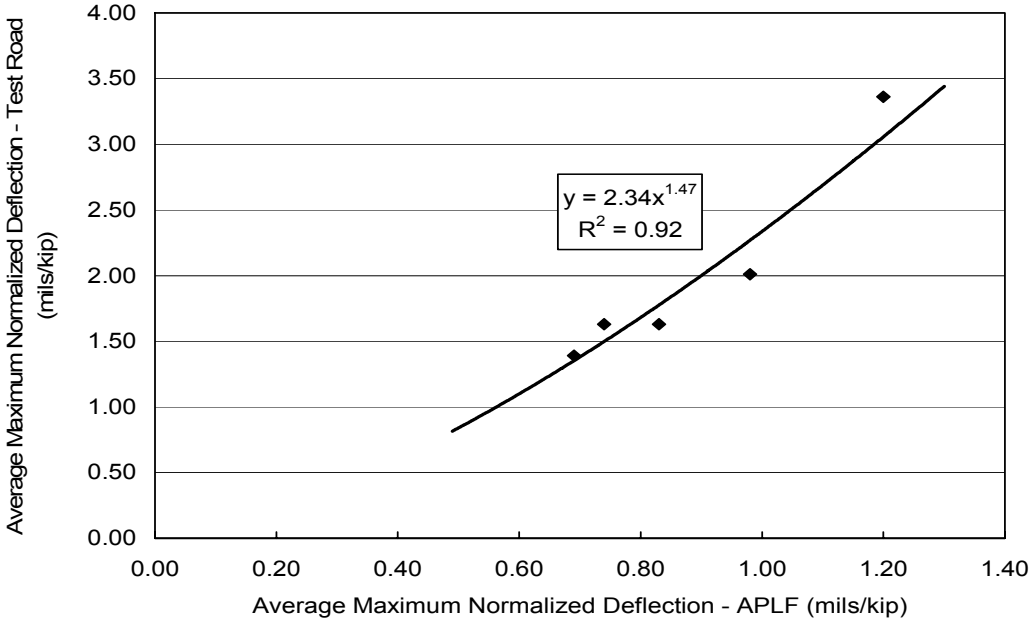

Figure 3.3 – Comparison of Average Normalized FWD Maximum Deflections on the Test Road and in the APLF – Pad A

Rolling Wheel Response Tests – Pad A

Two redundant Dynatest PAST II AC strain gauges were installed longitudinally at the bottom of the AC stabilized layers in Sections 101W (Z = 7”), 102 (Z = 4”) and 105 (Z = 8”) (17.8, 10.2 and 20.3 cm) in the APLF. No gauges were installed in Section 107 because of the presence of PATB, which was not expected to be used by ODOT on typical pavements. Single LVDTs referenced to the top of the subgrade and to a depth of about 6 feet (1.8 m) below the top of the pavement were also placed in each of the three instrumented sections. Prior to the application of repeated wheel loads, a response matrix consisting of two loads (6 and 9 kips) (2.7 and 4.1 Mg), three speeds (1, 3 and 5 mph) (1.6, 4.8 and 8.0 km/hr) and four lateral positions of the dual test tires (0, 2, 7 and 12 inches (0, 5.1, 17.8 and 30.5 cm) from midway between the dual tires) was run in each section at nominal air temperatures of 40, 70 and 100º F (4.4, 21.1, and 30.5º C). The dual tires were each 10 in. (25.4 cm) wide and spaced 4 in. (10.2 cm) apart, thereby having the sensors fall midway between the dual tires, under the inside edge of a tire, under the center of a tire and under the outside edge of a tire at the four lateral positions in the response matrix, as shown in Figure 3.4. Strains and deflections measured during these tests are summarized in Appendix B.

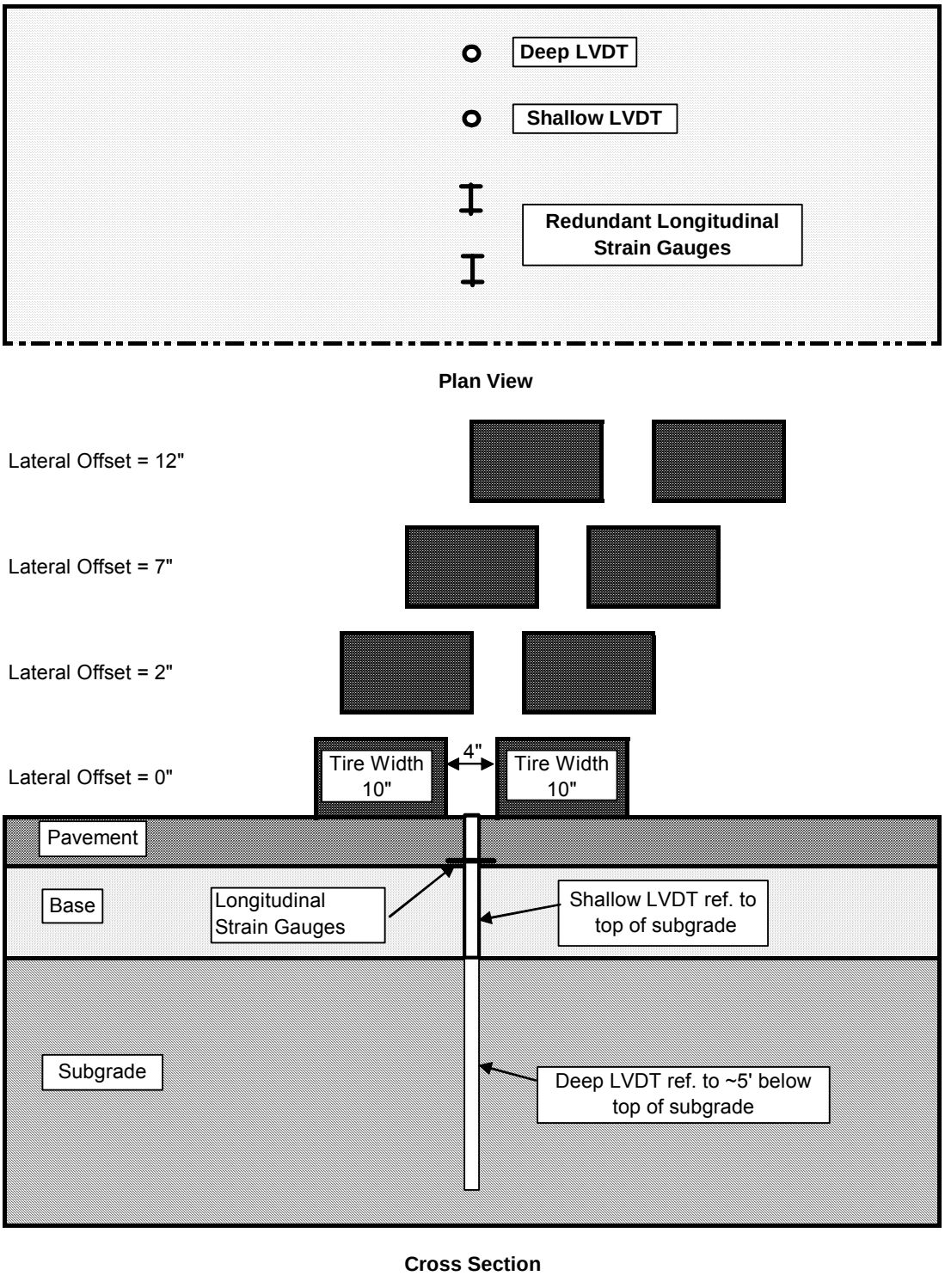

Figure 3.4 – Tire/Sensor Location during Response Testing

Because of the relatively uniform conditions existing in the APLF, differences in FWD and dynamic response between sections at the same temperature can be attributed to differences in the structural stiffness of the pavement structures at the time of the measurements. Further, changes in dynamic response with temperature can be attributed to changes in the moduli of the asphalt stabilized layers resulting from the changes in temperature, and differences between FWD and rolling wheel responses at 70º F (21.1º C) can be attributed to differences between the two loaded areas and the type of loading. Subgrade uniformity was confirmed both by Df6 measurements with the FWD and by backcalculation, as shown in Table 3.2.

A summary of total and normalized strains and deflections measured on the test road and in the APLF are shown in Tables 3.3 and 3.4. With no changes in subgrade moisture or pavement temperature in the APLF, FWD and LVDT measurements obtained at 70º F (21.1º C) can be compared directly on the three instrumented sections. In general, deflections measured in the APLF were slightly larger under the FWD load plate than under the dual test tires, and FWD deflections measured on the test road were 2 – 3 times higher than in the APLF with similar pavement temperatures. Deflections increased at both facilities with increasing temperature.

Figures 3.5 and 3.6 show total measured strain and deflection, respectively, as the set of dual tires loaded to 9 kips (4.08 Mg) and traveling at 5 mph (8.0 km/hr) was moved to different lateral positions at the three temperatures. These plots indicate little difference in dynamic response under or between the dual tires at 40º F (4.4º C), but higher response at the center of the tires and lower response at the outside edge of the tires with increasing temperature.

Graphs of strain and deflection versus load at the three nominal test temperatures are shown in Figures 3.7 and 3.8. Figure 3.7 indicates an elastic to softening response of strain vs. load, while Figure 3.8 generally shows a slight hardening response of deflection vs. load. Figures 3.9 and 3.10 show typical nonlinear responses of strain and deflection with changes in temperature on these thin pavement sections. Figure 3.11 shows a comparison of redundant longitudinal strains measured in the APLF during the rolling wheel response matrix. While variations in the Section 101W gauges were more than expected, variations in Sections 102 and 105 were reasonable.

Table 3.3

Total Dynamic Responses on Test Road and in the APLF – Pad A

Facility	Section	FWD		Wheels Moving @ Creep Speed							
					Single Tire		Dual Tires				
		Temp. (° F)	Total Dfl (mils)	Temp (° F)	Total Dfl (mils)	Total Strain (με)	Total Dfl (mils)	Total Strain (με)	Temp (° F)	Total Dfl (mils)	Total Strain (με)
Test Road	Load	~ 9 kips			4.76 kips		8.87 kips				
	390101	78	14.9								
	390102	77	31.6	114	56.3	1506	78.7	1627			
	390105	72	13.1	104	42.1	259	75.3	377			
	390107	77	18.5	104	78.3	1060	127.3	1285			
APLF (All Loads ~ 9K)		FWD		Dual Tires							
	390101	70	7.2	94			9.8	198	70	5.3	101
	390102	70	10.9	94			14.9	399	70	8.6	200
	390105	70	6.4	94			10.6	241	70	5.9	134
	390107	70	8.9								

Table 3.4

Normalized Dynamic Responses on Test Road and in the APLF – Pad A

Facility	Section	FWD		Wheels Moving @ Creep Speed							
					Single Tire		Dual Tires				
		Temp. (° F)	Norm. Dfl (mils) (kip)	Temp (° F)	Norm. Dfl (mils) (kip)	Norm. Strain (με) (kip)	Norm. Dfl (mils) (kip)	Norm. Strain (με) (kip)	Temp (° F)	Norm. Dfl (mils) (kip)	Norm. Strain (με) (kip)
Test Road	Load	~ 9 kips			4.76 kips		8.87 kips				
	390101	78	1.62								
	390102	77	3.34	114	11.8	316	8.87	183			
	390105	72	1.37	104	8.84	50	8.49	34			
	390107	77	2.01	104	16.5	222	14.4	145			
APLF (All Loads ~ 9K)		FWD		Dual Tires							
	390101	70	0.79	94			1.09	22	70	0.59	11
	390102	70	1.20	94			1.66	44	70	0.96	22
	390105	70	0.69	94			1.18	27	70	0.66	15
	390107	70	0.97								

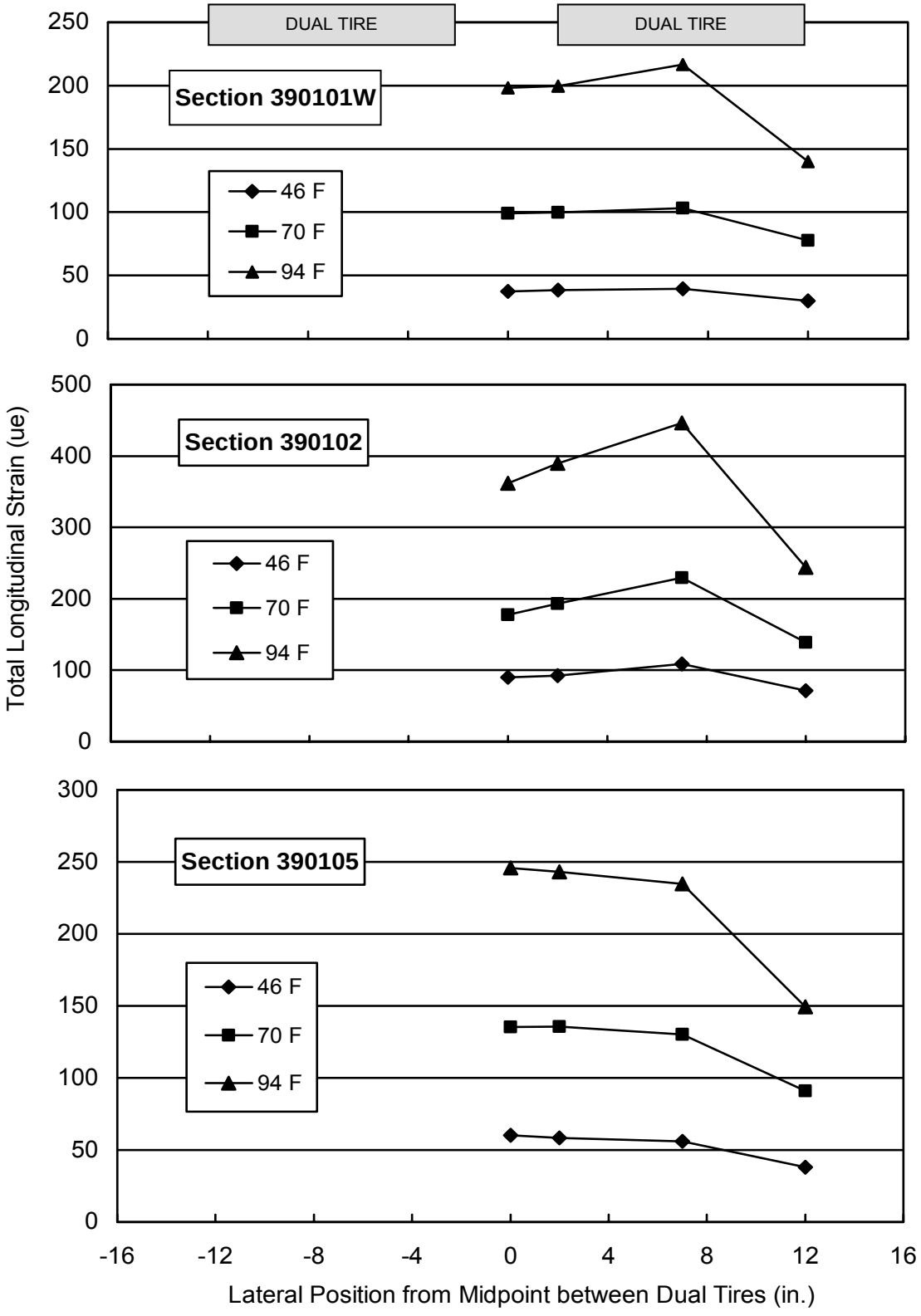

Figure 3.5 - Strain vs. Lateral Offset – Pad A; Load = 9000 lbs., Speed = 5 mph

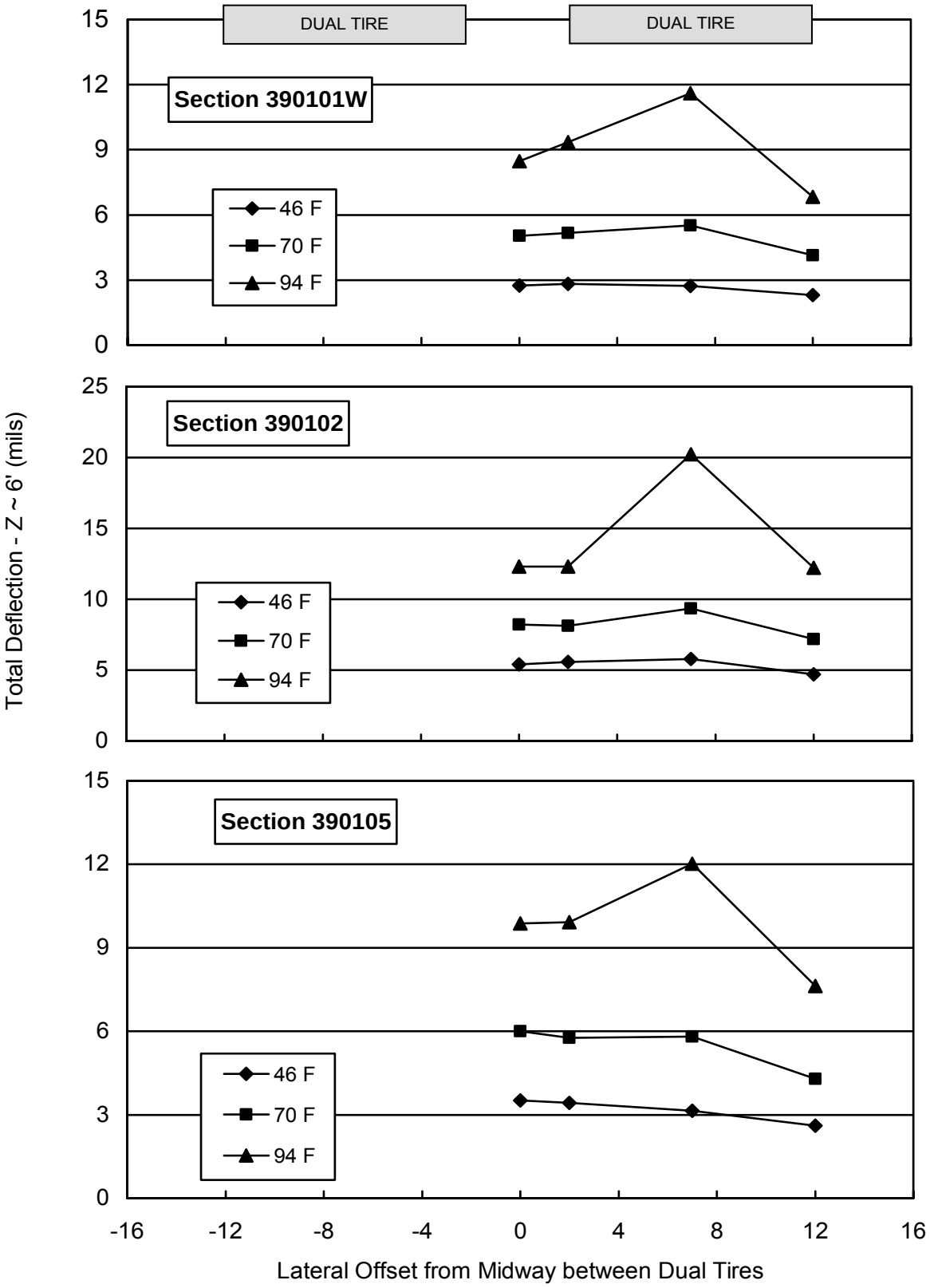

Figure 3.6 - Deflection vs. Lateral Offset – Pad A; Load = 9000 lbs., Speed = 5 mph

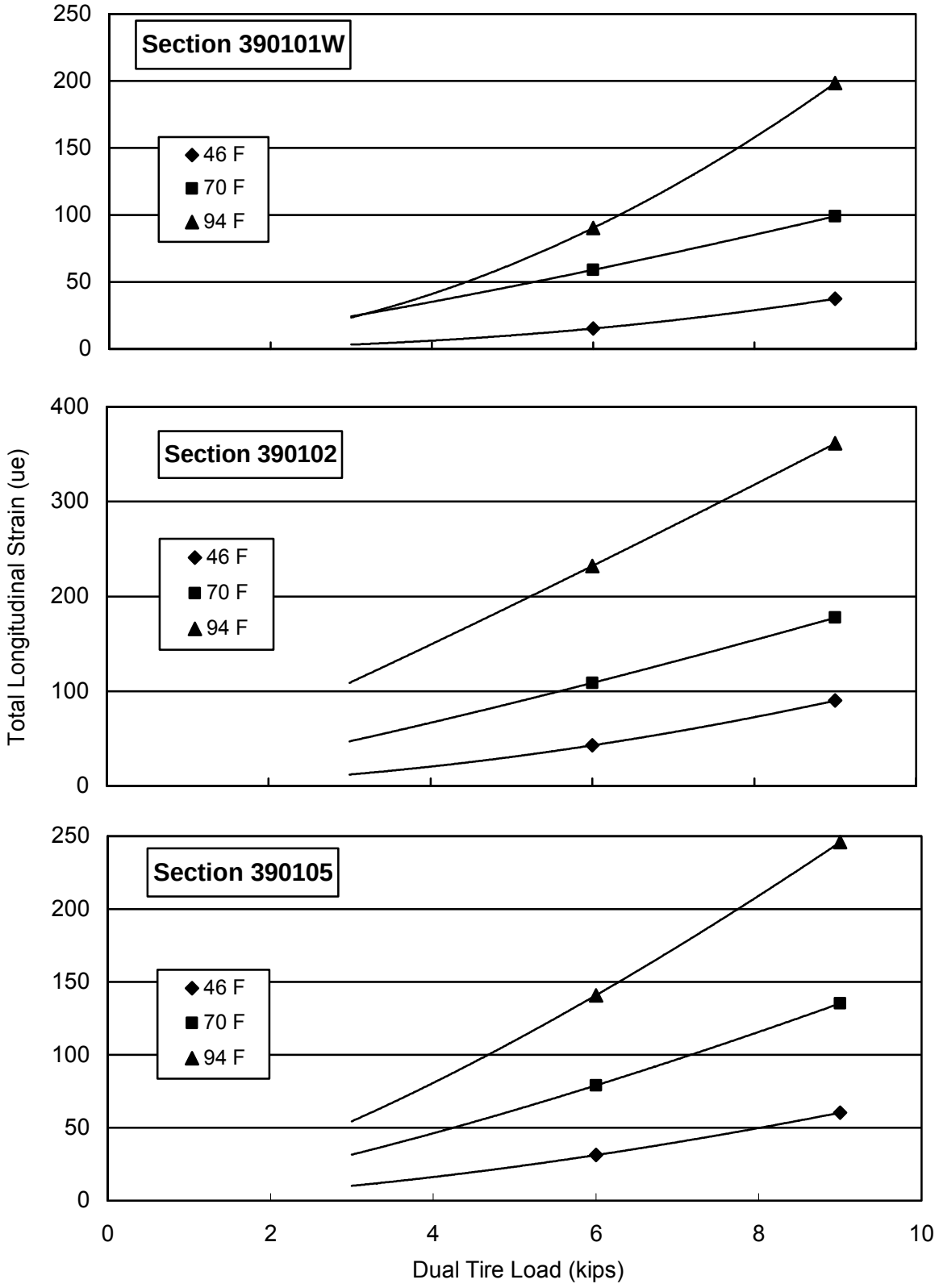

Figure 3.7 - Strain vs. Load – Pad A; Speed = 5 mph, Lateral Offset = 0 in.

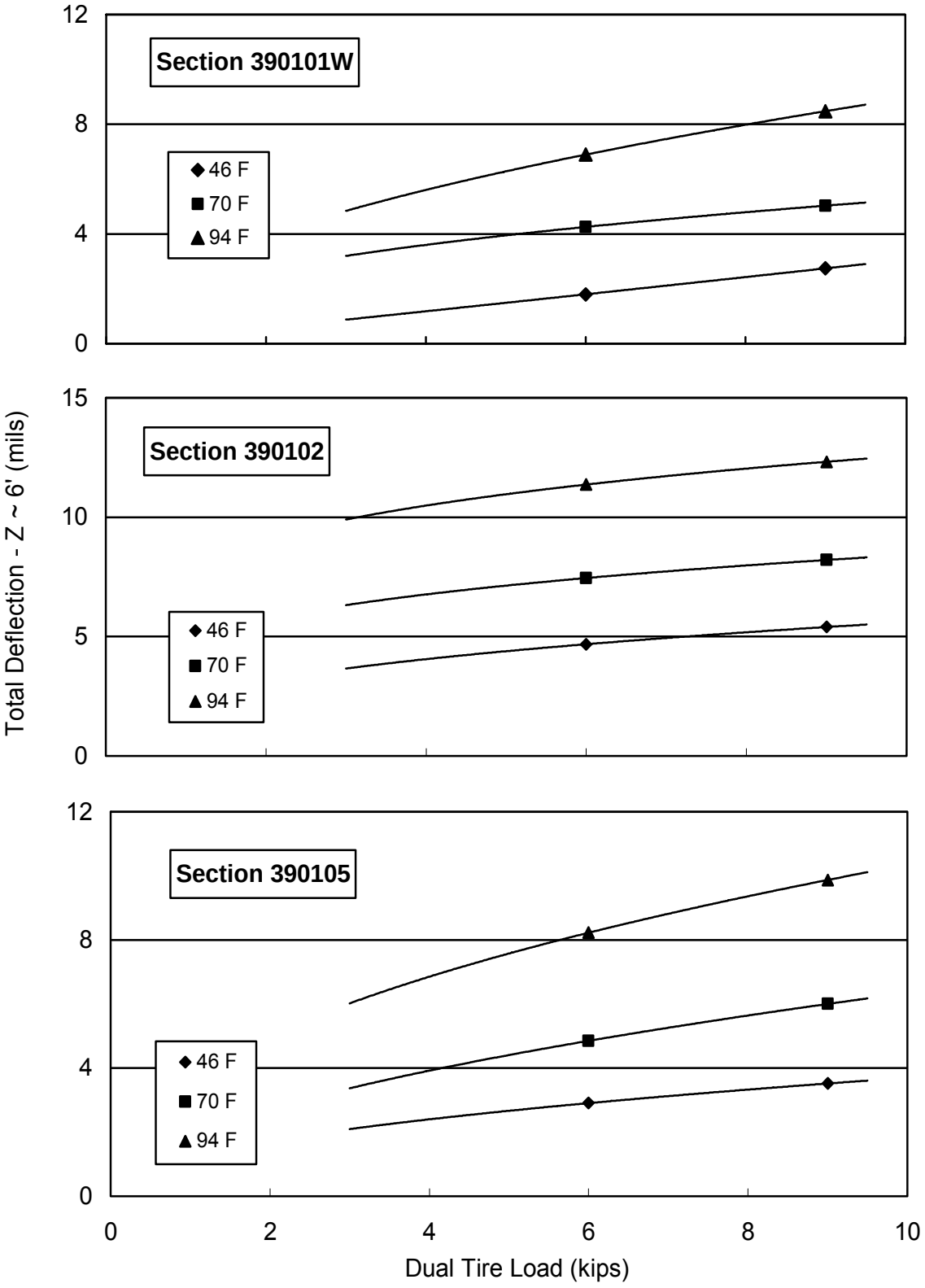

Figure 3.8 - Deflection vs. Load – Pad A; Speed = 5 mph, Lateral Offset = 0 in.

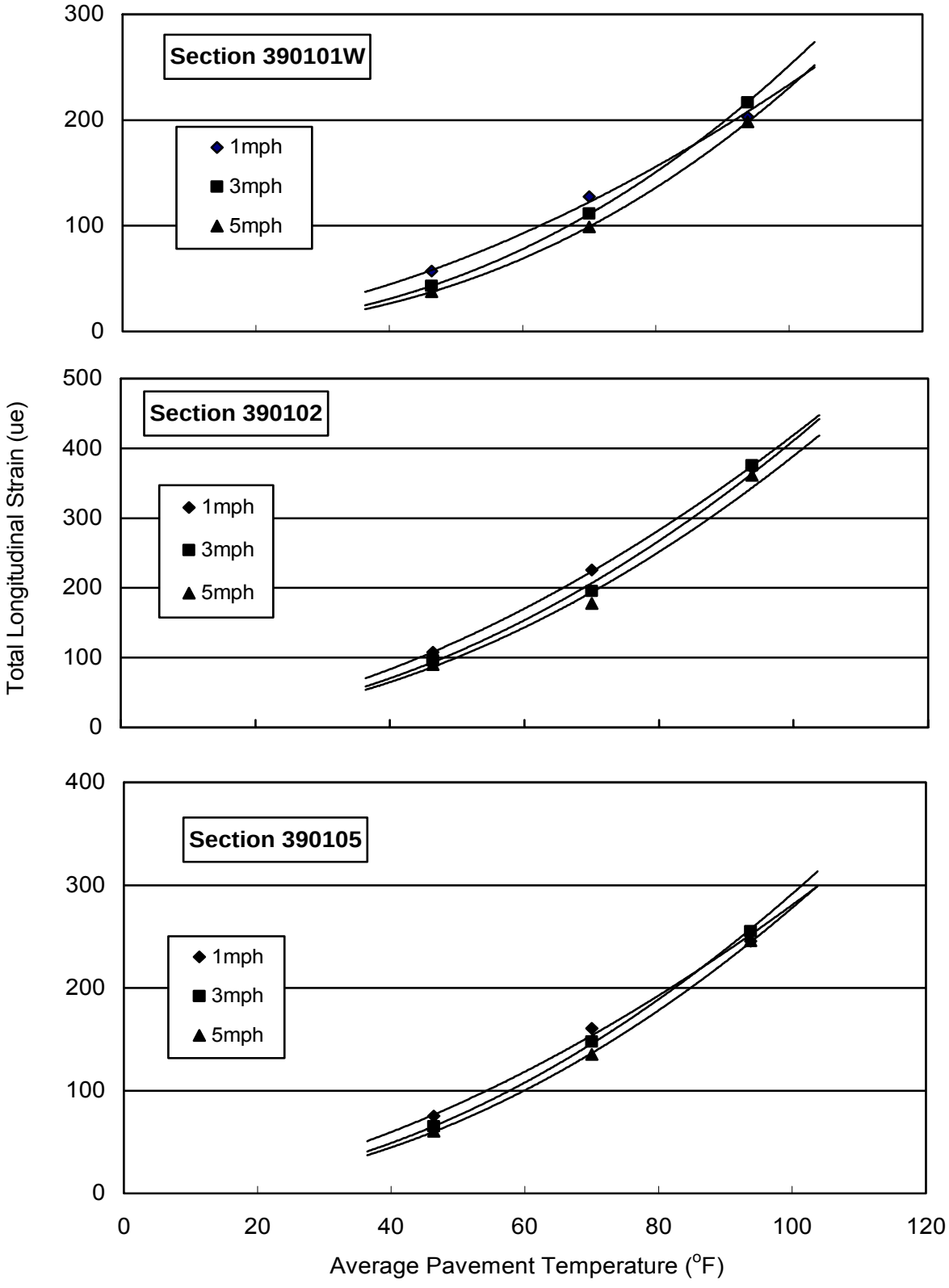

Figure 3.9 - Strain vs. Temperature – Pad A; Load = 9000 lbs., Lateral Offset = 0 in.

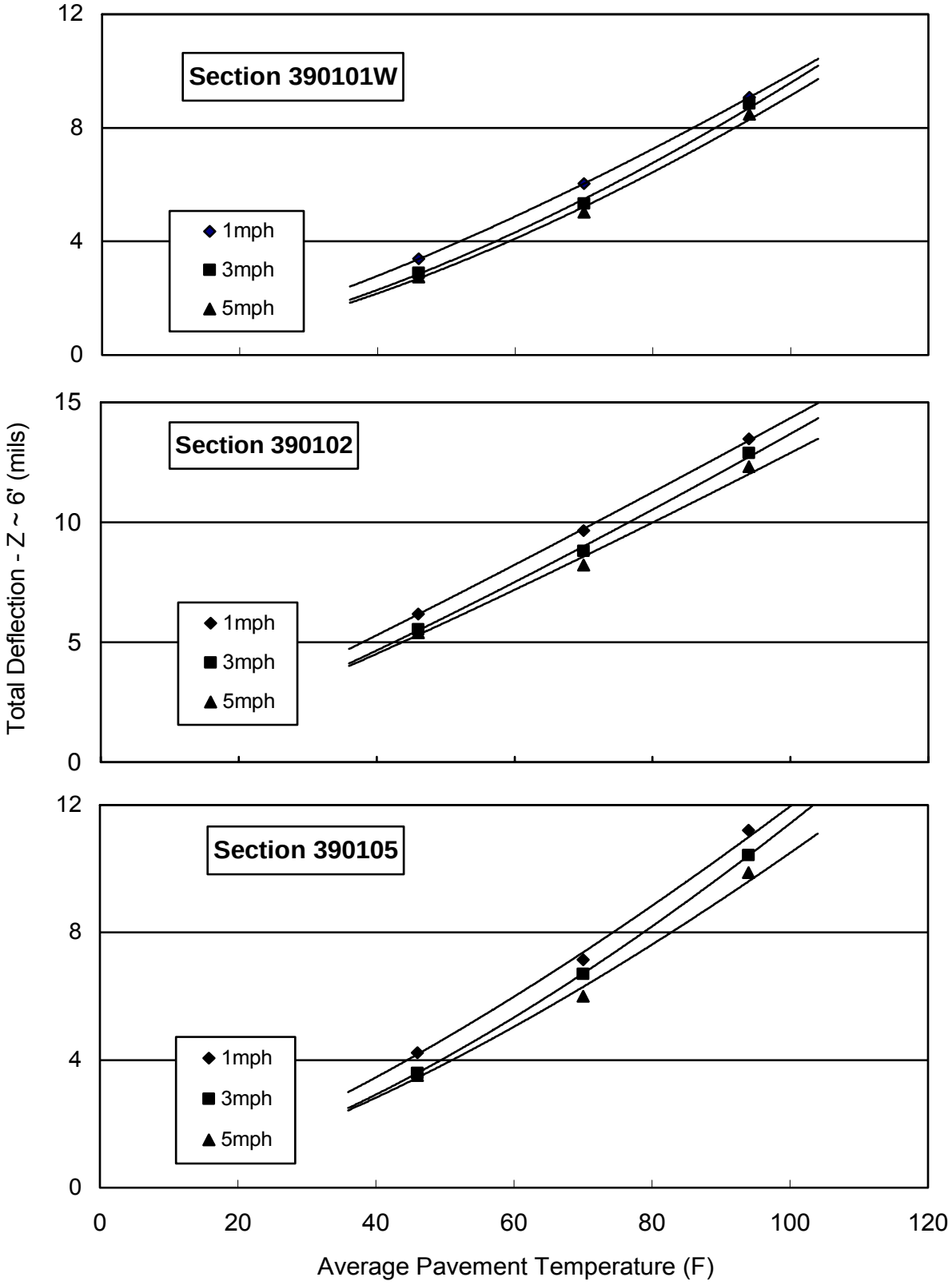

Figure 3.10 - Deflection vs. Temperature – Pad A; Load = 9000 lbs., Lateral Offset = 0 in.

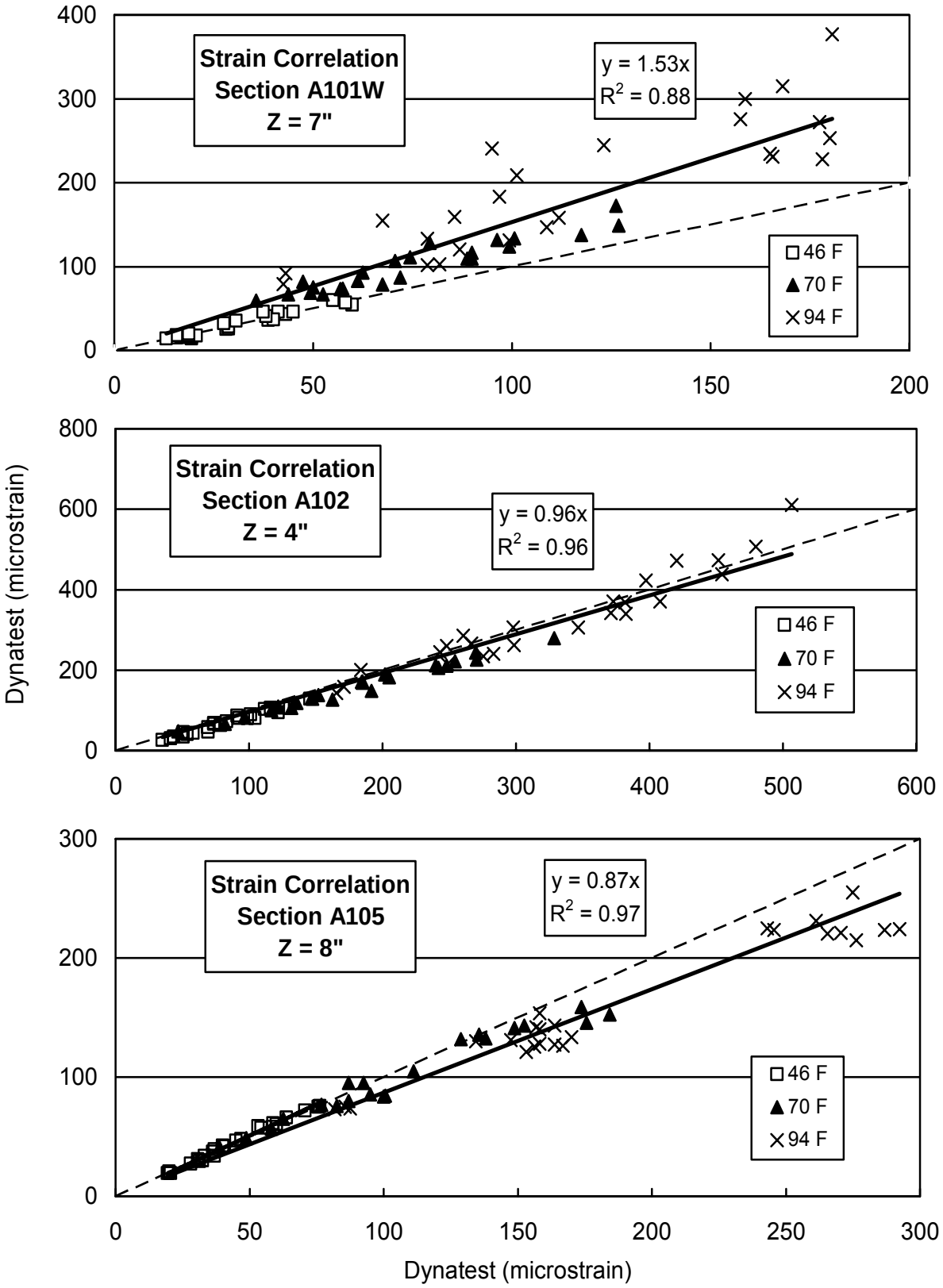

Figure 3.11 – Correlation of Redundant Strain Gauges – Pad A

Performance - Pad A

To measure performance on the four SPS sections in the APLF, the five test lanes were each divided into two 22.5 feet (6.9 m) long subsections and identified as either N or S for the north or south ends of the lanes. This resulted in ten subsections being available for performance testing. Tentative matrices in Table 3.5 were established to measure the rates of rutting over a range of environmental and loading conditions at the original subgrade moisture content (Pad A) and after water had been added to the subgrade (Pad B). The shorter section length limited wheel speed in the APLF to 3 mph (4.8 km/hr), as compared to the normal test speed of 5 mph (8.0 km/hr) when the wheel travels the entire 45-foot (13.7 m) lane length. This reduction in wheel speed was to prevent the braking system from overheating.

Table 3.5

Performance Matrices for SPS Testing in the APLF

Pad A – Original Subgrade Moisture				Pad B – Increased Subgrade Moisture			
Section	Temp.	Load	Wander	Section	Temp.	Load	Wander
A102S	70	9	None	B105S	70	9	None
A102N	70	12	None	B102S	70	9	None
A105S	70	9	None	B107S	70	9	None
A105N	70	15	None	B107N	70	12	None
A107S	70	9	None	B101WN	70	15	None
A101ES	70	9	None	B101WS	70	9	None
A107N	85	9	None	B102N	85	9	None
A101EN	104	9	None	B105N	104	9	None
A101WS	104	12	None	B101ES	104	15	None
A101WN	104	12	Random	B101EN	104	15	Random

Because of the rapid distress observed in these four SPS sections on the test road, unidirectional 9 kip (4.1 Mg) loading at 70º F (21.1º C) was selected for the initial test to avoid failure after only a few loads. If there was an early failure, the matrix would be altered to allow more load repetitions. Three temperatures, three loads and two levels of subgrade moisture were included in the matrix to develop performance trends for these variables on the Ohio SHRP Test Road. Actual pavement temperature, vehicle load and subgrade moisture histories observed during the time the four sections remained in service on the test road would be compared to trends developed in the APLF.

Pavement rutting was monitored periodically during the performance tests with a laser profilometer. To maintain a relatively constant horizontal position and vertical elevation for the profilometer throughout each performance test, large flat fender washers were epoxied to the pavement surface as references for the profilometer feet to sit on. Each profile measured on a pavement section spanned the entire six-foot (1.8 m) lane width at one millimeter intervals, and the average profile was comprised of the average of nine runs comprising three redundant profiles recorded at each of three locations. Any invalid profiles were eliminated from the computation. The dual tires were each 10 inches (25.4 cm) wide and separated by four inches (10.2 cm). To avoid tire edge effects, the average elevation of the center eight inches (21.0 cm) of each tire was calculated and both tires were then averaged together for an average elevation. To eliminate some inconsistencies that continued to occur between measurements, a 200 mm length of relatively flat profile outside the load affected area was used as a reference for each run. Average rut depth was then calculated as the change in elevation between this reference length and the average elevation of the two tires.

Performance testing was initiated on July 16, 2002 in Section A102S at a load of 9 kips and a temperature of 70º F (21.1º C). After the application of 6000 load cycles (12 hours), very little rutting was observed, thereby alleviating concern that the sections might fail too rapidly. However, the concern then became the length of time necessary to achieve the desired ½“ (13 mm) rut depth. One option was to use bidirectional loading instead of unidirectional loading which would effectively double the number of loads applied per hour, but there was no experience as to indicate whether rutting progressed at the same rate for both testing modes. To examine the effects of unidirectional and bidirectional loading, a series of tests was run at the interface of Lanes A101E and A101W. These sections were constructed the same and the interface was outside the path set aside for performance testing. The loading consisted of 2500 load cycles applied at 70º F (21.1º C), 2500 load cycles applied at 85º F (29.4º C) and 2000 load cycles applied at 104º F (40º C). Figure 3.12 shows rut depths measured during these tests.

The data in Figure 3.12 show little systematic difference in rut development for unidirectional and bidirectional testing. Larger ruts measured during the 70º F (21.1º C) runs did not get progressively larger with increasing cycles or temperature. The decrease noted for both

types of loading between 3500 and 5000 cycles was probably due to a glitch in the rut measurements. Each gridline on the vertical axis represents one millimeter of rutting. Based upon the results of these tests, all subsequent performance tests were conducted in the bidirectional mode.

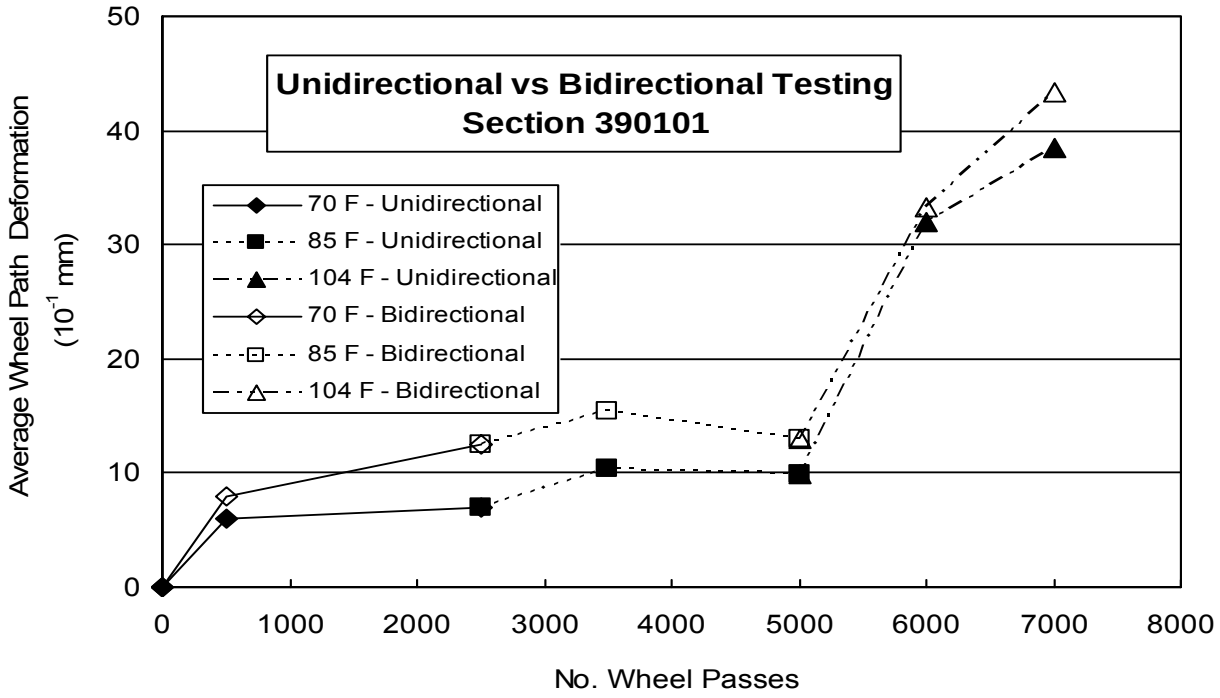

Figure 3.12 – Rut Depths for Unidirectional vs. Bidirectional Loading

Performance testing continued on Section A102S after conclusion of the unidirectional/bidirectional testing. Figure 3.13 shows how surface elevations measured under the test tires and over the reference strip changed as loads were applied to Section A102S, and why the use of a reference strip was necessary to calculate rut depth. While washers were used to minimize profile variations, the washers were not mounted exactly flat and the profilometer was not necessarily located at the same position on the washers during each set of measurements. Therefore, average rut depth was calculated by subtracting the measured elevation of the reference strip from the average measured elevation under the two test tires. Maximum rut depth was estimated from measured profiles, such as those in Figure 3.13, by adding the difference in elevation between the deepest points in the profile and the average elevation under the tires to the calculated average rut depth.

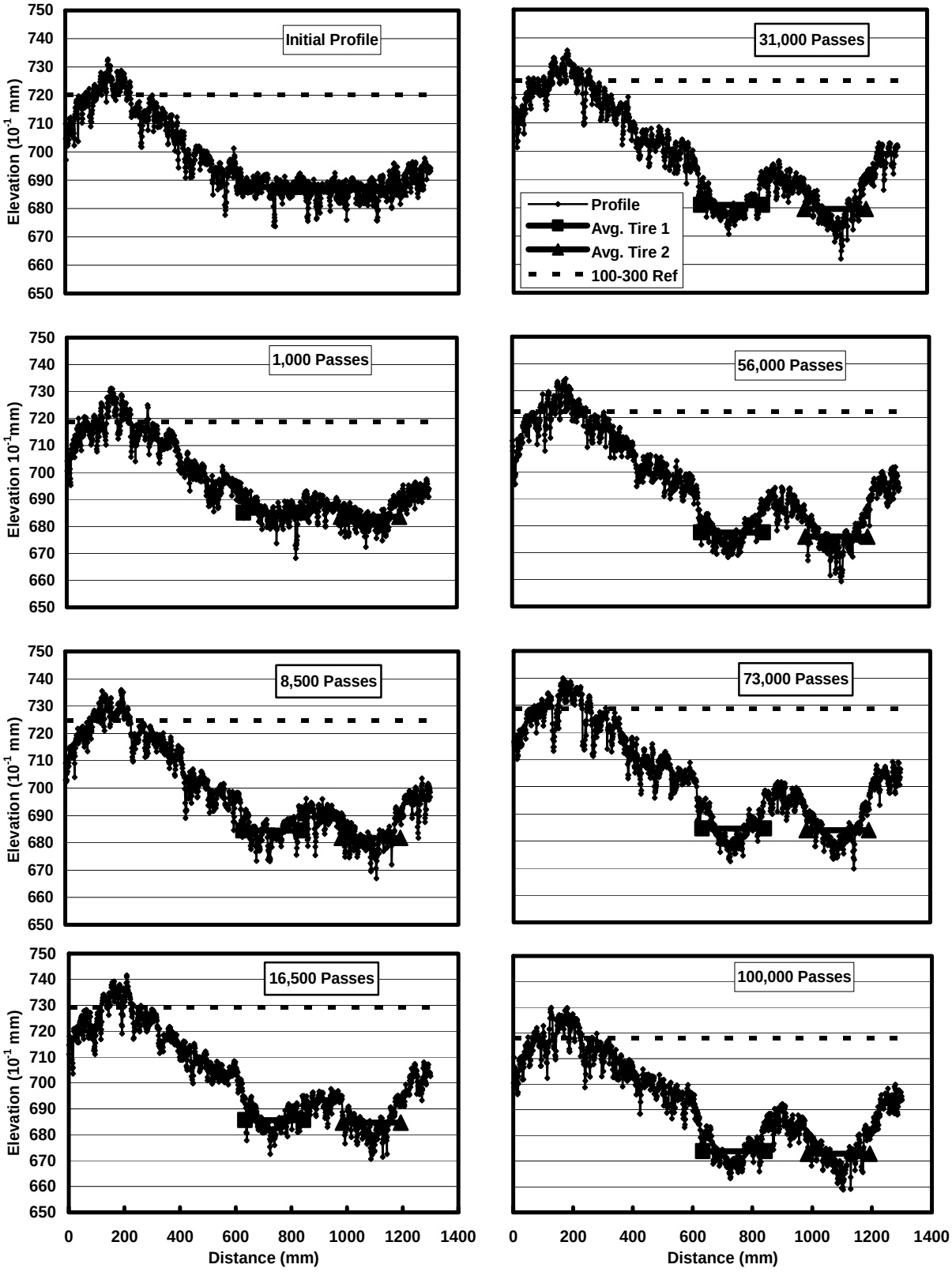

Figure 3.13 – Rutting on Section A102S; 9 kips, 70º F

Units on the y-axis are 10^{-1} mm making each gridline equal to one millimeter and the total deformation of the pavement surface about two millimeters after 100,000 load cycles. As a result of the minimal rutting observed during the early tests, it became obvious that the SPS sections constructed in the APLF were not going to rut as quickly as they did on the test road. This was due, no doubt, to the difference in subgrade stiffness at the two sites. Once Pad A was completed and water was added to the subgrade, rutting on Pad B was expected to be more indicative of that observed on the test road.

Figure 3.14 shows how surface elevations in Section A102S changed with the number of applied wheel loads and how, by subtracting the reference elevation between 100 and 300 mm from the wheel path elevation, the net change in wheel path elevation continued to increase positively with applied loads. Apparent fluctuations in the elevation of the reference washers over time was the reason rut depths were based on the reference and not on an assumed constant elevation of the washers epoxied to the pavement surface. Figure 3.15 shows how the use of semi-log plots provided a linear relationship between number of loads and rut depth in Section A102S. As expected, slopes of the logarithmic Excel trendlines increased with higher temperature and load, as shown in Figure 3.16. In these equations, the number of wheel passes (x) is expressed in thousands and the calculated average rut depth is in tenths of a millimeter. Data shown for Section A101WN should be viewed cautiously because of a hydraulic oil leak at 3000 cycles which may have softened the asphalt surface. Approximately three gallons (14 l) of oil misted over the 22.5-foot (6.9 m) long section length for a few minutes before the leak was detected. Testing was resumed on Section A101WN after the oil was cleaned up.

The coefficient of the Ln(x) term represents the slope of the trendline and the constant is the intercept of the trendline at 1000 wheel passes (or 1 on the graph). In general, these lines intercept the x-axis somewhere between 0.01 ($x10^3$) and 0.1 ($x10^3$) wheel passes for zero rut depth, indicating that a slight curvature in wheel passes vs. rut depth probably occurred during the first few passes since the intercept would be expected to be around .001 ($x10^3$) passes. The natural log trendlines provided by Excel can be converted to common logs by dividing the coefficient of the Ln(x) term by $\log_{10}$ (e) or 0.43429, changing Ln to log, and multiplying units along the x-axis (0.1, 1, 10 and 100) by 1000.

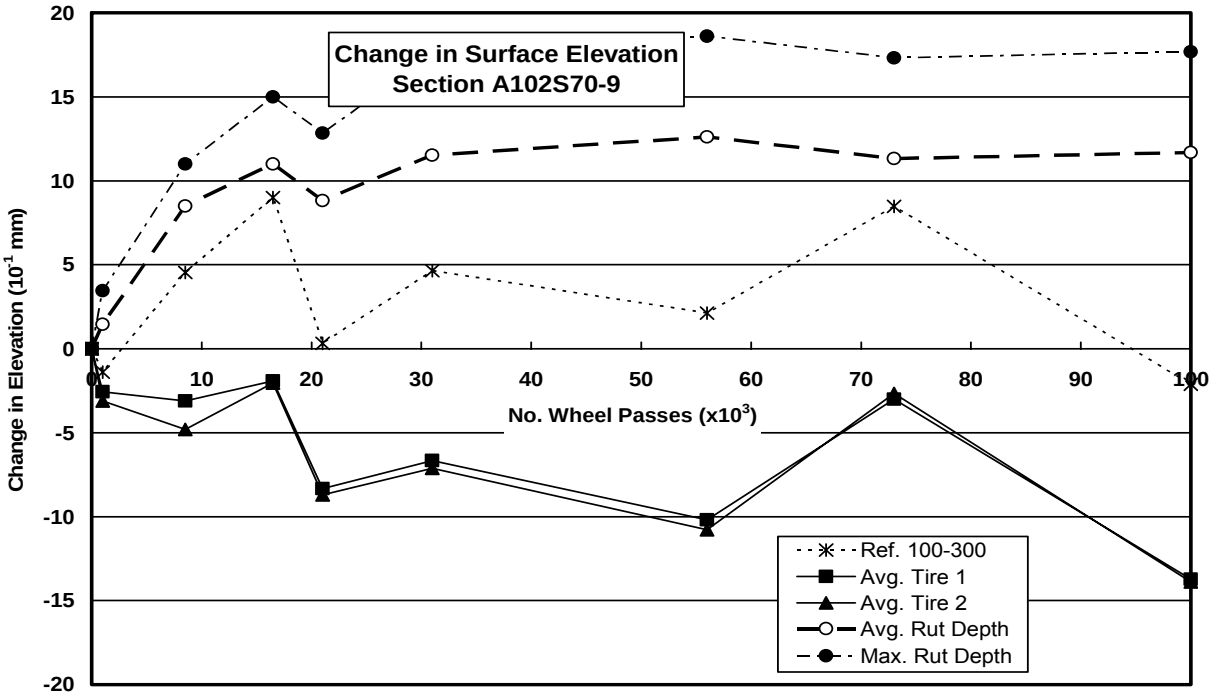

Figure 3.14 – Profile Calculations on Section A102S

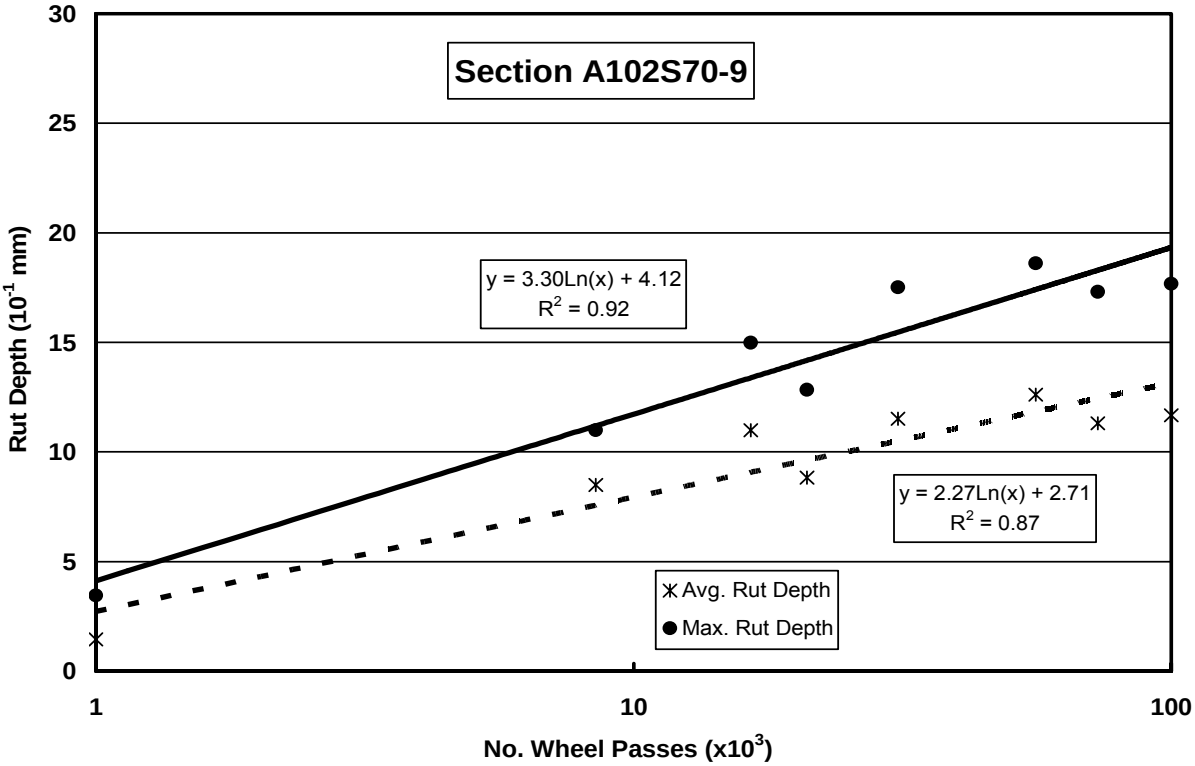

Figure 3.15 – Semi-Log Correlation of Deformation and Wheel Passes on Section A102S

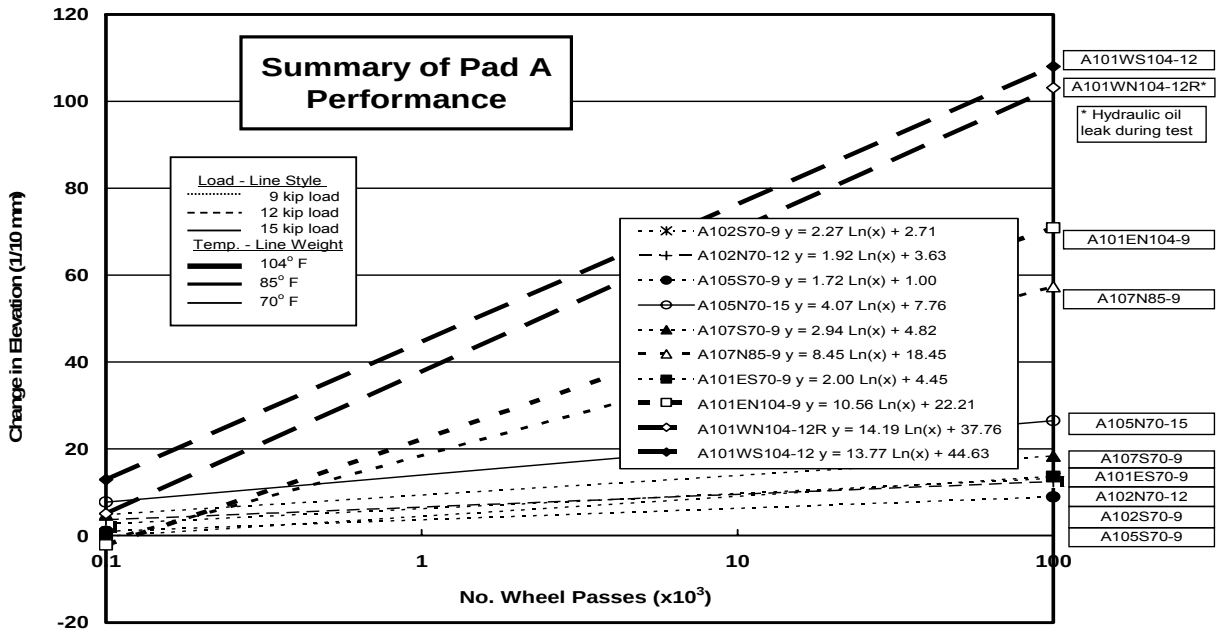

Figure 3.16 – Deformation Slopes on Pad A

The slopes of the initial best-fit trendlines calculated on Pad A can be used to estimate the effects on structural build-up, temperature and load on the rate of rutting. One subsection of each of the four sections was tested at 70º F and a 9 K wheel load. The rutting slopes for these tests were 2.00, 2.27, 1.72 and 2.94 for Sections 101ES, 102S, 105S and 107S, respectively, which tended to follow the order of the structural numbers calculated for these sections in a reverse order (3.57, 3.08, 3.36 and 2.52). That is, the weaker sections rutted faster than the more robust sections. Sections 101 and 107 had 9 K tests performed at two different temperatures. Rutting slopes on Section 101 were 2.00 at 70º F and 10.6 at 104º F, giving an acceleration factor of 5.3 for this increase in temperature. Rutting slopes on Section 107 were 2.94 at 70º F and 8.45 at 85º F, giving an acceleration factor of 2.87 for this increase in temperature. Sections 101, 102 and 105 had tests performed at the same temperature, but different loads. Tests run on Section 101 at 104º F had slopes of 10.6 at 9 K and 13.8 at 12 K loads, giving an acceleration factor of 1.30. Tests run on Section 102 at 70º F had slopes of 2.27 at 9 K and 1.92 at 12 K loads, giving an acceleration factor of 0.85, which is not reasonable. Tests run on Section 105 at 70º F had slopes of 1.72 at 9 K and 4.07 at 15 K loads, giving an acceleration factor of 2.37. Since rutting rates vary with pavement build-up, AC temperature, wheel loading and, probably subgrade stiffness, in multilayered AC pavement structures, all of these variables must be taken into consideration when calculating acceleration factors. Rutting plots for Pad A are shown in Appendix C.

Repeat of Response Tests – Pad A

At the conclusion of performance testing on Pad A, the original work plan called for the removal of that distressed pad and the construction of a second pad identical to it. Because of the excessive amount of time spent on the performance testing of the original pad and because of the minimal distress observed during these tests, the research team thought it might be prudent to not remove the pad, but add water and proceed on the same pad with a wetter subgrade. This decision would eliminate the need to account for any differences that might occur between Pads A and B. A set of response tests was rerun at a nominal air temperature of 104º F (40º C) to compare section stiffness before and after the performance testing.

Figure 3.17 shows how responses compared before and after testing at approximately 104º F (40º C). While Section 101W had higher responses during the second set of measurements, Sections 102 and 105 had mixed results. Because there were no consistent trends in all sections to indicate that the testing completed on Pad A might have caused some systematic structural deterioration, it was decided to proceed with the second round of tests on this pad after water was added to the subgrade. These data are summarized in Appendix D. Table 3.6 summarizes all tests conducted on Pad A.

Table 3.6
Summary of Events on Pad A

Section	Load (kips)	Speed (mph)	Temperature (° F)	Wander (in.)	Test Date(s)	No. Cycles
All	FWD		70		5/9/02	
Response Tests	6, 9	5	40, 70, 104	0, 2, 7, 12	7/1-12/02	
Rutting 102S	9	3	70	None	7/16–9/13/02	100,000
Uni. vs. Bi. Tests	9	3	70	None	7/22-30/02	12,000
Rutting 102N	12	3	70	None	9/16–10/31/02	100,000
Rutting 105S	9	3	70	None	11/20/02–1/24/03	100,000
Rutting 105N	15	3	70	None	1/28–2/27/03	73,500
Rutting 107S	9	3	70	None	2/28–4/10/03	77,500
Rutting 101ES	9	3	70	None	4/15–6/4/03	77,000
Rutting 107N	9	3	85	None	6/13-20/03	20,000
Rutting 101EN	9	3	104	None	6/26–30/03	10,000
Rutting 101WS	12	3	104	None	6/30–7/1/03	9,000
Rutting 101WN	12	3	104	Random	7/2–12/03	12,000
Response Tests	6, 9	5	104	0, 2, 7, 12	7/14/03	
					Total Pad A	591,000

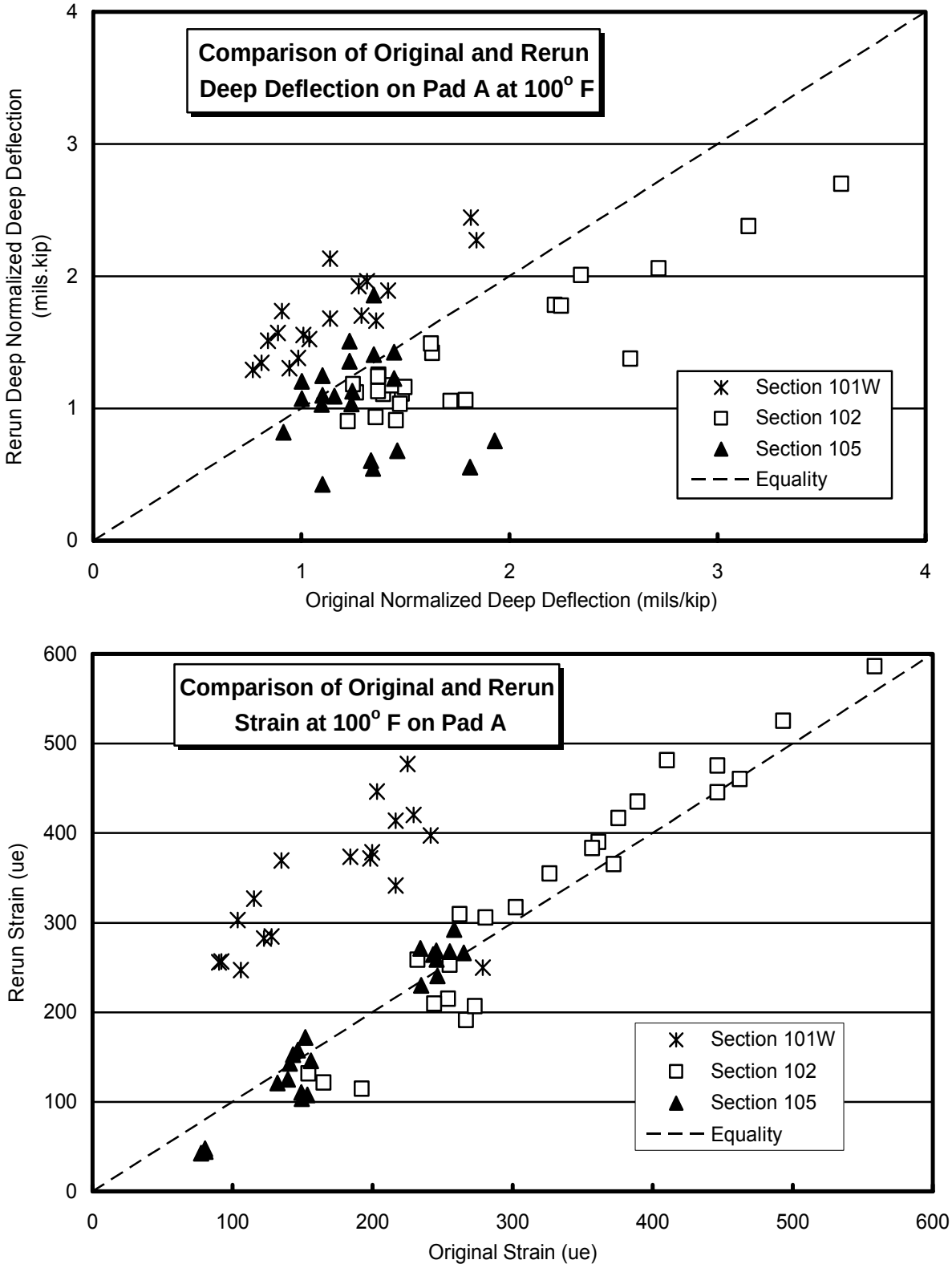

Figure 3.17 – Comparison of Original and Rerun Responses on Pad A at 104º F

Temperature Conditions – Pad A

Figure 3.18 compares temperature profiles measured down to a depth of 8.0 – 8.5 inches (20.3-21.6 cm) below the pavement surface during response testing in the APLF and on the test road. While no direct thermocouple measurements were recorded in the APLF during the 5/9/02 FWD testing, the FWD operator used an infrared sensor to measure the surface temperature. Since the test chamber was maintained at a constant 70º F (21.1º C) temperature for several days prior to FWD testing, and since the surface temperature of the pavements did not change during the testing, the pavement temperature was assumed to be a uniform 70º F (21.1º C) during the FWD tests. As shown in Figure 3.18, this assumption was consistent with temperatures measured in the APLF on 7/1/02 during the 70º F (21.1º C) rolling wheel tests. Average pavement temperatures obtained during the 6/11/96 FWD tests on the test road were only slightly higher. These three data sets can be compared with little effect from pavement temperature.

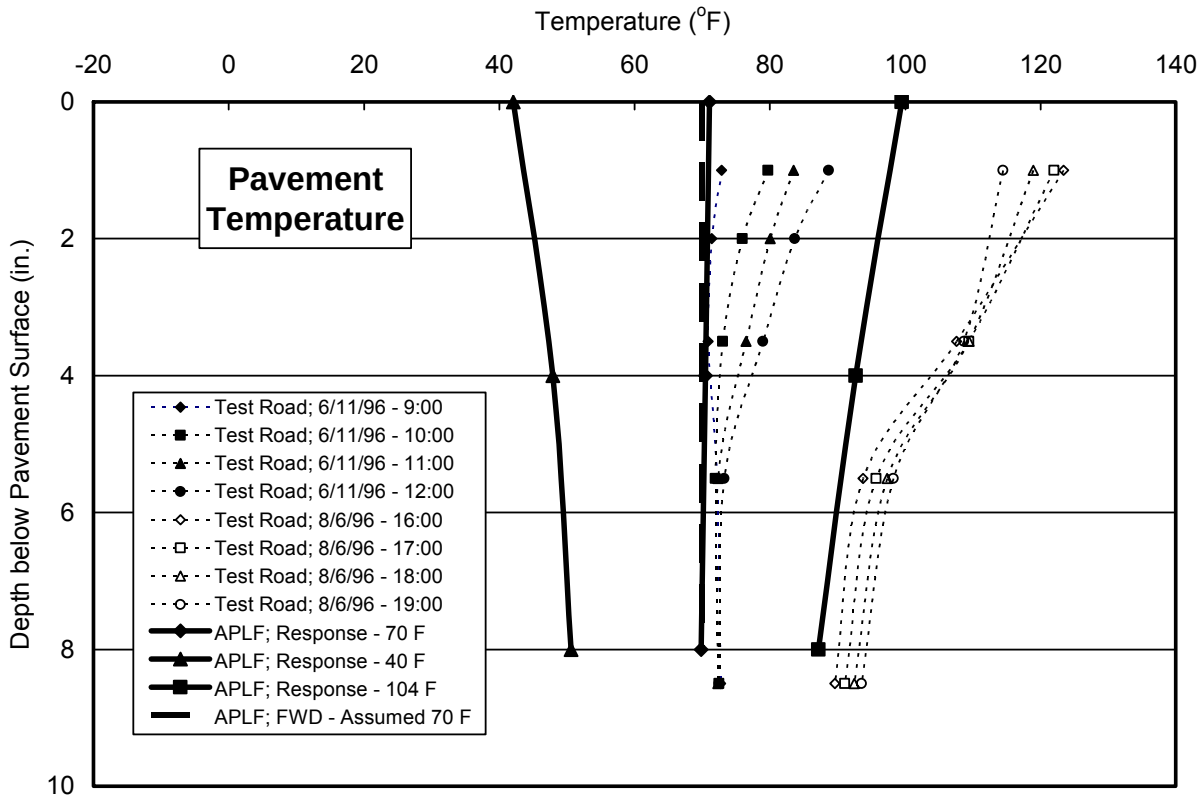

Figure 3.18 – Pavement Temperature on Test Road and in the APLF

Moisture Conditions – Pad A

Since base and pavement materials were designed to be similar in the APLF and on the test road, much of the difference between dynamic responses measured at the two facilities can be attributed to differences in pavement temperature and/or subgrade stiffness. Moisture in the APLF subgrade was unchanged since it was placed during construction of the facility in 1997, while subgrade moisture on the test road likely increased during the 1995-96 winter season and after placement of the base and pavement layers in the spring of 1996.

Figure 3.19 shows volumetric moisture measured with TDRs on the test road on July 25-26, 1996, which fell between the FWD measurements on June 11 and the controlled vehicle tests on August 6. Section 390107, which did not contain environmental instrumentation, was located between Sections 390101 and 390102, and Section 390108 was adjacent to Section 390105, which also did not contain environmental instrumentation. Also shown in Figure 3.19 is the average volumetric moisture measured in the APLF subgrade. Subgrade moisture remained constant during the FWD and response measurements on Pad A in the APLF.

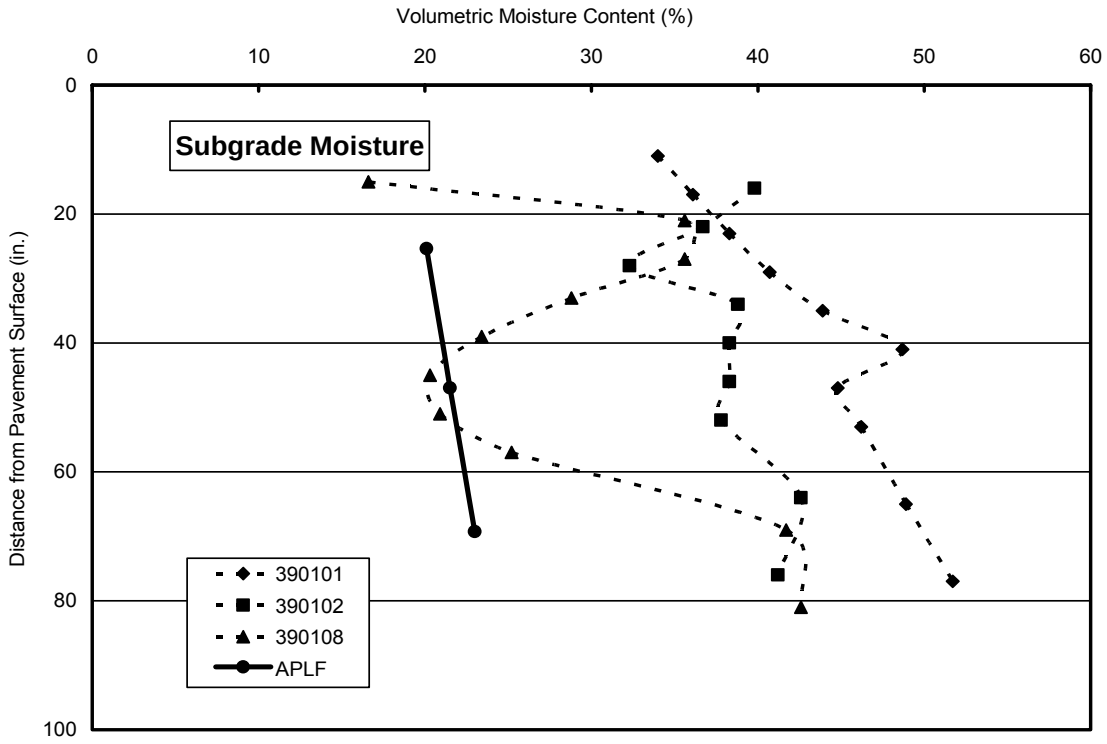

Figure 3.19 – Subgrade Moisture on Test Road and in the APLF

Pad B – General

The eight-foot (2.4 m) deep APLF test pit was designed with rows of 4-inch (10.2 cm) diameter slotted plastic drainage pipes in the bottom for excess water to be removed and rows of 2-inch (5.1 cm) diameter supply pipes above the drainage pipes for water to be added to the pit. No. 57 crushed limestone was added to a depth of approximately 12 inches (30.5 cm) above the bottom of the pit to cover the pipes and provide drainage for subgrade placed on the #57 aggregate. Fabric was placed over the aggregate to retard contamination from the subgrade. Vertical standpipes were installed on both sides of the pit to monitor the water table, and three time-domain reflectometry (TDR) probes were installed at different depths on two sides of the pit to monitor volumetric moisture in the subgrade. Water was to be added to the pit by opening the supply line until water stabilized approximately three feet from the pavement surface. At this level, water would be assumed to fill the #57 aggregate and infiltrate four feet into the subgrade. Capillary action might raise the water level even higher in the fine-grained A-6 subgrade. Figure 3.20 shows increased moisture measured with TDRs after water was added to the subgrade. After about two weeks of maintaining a steady elevation of water in the stand pipes without adding water and having no change in TDR output, it was decided to proceed with testing on Pad B.

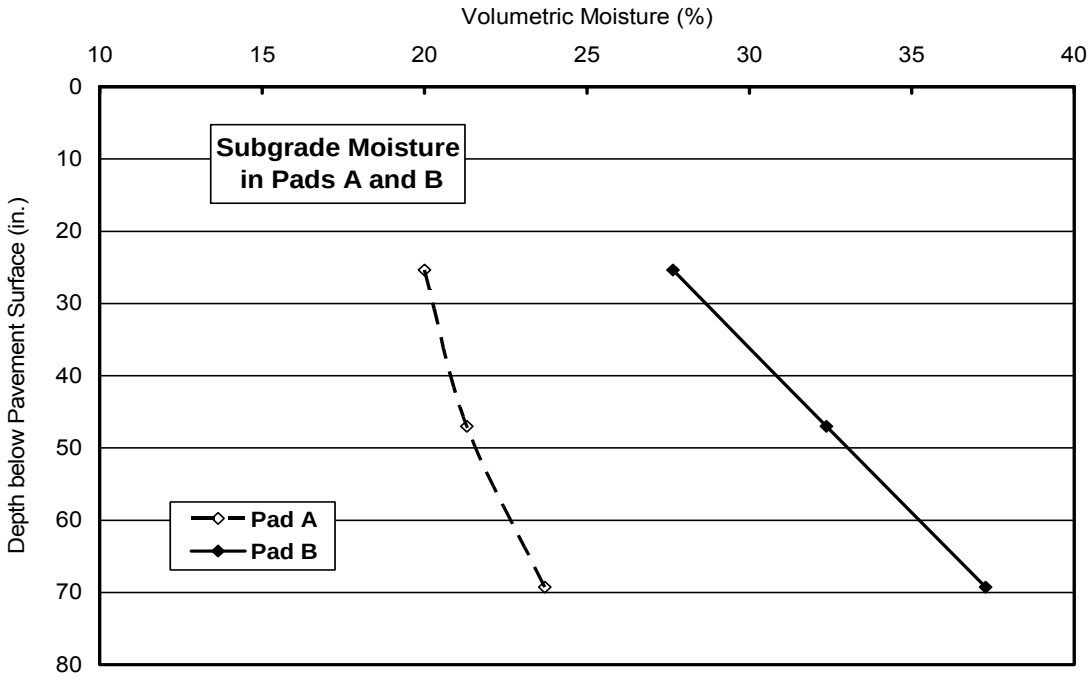

Figure 3.20 – Volumetric Moisture in Pads A and B

Rolling Wheel Response Tests – Pad B

A set of rolling wheel response measurements was performed on the three instrumented sections in Pad B at 70º F (21.1º C) to compare with the original responses measured on Pad A at the same temperature. Any differences in response could be attributed to changes in subgrade stiffness from the added moisture since no consistent changes in response were noted at the end of Pad A to indicate distress. Figure 3.21 shows a slight increase in deflection in Section 101W, a slight decrease in deflection in Section 102, no change in deflection in Sections 105, and some increased strain in all three sections. The responses on Pad B were expected to be much higher, raising concern about the amount of water that actually infiltrated the subgrade. Water in the stand pipes remained three feet below the pavement surface during these tests, indicating that the water table was stable at that elevation. Response data from Pad B are shown in Appendix E.

Performance – Pad B

Section 105S was the first section tested on Pad B. Since it was unknown how quickly ruts would develop after water had been added to the subgrade, testing was initiated again at 70º F (21.1º C) and 9,000 lbs (4.08 Mg). Adjustments would be made to the test matrix in accordance with the results of this test. If the subgrade was saturated up to a level of three feet (0.9 m) below the pavement surface, as expected, there was concern that the kneading action of the test wheel rolling back and forth on the pavement might cause subgrade moisture to migrate upward under the wheel load and accelerate the rutting. If this occurred, moisture readings monitored along the edge of the pit would not be indicative of actual moisture under the wheel during testing. To monitor subgrade moisture under the wheel, a TDR was placed in the centerline of Section 105S to monitor moisture at the top of the subgrade during the rutting tests.

A total of 25,000 load cycles were applied to Section 105S with little additional rutting being observed. With project time running out, it then became obvious that significant changes would have to be made in the test matrix. Load was increased to 12,000 lbs. (5.44 Mg) and another 10,000 cycles were run on this section, again with little effect. Load was increased to 15,000 lbs. (6.80 Mg) and another 10,000 cycles were applied. No change in moisture was detected by the extra TDR placed under the wheel path in Section 105S.

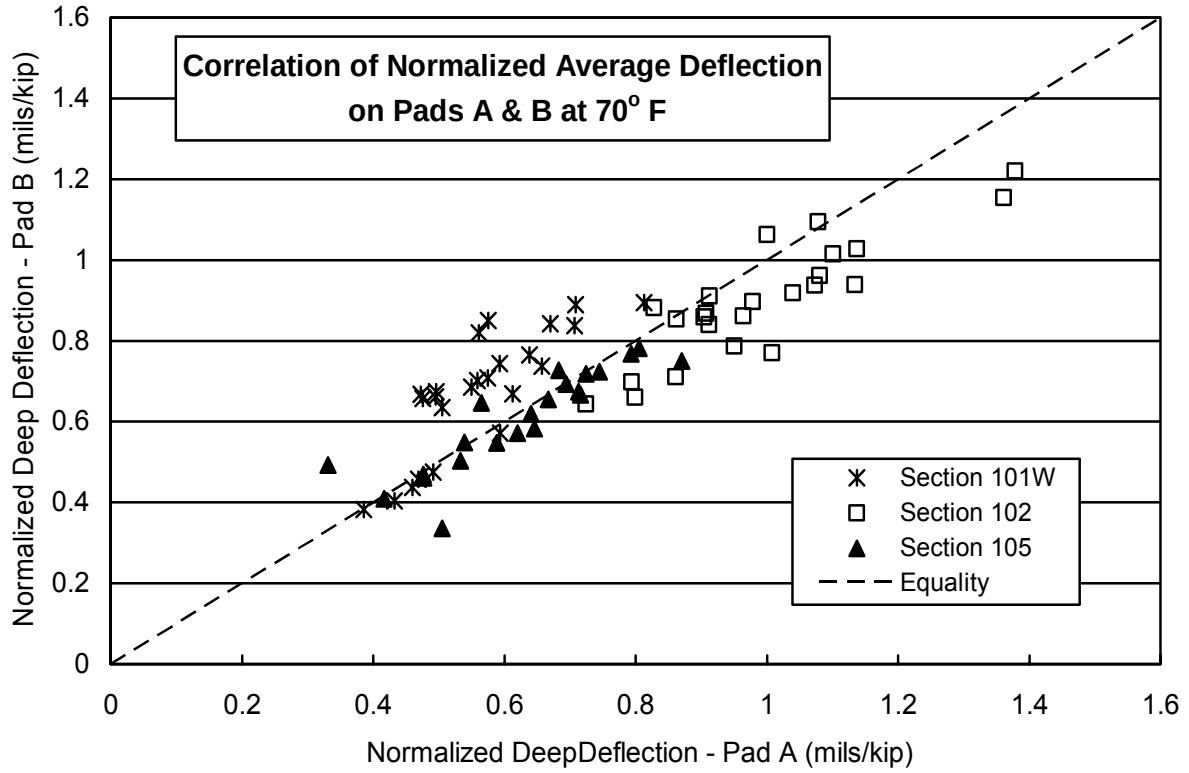

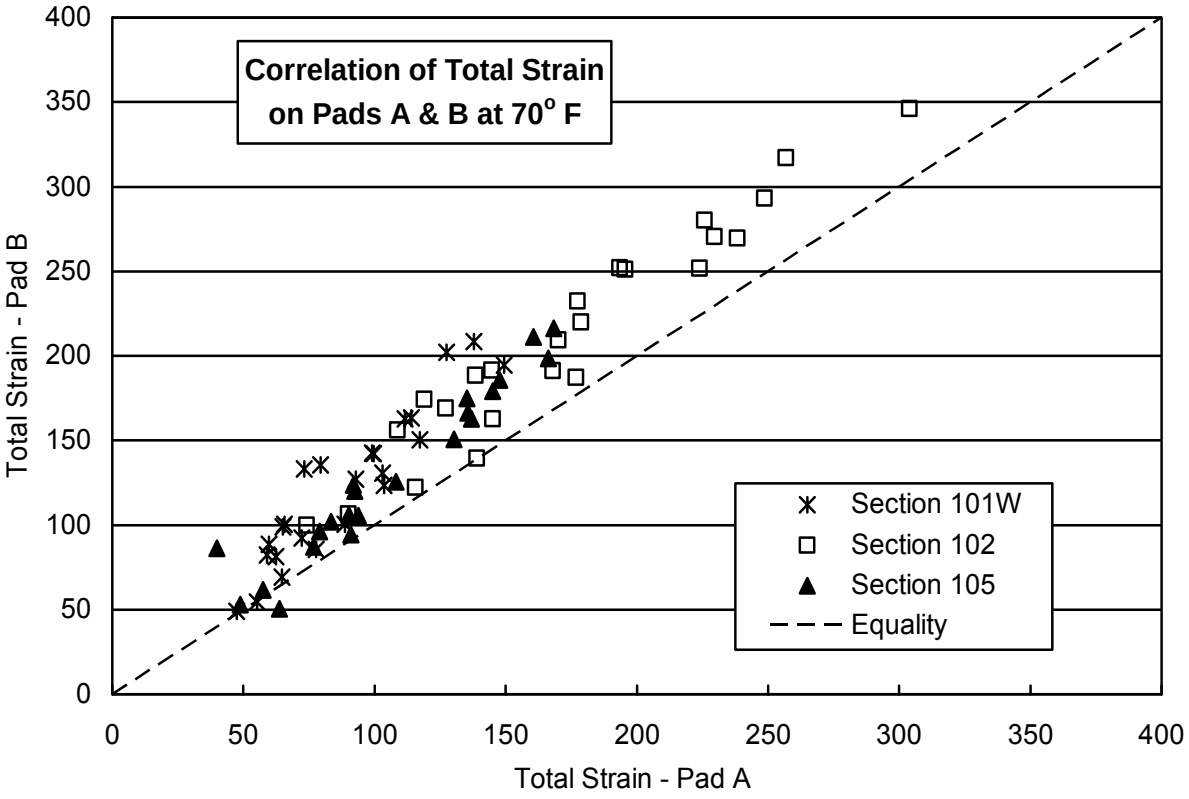

Figure 3.21 – Comparison of Responses on Pads A and B at 70º F

Attention was then directed to Section 107, which was the weakest of the four sections. While temperature was maintained at 70º F (21.1º C), 10,000 cycles were applied at 9,000 lbs. (4.089 Mg) and 5,100 cycles were applied at 12,000 lbs. (5.44 Mg), with only minimal additional rutting. To expedite the remainder of testing on Pad B, air temperature was raised to 104º F (40º C) and the entire 45-foot (13.7 m) long lanes were tested at 9,000 lbs. (4.089 Mg) and 15,000 lbs. (6.80 Mg). All previous tests on the 22.5-foot (6.9 m) long sections were conducted at 3 mph (4.8 km/hr), while tests over the entire 45-foot (13.7 m) lane lengths were conducted at 5 mph (8.0 km/hr). Test speed over the shorter distance was reduced automatically by the loading mechanism to prevent overheating of the braking system. Table 3.7 summarizes all testing activities on Pad B.

Table 3.7
Summary of Events on Pad B

Section	Load (kips)	Speed (mph)	Temperature (° F)	Wander (in.)	Test Date(s)	No. Cycles
Response Tests	6, 9	5	70	0, 2, 7, 12	7/31/03	
Rutting 105S	9	3	70	None	8/5-8/15/03	25,000
Rutting 105S	12	3	70	None	8/18-8/26/03	10,000
Rutting 105S	15	3	70	None	8/26-9/10/03	10,000
Rutting 107S	9	3	70	None	9/10–9/15/03	10,000
Rutting 107S	12	3	70	None	9/19–9/23/03	5,000
Rutting 107S	9	5	104	None	9/23–10/01/03	9,000
Rutting 107N	9	5	104	None	9/23–10/01/03	9,000
Rutting 107S	15	5	104	None	10/1–10/3/03	2,500
Rutting 107N	15	5	104	None	10/1–10/3/03	2,500
Rutting 105S	9	5	104	None	10/3–10/7/03	3,000
Rutting 105N	9	5	104	None	10/3–10/7/03	3,000
Rutting 105S	15	5	104	None	10/8–10/10/03	5,000
Rutting 105N	15	5	104	None	10/8–10/10/03	5,000
Rutting 102S	9	5	104	None	10/10-10/13/03	4,000
Rutting 102N	9	5	104	None	10/10-10/13/03	4,000
Rutting 102S	15	5	104	None	10/15-10/17/03	2,990
Rutting 102N	15	5	104	None	10/15-10/17/03	2,990
Rutting 101ES	9	5	104	None	10/17-10/22/03	4,000
Rutting 101EN	9	5	104	None	10/17-10/22/03	4,000
Rutting 101ES	15	5	104	None	10/23/03	3,000
Rutting 101EN	15	5	104	None	10/23/03	3,000
					Total Pad B	126,980

Rut depths were measured the same on Pad B as on Pad A. When the entire lane length was tested on Pad B, the north and south sections were monitored separately because of differences in the initial rut depth from previous tests. Table 3.8 summarizes all incremental rut depths measured on Pads A and B. If rut depths from different series of tests on Pad B were plotted continuously as wheel loads were applied, they would appear as shown in Figure 3.22 for Sections 101ES and 101EN. The individual trendlines on Pad B became much more useful when they were adjusted back to a position where they became a segment of a complete trendline that would have developed if those conditions had been maintained throughout the entire testing period. Once the Pad B trendlines were adjusted, they could be compared directly with each other and with Pad A trendlines to determine the effects of load, temperature and section design on rut development. The comparison with Pad A trendlines was possible here because subgrade stiffness was essentially the same for both pads.

To adjust the Pad B trendlines, it was first necessary to assume that the rate of rut growth measured under current conditions was not affected by conditions applied during earlier tests to generate the initial rut for the current test. In other words, rut growth is determined only by current test conditions and not by how the initial rut was formed. This seems reasonable, at least as a first order assumption. When a second or third test series was initiated on a section of pavement, therefore, the starting rut depth (Y0) was known from the previous test, but the number of wheel passes (X0) that would have been required to form that rut entirely under the new conditions was not known. A spreadsheet was set up to calculate this number of wheel passes through an iterative process by assuming some number of wheel passes, calculating the corresponding X1, X2, Y1 and Y2 coordinates from rut measurements obtained during the test series in question using the assumed X0, plotting these three (or more) points on a graph, calculating the best-fit trendline, and adjusting X0 until the trendline intersected the x-axis at a selected number of wheel passes. Since trendlines on Pad A tended to intersect the x-axis around X = 0.1 (100 passes), this same point was selected for the Pad B trendlines. Also, because the constant in the trendline equations was equal to Y at X = 1, and because the Ln of 0.1 is -2.30, the slope of the trendline equation (or coefficient of Ln(x)) times 2.30 should be equal to the constant when the trendline crosses the x-axis at X = 0.1. Figure 3.23 shows the adjusted trendlines for Section 101ES. Plots of trendlines for all sections are shown in Appendix F.

Table 3.8 – Incremental Rut Depths Measured in the APLF

Incremental Rut Measurements in APLF

Pad	101EN		101ES		101WN		101WS		102N		102S		105N		105S		107N		107S	
	No. Cycles (10^3)	Rut Depth (10^{-1} mm)	No. Cycles (10^3)	Rut Depth (10^{-1} mm)	No. Cycles (10^3)	Rut Depth (10^{-1} mm)	No. Cycles (10^3)	Rut Depth (10^{-1} mm)	No. Cycles (10^3)	Rut Depth (10^{-1} mm)	No. Cycles (10^3)	Rut Depth (10^{-1} mm)	No. Cycles (10^3)	Rut Depth (10^{-1} mm)	No. Cycles (10^3)	Rut Depth (10^{-1} mm)	No. Cycles (10^3)	Rut Depth (10^{-1} mm)	No. Cycles (10^3)	Rut Depth (10^{-1} mm)
	104° F, 9 kips		70° F, 9 kips		104° F, 12 kips		104° F, 12 kips		70° F, 12 kips		70° F, 9 kips		70° F, 15 kips		70° F, 9 kips		85° F, 9 kips		70° F, 9 kips	
	0.00	0	0.00	0	0.00	0	0.00	0	0.00	0	0.00	0	0.00	0	0.00	0	0.00	0	0.00	0
	0.10	2.06	0.10	1.56	0.10	8.51	0.10	16.06	0.10	-0.01	1.00	1.45	0.10	1.50	1.00	1.69	0.10	4.02	0.10	-0.11
	1.00	14.64	0.90	2.15	1.00	31.72	1.00	39.34	1.00	3.33	8.50	8.50	1.00	5.24	15.00	4.24	1.00	13.42	1.00	3.98
	4.00	34.91	21.00	8.54	4.50	56.93	2.00	51.83	12.00	6.78	16.50	10.99	5.00	11.77	44.00	7.01	2.00	19.16	9.00	7.70
A	10.00	51.87	44.00	12.72	9.50	72.07	6.55	73.81	28.75	9.57	21.00	8.83	10.00	15.19	75.00	8.09	14.00	41.60	33.00	14.11
			73.00	14.69	11.00	74.21	9.00	76.08	65.50	12.02	31.00	11.52	20.50	20.07	100.00	10.50	20.00	48.04	57.00	16.64
									100.00	13.74	56.00	12.61	35.50	23.16					76.00	21.20
											73.00	11.31	53.00	24.97						
											100.00	11.68	73.50	27.18						
	104° F, 9 kips		104° F, 9 kips						104° F, 9 kips		104° F, 9 kips		104° F, 9 kips		70° F, 9 kips		104° F, 9 kips		70° F, 9 kips	
	0.00	0	0.00	0					0.00	0	0.00	0	0.00	0	0.00	0	0.00	0	0.00	0
	0.10	12.81	0.10	6.51					0.10	0.10	0.10	1.65	0.10	0.77	25.00	No Profiles	0.10	6.78	0.10	-0.81
	1.00	12.89	1.00	22.78					1.00	7.65	1.00	4.25	1.00	8.52			1.00	13.11	1.00	-0.61
	4.00	31.07	4.00	43.83					4.00	7.08	4.00	13.03	3.00	15.07			4.00	29.90	6.00	2.09
																	9.00	31.67	10.00	2.35
	104° F, 15 kips		104° F, 15 kips						104° F, 15 kips		104° F, 15 kips		104° F, 15 kips		70° F, 12 kips		104° F, 15 kips		70° F, 12 kips	
	0.00	0	0.00	0					0.00	0	0.00	0	0.00	0	0.00	0	0.00	0	0.00	0
	0.10	10.72	0.10	2.59					0.10	-12.93	0.10	-2.20	0.10	2.28	0.10	3.04	0.10	9.18	0.10	-5.71
	1.00	19.54	1.00	22.59					1.00	5.98	1.00	8.97	1.00	14.94	1.00	2.38	1.00	25.55	1.00	-0.46
	3.00	37.94	3.00	47.44					2.99	12.61	2.99	13.95	5.00	45.51	5.00	4.04	2.50	47.79	4.00	3.36
															10.00	6.05				
															70° F, 15 kips				104° F, 9 kips	
															0.00	0.00			0.00	0
B															0.10	-0.56			0.10	-1.44
															1.00	-0.20			1.00	11.47
															3.00	0.21			4.00	32.11
															8.00	4.32			9.00	38.32
															10.00	6.12				
															104° F, 9 kips				104° F, 15 kips	
															0.00	0.00			0.00	0
															0.10	-6.90			0.10	2.48
															1.00	8.22			1.00	19.52
															3.00	15.53			2.50	43.63
															104° F, 15 kips					
															0.00	0.00				
															0.10	13.63				
															1.00	14.68				
															5.00	41.27				

Shaded tests conducted at 5 mph, unshaded tests conducted at 3 mph

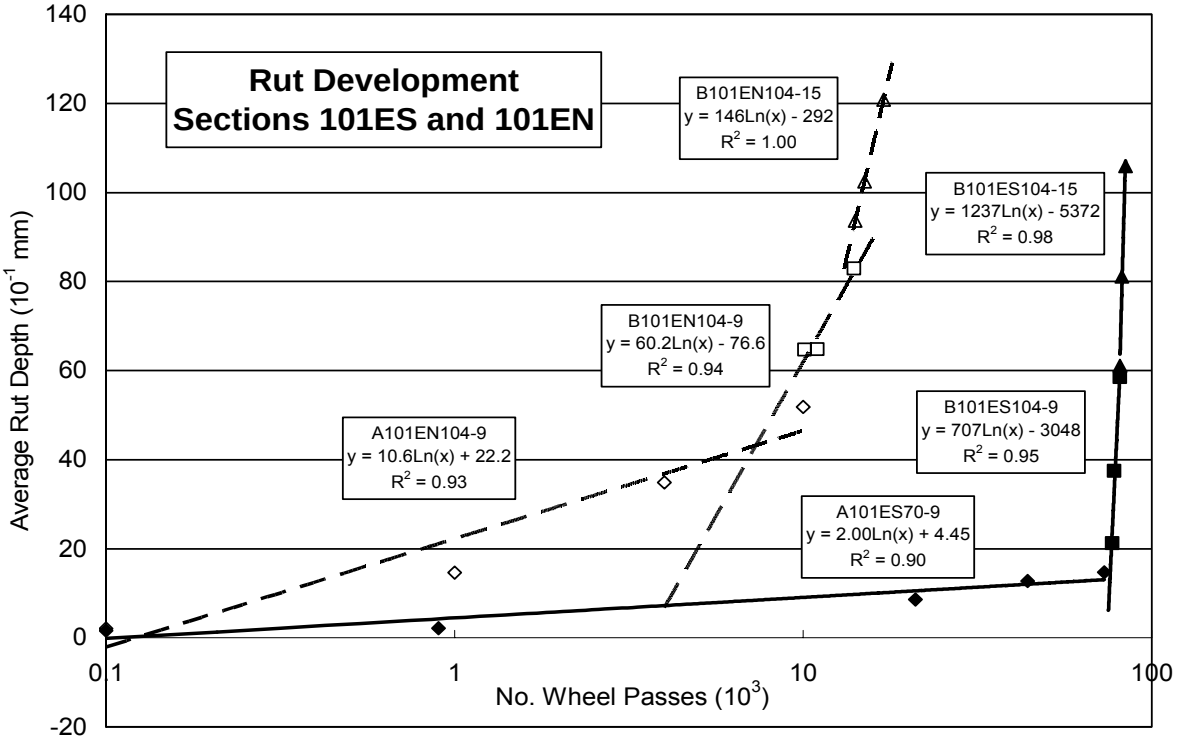

Figure 3.22 – Rutting Histories for Sections 101ES and 101EN

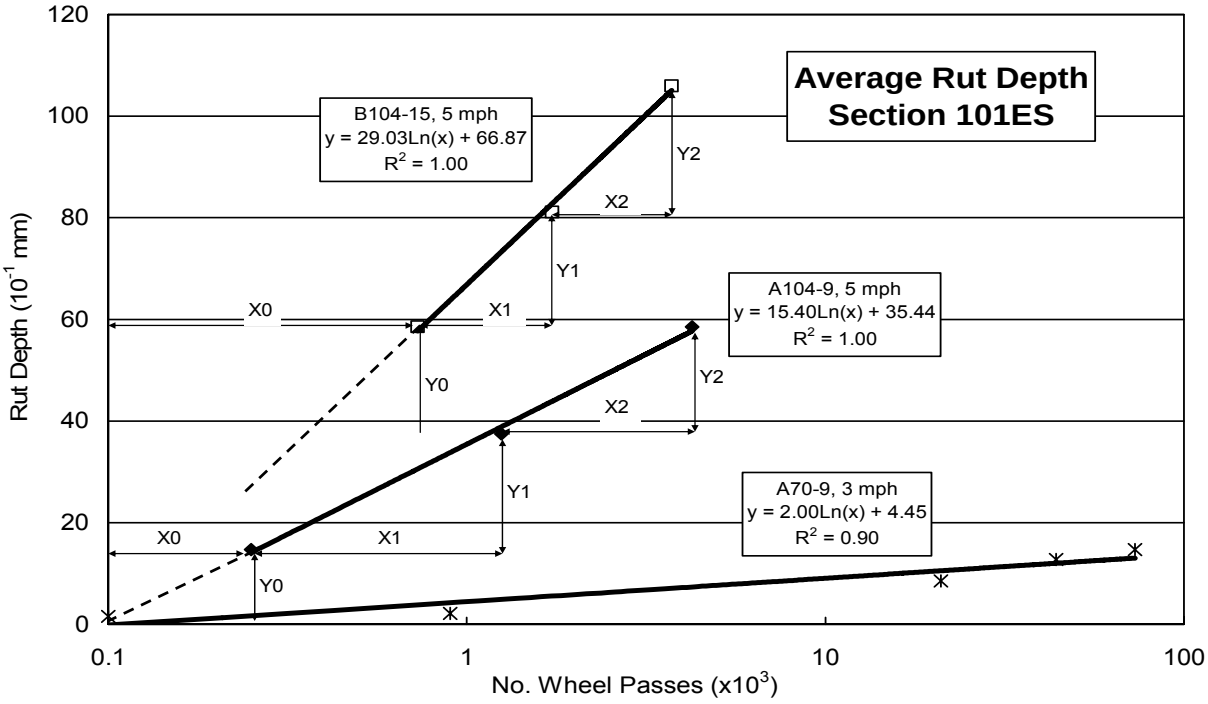

Figure 3.23 – Adjusted Best-Fit Trendlines for Section 101ES

Table 3.9 summarizes the trendline equations calculated for all tests on Pads A and B with the coefficients of variation, and the incremental and total accumulated rut depths measured at the conclusion of each test series. The trendlines for Pad B tests were adjusted back to where each would have been if all wheel passes had been applied at conditions specified for those tests. Rut depths were left in tenths of a millimeter which were units used by the laser profilometer. Care must be taken when using trendlines calculated for different series of tests on one section. Initial rutting occurred along the Pad A trendline until that test was stopped at rut depth Y0. The second series of tests (Pad B) begins at the same rut depth, but back at the number of wheel passes (X0) that would have been required to generate the rut under current conditions. The third series of tests begins at the total accumulated rut depth developed during the first two tests (Y0+Y1), but the number of wheel passes goes back again to X0+X1.

Table 3.9 - Adjusted Rutting Trendlines

Test Section	Test Series	Test Date	Start Passes (10^3)	End Passes (10^3)	Rut Equation (Pad B Trendlines Adjusted to Y0, X0)	R^2	Adjusted Trendline		Incremental Rut Depth (10^{-1} mm)	Accumulated Rut Depth (10^{-1} mm)
							Y0 (10^{-1} mm)	X0 (10^3 Passes)		
101ES	A70-9	4/15-6/4/03	0	77	2.00Ln(x) + 4.45	0.90			14.69	14.69
	B104-9	10/17-10/22/03	77	81	15.4Ln(x) + 35.4	1.00	14.69	0.25	43.83	58.52
	B104-15	10/22-10/23/03	81	84	29.0Ln(x) + 66.9	1.00	58.52	0.73	47.44	105.96
101EN	A104-9	6/26-6/30/03	0	10	10.6Ln(x) + 22.2	0.93			51.87	51.87
	B104-9	10/17-10/22/03	10	14	21.0Ln(x) + 48.4	1.00	51.87	1.18	31.07	82.94
	B104-15	10/22-10/23/03	14	17	32.2Ln(x) + 74.1	1.00	82.94	1.34	37.94	120.88
101WS	A104-12	6/30-7/1/03	0	9	13.8Ln(x) + 44.6	0.98			58.61	58.61
101WN	A104-12R	7/2-7/12/03	0	12	14.2Ln(x) + 37.8	0.98			66.42	66.42
102S	A70-9	7/16-9/13/02	0	100	2.27Ln(x) + 2.71	0.87			11.51	11.51
	B104-9	10/10-10/13/03	100	104	6.23Ln(x) + 14.4	0.97	11.51	0.56	13.03	24.54
	B104-15	10/15-10/17/03	104	106.99	9.85Ln(x) + 22.8	0.93	24.54	1.36	13.95	38.49
102N	A70-12	9/16-10/31/02	0	100	1.92Ln(x) + 3.63	0.96			14.29	14.29
	B104-9	10/10-10/13/03	100	104	9.21Ln(x) + 21.08	1.00	14.29	1.45	7.08	21.37
	B104-15	10/15-10/17/03	104	106.99	9.11Ln(x) + 21.3	1.00	21.37	1.02	12.61	33.98
105S	A70-9	11/20/02-1/24/03	0	100	1.72Ln(x) + 1.00	0.89			10.94	10.94
	B70-9	8/5-8/15/03	100	125	1.53Ln(x) + 3.61	0.98	10.94	121	0.40	11.34
	B70-12	8/18-8/26/03	125	135	4.21Ln(x) + 9.71	1.00	11.34	1.29	6.05	17.39
	B70-15	8/26-9/10/03	135	145	5.55Ln(x) + 12.8	0.85	21.43	4.11	6.12	23.51
	B104-9	10/3-10/7/03	145	148	11.8Ln(x) + 27.2	1.00	28.11	1.10	15.53	39.04
	B104-15	10/8-10/10/03	148	153	20.7Ln(x) + 47.9	0.99	43.64	0.78	41.27	80.31
105N	A70-15	1/28-2/27/03	0	73.5	4.07Ln(x) + 7.76	0.95			24.62	24.62
	B104-9	10/3-10/7/03	73.5	76	10.9Ln(x) + 25.0	0.99	24.62	1.00	15.07	39.69
	B104-15	10/8-10/10/03	76	81	20.8Ln(x) + 47.8	0.99	39.69	0.62	45.51	85.20
107S	A70-9	2/28-4/10/03	0	77.5	2.94Ln(x) + 4.82	0.91			21.22	21.22
	B70-9	9/10-9/15/03	77.5	87.5	4.67Ln(x) + 10.8	0.94	21.22	9.59	2.35	23.57
	B70-12	9/19-9/23/03	87.5	92.5	7.84Ln(x) + 18.1	0.91	24.38	2.58	3.36	26.93
	B104-9	9/26-10/1/03	92.5	101.5	15.2Ln(x) + 35.0	1.00	33.45	0.91	38.32	65.25
	B104-15	10/1-10/3/03	101.5	104	31.7Ln(x) + 73.1	0.98	69.8	0.86	43.63	108.88
107N	A85-9	6/13-6/20/03	0	20	8.45Ln(x) + 18.45	0.93			48.04	48.04
	B104-9	9/26-10/1/03	20	29	17.2Ln(x) + 39.5	0.96	48.04	1.91	31.67	79.71
	B104-15	10/1-10/3/03	29	31.5	36.1Ln(x) + 82.7	1.00	79.71	0.91	47.79	127.50

Table 3.10 summarizes the slopes of all trendline slopes calculated on Pads A and B and groups them by wheel load and temperature. It also shows acceleration factors derived by comparing slopes for changes in either load or temperature. Slope is the coefficient of the Ln(x) term and is a measure of how fast rutting proceeds under specific conditions. In general, stiff pavement structures would be expected to rut slower than weak pavement structures, warm AC material would be expected to rut faster than cold AC material, heavy wheel loads would be expected to generate ruts faster than light wheel loads, and pavements with weak subgrade would be expected to rut faster than pavements with stiff subgrade. Also, material in each pavement layer has some potential for rutting, either by compressing vertically and/or shoving horizontally as loads are applied, depending upon the characteristics of the materials in these layers and the magnitude of stress carried by the layers. All of these factors can contribute to rutting to some extent. As AC temperature, subgrade moisture and/or traffic loading changes, the rate of rutting will also change accordingly.

Table 3.10 is particularly useful in evaluating the effects of design build-up, load and temperature on rutting performance in the APLF. Overall, these data appear to be quite good judging by the high coefficients of variation associated with the trendlines and the excellent agreement between rutting slopes developed on the same pavement build-up at different times under identical conditions. This was especially true at 104º F in all four pavement structures with loads of 9 and 15 kips. The largest difference in slopes for identical conditions was for the 9 kip, 104º F tests in Lane 101E where two tests were run at 5 mph and one test was run at 3 mph. Any differences in rutting between the 3 and 5 mph tests would be expected to be explained by the effects in speed, except that the 3 mph test would be expected to generate more rutting per pass of the test wheel or have a higher slope. Since the 3 mph test had the lower slope, the three tests in Section 101EN were averaged together with any differences in slope between the 3 and 5 mph tests being assumed to be negligible.

As was stated earlier under the discussion for Pad A, slopes of the four pavement sections in Pad A tested at 9 kips and 70º F tended to be inversely proportional to the structural numbers of the sections, thereby indicating that the lighter sections rutted faster than the heavier sections. These structural numbers were as follows: 101 – 3.57, 102 – 3.08, 105 – 3.36 and 107 – 2.52.

Table 3.10
Summary of Trendline Slopes

Trendline Slopes by Section, Temperature and Load						
Wheel Load	Nominal Air Temperature			Temperature Acceleration		
	70º F	85º F	104º F	85º F/70º F	104º F/85º F	104º F/70º F
9 K	A101ES - 2.00		A101EN - 10.56			101 - 7.83
			B101EN - 21.00			
			B101ES - 15.40			
	A102S - 2.27		B102S - 6.23			102 - 2.74
	A105S - 1.72		B105N - 10.87			105 - 6.30
			B105S - 10.80			
	A107S - 2.94	A107N - 8.45	B107N - 17.18	107 - 2.22	107 - 1.92	107 - 4.25
	B107S - 4.67		B107S - 15.20			
12 K			A101WN - 14.19			
			A101WS - 13.77			
	A102N - 1.92					
	B105S - 4.21					
	B107S - 7.84					
15 K			B101EN - 32.24			
			B101ES - 29.03			
			B102N - 9.11			
			B102S - 9.85			
	A105N - 4.07		B105N - 20.83			105 - 4.32
	B105S - 5.55		B105S - 20.74			
			B107N - 36.10			
			B107S - 31.68			
Load Acceleration						
12K/9K			101 - 1.12			
	102 - 0.85					
	105 - 2.45					
	107 - 1.68					
15K/12K			101 - 0.89			
	105 - 0.80					
15K/9K			101 - 1.96			
			102 - 1.52			
	105 - 2.80		105 - 1.92			
			107 - 2.09			

Shaded tests conducted at 5 mph, unshaded tests conducted at 3 mph

When temperature was raised to 104º F, however, the magnitudes of the rutting slopes increased more with increased thickness and asphalt content of the stabilized materials, as indicated by the temperature acceleration factors shown in Table 3.10. In fact, the acceleration factors were highest for Section 101 (7” AC), followed by Section 105 (4” AC & 4” ATB),

followed by Section 107 (4" AC & 4" PATB), and followed finally by Section 102 (4" AC). The order of rutting slopes by section at 104º F was identical at the 9 kip and 15 kip loads, with the 15 kip slopes being about twice as high as those at 9 kips. It was interesting that the lowest acceleration factors for temperature and load were in Section 102 with the thinnest layer of asphalt stabilized material.

Raising the temperature from 70º F to 104º F accelerated rutting about two to three times more than by increasing the load from 9 kips to 15 kips. At 9 kips on Section 107, rutting doubled as temperature was raised from 70º F to 85º F and doubled again as temperature was raised from 85º F to 104º F. This resulted in a total acceleration factor of 4.25 when temperature was raised from 70º F to 104º F. At 15 kips on Section 105, the acceleration factor was 4.32 when raising temperature from 70º F to 104º F. Also on Section 105, rutting accelerated 12.09 times when load was increased from 9 kips to 15 kips and temperature was increased from 70º F to 104º F. This combined effect can be derived either by dividing the final slopes directly (20.79/1.72), or by multiplying the individual acceleration factors (2.80 x 4.32 or 6.30 x 1.92).

Pavement rutting becomes quite complex in the field as spectra of wheel loads are applied at different lateral positions, AC temperatures, and subgrade moisture levels to incrementally develop ruts in AC pavements. Another variable associated with the rutting of AC pavements is distress mode. When simulating field conditions in a controlled environment, it is certainly desirable to generate similar types of distress in the APLF that would be observed in the field, whether it is cracking or consolidation of the AC, and/or deformation of the base and subgrade. It appears from these tests that, if the APLF subgrade had been similar to that in the field, hourly pavement loadings from the WIM could have been combined with hourly combinations of temperature and moisture on the test road to estimate rutting performance based on rutting slopes developed in the APLF. Unfortunately, the A-6 subgrade in the APLF did not absorb sufficient moisture to adequately to simulate conditions on the test road.

Environmental Conditions – Pad B

Actual pavement temperatures on Pad B were quite similar to those measured on Pad A during response and performance monitoring. While TDRs mounted along the pit wall indicated higher moisture under Pad B than Pad A, response measurements, rut measurements and observations as the subgrade was being removed at the completion of the study indicated little difference between the two pads.

Acceleration factors for structural number, temperature and load were calculated by dividing the rutting slopes determined for two tests where the parameter in question was the only variable. Structural numbers tended to be inversely proportional to rutting slope, thereby indicating that the weaker sections rutted faster, at least at 70^{o} F (21.1^{o} C). Rutting was accelerated by a factor of 2.22 on Section 107, Pad A by raising the temperature from 70 to 85^{o} F (21.1-29.4^{o} C), and by factors of 2.74 to 7.83 on the four lanes in Pads A and B by raising the temperature from 70º F to 104^{o} F (21.1-40.0^{o} C). Increasing load from 9-12 kips (4.08-5.44 Mg) at 70º F (21.1º C) accelerated rutting by an average of 1.66 on Sections 102 and 105, and increasing load from 9-15 kips (4.08-6.80 Mg) accelerated rutting by an average rate of 2.06 on the two pads. Since the rate of rutting appears to be affected by structural number and/or thickness of the AC material, acceleration rates for temperature and load are likely to be influenced by pavement build-up.

Forensics – Pad B

At the conclusion of testing, the AC pavement sections were removed and replaced with new pavements for another research project. During the removal process, observations were made as to how much deformation was visible in the pavement, base and subgrade layers, and how wet the subgrade was after water was added for Pad B. Figures 3.24 and 3.25 show pieces of pavement being removed from Sections 102N and 107S, respectively. While deformation was visible in the pavement surfaces, no deformation was present at the bottom of the slabs or in the supporting layers. These sections were typical of the other sections, which also showed no deformation at the bottom of the AC layers indicating that all surface rutting resulted from consolidation of the AC mixes.

Figure 3.24 –Slab from Section 102N being Removed

Figure 3.25 –Slab from Section 107S being Removed

Figure 3.26 shows removal of the subgrade after all testing was completed. With water in the standpipes remaining constant at approximately three feet (0.9 m) below the pavement surface or four feet (1.2 m) above the bottom of the subgrade, the soil would have been expected to be near saturation to that level. Sensor responses and deformation slopes suggested the stiffness of Pad B was very similar to the stiffness of Pad A, indicating little change in subgrade moisture. Figure 3.26 confirms that there was no excess moisture in the subgrade. Workers could walk on the subgrade without mud sticking to their boots and equipment could operate quite easily in the pit without picking up soil in the tires or sinking into the soil. Soil around the TDRs along the two sides of the pit appeared darker and felt slightly wetter than soil farther away from the pit edges, explaining why the TDRs showed higher moisture. Some moisture had evidently moved up along the pit walls, but did not migrate under the pavement sections.

Figure 3.26 – Subgrade Removal after Completion of Testing in APLF

Material Properties

Cores were removed from the pavement lanes after construction in the APLF and tested in the lab in accordance with SHRP protocol. Figure 3.27 shows the results of resilient modulus tests on the asphalt stabilized materials on the test road with results of the Types 1 and 2 surface mixes in the APLF added for comparison. The moduli of the surface mixes in the APLF were about twice as high as those on the test road. One possible explanation was the stiffer subgrade in the APLF which provided better support during compaction of these mixes.

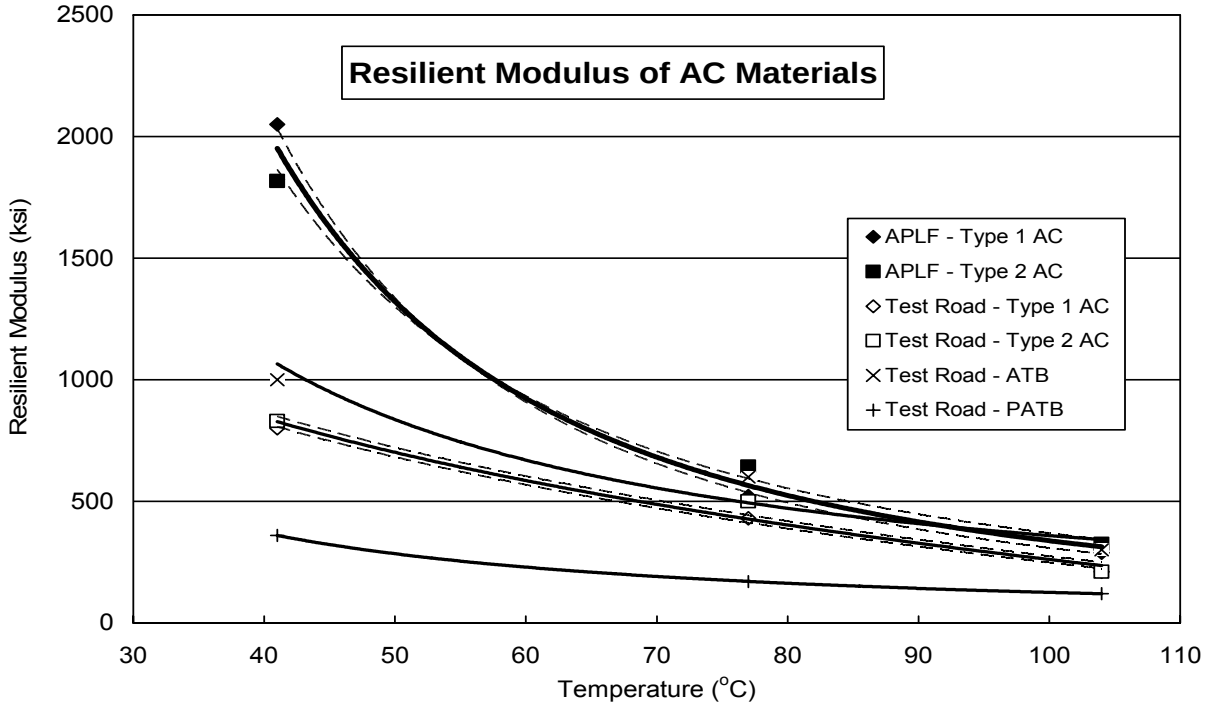

Figure 3.27 – Resilient Modulus of AC Materials on Test Road and in the APLF

Calculated Rutting

The rutting of flexible pavements can be divided into two main categories: rutting caused by compaction or consolidation of the asphalt concrete mix and rutting caused by deformation of the underlying support layers. While both forms of rutting can develop simultaneously, forensic investigations showed rutting on the test road to be confined to the support layers while rutting in the APLF was confined to the AC mixes. The type and magnitude of rutting on any pavement

depends upon the stability and compaction of the AC mixes, and the stiffness and stability of the support layers. On the test road, high moisture present in the bases and in the fine-grained subgrade resulted in low support stiffness. Heavy traffic loads traveling on thin pavement sections caused overstressing and rutting of the support layers. In the APLF, the subgrade was constructed at about optimum moisture which provided stiff support for compaction of the base and AC layers. Repeated loads in the APLF generated some rutting in the AC sections but, because of the stiff support layers, the rutting was confined to the AC layer. The different modes of distress at the two sites made it difficult to compare performance.

Two rutting equations are presented in a textbook entitled "Pavement Design and Analysis" and authored by Dr. Yang H. Huang. One equation is for HMA thicknesses less than six inches and the other equation is for HMA thicknesses six inches or greater. These equations are as follows:

$$\text{Log RR} = -5.617 + 4.343 \log w_o - 0.167 \log(N_{18}) - 1.118 \log \sigma_c \qquad (t_{AC} < 6\text{"})$$

$$\text{Log RR} = -1.173 + 0.717 \log w_o - 0.658 \log(N_{18}) + 0.666 \log \sigma_c \qquad (t_{AC} \geq 6\text{"})$$

Where: RR is the rate of rutting in microinches per axle load

W_o is the surface deflection in mils (see Figure 2.17 in textbook)

σ_c is the vertical compressive stress under the HMA in psi (see Figure 2.15 in textbook)

N_{18} is the equivalent 18 kip single-axle loads in 10^5

Table 3.11 summarizes incremental rut depths measured with the laser profilometer, calculated from best-fit trendlines of measured profiles, and calculated with the above equations for each series of tests in the APLF. Because rut depths determined for Section 102, with a t_{AC} of 4 inches (100 mm), were unrealistically low and not shown in the table.

Table 3.11

Summary of Measured and Calculated Rut Depths

Test Section	Test Series	Measured Rut Depth (mm)	Best-Fit Trendline (mm)	Calculated Rut Depth (mm)
APLF				
101ES	A70-9	1.47	1.31	3.95
	B104-9	4.38	3.58	4.20
	B104-15	4.74	4.50	5.56
101EN	A104-9	5.19	4.66	3.07
	B104-9	3.11	2.03	2.03
	B104-15	3.79	2.83	4.38
101WS	A104-12	7.61	7.50	8.41
101WN	A104-12R	7.42	7.30	2.65
102S	A70-9	1.17	1.32	
	B104-9	1.30	1.17	
	B104-15	1.40	1.52	
102N	A70-12	1.37	1.25	
	B104-9	0.71	0.52	
	B104-15	1.26	1.26	
105S	A70-9	1.05	0.89	1.39
	B70-9	(1)	(1)	3.55
	B70-12	0.61	0.34	1.03
	B70-15	0.61	0.62	2.46
	B104-9	1.55	1.48	2.26
	B104-15	4.13	3.69	2.62
105N	A70-15	2.72	2.52	1.80
	B104-9	1.51	0.84	2.26
	B104-15	4.55	4.27	2.62
107S	A70-9	2.12	1.76	2.02
	B70-9	0.24	0.35	2.23
	B70-12	0.34	0.79	6.46
	B104-9	3.83	3.77	2.32
	B104-15	4.36	4.26	3.56
107N	A85-9	4.80	4.38	5.59
	B104-9	3.17	2.52	2.32
	B104-15	4.78	4.00	3.56
Test Road				
390101		~ 13		7.94
390102		~ 13		0.53
390105		~ 13		8.44
390107		~ 13		4.42

CHAPTER 4

THEORETICAL ELASTIC RESPONSES

General

During the construction of flexible pavements, individual material layers assume some level of structural stiffness, depending upon the materials used, the methods of placement and environmental conditions existing at the time. Subsequent temperature cycling causes changes in the stiffness of materials stabilized with asphalt cement and moisture cycling causes changes in the stiffness of the fine-grained subgrade. Other material variations may occur as environmental conditions change, but the temperature of asphalt concrete and the moisture content of fine-grained subgrades are the primary causes for time related environmental changes in AC pavement stiffness.

When comparing dynamic responses generated by rolling tires and the FWD on different pavement systems, it is necessary to consider design and material parameters in the pavement structures, environmental conditions, and the geometry associated with each type of loading. Design parameters for the four SPS pavements studied in this project are summarized in Table 2.1. While efforts were made to replicate pavement sections from the test road in the APLF, the subgrade was much stiffer and the resilient modulus of the AC pavement was higher in the APLF than on the test road. Environmental conditions were controlled and relatively stable in the APLF, while conditions on the test road changed continuously. Dump trucks applied loads with a front single tire and rear dual tires at speeds of up to 50 mph (80 km/hr) on the test road. Dual tires in the APLF traveled up to 5 mph (8 km/hr), and were ¼-inch (6.4 mm) wider and separated by one more inch (2.5 cm) than dual tires on the dump truck. The same FWD, with a 300 mm diameter load plate, was used on the test road and in the APLF.

At the time dynamic responses are measured on AC pavements, the in-situ elastic moduli of the pavement and subgrade are not usually known precisely. The moduli of other materials not substantially affected by temperature or moisture can be reasonably estimated from past experience. Therefore, multiple response measurements must be obtained to determine the environmentally dependant moduli. Load applied by the FWD provides seven surface deflections

spaced along the radius of the resulting basin, which can be used with elastic-layer programs to backcalculate the moduli of individual material layers. An alternative procedure involves the estimation of E_2 or $E_{subgrade}$ from Df6 and combining E_2 with Df1 to determine E_1 or $E_{pavement}$. Deflection of the pavement surface and longitudinal strain at the bottom of the asphalt stabilized materials were monitored during controlled vehicle tests on the test road and during rolling wheel tests in the APLF. Graphical models were devised to estimate moduli of the asphalt pavement and subgrade from these various types of measurements.

Elastic Layer FWD Model for One and Two-Layer Systems

The first step in using FWD data to determine layer moduli on one or two layer pavement systems was to assess the feasibility of using DF6 or Df7 to directly determine E_2. This analysis was provided in a previous report, but is included here for reference. The top graph in Figure 4.1 shows the theoretical relationship between surface deflection and layer modulus for the seven FWD geophone locations used in this project on a one-layer elastic system. The slopes of the lines in the top graph are shown as constant "a" in the inserted table. The linearity shown in this graph permits the development of simple relationships between elastic layer modulus and normalized deflection at any distance from the load, as shown in the bottom graph of Figure 4.1.

When a second elastic layer is added to a one-layer elastic system, the relationship between load and deflection remains linear, but the interaction between layer thickness and modulus on deflection becomes more complex. Figure 4.2 shows how deflection is related to the modulus of the top layer for a hypothetical two-layer system with t_1 = 10 inches (25.4 cm) and E_2 = 10,000 psi (69 MPa). Of particular interest is the manner in which FWD geophones Df6 and Df7, located 36 and 60 inches (0.91 and 1.52 m), respectively, from the center of the load plate, remain relatively constant with changing moduli of the top layer. This suggests that output from these geophones is indicative of the stiffness of the pavement subgrade, regardless of the stiffness of the top layer, and that the slopes indicated for Df6 and Df7 on a one-layer system can be used with reasonable accuracy on multiple layer systems. Figure 4.3 shows similar plots for DF6 and Df7 on two-layer systems with E_2 ranging from 10,000 – 100,000 psi (69-690 MPa), and pavement thickness ranging from 4–16 inches (10.2-40.6 cm). Additional DGAB and PATB layers between the pavement and subgrade are not likely to cause much practical difference in

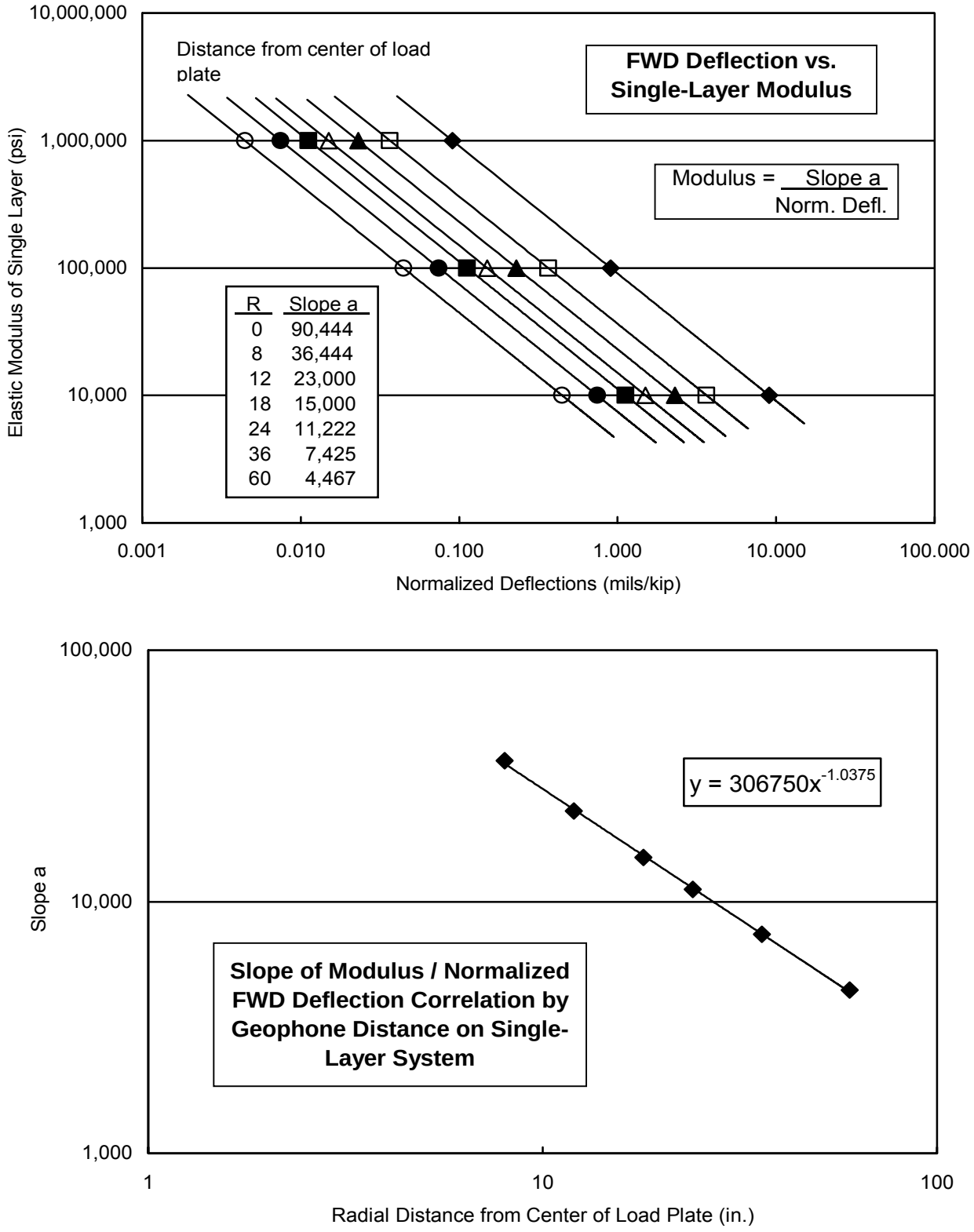

Figure 4.1 – Theoretical Relationship between FWD Distance/Deflection and Elastic Modulus on a Single-Layer System

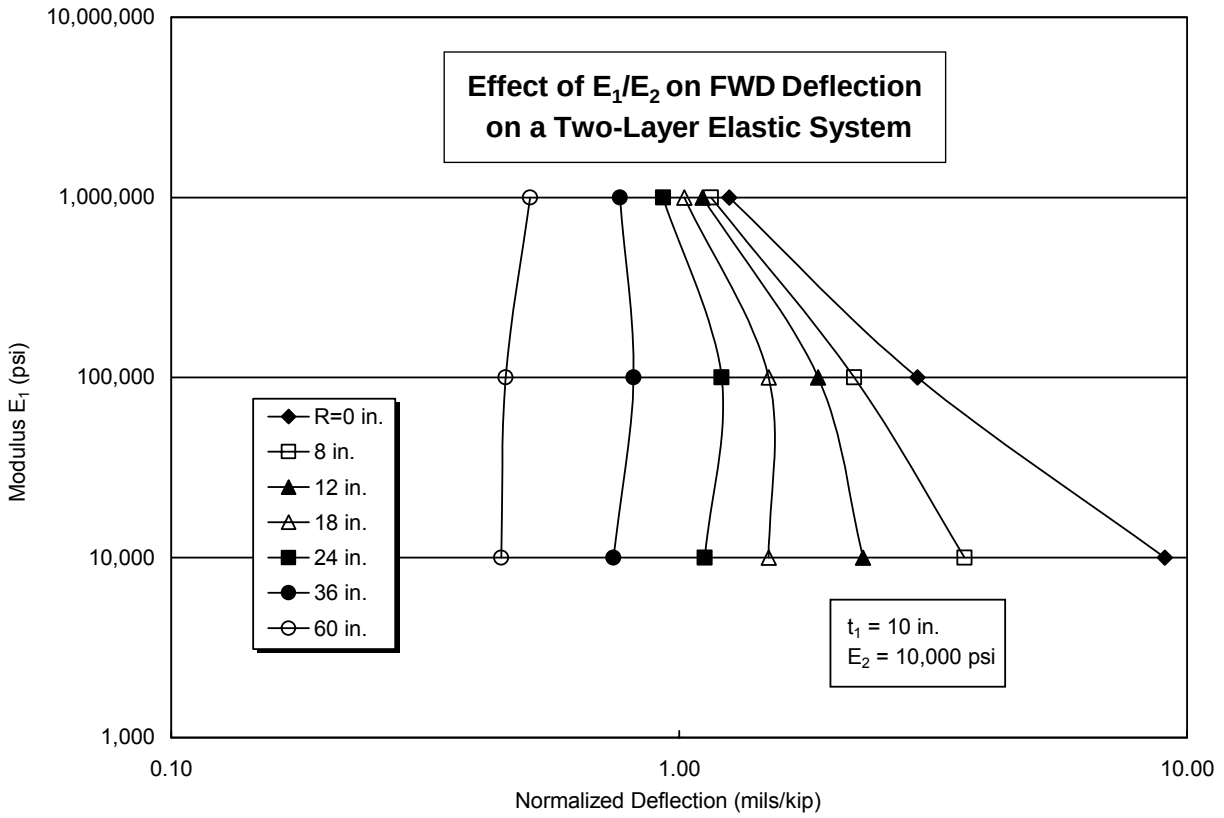

Figure 4.2 – Effect of E_1/E_2 on FWD Deflection on a Two-Layer Elastic System

the deflection calculations. It appears from Figure 4.3 that geophone Df7 has less variation than geophone Df6, but a one digit difference in Df7 will cause more variation in E_2 than will a one digit difference in Df6. Most variations in Df6 occurred with a very stiff pavement over a weak subgrade or a very weak pavement over a stiff subgrade. When calculating E_2 with Df6 or Df7, simply normalize the Df6 or Df7 deflections measured with the FWD to 1,000 lbs. and refer to Figure 4.1 for an estimation of subgrade modulus, or divide the appropriate slope "a" by the normalized deflection measured with Df6 or Df7. Based upon the sensitivity of Df6 and Df7, it appears that DF6 would be the better sensor for estimating E_2.

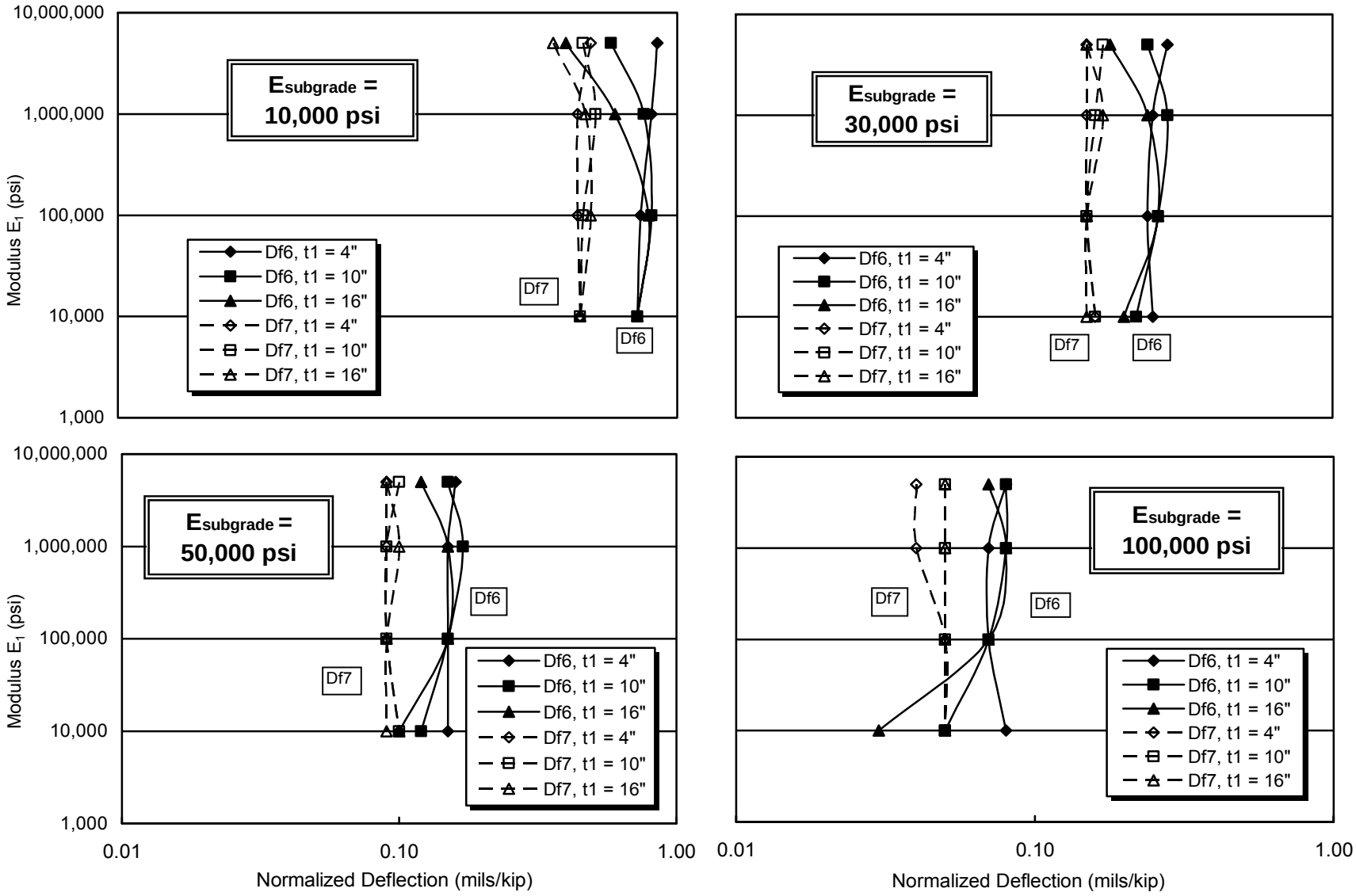

Figure 4.3 – Effect of E_1, E_2 and Pavement Thickness on FWD Df6 and Df7 Deflections

Elastic Layer Models for SPS Sections

While many elastic layer programs are currently available, WinJULEA, developed by the Waterways Experiment Station, Engineering Research and Development Center in Vicksburg, MS, was used for modeling theoretical responses on the four SPS sections included in this project. Models were set up for each of the four SPS sections with an 11.8-inch (30 cm) diameter FWD load plate, an 8.5-inch (21.6 cm) diameter single truck tire, a set of 9.75-inch (24.8 cm) diameter dual tires separated by 3 inches (9.6 cm) (test road) and a set of 10-inch (25.4 cm) diameter dual tires separated by 4 inches (10.2 cm) (APLF). Diameters for the single and dual tire configurations were based on the measured contact widths of tires on the ODOT single-axle test truck used for controlled vehicle tests on the test road and the dual tires in the APLF. Differences in calculated deflection and strain between the two dual tire geometries is believed to be less than errors caused by the assumption that the actual tire footprints were round and applied uniform pressure. Therefore, either one of the dual tire configurations could probably be used for both test geometries.

One of the inputs for WinJULEA is slippage between pavement layers. Figure 4.4 shows calculations performed using assumptions of full slip and no slip at the DGAB interfaces in all four sections with dual tires and one set of stiffness parameters. As expected, strain profiles were smoother with no slippage between layers, and strain at the bottom of the AC layers was higher when slippage does occur. While the difference in longitudinal strain at the bottom of the AC layer with and without slippage varied from approximately 70 to 170 με on the four sections, any assumption of partial slippage would give results somewhere between the two limits. Differences in longitudinal strain with and without slippage became less toward the pavement surface. Longitudinal strain on top of the underlying material layers was dramatically different and in the opposite direction. Graphs of longitudinal strain with and without slippage under the FWD, single truck tire, and dual truck tires on all four sections are shown in Appendix G. With all four sections containing a layer of DGAB, there was probably some slippage associated with that layer, but the actual magnitude is unknown. On this basis, WinJULEA models were developed for FWD loading on all four pavement sections, and single and dual tire loading on three sections tested on the test road using the assumption of no slippage.

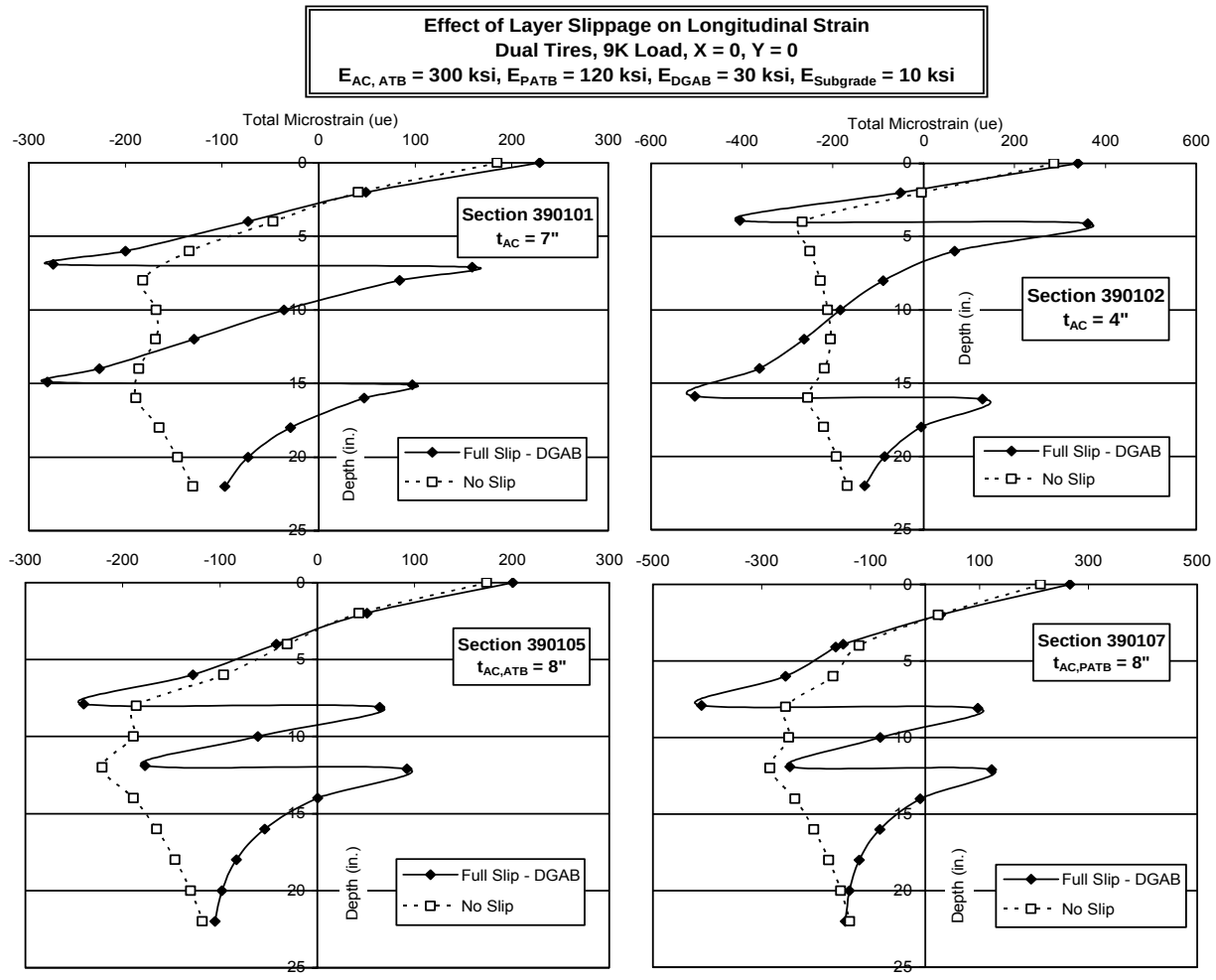

Figure 4.4 – Theoretical Strain Calculations With and Without Layer Slippage

To compare measured and calculated responses on the test road, responses calculated from WinJULEA using resilient moduli determined in the lab for asphalt concrete and subgrade are shown in Figures 4.5 – 4.7. Calculated responses on Pad A in the APLF were obtained by using WinJULEA, resilient moduli determined in the lab, and the APLF dual tire geometry. One point was also added using moduli back calculated from FWD measurements obtained at a pavement temperature of 70º F. Figures 4.8 – 4.10 show the calculated and measured responses on the three instrumented APLF sections. PATB and DGAB were assumed to have constant moduli of 120,000 psi and 30,000 psi (827 and 207 MPa), respectively, for all calculations. In general, measured responses were higher than calculated responses on the test road. In the APLF, measured and calculated strains were similar and calculated deflections were higher than measured deflections.

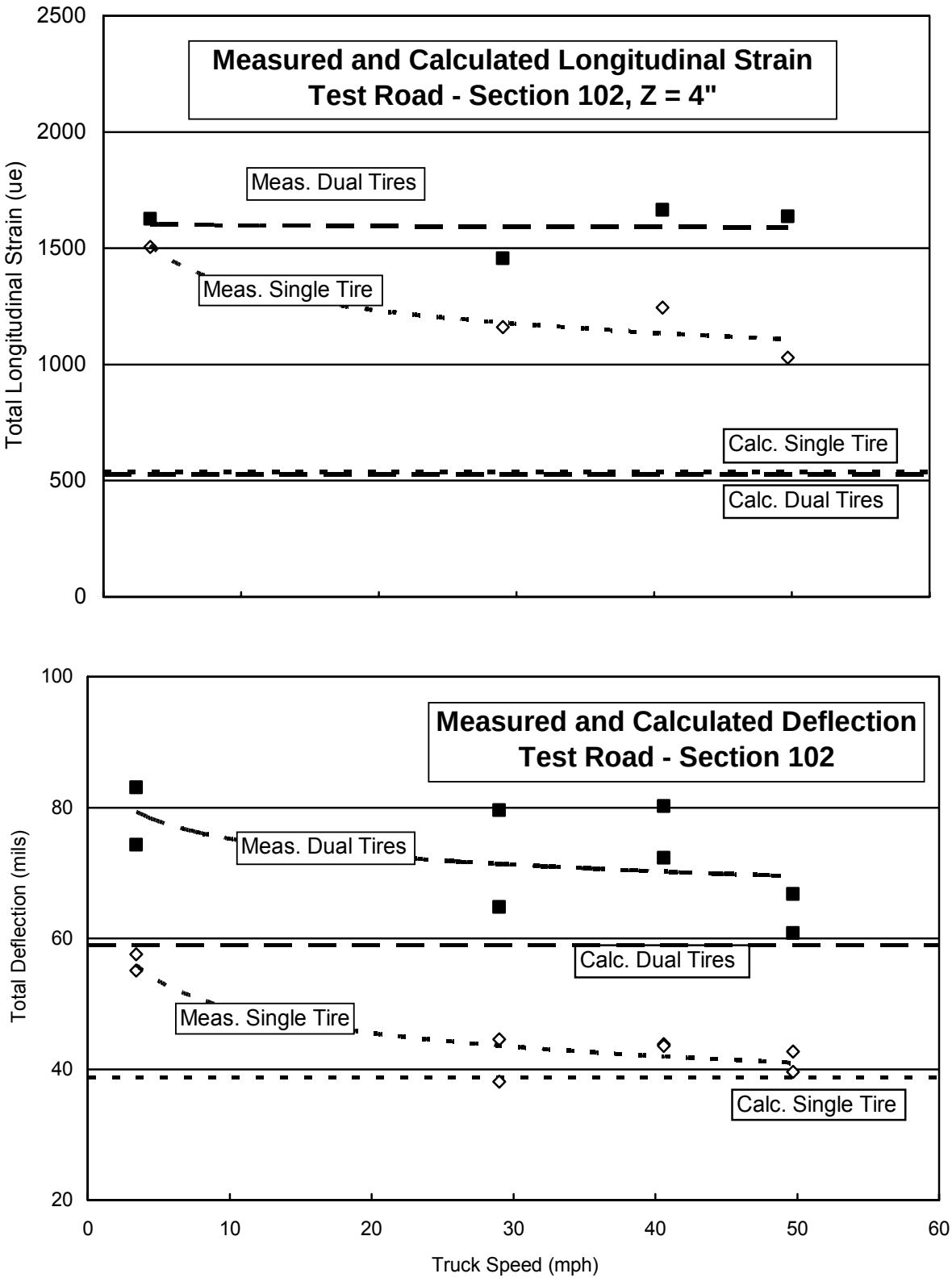

Figure 4.5 – Measured vs. Calculated Responses on Test Road Section 390102

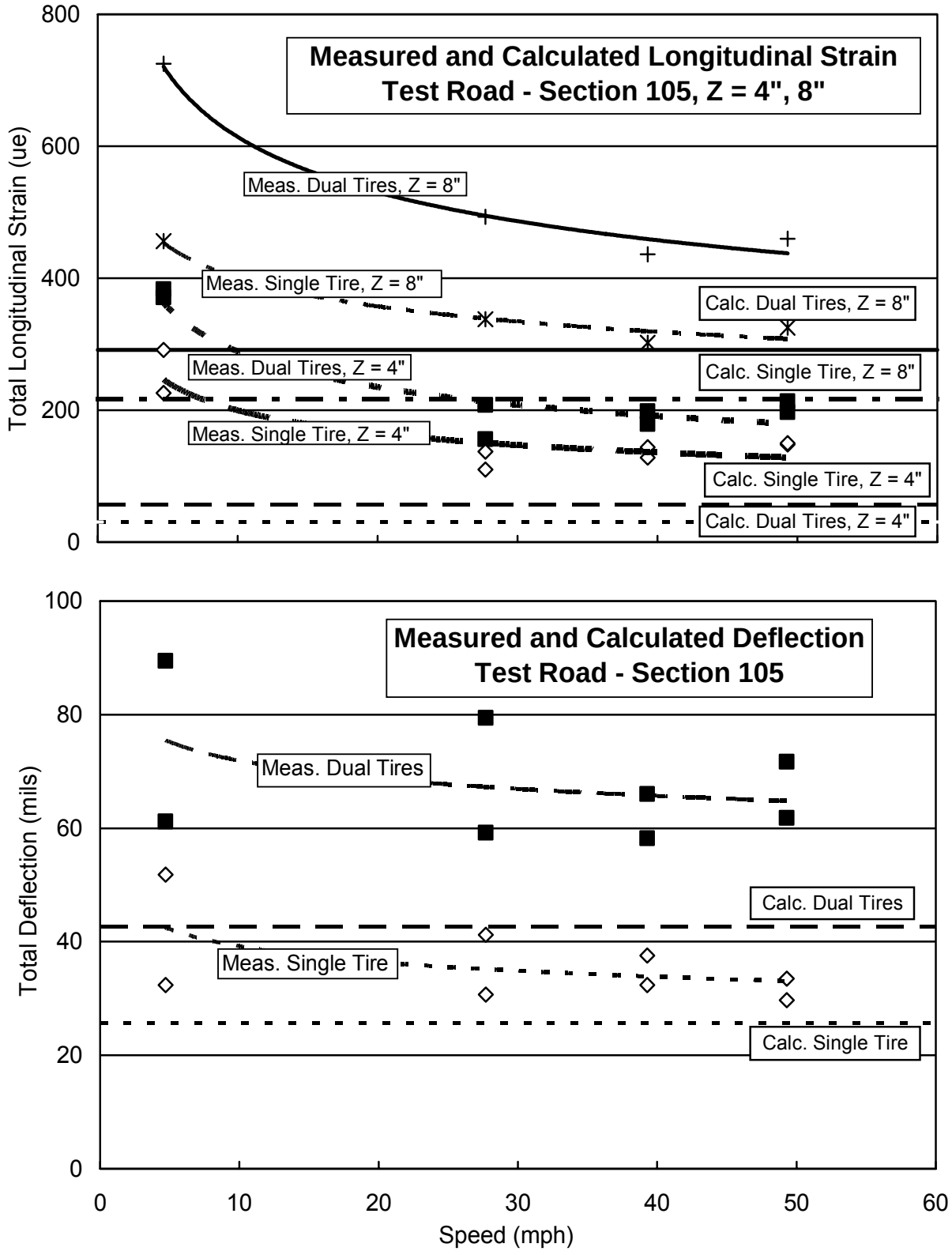

Figure 4.6 – Measured vs. Calculated Responses on Test Road Section 390105

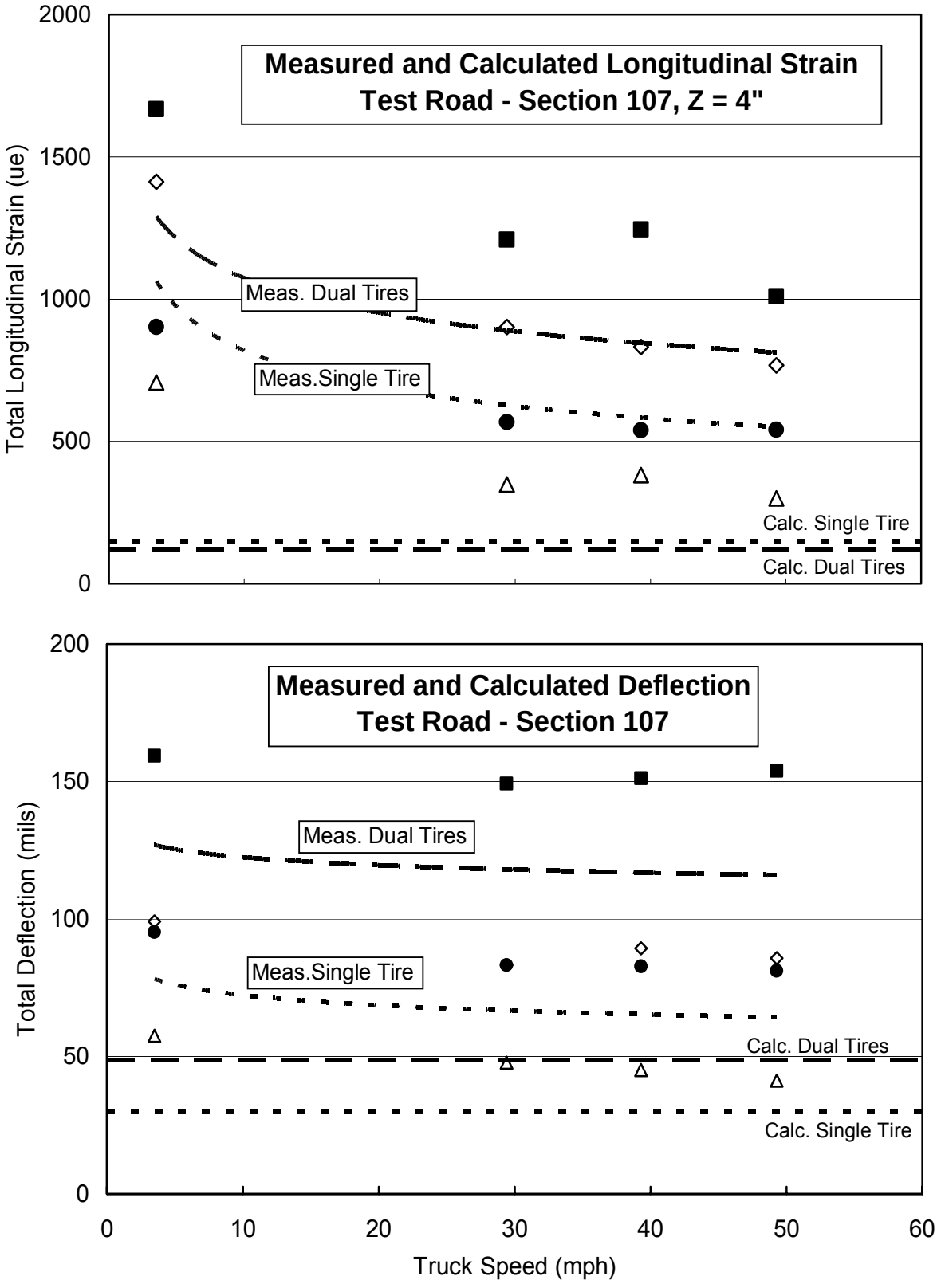

Figure 4.7 – Measured vs. Calculated Responses on Test Road Section 390107

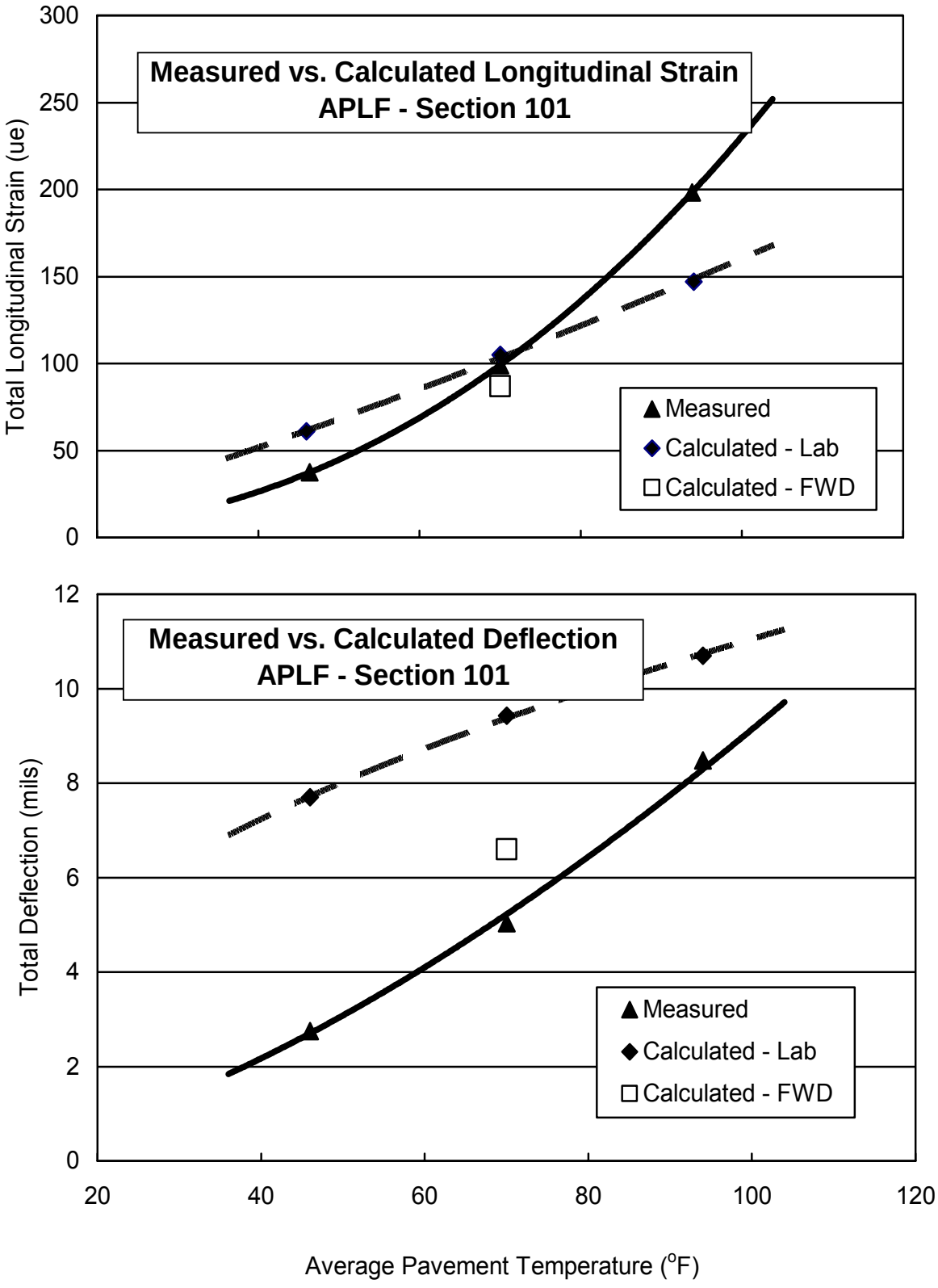

Figure 4.8 – Measured vs. Calculated Responses on APLF Section 101

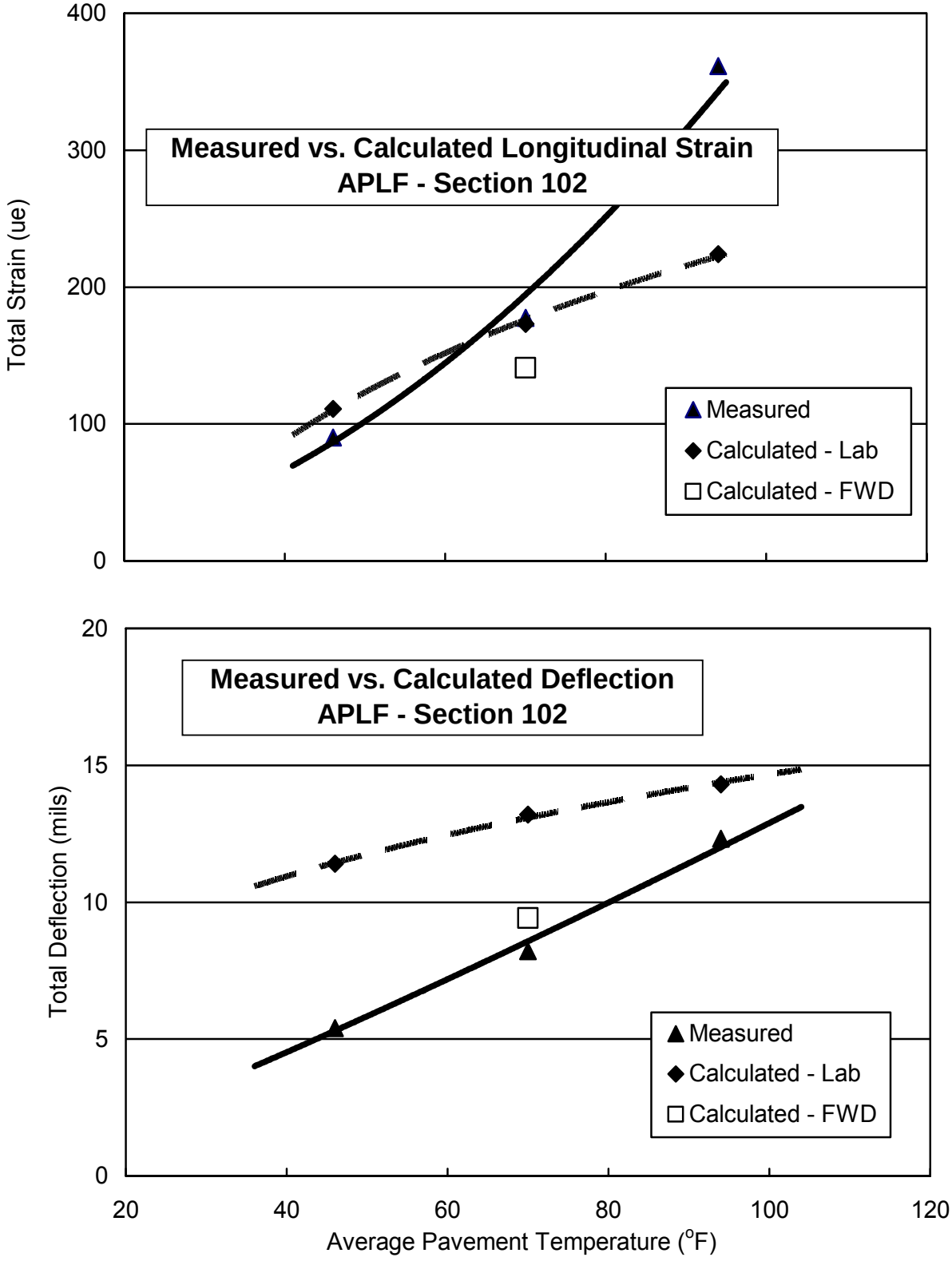

Figure 4.9 – Measured vs. Calculated Responses on APLF Section 102

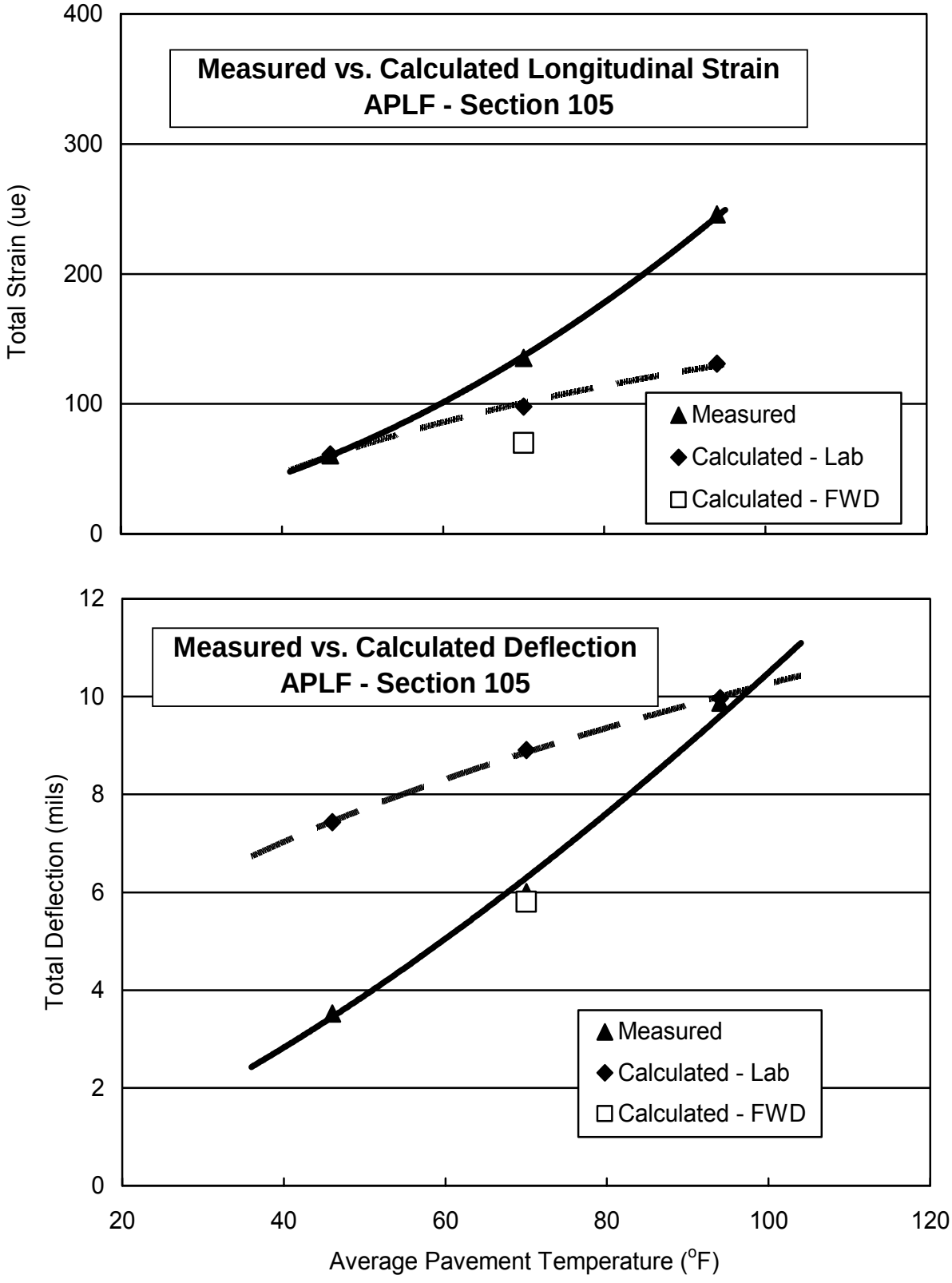

Figure 4.10 – Measured vs. Calculated Responses on APLF Section 105

The development of a model for FWD responses on test road Section 390101 is shown here as an example of how graphical solutions developed with WinJULEA can be used to relate vertical surface deflection, longitudinal strain at the bottom of the AC pavement, $E_{pavement}$, and $E_{subgrade}$ in one figure. Because the graphics are limited to two layer moduli, the pavement and subgrade were selected since they are affected most by environmental cycling. The elastic moduli of the DGAB and PATB in these sections were assumed to be a constant 30,000 and 120,000 psi (207 and 827 MPa), respectively, for all models. Since laboratory tests showed properties of the ATB to be similar to the AC pavement, these layers were combined in the Section 390105 model. No slippage was assumed at the material interfaces, and Poisson's ratios for the various materials were 0.40 for the AC, ATB and subgrade, and 0.35 for the PATB and DGAB.

Figure 4.11 shows separate plots for the relation between E_2, and longitudinal strain and deflection for a one kip FWD load and various values of E_1. All moduli are shown in ksi. While the power curves used in these plots to fit the data are not exact, they do provide a good approximation of the data and have a high coefficient of variation. The major problem occurs at low very values of E_2 where strain and deflection increase rapidly with decreasing E_1. Using the best-fit equations for deflection and strain shown in Figure 4.11, values of E_2 were calculated for assumed levels of deflection and strain over a range of E_1. Figure 4.12 shows the combined plot relating pavement and subgrade moduli with normalized deflection and strain responses for FWD geometry. Data points were added to illustrate how Df1 and subgrade modulus calculated from Df6 readings obtained with the FWD compared to moduli backcalculated from all seven FWD geophones. Plots of the relationship between E_1 and E_2, and longitudinal strain and deflection, and the combined plots for FWD geometry on all four pavement sections are shown in Appendix H. Similar figures are shown for the single tire and dual tire geometries in Appendices I and J, respectively.

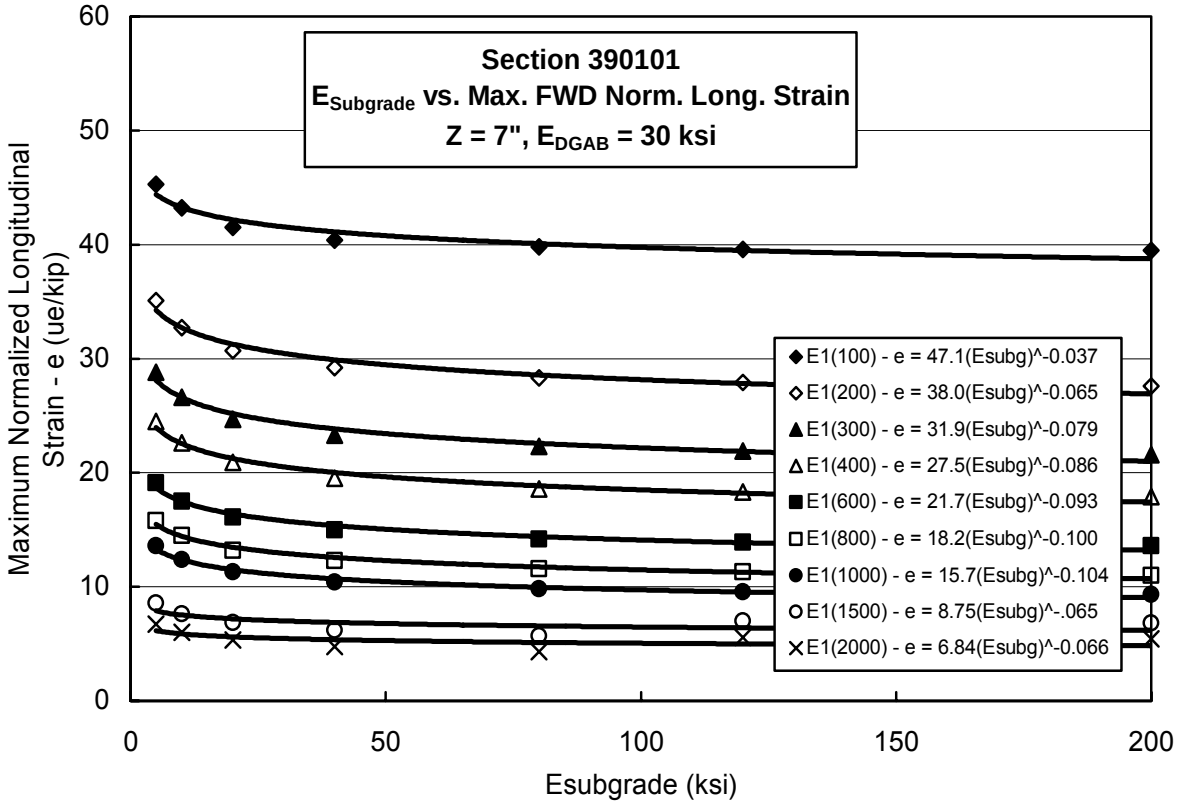

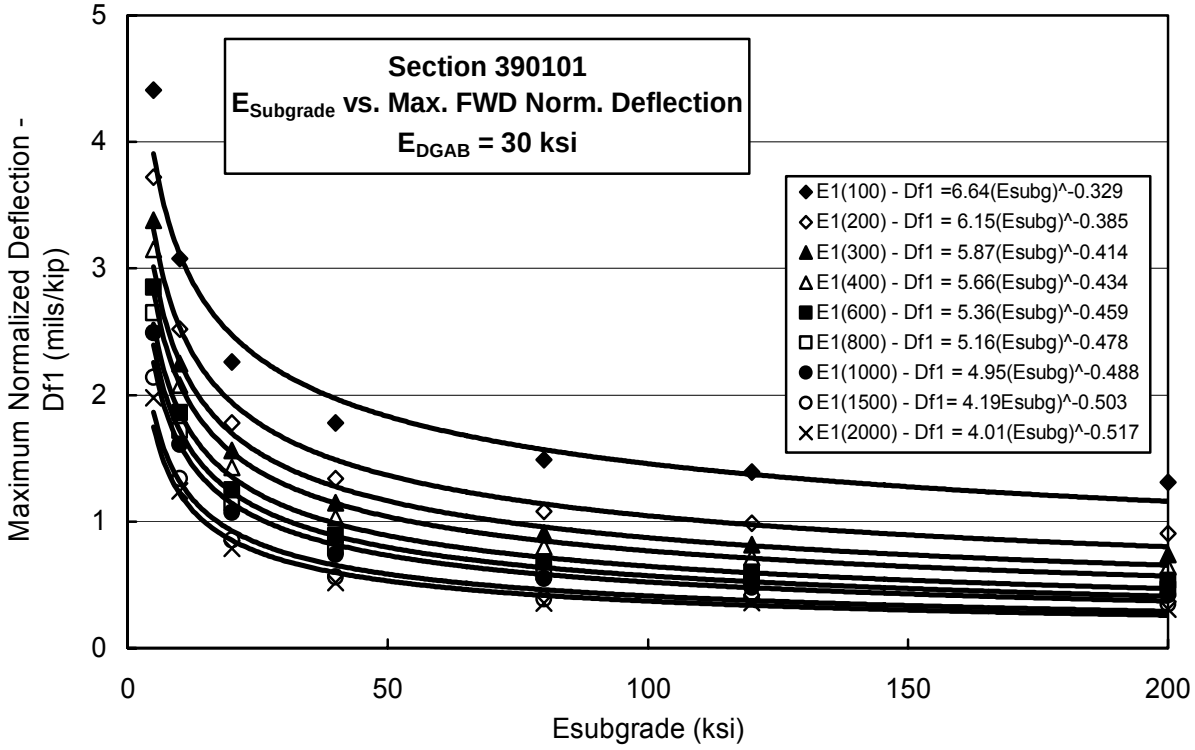

Figure 4.11 – Relations between Layer Moduli, and Deflection and Strain on Section 390101

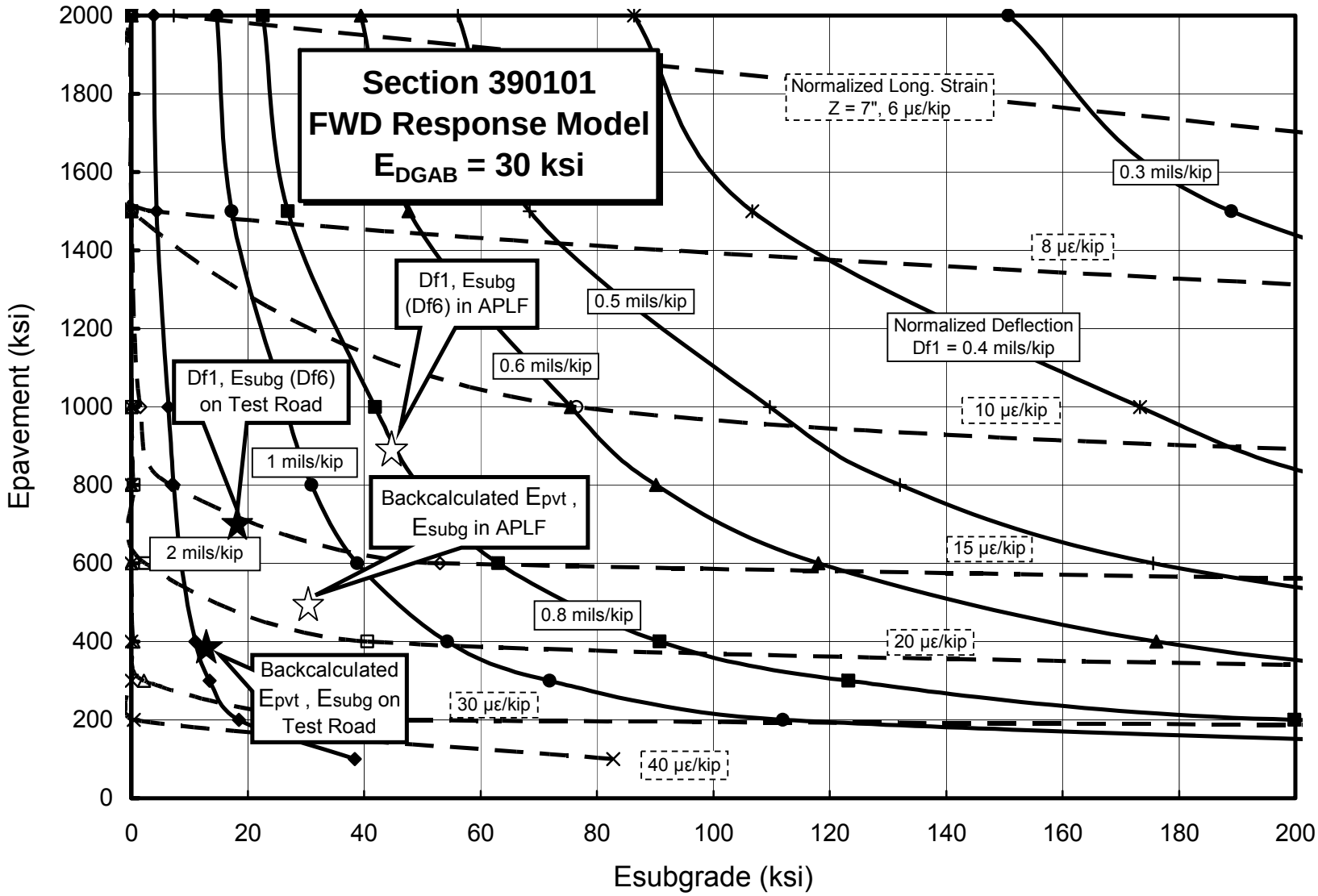

Figure 4.12 – Combined Relationship between Layer Moduli, Deflection and Strain Using FWD Geometry on Section 390101

CHAPTER 5
TRAFFIC LOADING ON TEST ROAD

General

A Mettler-Toledo (MT) weigh-in-motion (WIM) system was installed in the mainline test pavement at the time of construction to continuously monitor traffic loading in all four pavement lanes. In 1999, ODOT reported a truck loading of approximately 46,700 ESALs per month or 560,400 ESALs per year in the southbound driving lane and approximately 88,000 ESALs per month or 1,056,000 ESALs per year in the northbound driving lane between November 1997 and July 1998. In 2002, these estimates were revised to approximately 38,500 ESALs per month or 462,000 ESALs per year in both driving lanes between November 1997 and December 2001. Both estimates showed very consistent ESAL loadings over the reporting periods. Differences in the 1999 and 2002 ODOT estimates and the lack of traffic information from LTPP warranted this in-depth investigation of traffic loading on the test road. ODOT furnished ORITE with a copy of the unedited raw WIM files from the time the test road was opened to traffic in August 1996 through March 2003. Since the scope of this project was limited to the time the four distressed SPS-1 sections remained in service, this analysis of WIM data only extended through 1998.

Data Assessment

The southbound lanes of the test road were opened to traffic on Wednesday, 8/14/96 and the northbound lanes were opened the next day. The WIM system was calibrated on 8/15/96. A 13-axle superload weighing 209,820 lbs. (95 MPa) was monitored as it traveled in the northbound driving lane at 10:50 am on 8/15/96. The first regular WIM file recorded by ODOT was dated Thursday, 8/22/96. On this date, a total of 2,464 trucks were recorded in all four lanes during Hours 09-15 and in two lanes during Hours 16-23. From 8/23/96 to 10/27/96, data were only collected in the southbound passing lane. The 10/28, 10/29, 10/30, 11/1, 11/10 and 11/18 daily files were incomplete, in that data were only recorded during certain hours. With the exception of a few days when files were missing or unreadable, the magnitude of the daily WIM files from 10/28/96-12/2/96 appeared to be reasonable. From about noon on 12/3/96 until 11/11/97, all lanes on the test road were closed for the replacement of Sections 390101, 390102 and 390107. Therefore, the most complete WIM data for 1996 was between 10/28 and 12/2.

Tables 5.1 and 5.2 summarize lane closure dates and WIM maintenance activities on the mainline test road as documented by ODOT.

Table 5.1
Lane Closure Dates

Closure Dates	Direction	Reason for Closure
9/3/96-9/10/96	SB	Temporary repair of Sections 390102 and 390107
12/2/96-11/9/97	NB	Replacement of Sections 390101, 390102 and 390107
12/3/96-11/10/97	SB	Replacement of Sections 390101, 390102 and 390107
9/8/98-10/19/98	NB & SB	Replacement of Section 390105
3/28/01-6/1/01	SB	Controlled vehicle testing
3/28/01-5/31/01	NB	Controlled vehicle testing
3/7/02	SB	Section 390103 closed
4/24/02-11/20/03	SB	Replacement of Sections 390103, 390108, 390109 and 390110

Table 5.2
WIM Maintenance Records

Date	Maintenance Details
8/15/96	MT letter indicated calibration and start of 60 day acceptance period
1/2/97	MT letter indicated that the three load cells changed in the southbound lanes had been damaged by lightning. Nine damaged load cells in the northbound lanes will also be replaced.
7/8/97	MT work order indicated load cells 1-1, 1-2, 2-1, 2-3, and 2-4 were replaced
7/9/97	MT work order indicated load cells 3-1, 4-1 and 4-3 were replaced and two others were determined to be defective
7/9/97	MT work order indicated load cells 4-4 and 8-1 were replaced
5/20/98	MT work order indicated regular inspection and service. Replaced cell 4-1 and DSP3's. System working OK
5/21/98	MT work order indicated CPU was replaced
7/23/99	MT work order indicated surge protectors were replaced
8/4/99	MT work order indicated surge protector was replaced and phone wiring corrected

There was a reoccurring problem early on with electrical surges from lightning strikes entering the WIM and shutting it down. This happened shortly after the test road was opened to traffic and intermittently thereafter until Mettler-Toledo devised an adequate protection system. These surges and other problems caused the system to perform poorly until the load cells were replaced in July 1997, as indicated by the numerous small daily files recorded in 1996. This review of the WIM files included an assessment of how well the system functioned during the time Sections 390101, 390102, 390105 and 390107 remained in service, and an estimation of traffic loading during this time using the best data available.

During times when the SPS experiments were closed for extended maintenance or data collection, traffic was diverted to the service lanes where there was no traffic monitoring. On dates when the test road was open, traffic in the driving lanes was occasionally diverted to the passing lanes a few hours for short term maintenance or testing. Table 5.3 summarizes the size of the daily WIM files recorded during 1996-98 to provide an indication of their completeness. Weekday files would be expected to contain 200-300 KB of data, while weekends and holidays typically contained half this amount of data or less. Daily files in Table 5.3 fall into three general categories; very small files with little useful data such those recorded during the first couple of months after the test road was opened in 1996, files with the expected 200-300 KB of data, and files that appear to be excessively large such as those in 12/97 to 3/98. Shaded cells in Table 5.3 indicate when lanes on the test road were closed to traffic for substantial lengths of time.

Table 5.3
Magnitude of Daily WIM Files

WIM File Size (kb)																			
Date	1996					1997		1998											
	Aug	Sept	Oct	Nov	Dec	Nov	Dec	Jan	Feb	Mar	Apr	May	Jun	Jul	Aug	Sept	Oct	Nov	Dec
1		2	6	79	114		973	518	836	893	290	270	258	42	96	287	1	79	276
2		2	0	145	201		991	932	899	952	289	95	278	178	72	289	1	252	280
3		13	58	112	56		1020	842	933	952	270	80	287	130	65	291	0	271	285
4		12	13	281	1		1030	818	939	988	95	261	291	43	260	262	0	279	261
5		19	4		1		1060	877	862	474	83	282	263	66	277	87	1	278	95
6		15	6		1		811	719	1110	1240	254	278	107	121	268	52	0	253	69
7		4	13	0	0		726	916	867	1000	294	272	83	251	256	81	0	97	252
8		2	6	292	0		939	939	804	863	292	266	259	266	104	206	1	76	276
9		12	42	135	0		964	1020	422	930	288	102	280	259	66	1	2	257	274
10		12	13	33	0		987	808	993	923	207	77	288	248	72	1	0	81	271
11		10	6	265	0		1000	738	981	973	71	264	64	95	272	1	0	282	260
12		15	0	298			1120	873	999	1050	53	288	258	88	294	1	0	270	93
13		13	4	308		0	875	920	1160	570	242		103	241	269	0	0	248	76
14		6	13	304		0	782	962	908	90	273		91	250	263	1	2	91	248
15		4	15	285		0	969	896	893	33	284		258	268	108	1	2	75	278
16		11	57	132			1010	1110	1010	31	240		31	253	96	1	1	257	279
17		13	13	107		0	1020	812	951	157	265		95	237	152	1	0	277	277
18		3	14	199			1060	741	958	344	104		271	96	8	3	0	286	253
19		13	4	294			1150	960	1000	283	77		252	14	291	0	2	281	94
20		15	2	297			978	939	1150	257	258		102	233	283	0	58	271	73
21		5	6	310			879	946	608	87	285		73	252	260	1	290	105	253
22	137	5	13	289			1020	944	896	76	165		253	260	103	0	283	83	255
23	10	25	32	143			905	1050	931	260	296		272	259	86	0	258	258	238
24	6	10	13	115			1050	816	942	292	270		278	242	42	1	106	290	79
25	2	68	13	303		1120	749	693	513	288	64		278	99	182	1	80	149	9
26	10	7	5	311			1070	910	1000	285	78		262	85	278	2	257	53	19
27	6	10	4	286		1030	1030	928	1190	259	265	299	99		281	0	291	96	29
28	11	3	107	82		1020	979	952	936	27	294	298	10	244	259	2	290	62	111
29	12	5	91	141		1060	991	953		70	294	59	222	260	104	3	288	72	128
30	14	12	221	106		1200	932	1120		253	291	118	177	256	83	3	248	249	117
31	6		0				896	894		268		23		242	256		95		96
	SB lanes only					NB and SB lanes													

Each vehicle crossing the WIM system generated a row of data in the daily file delineated by fixed column widths, as shown in Figure 5.1. Additional spaces are available in the files to record more than the five axle weights and four axle spacings shown. Lanes were identified as NB driving (11), NB passing (12), SB passing (52) and SB driving (51). The objective of this research was to predict field performance from load and environmental trends developed in the APLF. One task within this objective was to determine hourly pavement loadings from WIM data on the test road during the period of time the four distressed SPS sections were in service.

Typical Data Showing Number of Digits in Field																			
W39	000721	51 (SBD), 52 (SBP), 11 (NBD), 12 (NBP)	98	03	29	04	09	000	0258 (2580 kg)	05	045 (4500 kg)	034 (3.4 m)	055 (5500 kg)	013 (1.3 m)	052 (5200 kg)	100 (10.0 m)	052 (5200 kg)	012 (1.2 m)	053 (5300 kg)
Card - State	Site	Dir. - Lane	Year	Month	Day	Hour	Vehicle Class	Open	Gross Wt.	No. Axles	W1	S1	W2	S2	W3	S3	W4	S4	W5

Figure 5.1 - WIM Data Format

An Excel spreadsheet was developed to calculate hourly traffic loadings by lane on the Ohio SHRP Test Road from the raw WIM files. ESALs were calculated using the following structural parameters for concrete: thickness (D) = 9.5" (24.1 cm), which was the average thickness of the 8 and 11-inch (20.3 and 27.9 cm) pavements in the SPS-2 experiment, initial serviceability (p_i) = 4.2, terminal serviceability (p_t) = 2.5, and serviceability at failure (p) = 1.5. Asphalt pavement parameters included a structural number (SN) of 4.75, p_i = 4.5, p_t = 2.5, and p = 1.5. The spreadsheet was limited to seven axles which covered all but a handful of trucks each day. Even on trucks with more than seven axles, the first seven axles were counted as a vehicle, so the only data lost were those few axles past the seventh axle. Class 2, 3, 14 and 15 vehicles, and vehicles with zero weight recorded on the first or second axle were filtered out. Loadings for the remaining vehicles were then converted into hourly weight and ESALs distributions by lane. Examples of the two-page spreadsheet summary for 12/11/98 are shown in Tables 5.4 and 5.5 .

Table 5.4

First Summary Page of Excel WIM Spreadsheet

DAILY/HOURLY WIM SUMMARY (1/2)

Print Page 1

Card:	W39	Site	721	Date:	12	11	98	Location:	DEL 23

Hourly Weight Summary - 11/24/96

Hour	Total Vehicle Wt. (K)	Total Number Vehicles	Wt. per Vehicle (K)	Total Weight by Lane (kips)				% Weight by Lane				Total Class 9 Wt. (K)	% Wt. Class 9
				11	12	52	51	11	12	52	51		
0	6593	124	53.2	3666	313	0	2614	55.6	4.7	0.0	39.6	5607	85.1
1	5479	107	51.2	3914	161	0	1404	71.4	2.9	0.0	25.6	4600	84.0
2	6247	117	53.4	3620	135	0	2493	57.9	2.2	0.0	39.9	5307	84.9
3	7607	156	48.8	4253	172	35	3147	55.9	2.3	0.5	41.4	6000	78.9
4	7147	129	55.4	3919	283	248	2697	54.8	4.0	3.5	37.7	6112	85.5
5	7624	153	49.8	4541	10	36	3037	59.6	0.1	0.5	39.8	6016	78.9
6	7992	164	48.7	3413	263	296	4020	42.7	3.3	3.7	50.3	6604	82.6
7	9628	188	51.2	3822	409	621	4776	39.7	4.2	6.4	49.6	7767	80.7
8	10414	226	46.1	4815	456	480	4663	46.2	4.4	4.6	44.8	8628	82.8
9	12824	269	47.7	6034	784	401	5605	47.1	6.1	3.1	43.7	11223	87.5
10	13441	296	45.4	5446	936	927	6132	40.5	7.0	6.9	45.6	11455	85.2
11	13325	292	45.6	6093	851	993	5388	45.7	6.4	7.4	40.4	11368	85.3
12	12891	294	43.8	5932	694	754	5510	46.0	5.4	5.9	42.7	11218	87.0
13	13919	305	45.6	6554	639	938	5788	47.1	4.6	6.7	41.6	12082	86.8
14	12298	280	43.9	4128	827	576	6767	33.6	6.7	4.7	55.0	10499	85.4
15	11257	252	44.7	4270	635	672	5680	37.9	5.6	6.0	50.5	10004	88.9
16	11920	254	46.9	4270	772	850	6028	35.8	6.5	7.1	50.6	10485	88.0
17	10217	222	46.0	3076	385	948	5808	30.1	3.8	9.3	56.8	9076	88.8
18	8801	188	46.8	3174	343	261	5023	36.1	3.9	3.0	57.1	7955	90.4
19	8393	168	50.0	3075	526	401	4391	36.6	6.3	4.8	52.3	7528	89.7
20	8060	161	50.1	3453	204	360	4043	42.8	2.5	4.5	50.2	7484	92.9
21	6431	131	49.1	2322	180	230	3699	36.1	2.8	3.6	57.5	5737	89.2
22	6131	111	55.2	2196	418	201	3317	35.8	6.8	3.3	54.1	4998	81.5
23	5086	97	52.4	2366	248	105	2367	46.5	4.9	2.1	46.5	4210	82.8
Total	223726	4684	47.8	98354	10642	10334	104396					191963	
Averge (%)								44.0	4.8	4.6	46.7		85.8

ESAL Input
(Fill in all blue cells)

Concrete	
D (in.)	9.5
pi (initial)	4.2
pt (terminal)	2.5
p (failure)	1.5

Asphalt	
Structural No.	4.75
pi (initial)	4.5
pt (terminal)	2.5
p (failure)	1.5

Reference Load	
Ref. Wt. (K)	18
Ref. Axles	1

Pavement Type Code	
Lane ID (Max - 4 Lanes)	AC - 1 PCC - 2
11	2
12	2
52	1
51	1

Daily Volume/Weight Summary

Parameter	Daily Volume						Daily Weight (Kips, Kips/Vehicle)					
	Lane					Class 9	Lane					Class 9
	All	11	12	52	51		All	11	12	52	51	
Total	4682	2123	241	212	2106	3669	223726	98354	10642	10334	104396	191963
%		45.3	5.1	4.5	45.0	78.4		44.0	4.8	4.6	46.7	85.8
Per Vehicle							47.78	46.33	44.16	48.75	49.57	52.32

Lane Code	
Lane No.	Lane Description
11	NB Driving
12	NB Passing
52	SB Passing
51	SB Driving

Table 5.5

Second Summary Page of Excel WIM Spreadsheet

DAILY/HOURLY WIM SUMMARY (2/2)

Print Page 177

Card:	W39	Site:	721	Date:	12	11	98	Location:	DEL 23

Hourly ESAL Summary - 11/24/96

Hour	Total Vehicle ESALs	Total Number Vehicles	ESALs per Vehicle	Total ESALs by Lane				% ESALs by Lane			
				11	12	52	51	11	12	52	51
0	133	124	1.07	81	9	0	44	60.6	6.5	0.0	32.9
1	102	107	0.95	80	4	0	18	78.9	3.9	0.0	17.2
2	127	117	1.08	81	5	0	41	64.0	3.6	0.0	32.4
3	133	156	0.85	87	2	0	44	65.0	1.6	0.1	33.3
4	164	129	1.27	104	6	4	49	63.5	3.7	2.7	30.1
5	162	153	1.06	101	0	0	60	62.6	0.0	0.1	37.3
6	146	164	0.89	63	3	4	76	43.4	2.2	2.8	51.6
7	242	188	1.29	93	12	20	116	38.7	4.9	8.4	48.0
8	208	226	0.92	101	8	10	88	48.9	3.9	4.9	42.3
9	266	269	0.99	137	19	6	105	51.3	7.1	2.3	39.3
10	238	296	0.80	108	15	13	102	45.4	6.4	5.3	43.0
11	260	292	0.89	116	18	26	100	44.7	6.9	10.0	38.4
12	216	294	0.73	111	10	17	77	51.5	4.6	8.0	35.8
13	244	305	0.80	128	13	14	89	52.5	5.4	5.8	36.3
14	225	280	0.80	67	14	10	134	29.6	6.1	4.6	59.7
15	192	252	0.76	77	11	12	92	40.1	5.8	6.3	47.8
16	229	254	0.90	73	18	18	120	31.7	7.7	8.1	52.5
17	178	222	0.80	55	6	15	101	30.9	3.6	8.6	56.8
18	161	188	0.85	58	6	14	83	36.4	3.4	8.6	51.5
19	163	168	0.97	74	10	6	73	45.4	6.1	3.6	44.9
20	157	161	0.97	76	2	7	72	48.3	1.1	4.7	45.8
21	114	131	0.87	41	3	5	65	36.2	2.3	4.7	56.8
22	134	111	1.20	44	11	2	77	32.6	8.3	1.8	57.2
23	93	97	0.96	43	4	1	44	46.4	4.8	0.9	47.8
Total	4286	4684	0.91	2001	208	207	1869				
Average (%)								46.7	4.9	4.8	43.6

Daily ESAL Summary

Daily Loading (ESALs, ESALs/Vehicle)						Daily Class 9 Loading (ESALs, ESALs/Vehicle)					
Parameter	Lane					Parameter	Lane				
	All	11	12	52	51		All	11	12	52	51
Total ESALs	4286	2001	208	207	1869	ESALs	3704	1731	195	180	1599
% in Lane		46.7	4.9	4.8	43.6	No. 9 Veh.	3670	1664	196	165	1642
ESALs/Truck	0.92	0.94	0.86	0.98	0.89	ESAL/Veh.	1.01	1.04	0.99	1.09	0.97

Daily Weight Distribution

Load Range (K)	Number of Trucks in Range				
	Lane				Class 9 All lanes
	11	12	52	51	
0-10	22	12	8	31	1
10-20	157	21	17	122	21
20-30	212	19	17	122	142
30-40	611	74	49	582	1166
40-50	300	31	28	329	594
50-60	233	28	23	297	514
60-70	180	15	22	138	303
70-80	351	25	23	275	648
80-90	54	16	23	194	269
90-100	2	0	0	5	3
100-110	0	0	1	5	5
110-120	1	0	0	5	3
120-130	0	0	0	1	0
130-140	0	0	1	0	0
140-150	0	0	0	0	0
150-160	0	0	0	0	0

Daily ESAL Distribution

ESALs / Truck	No. Trucks in Range				
	11	12	52	51	Class 9
0-2	1666	182	165	1685	2829
2-4	386	32	27	362	756
4-6	36	10	5	10	55
6-8	3	0	1	1	3
8-10	1	0	1	2	3
10-12	0	0	1	2	3
12-14	0	0	0	2	2
14-16	0	0	0	0	0
16-18	0	0	0	0	0
18-20	0	0	0	1	1
20-22	0	0	0	0	0
22-24	0	0	0	0	0
24-26	0	0	0	0	0
26-28	0	0	0	0	0
28-30	0	0	0	0	0

File sizes in Table 5.3 suggested the 1996 WIM data was most complete between 10/28 and 12/2, which was just before the test road was closed for the replacement of Sections 390101, 390102 and 390107. These files, which were about the correct size, contained truck weights larger than those normally observed on similar pavements around Ohio and larger than seemed likely for the indicated vehicle geometries. Table 5.6 shows the distributions of gross truck weights on 11/11/96 and 12/11/98. These dates were selected for comparison because of the similarity in the size of these two WIM files. The 12/11/98 loading distribution is representative of that normally observed on major routes in Ohio, while the 11/11/96 loading distribution, though reasonable in Lanes 11, 12 and 52, is clearly quite suspicious in Lane 51. At a minimum, there are too many light vehicles weighing less than 20 kips (9.1 MPa) and too many exceptionally heavy vehicles weighing more than 90 kips (40.8 MPa).

Table 5.6
Distribution of Truck Weights

Daily Distribution of Gross Truck Weights										
Load Range (kips)	11/11/96 (265 KB)					12/11/98 (260 KB)				
	Lane				Class 9 All lanes	Lane				Class 9 All lanes
	11	12	52	51		11	12	52	51	
0-10	11	10	27	794	4	22	12	8	31	1
10-20	113	15	24	244	20	157	21	17	122	21
20-30	129	22	33	102	77	212	19	17	122	142
30-40	488	57	48	186	620	611	74	49	582	1166
40-50	242	24	22	381	561	300	31	28	329	594
50-60	191	17	21	224	387	233	28	23	297	514
60-70	123	11	14	171	277	180	15	22	138	303
70-80	343	22	19	148	508	351	25	23	275	648
80-90	89	12	5	123	204	54	16	23	195	270
90-100	13	1	4	170	170	2	0	0	5	3
100-110	4	0	3	158	150	0	0	1	5	5
110-120	0	0	2	103	90	1	0	0	5	3
120-130	0	0	0	40	36	0	0	0	1	0
130-140	0	0	0	12	12	0	0	1	0	0
140-150	0	0	0	2	2	0	0	0	0	0
Total	1746	191	223	2859	3118	2123	241	212	2107	3670

An examination of the first set of tandem axles also suggested there was a problem with axle spacings in the 1996 Lane 51 data. Figures 5.2 and 5.3 show the distribution of axle spacings between the second and third axles in Lane 51 on 11/11/96 and 12/11/98, respectively,

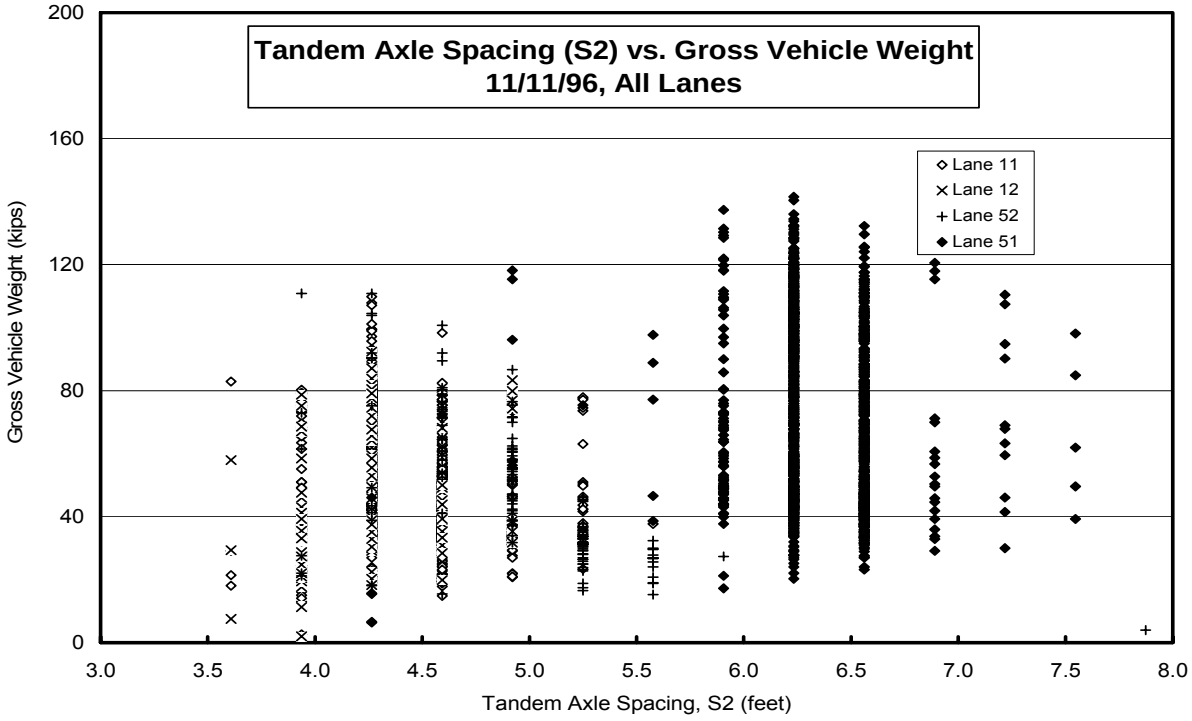

Figure 5.2 – Tandem Axle Spacing on 11/11/96

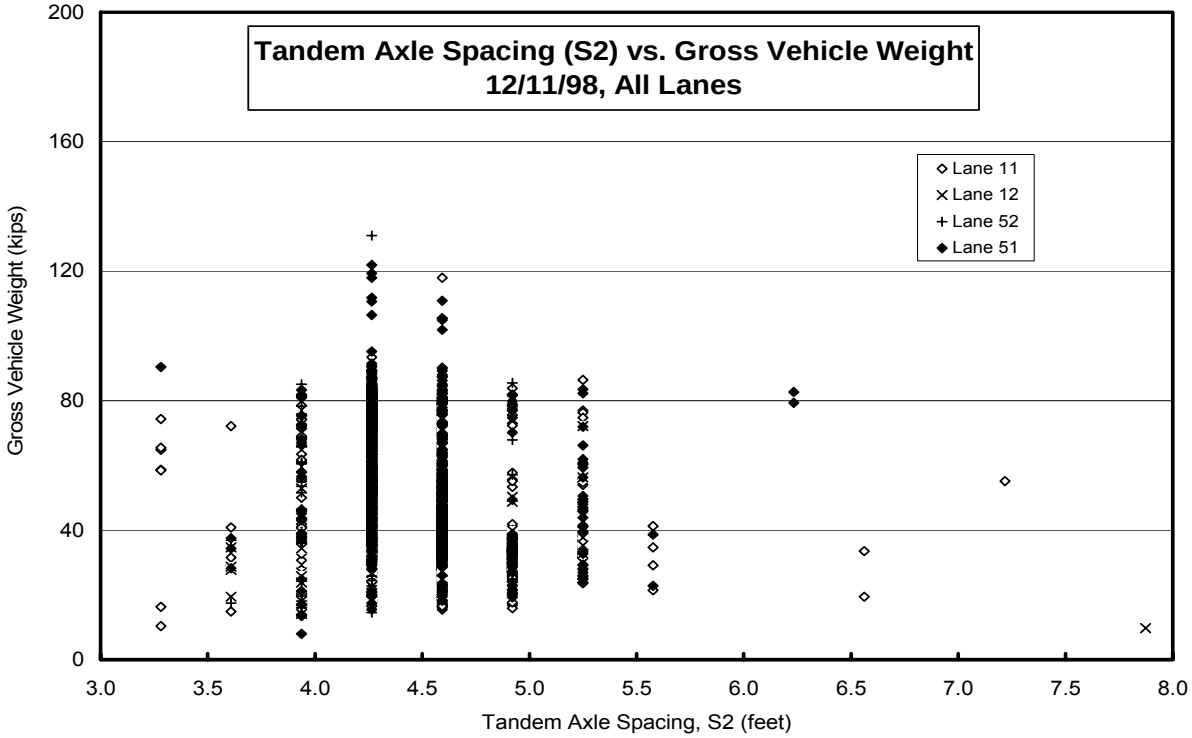

Figure 5.3 – Tandem Axle Spacing on 12/11/98

which represents the first set of tandem axles on Class 9 vehicles. Axle spacings of 4.9 – 7.5 feet (1.5-2.3 m) in Lane 51 on 11/11/96 were consistently higher than the 3.3 – 5.6 feet (1.0-1.7 m) observed in the other three lanes on that date and in all four lanes on 12/11/98. Consequently, the 1996 Lane 51 axle spacings are considered to be too high, which would contribute to the exceptionally large number of vehicles at the lower end of the distribution through a misclassification of Class 2 and 3 vehicles as Class 4 and 5 vehicles. It appears as though the 1996 axle spacings in Lane 51 were approximately 50% too high. A similar problem with the axle weights would account for the upward shift of vehicles in the weight distribution and the unusually large number of vehicles in the high weight ranges.

An examination of the large files between 11/25/97 and 3/13/97 revealed two problems. First, these files consisted of about 80% Class 2 and Class 3 vehicles, which are not typically recorded at WIM sites because of their negligible effect on ESAL loading and overall pavement performance. These vehicles were filtered out for this study. Second, vehicles in Lane 51 were recorded as being in Lane 52 and visa versa. Although this error continued through 12/9/98, WIM data after the middle of March 1998 was vastly improved. The incorrect lane designations in 1998 were also corrected during this analysis.

Weekly vehicle counts were adopted as the basic WIM unit to estimate traffic loading because they include both weekday and weekend counts which, as expected, were significantly different. Weekly counts also include cycles where trucks leave their home base loaded on certain days of the week and return lighter on other days within the same week. Weekly samples of WIM data were selected during November 1996 (Lanes 11, 12 and 52 only), December 1997, and ten months in 1998 to determine average weekly traffic loading on the test road. Table 5.7 summarizes the volume, weight and ESAL data calculated for these fourteen weekly periods. Selected data in the table for the two weeks in 1996 were shaded as a reminder that weights and ESALs in Lane 51 were incorrect. This problem not only affects the data for lane 51, but also other parameters containing Lane 51 data, such as totals and averages for all lanes and for Class 9 vehicles. Separate averages are shown for 1996 and 1997-98 data. WIM summaries for each day within these fourteen weeks are shown in Appendix K.

Table 5.7 – Weekly WIM Totals

Ohio SHRP Test Road Total Weekly WIM Totals																						
Week	Avg. Date	Total Weekly Volume (Classes 4-13)						Total Weekly Weight (Kips)						Total Weekly ESALs					Total Weekly Class 9 ESALs				
		Lane					Class 9	Lane					Class 9	Lane					Lane				
		All	11	12	52	51		All	11	12	52	51		All	11	12	52	51	All	11	12	52	51
11/11-17/96	11/14/96	32426	11214	1105	1571	18536	19520	1449522	553425	50144	58995	786958	1187272	45697	12358	1094	941	31304	39691	10500	1004	814	27374
11/18-24/96	11/21/96	32471	11274	1210	1795	18192	19808	1436224	552638	53352	66472	763762	1181712	42820	12158	1131	1002	28529	37252	10407	1022	887	24936
Weekly Avg.	1996	32449	11244	1158	1683	18364	19664	1442873	553032	51748	62733	775360	1184492	44259	12258	1112	972	29917	38472	10454	1013	850	26155
Note: Data in the shaded cells are incorrect due to axle weights in Lane 51 being too high																							
12/15-21/97	12/18/97	29517	13460	1554	1338	13165	21527	1383429	616056	62169	56957	648247	1160342	28471	13387	1339	1025	12720	24150	11322	1198	861	10768
1/19-25/98	1/22/98	27021	12315	1391	1245	12070	19692	1275218	566701	55897	52944	599676	1071457	26563	12362	1243	1000	11959	22734	10669	1136	887	10042
2/16-22/98	2/19/98	28269	12822	1548	1329	12570	20119	1315825	585597	62842	56470	610915	1073612	26972	12431	1362	1114	12064	22044	10255	1122	941	9726
4/4-10/98	4/7/98	27250	12326	1456	1221	12247	20750	1340353	580421	64333	58007	637591	1131603	27851	12432	1413	1163	12844	23832	10708	1247	1025	10852
5/4-10/98	5/7/98	27772	11880	2063	1256	12573	20973	1344007	562840	94247	57103	629818	1135101	27263	12279	2221	967	11795	23250	10543	1938	835	9934
6/1-7/98	6/4/98	28377	12804	1573	1235	12765	21049	1360168	601779	70693	52882	634813	1140844	27662	13178	1644	899	11941	23535	11250	1483	795	10007
7/11-17/98	7/14/98	26079	11846	1537	1165	11531	18793	1213890	534990	64108	50886	563905	1009222	24693	11399	1352	1003	10940	20985	9814	1175	881	9115
8/11-17/98	8/14/98	27294	12360	1645	1333	11956	19788	1278021	568598	68923	56650	583850	1070723	25947	12276	1497	1068	11107	22244	10590	1322	929	9403
8/31-9/6/98	9/2/98	27575	12327	1583	1187	12478	20339	1321567	572484	68191	53089	627803	1096796	26987	12262	1467	993	12265	22747	10510	1276	837	10124
11/2-8/98	11/5/98	27144	12352	1438	1058	12296	20894	1324034	583726	62313	48719	629277	1124811	27577	12779	1360	942	12496	23628	11025	1253	826	10525
12/7-13/98	12/10/98	27007	12470	1376	1091	12070	20921	1314281	587170	60532	53282	613297	1116583	26517	12294	1271	1103	11849	22781	10663	1168	989	9961
12/14-20/98	12/17/98	26927	12252	1458	1223	11994	21016	1311524	578222	66524	57686	609092	1117459	26031	11987	1409	1069	11566	22271	10274	1266	956	9774
Weekly Avg.	1997-98	27519	12435	1552	1223	12310	20488	1315193	578215	66731	54556	615690	1104046	26878	12422	1465	1029	11962	22850	10635	1299	897	10019

Ohio SHRP Test Road Weekly WIM Averages per Vehicle																						
Week	Avg. Date							Average Weekly Weight /Vehicle (Kips)						Avg. Weekly ESALs/Vehicle					Avg. ESALs/Class 9 Vehicle				
								Lane					Class 9	Lane					Lane				
								All	11	12	52	51		All	11	12	52	51	All	11	12	52	51
11/11-17/96	11/14/96							44.70	49.35	45.38	37.55	42.46	60.82	1.41	1.10	0.99	0.60	1.69	1.22	0.94	0.91	0.52	1.48
11/18-24/96	11/21/96							44.23	49.02	44.09	37.03	41.98	59.66	1.32	1.08	0.93	0.56	1.57	1.15	0.92	0.84	0.49	1.37
Average/Veh.	1996							44.47	49.19	44.74	37.29	42.22	60.24	1.36	1.09	0.96	0.58	1.63	1.19	0.93	0.88	0.51	1.42
Note: Data in the shaded cells are incorrect due to axle weights in Lane 51 being too high																							
12/15-21/97	12/18/97							46.87	45.77	40.01	42.57	49.24	53.90	0.96	0.99	0.86	0.77	0.97	0.82	0.84	0.77	0.64	0.82
1/19-25/98	1/22/98							47.19	46.02	40.18	42.53	49.68	54.41	0.98	1.00	0.89	0.80	0.99	0.84	0.87	0.82	0.71	0.83
2/16-22/98	2/19/98							46.55	45.67	40.60	42.49	48.60	53.36	0.95	0.97	0.88	0.84	0.96	0.78	0.80	0.72	0.71	0.77
4/4-10/98	4/7/98							49.19	47.09	44.18	47.51	52.06	54.54	1.02	1.01	0.97	0.95	1.05	0.87	0.87	0.86	0.84	0.89
5/4-10/98	5/7/98							48.39	47.38	45.68	45.46	50.09	54.12	0.98	1.03	1.08	0.77	0.94	0.84	0.89	0.94	0.67	0.79
6/1-7/98	6/4/98							47.93	47.00	44.94	42.82	49.73	54.20	0.97	1.03	1.05	0.73	0.94	0.83	0.88	0.94	0.64	0.78
7/11-17/98	7/14/98							46.55	45.16	41.71	43.68	48.90	53.70	0.95	0.96	0.88	0.86	0.95	0.80	0.83	0.76	0.76	0.79
8/11-17/98	8/14/98							46.82	46.00	41.90	42.50	48.83	54.11	0.95	0.99	0.91	0.80	0.93	0.81	0.86	0.80	0.70	0.79
8/31-9/6/98	9/2/98							47.93	46.44	43.08	44.73	50.31	53.93	0.98	0.99	0.93	0.84	0.98	0.82	0.85	0.81	0.70	0.81
11/2-8/98	11/5/98							48.78	47.26	43.33	46.05	51.18	53.83	1.02	1.03	0.95	0.89	1.02	0.87	0.89	0.87	0.78	0.86
12/7-13/98	12/10/98							48.66	47.09	43.99	48.84	50.81	53.37	0.98	0.99	0.92	1.01	0.98	0.84	0.86	0.85	0.91	0.83
12/14-20/98	12/17/98							48.71	47.19	45.63	47.17	50.78	53.17	0.97	0.98	0.97	0.87	0.96	0.83	0.84	0.87	0.78	0.81
Average/Veh.	1997-98							47.80	46.51	42.94	44.69	50.02	53.89	0.98	1.00	0.94	0.84	0.97	0.83	0.86	0.83	0.74	0.81

Figures 5.4 and 5.5 show plots of the data presented in Table 5.7. Lanes 11, 12 and 52 in 1996 were added to the plots to provide some visual indication as to traffic loading trends over this two year period of time. In general, total volume, weight and ESALs increased slightly in Lanes 11 and 12 between 1996 and 1998, while total volume and weight decreased in Lane 52. The simultaneous decreases of volume and weight in Lane 52 resulted in total ESALs remaining constant. Lanes 11 and 12 showed notable decreases in average weight and ESALs per vehicle from 1996 to 1997, followed by a slight continuous increase into 1998. Lane 52 was different in that average weight and ESALs per vehicle both jumped from 1996 to 1997 and continued to increase slightly into 1998. These trends are somewhat tenuous since the 1996 data are based on only two consecutive weekly periods in November. Overall, the weekly ESAL loadings, while having some hourly and daily cycles, appear to be quite uniform from 1996 through 1998.

Accumulated ESAL Loading

Considering the scarcity of valid WIM data on the test road until the latter part of 1997, any projections of ESAL loading for 1996, especially in Lane 51, will require some assumptions and a leap of faith. Procedures for estimating 1996 ESAL loading in Lane 51 included: 1) extrapolation of the 1997-98 weekly loadings directly back to 1996, and 2) adjustments of the 1997-98 weekly loading in Lane 51 back to 1996 using comparisons of Lanes 11 and 52 data recorded in 1996 and in 1997-98. Since there are no independent means to determine which projection is best, all were used to define a band of accumulated ESAL loadings on the test road, in the hope that there would be little practical difference between the band limits.

To calculate accumulated traffic loadings, weekly ESAL loadings in Table 5.7 were divided by seven to obtain daily averages prorated for five weekdays and two weekend days. The average daily loading for Lane 11 in 1996 was 1,751 (12,258/7) ESALs per day while the average daily loadings for Lanes 11 and 51 in 1997-98 were 1,775 (12,422/7) and 1,709 (11,962/7) ESALs per day, respectively. Adjusting the 1,709 ESALs per day in Lane 51 by the ratio of Lane 11 ESALs measured in 1996 and 1997-98 gives 1,686 ESALs per day, and adjusting the 1,709 ESALs per day in Lane 51 by the ratio of Lane 52 ESALs measured in 1996 and 1997-98 gives 1,616 ESALs per day. Thus, the 1996 estimated loading rates of 1,616, 1,686 and 1,709 ESALs per day in Lane 51 can be represented by a band bounded by daily rates of 1,616 and 1,709 ESALs.

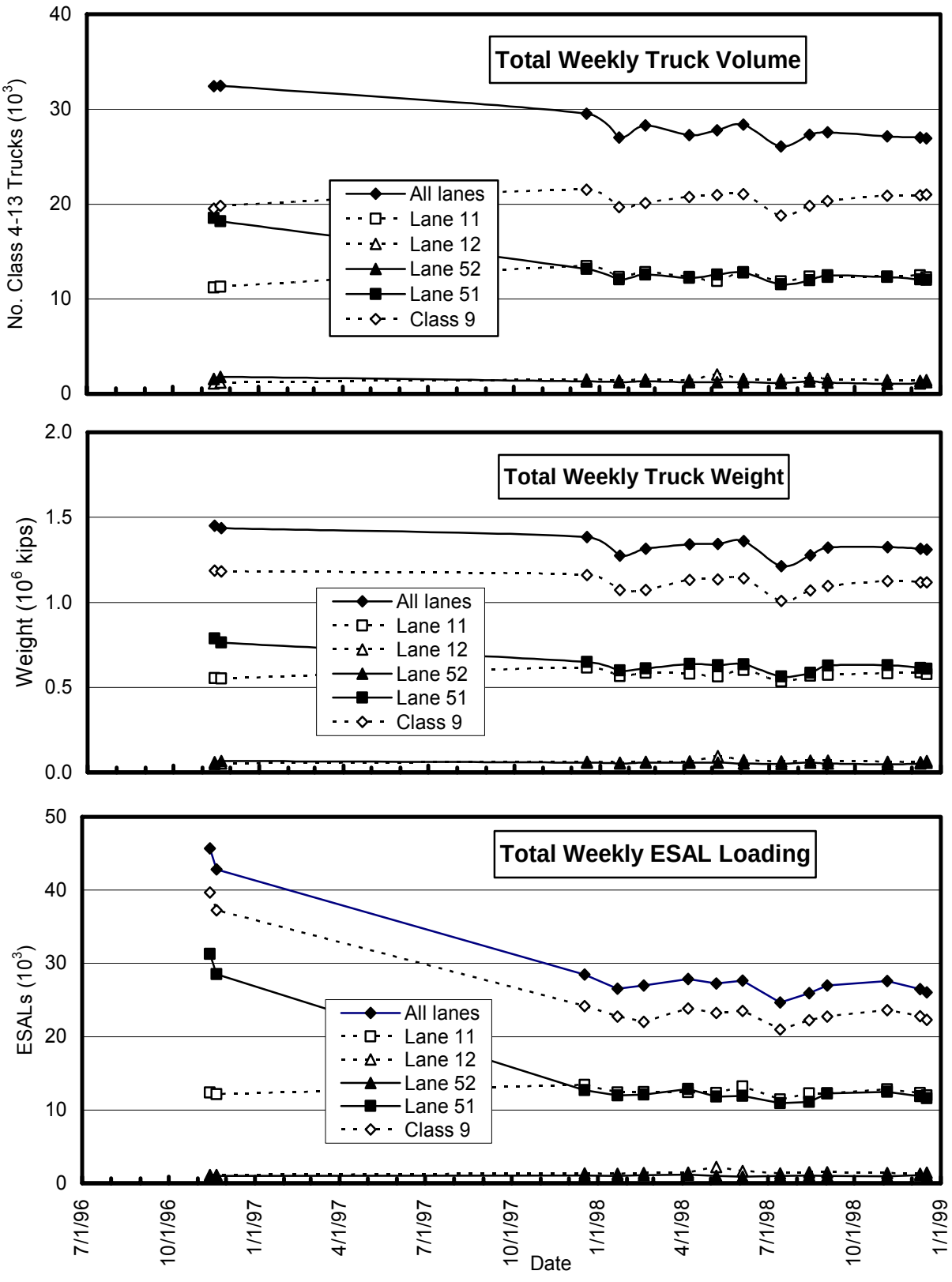

Figure 5.4 – Total Weekly Lane Loadings during 1996-98

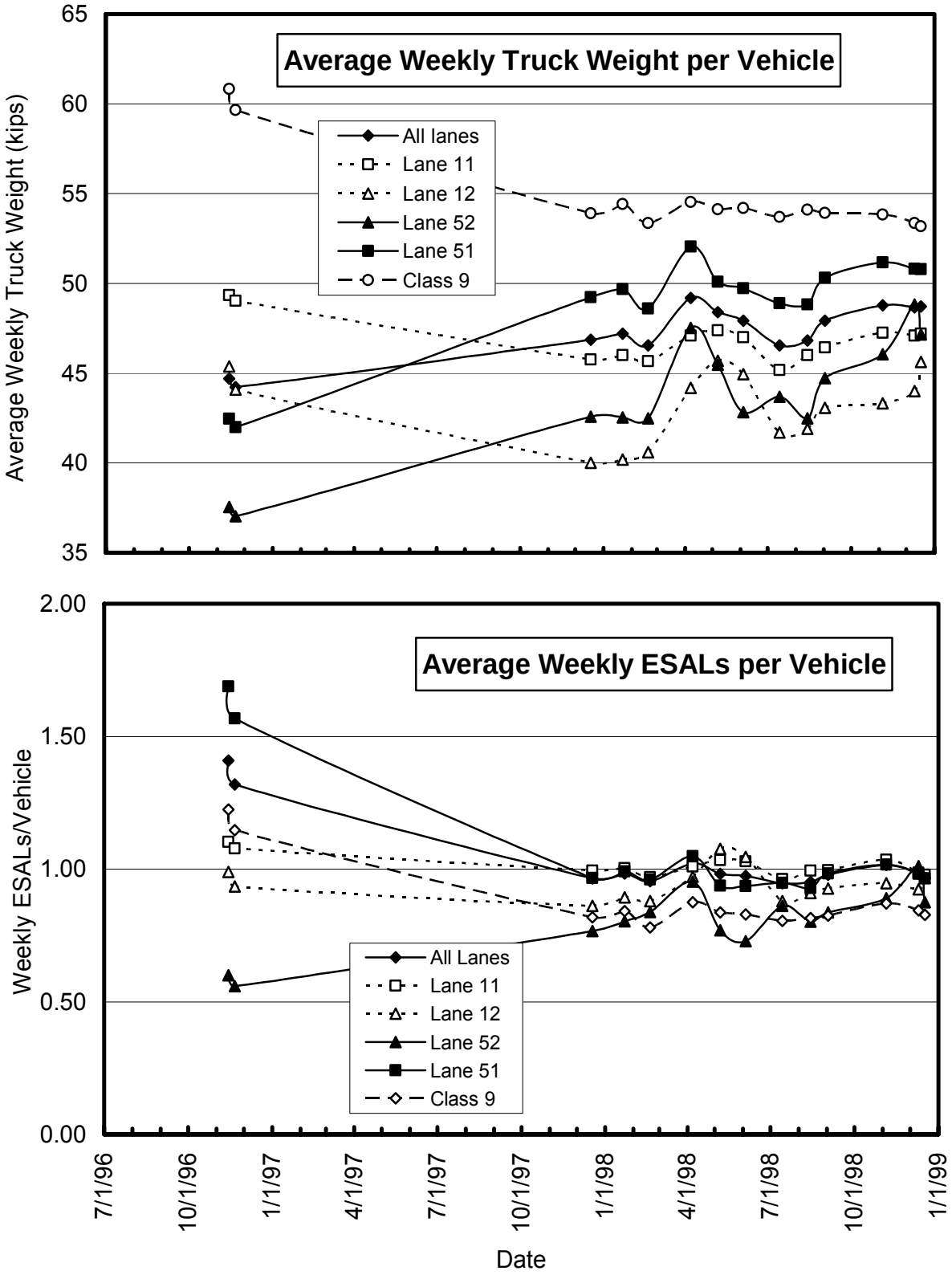

Figure 5.5 – Unit Truck Loading during 1996-98

Figure 5.6 shows plots of the estimated number of accumulated ESALs in Lanes 11 and 51 using daily loadings of 1,751 (1996) and 1,775 (1997-98) ESALs for Lane 11, and daily loadings of 1,616 (adjusted 1996, Lane 52) and 1,709 (1997-98) ESALs for Lane 51. Also shown for both lanes are the 1997-98 loadings extrapolated back through 1996. Because of the lack of early data and the uniform rates of loading observed in 1998, the straight line representations of ESAL loadings in Figure 5.6 seem quite appropriate. Figure 5.6 shows no practical difference between the methods used to calculate ESALs in either lane, and approximately the same ESAL loading rate occurred in the northbound (Lane 11) and southbound (Lane 51) driving lanes. Differences in accumulated ESAL loadings in the northbound and southbound directions on a given date can be attributed to the 9/3-9/10/96 closure in Lane 51 only and the difference in average weekly ESAL loading. The average daily ESAL rate of 1,763 in Lane 11 translates to 12,340 ESALs per week, 52,890 ESALs per month or 643,495 ESALs per year, and the average daily ESAL rate of 1,663 in Lane 51 translates to 11,640 ESALs per week, 49,890 ESALs per month or 606,995 ESALs per year. Lane 12 carried 10.1% of the ESALs carried in Lane 11, and Lane 52 carried 8.6% of the ESALs carried in Lane 51 during the fourteen weeks sampled.

Based upon the calculated loading rate for Lane 51, Sections 390102 and 390107 carried some 33,000 ESALs by the time the southbound lanes were closed to traffic on 9/3/96 for temporary rehabilitation of these sections. By this time, both sections had developed rut depths approximately ½-inch (1.3 cm) deep in less than three weeks of service. Section 390101 carried some 170,000 ESALs by 12/3/96 when the test road was closed for the replacement of three distressed SPS-1 sections. It also had ruts about ½-inch (1.3 cm) deep at the time of closure. By 5/29/98, when Section 390105 experienced a sudden localized failure in the right wheel path, the southbound driving lane had carried approximately 510,000 ESALs.

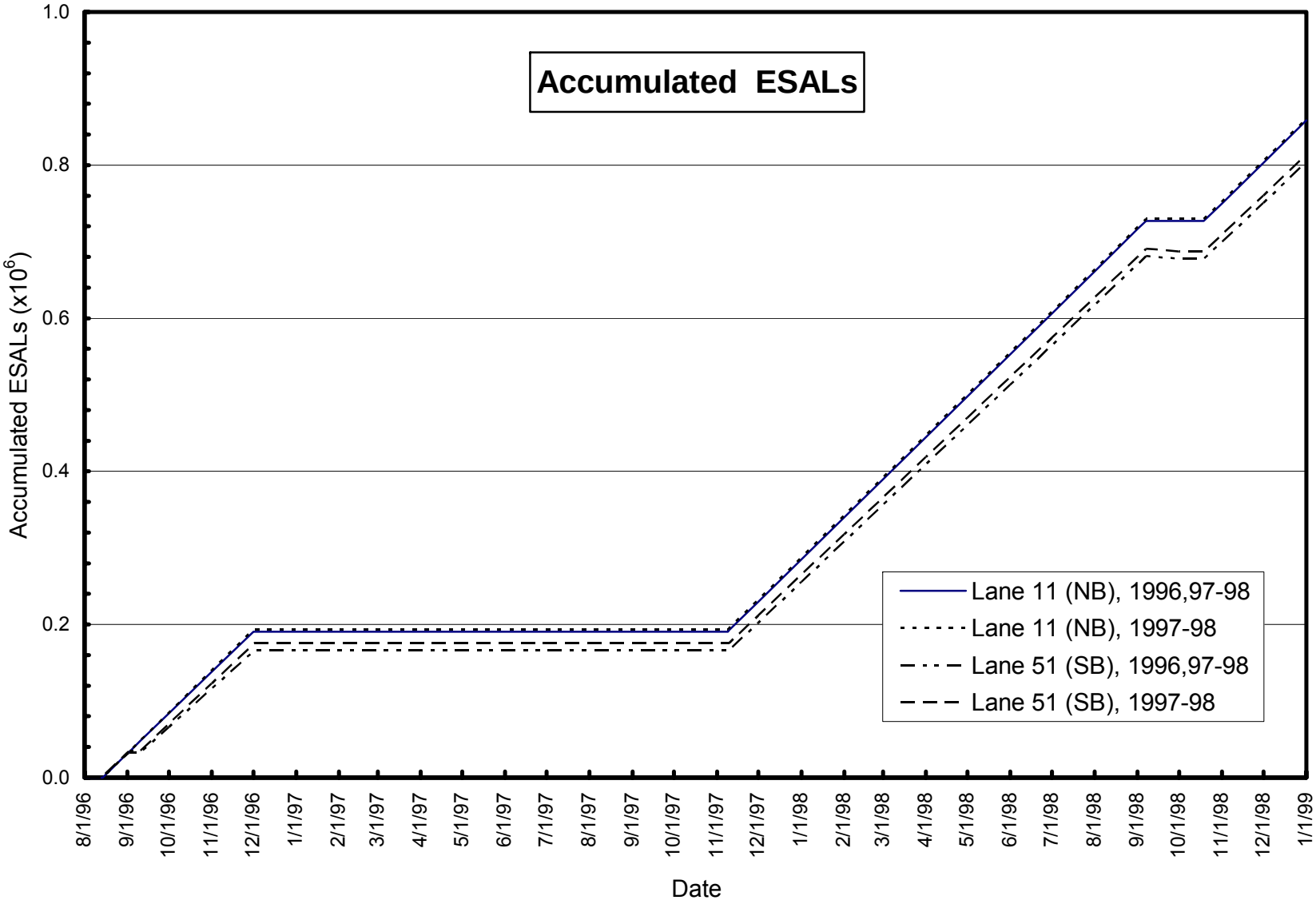

Figure 5.6 – Accumulated ESALs for 1996-98

Loading Patterns

Total hourly truck volumes, weights and ESALs calculated for the week of 1/19-25/98 are plotted in Figure 5.7 to show hourly and daily loading patterns. All three load parameters displayed sinusoidal daily cycles with the midday peaks being two to three times higher than the night time valleys. The magnitudes and loading patterns were quite similar on all five week days. The percentage of Class 9 vehicles, which are the standard 18-wheel, five-axle semi-tractor trailer, varied from about 60 – 70% at midday to about 80 – 90% at night. The passing lanes carried approximately 10% of the load carried in the driving lanes and the northbound loading was about the same as the southbound loading.

Figure 5.8 shows the same sinusoidal cycling for average weight and average ESALs measured per truck, except that the peaks are shifted 180º or 12 hours. This shift resulted from the higher volume of light trucks being observed during the day and a higher percentage of Class 9 trucks traveling at night. These differences provide higher average weights and higher average ESALs per truck at night than during the day.

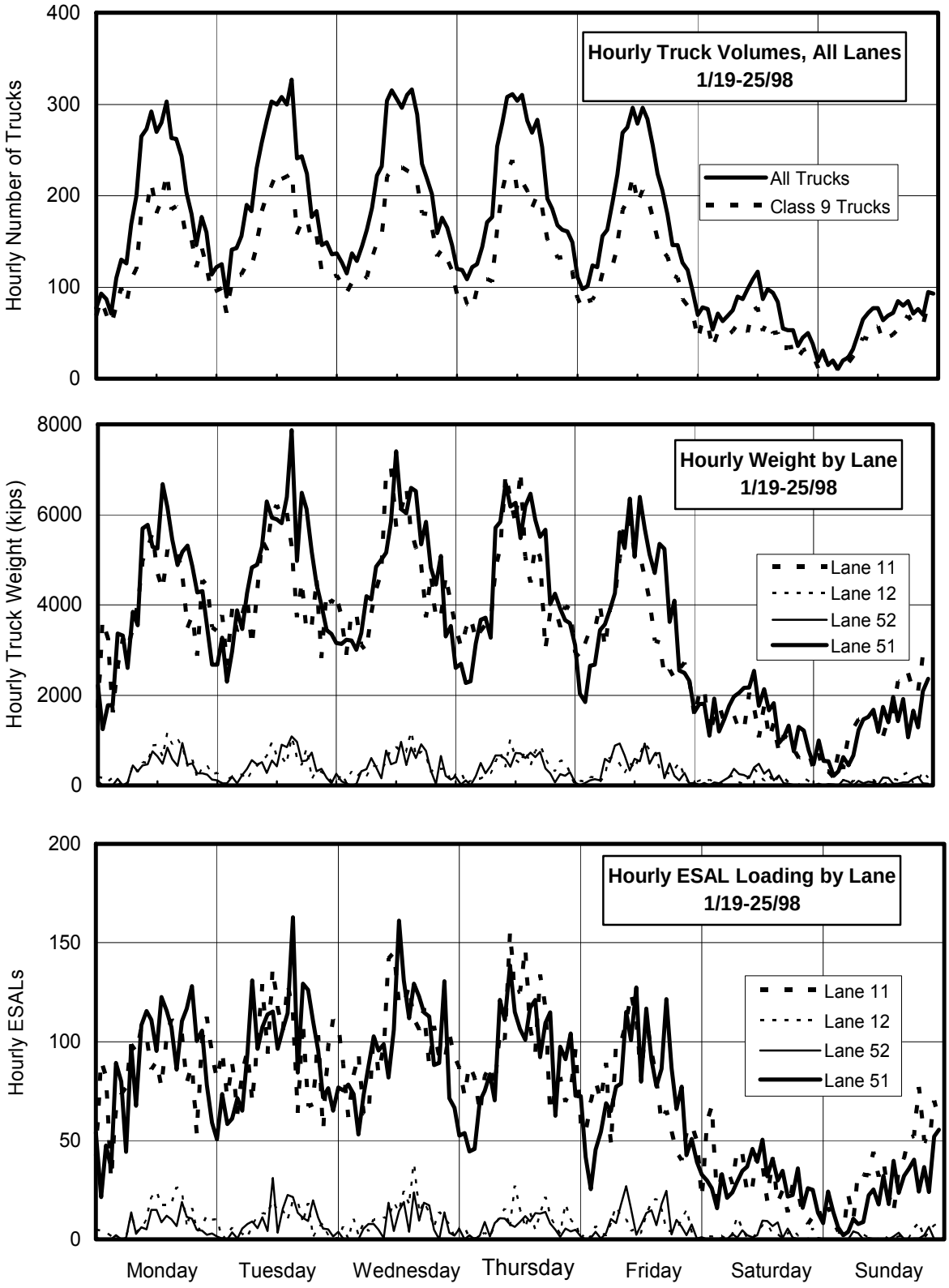

Figure 5.7 – Total Hourly Truck Volumes, Weights and ESALs during Week of 1/19-25/98

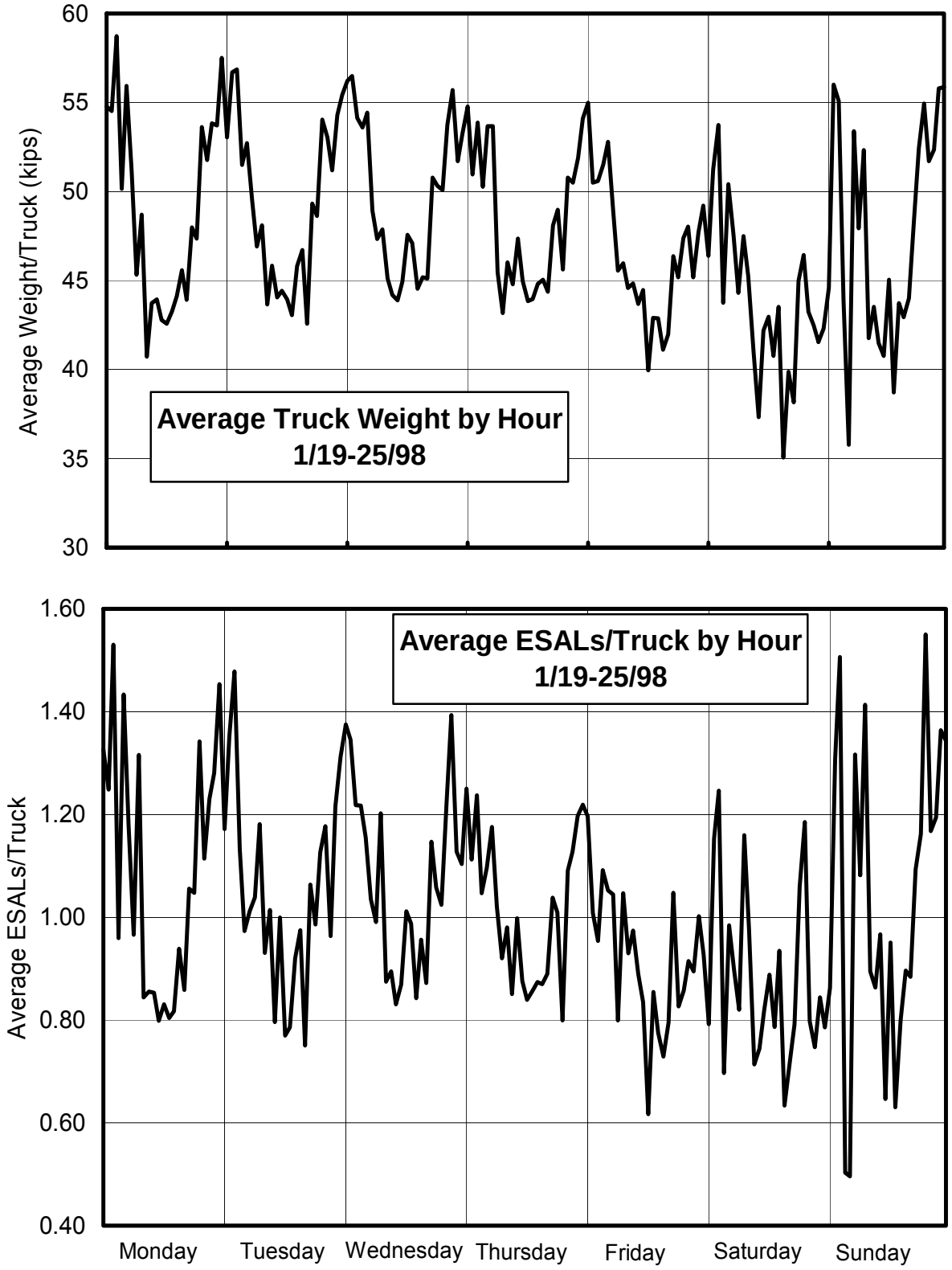

Figure 5.8 – Unit Hourly Weights and ESALs during Week of 1/19-25/98

CHAPTER 6

CONCLUSIONS

1. The relative order of FWD composite stiffness was the same for the four test sections on the test road and in the APLF. However, the APLF sections were stiffer than the test road sections because of less subgrade moisture in the APLF.

2. All responses measured during the controlled vehicle tests on the test road were much larger than responses measured in the APLF. These differences were largely due to a weaker subgrade on the test road caused by higher levels of moisture.

3. Redundant sensors generally compared quite well on the test road and in the APLF. Three redundant strain gauges and two redundant LVDTs are recommended for a field environment. Two of each worked well in the APLF.

4. The comparison of measured and calculated responses in the APLF showed that elastic-layer theory approximated longitudinal strain reasonably well at 46º F and 70º F using laboratory determined moduli. Measured strains were higher than calculated strains at 94º, probably due to the increased nonlinearity of AC material at higher temperatures. Calculated deflections were higher than measured deflections, but this difference tended to decrease with higher temperature.

5. At 70º F, strains determined with FWD backcalculated moduli were slightly lower than strains determined with laboratory determined moduli. Deflections with FWD moduli were lower than those calculated with laboratory moduli and agreed quite well with measured deflections.

6. Total and normalized responses must be used carefully when comparing different types of load. Total responses were larger under dual tires than under single tires because of the

larger total load. Normalized responses were larger under single tires because of the smaller contact area.

7. When comparing responses from different types of load and at different times, material properties, load geometry, load position, and tire speed all must be taken into account.

8. Logarithmic plots of rut depth vs. number of wheel loads provided a linear relationship between these parameters in the APLF. The slopes of these lines were the rate of rutting associated with each combination of load, temperature and section design. Since these plots were linear to 100,000 cycles, rutting can be adequately characterized by applying 10,000 to 20,000 load cycles.

9. Parameters which mainly affect rut growth in AC pavements include: section design, AC thickness, AC temperature, wheel load, and subgrade stiffness, as determined by soil type and moisture content.

10. Increasing pavement temperature from 70º F to 104º F accelerated rutting 2 – 3 times faster than increasing the applied dual wheel load from 9 kips to 15 kips in these SPS-1 sections.

11. Structural numbers tended to be inversely proportional to rutting slope at 70º F, thereby indicating that weaker pavement sections rutted faster at that temperature. As temperature increased, the rates of rutting accelerated faster on pavements with thicker layers of asphalt stabilized materials.

12. On the test road, traffic loading accumulated at the rate of 643,500 ESALs per year in the northbound driving lane and at the rate of 607,000 ESALs per year in the southbound driving lane during 1996, 1997 and 1998.

13. Sections 390102 and 390107 carried 33,000 ESALs, Section 390101 carried 170,000 ESALs, and Section 390105 carried 510,000 ESALs by the time they were closed for

rehabilitation. Sections 390101, 390102 and 390107 had ruts about ½" deep at the time of closure and Section 390105 had a dramatic localized failure.

14. The inability to get adequate moisture into the APLF subgrade did not permit a complete simulation of subgrade conditions on the test road. Rutting on the test road developed in the base and subgrade, while rutting in the APLF was limited to the AC pavement layer. Performance, therefore, could not be correlated at the two sites.

15. To properly simulate field conditions in the APLF, the material and structural properties of all pavement layers must be closely replicated.

CHAPTER 7

IMPLEMENTATION

Pavement response can be measured effectively in the APLF with the FWD and with sensors installed during construction of the pavement sections. These measurements permit the backcalculation of layer moduli, and the validation and calibration of new design procedures and other theoretical calculations. To properly simulate the structural response and performance of actual pavements in the APLF, however, care must be taken to adequately replicate the material and structural properties of each pavement layer in the field. This replication is necessary to attain the same structural behavior and, ultimately, the same modes of distress in both settings.

Rut depth vs. number of load applications in the APLF plotted out as straight lines up to 100,000 cycles on semi-log graphs. Consequently, 10,000 - 20,000 loading cycles can be used to characterize the rutting characteristics of an AC pavement in the APLF, which would require about one week when testing eight hours per day. At least two or three different tests can be run on the same section of pavement, as long as the best-fit trendline for each test is adjusted to where it would be if all previous loading had been performed under those conditions. With the findings from these tests in the APLF, and with the determination of how to calculate, adjust and compare rates of rutting, future testing of AC pavements can be performed very effectively.

The Excel spreadsheet developed for processing WIM data on the Ohio SHRP Test Road will allow pavement engineers at ODOT to quickly analyze WIM data from other Mettler-Toledo sites using desktop or laptop computers. With this spreadsheet, engineers can also adjust the various parameters used in the calculation of ESALs.

Because of the inability to saturate the A-6 subgrade in the APLF, it was not possible to fully simulate structural conditions on the test road and to develop performance correlations at the two sites. Pavement sections on the test road rutted in the base and subgrade layers, while rutting in the APLF was limited to consolidation of the AC layers. By controlling load and environmental conditions in the APLF, however, considerable information was gathered on how

load and temperature affected the response and performance of the four SPS-1 sections selected for this study. Trends regarding the effects of speed and load on measured strain and deflection were also obtained during controlled vehicle testing on the test road. All pertinent data were included in this report to serve as a reference for future studies on accelerated pavement testing and for peripheral investigations of pavement response and performance.

The problem encountered on this project with introducing moisture into the APLF subgrade has been addressed by closing all open ducts from the bottom of the APLF pit to the pavement surface. This change will allow water to be added to the subgrade under pressure. Other options are also available, such as the use of more porous subgrade materials, the addition of porous layers in the subgrade during construction to facilitate the distribution of water, or adding water at the pavement surface. The APLF is extremely useful in monitoring AC and PCC pavement response and performance under closely controlled environmental and loading conditions. This capability permits engineers to evaluate the effects of various design, material and construction parameters under controlled conditions without having to construct expensive test sections in the field and having to make various assumptions regarding the effects of environment and traffic loading on the parameters in question.

APPENDIX A

FWD MEASUREMENTS ON TEST ROAD

Table A1
Initial Normalized Maximum FWD Deflection Profiles on Test Road

OHIO SHRP TEST ROAD																										
Normalized FWD Deflection Profiles																										
Section	Path	Layer	Load	Date	Normalized FWD Df1 Deflection (mils/kip) at Station																					
Station					0+00	0+25	0+50	0+75	1+00	1+25	1+50	1+75	2+00	2+25	2+50	2+75	3+00	3+25	3+50	3+75	4+00	4+25	4+50	4+75	5+00	Avg.
SPS-1																										
390101*	C/L	Subgrade	5.10	8/29/95		4.06		3.56		3.20		4.54		6.39		6.73		4.18		5.98		18.4		16.0		7.30
		8"DGAB	9.02	9/12/95		3.02		4.19		4.36		2.67		3.18		4.66		3.48		3.40		3.33		4.15		3.64
		7"AC	9.25	6/11/96	1.39		1.59		1.50		1.66		1.56		1.59		2.08		1.52		1.53		1.85		1.85	1.65
	RWP	Subgrade	5.11	8/29/95	8.13		7.16		8.83		10.0		5.41		11.81		9.00		3.41		6.50		16.35		15.3	9.26
		8"DGAB	8.87	9/12/95	4.16		5.49		5.47		4.17		3.69		7.08		5.22		3.80		4.11		5.08		4.83	4.83
		7"AC	9.18	6/11/96	1.46		1.52		1.48		1.53		1.50		1.61		2.17		1.50		1.48		1.68		1.71	1.60
390102*	C/L	Subgrade	5.77	8/29/95		2.43		3.54		4.62		4.78		5.76		9.58		2.90		2.13		2.08		4.10		4.19
		12"DGAB	8.99	9/12/95		3.98		3.23		3.62		4.12		4.19		4.32		3.51		3.32		3.14		3.10		3.65
		4"AC	9.49	6/11/96	3.14		2.78		3.25		3.70		4.00		3.53		3.68		3.13		3.06		4.39		3.86	3.50
	RWP	Subgrade	5.66	8/29/95	2.83		3.09		3.82		7.21		7.20		8.73		3.22		2.18		4.88		2.43		3.18	4.43
		12"DGAB	8.99	9/12/95			3.17		3.99		4.89		4.48		6.06		4.13		3.65		3.02		3.44		3.82	4.07
		4"AC	9.42	6/11/96	3.36		2.82		3.02		3.36		3.63		3.68		3.61		2.75		2.55		3.51		3.11	3.22
390105*	C/L	Subgrade	5.26	8/28/95		5.77		5.97		4.37		4.32		3.95		4.03		4.15		4.38		4.70		5.02		4.67
		4"DGAB	9.21	9/11/95		3.45		4.25		5.82		4.63		4.92		4.82		4.78		5.58		4.84		6.12		4.92
		4"ATB	9.14	9/25/95		2.42		2.10		1.53		1.63		2.24		1.92		1.95		1.74		2.09		2.14		1.98
		4"AC	9.71	6/11/96	1.39		1.27		1.30		1.33		1.20		1.47		1.31		1.26		1.25		1.55		1.61	1.36
	RWP	Subgrade	5.29	8/28/95	4.10		5.26		3.21		3.67		3.65		4.91		5.50		6.22		5.95		5.83		6.04	4.94
		4"DGAB	9.08	9/11/95	4.13		4.70		3.77		4.47		5.30		4.54		5.50				5.09		5.69		7.51	5.07
		4"ATB	9.19	9/25/95	2.37		2.45		2.58		2.30		2.66		2.16		2.10		1.52		1.61		2.05		2.18	2.18
		4"AC	9.47	6/11/96	1.55		1.35		1.44		1.29		1.33		1.47		1.41		1.20		1.34		1.59		1.48	1.41
390107	C/L	Subgrade	5.81	8/29/95		9.39		3.70		6.13		4.00		3.31		3.17		6.67		3.33		7.54		7.36		5.46
		4"DGAB	9.06	9/12/95		7.35		4.23		4.31		5.16		5.54		5.69		9.69		5.40		5.30		4.80		5.75
		4"PATB	8.35	10/19/95		5.97		5.74		5.62		5.51		6.88		5.52		5.97		4.81		5.06		4.69		5.58
		4"AC	9.20	6/11/96	1.90		1.96		2.35		2.09		2.37		1.99		1.87		2.30		1.93		2.34		2.21	2.12
	RWP	Subgrade	5.83	8/29/95	3.99		2.53		3.80		3.35		4.19		5.02		3.20		3.58				9.64		7.98	4.73
		4"DGAB	8.92	9/12/95	6.27		4.79		3.66		4.47		5.32		5.82		4.36		7.98		5.38		5.15			5.32
		4"PATB	8.75	10/19/95	4.50		4.50		4.91		4.65		9.04		5.38		4.11		4.61		4.08		4.76		3.52	4.91
		4"AC	9.19	6/11/96	1.77		1.74		2.25		1.77		2.19		1.74		1.79		1.75		1.79		2.07		2.04	1.90

* Undrained section

Table A2
Average Normalized FWD Basins by Layer on Test Road

OHIO US 23 SHRP TEST ROAD																			
Average FWD Deflection Basins by Layer																			
Section	Layer	Date	Centerline									Right Wheelpath								
			Load (kips)	Avg. Norm. Deflection (mils/kip) @ R = (in.)							SPR (%)	Load (kips)	Avg. Norm. Deflection (mils/kip) @ R = (in.)							SPR (%)
				0	8	12	18	24	36	60			0	8	12	18	24	36	60	
390101	Subgrade	8/29/95	5.10	7.30	4.24	2.50	1.35	0.78	0.43	0.21	32.9	5.11	9.26	4.43	2.70	1.41	0.86	0.49	0.23	29.9
	8" DGAB	9/12/95	9.02	3.64	2.28	1.41	0.79	0.56	0.37	0.19	36.4	8.87	4.83	2.23	1.14	0.64	0.54	0.34	0.18	29.4
	7" AC	6/11/96	9.25	1.65	1.35	1.15	0.88	0.66	0.39	0.17	54.8	9.18	1.60	1.33	1.12	0.86	0.64	0.38	0.18	54.5
390102	Subgrade	8/29/95	5.77	4.19	1.86	1.22	0.74	0.53	0.34	0.18	30.9	5.66	4.43	2.11	1.47	0.94	0.60	0.37	0.19	32.6
	12" DGAB	9/12/95	8.99	3.65	2.01	1.09	0.55	0.39	0.29	0.18	31.9	8.99	4.07	2.09	1.03	0.54	0.41	0.33	0.20	28.3
	4" AC	6/11/96	9.50	3.50	2.72	2.16	1.43	0.92	0.42	0.20	46.7	9.42	3.22	2.51	2.00	1.33	0.86	0.42	0.22	47.0
390105	Subgrade	8/28/95	5.26	4.67	2.74	1.68	0.83	0.66	0.37	0.19	34.1	5.29	4.94	2.79	1.32	0.79	0.51	0.34	0.18	31.4
	4" DGAB	9/11/95	9.21	4.92	2.54	1.07	0.61	0.47	0.32	0.17	29.3	9.08	5.07	2.33	1.18	0.70	0.51	0.35	0.19	29.3
	4" ATB	9/25/95	9.14	1.98	1.56	1.24	0.84	0.57	0.32	0.17	48.3	9.19	2.18	1.70	1.32	0.87	0.57	0.31	0.16	46.6
	4" AC	6/11/96	9.71	1.36	1.16	1.03	0.83	0.65	0.40	0.17	59.6	9.47	1.41	1.23	1.09	0.88	0.69	0.44	0.18	60.1
390107	Subgrade	8/29/95	5.81	5.46	2.05	1.32	0.79	0.52	0.32	0.19	27.9	5.83	4.73	2.05	1.19	0.78	0.50	0.35	0.20	29.8
	4" DGAB	9/12/95	9.06	5.75	2.28	1.02	0.60	0.45	0.31	0.17	27.0	8.92	5.32	2.31	0.95	0.60	0.49	0.35	0.20	27.8
	4" PATB	10/19/95	8.35	5.58	3.27	1.74	0.58	0.30	0.29	0.19	30.6	8.75	4.91	2.85	1.40	0.47	0.27	0.26	0.18	30.2
	4" AC	6/11/96	9.20	2.12	1.69	1.39	0.99	0.69	0.37	0.18	50.3	9.19	1.90	1.52	1.26	0.91	0.64	0.36	0.18	50.9

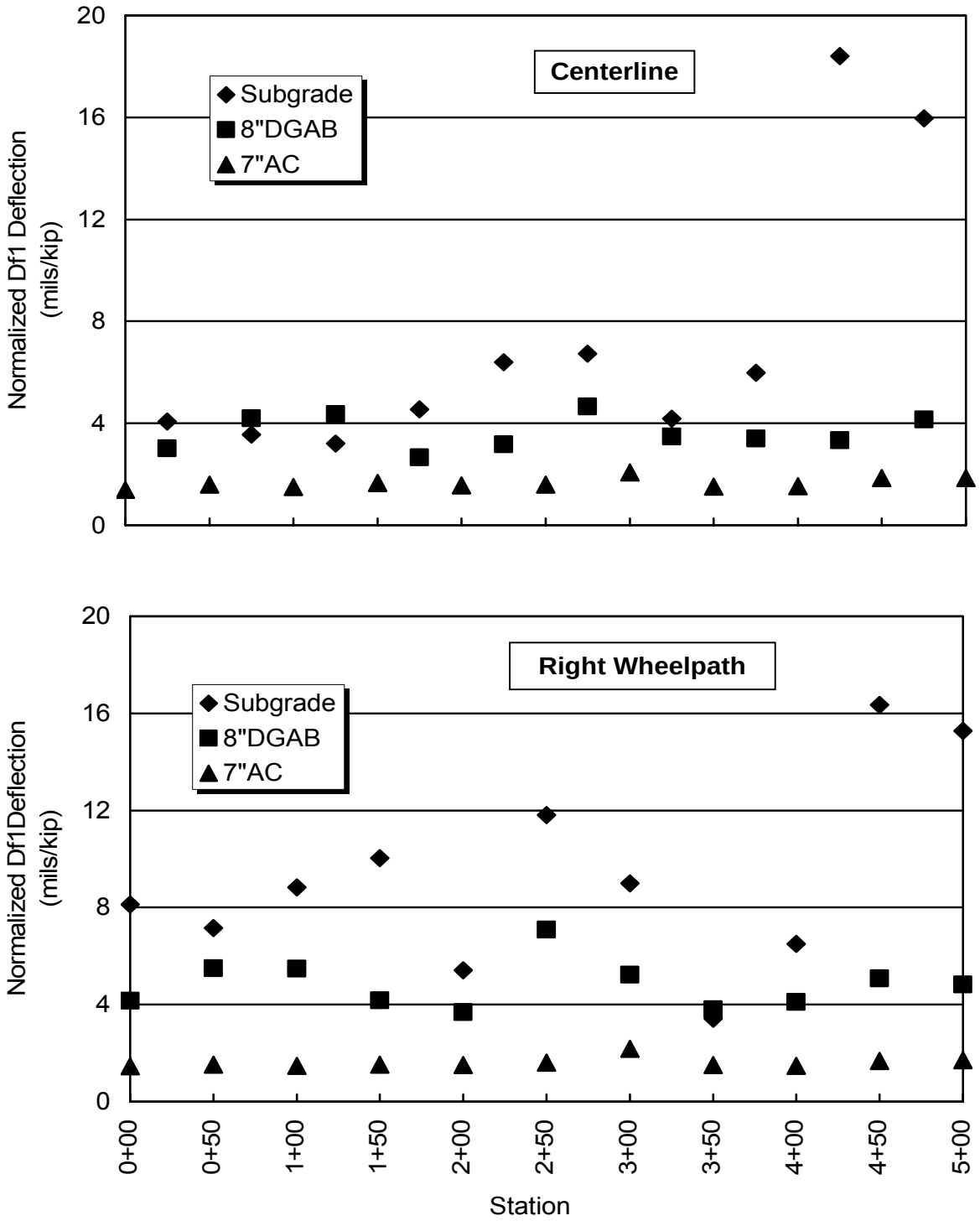

Figure A1 – FWD Profiles on Section 390101

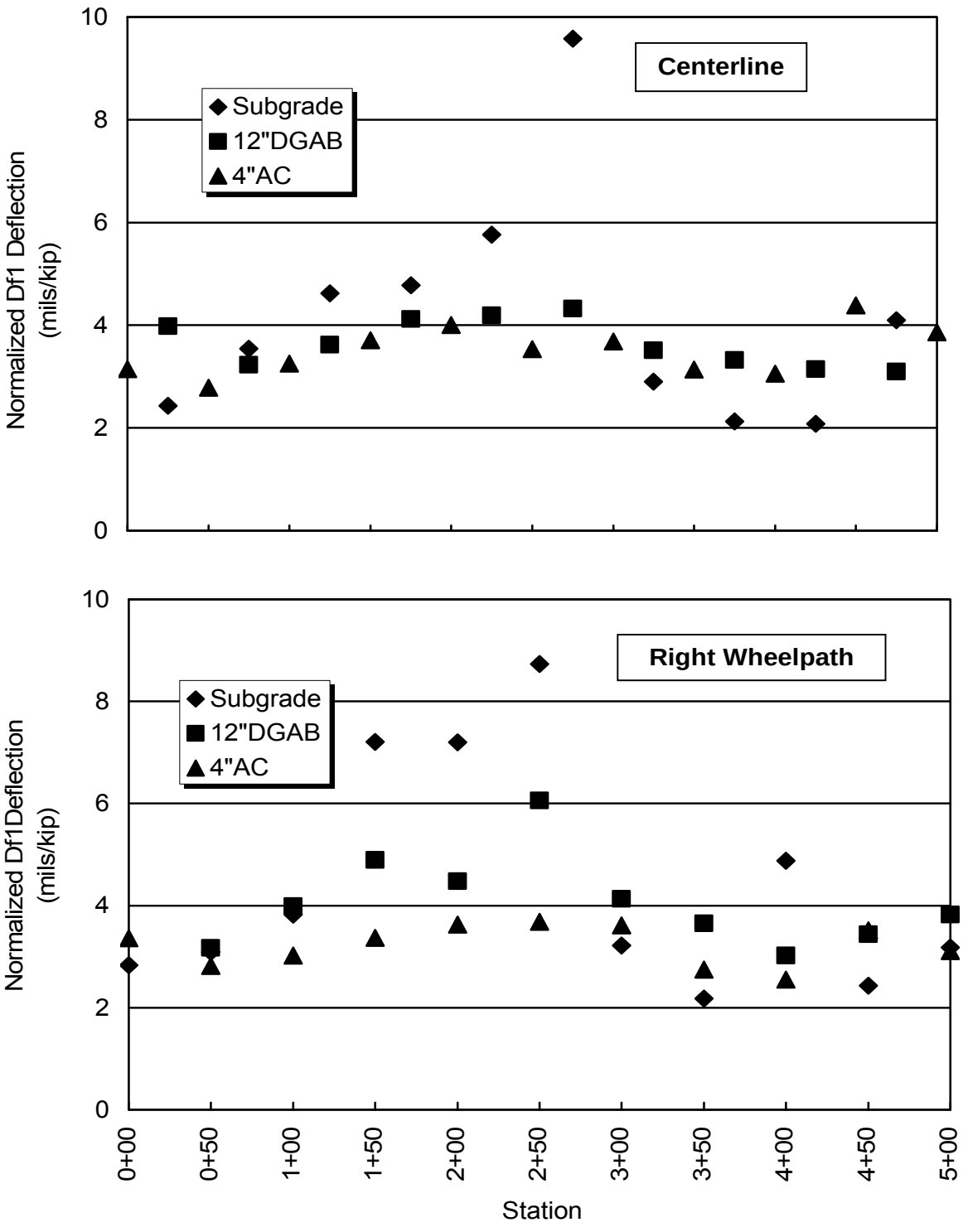

Figure A2 - FWD Profiles on Section 390102

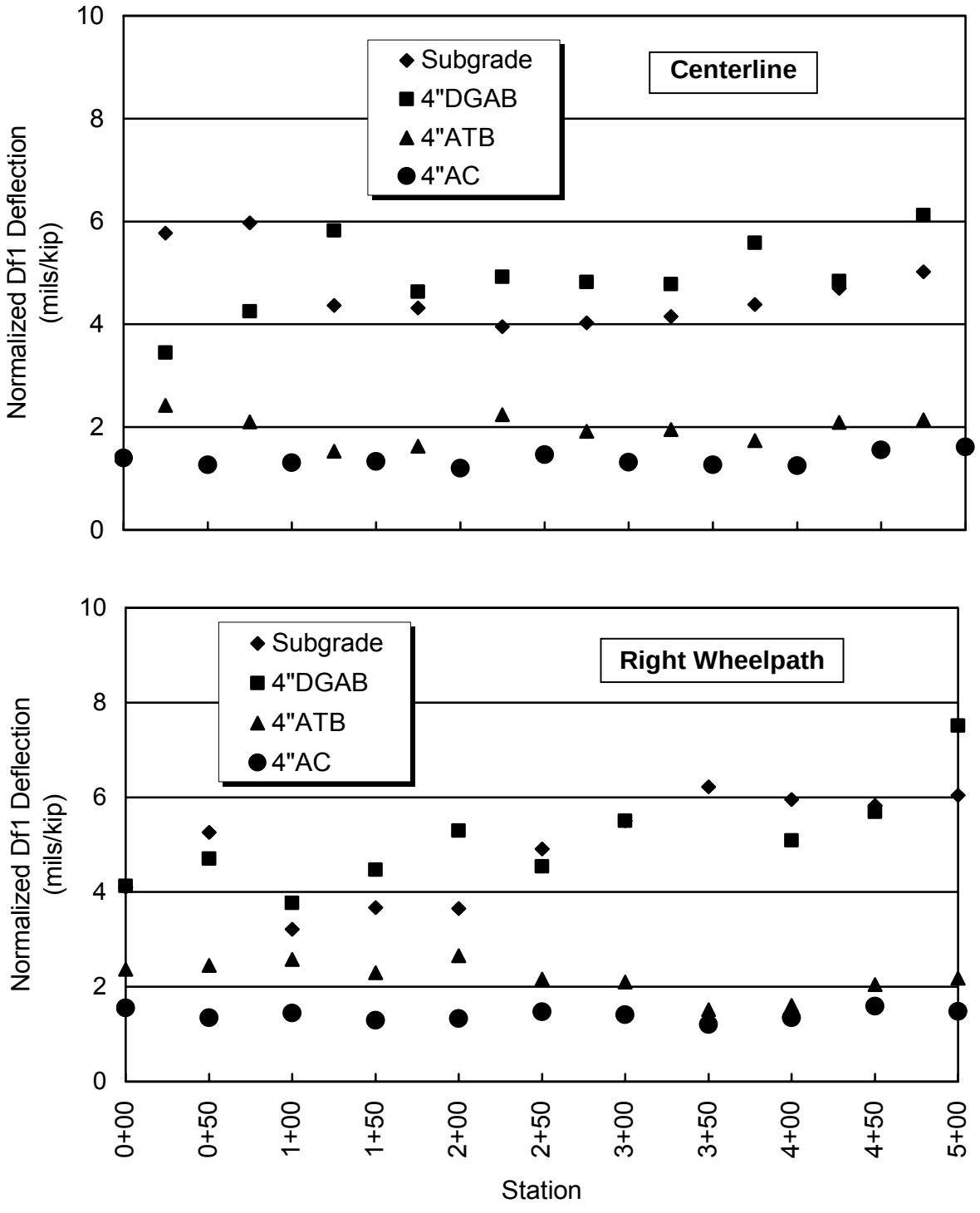

Figure A3 - FWD Profiles on Section 390105

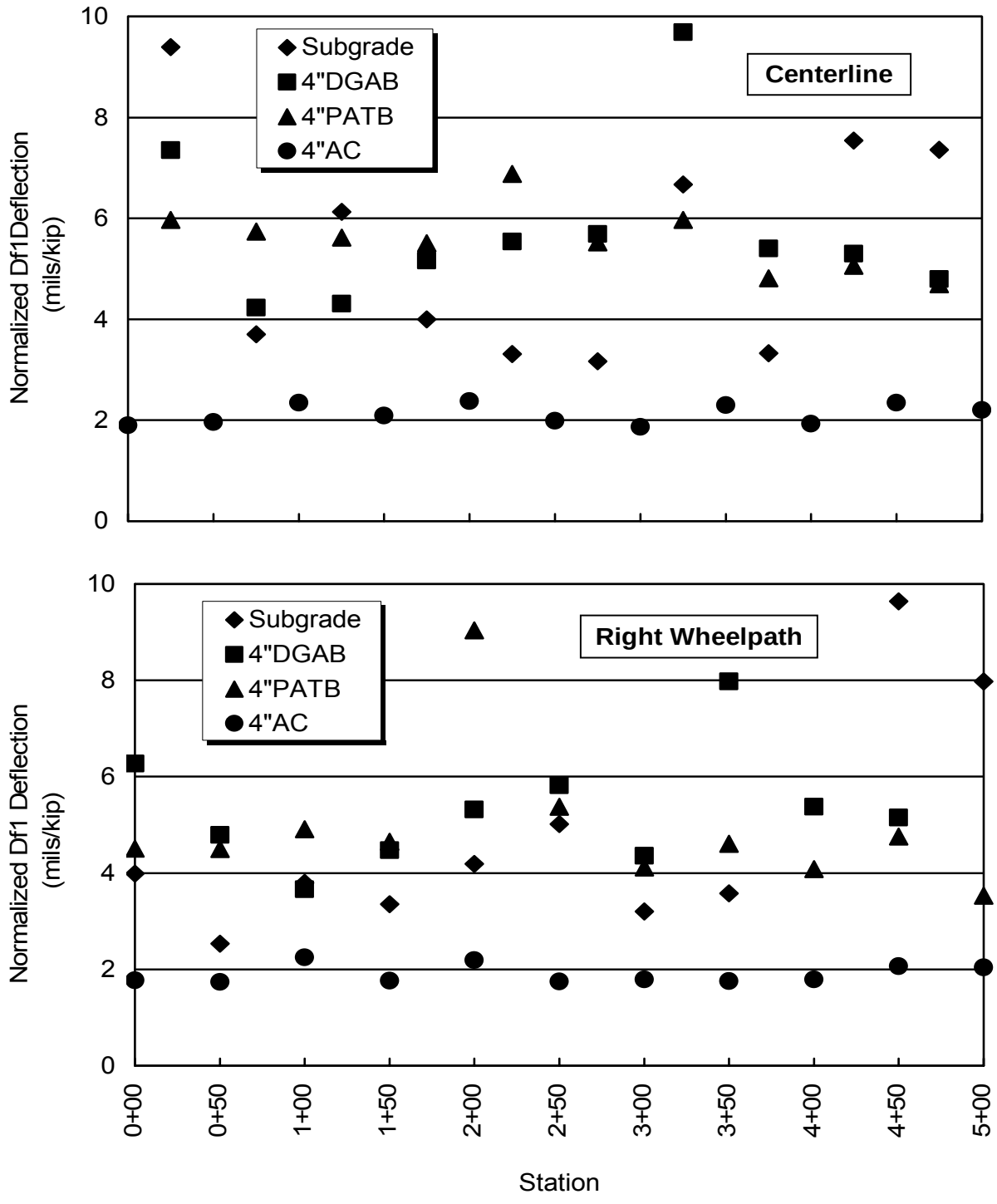

Figure A4 - FWD Profiles on Section 390107

APPENDIX B

RESPONSE MEASUREMENTS ON PAD A

Table B1 - Dynamic Response in Section A101W

Dynamic Response in Section A390101W																								
Temp. (°F)	Nominal Load (kips)	Wheel Speed (mph)	Maximum Strain @ Offset in inches								Maximum Voltage Output @ Offset in inches											
			Gauge No. 3 (Z = 7")				Gauge No. 4 (Z = 7")				Short LVDT No. 5 (Z = 5')				Long LVDT No. 6 (Z = 15")				Diff. between Shallow and Deep LVDTs			
			0	2	7	12	0	2	7	12	0	2	7	12	0	2	7	12	0	2	7	12
46.4	6										Maximum Voltage											
		1	28.12	28.74	28.74	18.74	25.62	26.24	28.74	19.99	0.072	0.075	0.076	0.058	0.019	0.020	0.022	0.015	0.053	0.055	0.054	0.043
		3	19.37	19.37	20.62	15.62	14.37	16.24	17.49	18.12	0.060	0.061	0.063	0.050	0.018	0.018	0.019	0.014	0.042	0.043	0.043	0.036
		5	15.62	16.87	18.74	13.12	14.99	15.62	17.49	14.37	0.048	0.046	0.053	0.043	0.018	0.017	0.018	0.011	0.031	0.028	0.035	0.032
			Average Gauges 3 & 4								Maximum Deflection (mils/kip)											
			Total Strain				Norm. Strain (με/kip)				Calibration; Long LVDT = 20 volts/in., Short LVDT = 40 volts/in.											
		1	26.87	27.49	28.74	19.37	4.48	4.58	4.79	3.23	0.301	0.311	0.316	0.242	0.162	0.164	0.180	0.123	0.139	0.147	0.136	0.120
		3	16.87	17.81	19.06	16.87	2.81	2.97	3.18	2.81	0.250	0.253	0.260	0.207	0.148	0.148	0.162	0.114	0.102	0.104	0.099	0.093
		5	15.31	16.25	18.12	13.75	2.55	2.71	3.02	2.29	0.200	0.190	0.220	0.178	0.146	0.143	0.148	0.088	0.055	0.047	0.072	0.090
	9										Maximum Voltage											
		1	59.87	58.12	54.99	37.49	54.37	56.87	59.99	46.24	0.135	0.136	0.136	0.106	0.033	0.033	0.036	0.027	0.102	0.103	0.100	0.079
		3	43.12	41.24	44.99	30.62	43.12	46.24	46.24	35.62	0.116	0.114	0.119	0.093	0.030	0.033	0.034	0.025	0.086	0.081	0.085	0.068
		5	38.74	39.99	38.12	27.49	36.24	36.87	40.62	32.49	0.110	0.113	0.109	0.093	0.030	0.031	0.033	0.025	0.079	0.082	0.077	0.068
			Average Gauges 3 & 4								Maximum Deflection (mils/kip)											
			Total Strain				Norm. Strain (με/kip)				Calibration; Long LVDT = 20 volts/in., Short LVDT = 40 volts/in.											
		1	57.12	57.50	57.49	41.87	6.35	6.39	6.39	4.65	0.376	0.377	0.377	0.294	0.186	0.182	0.198	0.151	0.190	0.194	0.179	0.143
		3	43.12	43.74	45.62	33.12	4.79	4.86	5.07	3.68	0.321	0.317	0.331	0.259	0.167	0.182	0.188	0.139	0.154	0.135	0.143	0.121
		5	37.49	38.43	39.37	29.99	4.17	4.27	4.37	3.33	0.305	0.313	0.304	0.257	0.168	0.172	0.182	0.139	0.136	0.142	0.122	0.118
70	6										Maximum Voltage											
		1	67.49	71.87	74.37	47.49	78.74	86.87	111.2	81.86	0.135	0.138	0.170	0.113	0.037	0.035	0.052	0.040	0.098	0.103	0.118	0.072
		3	56.87	57.49	61.24	43.74	73.11	73.74	83.11	66.87	0.119	0.119	0.132	0.104	0.034	0.032	0.041	0.033	0.085	0.088	0.091	0.070
		5	49.37	52.49	49.99	35.62	68.74	66.87	74.99	59.37	0.113	0.114	0.121	0.093	0.034	0.032	0.041	0.029	0.079	0.082	0.080	0.063
			Average Gauges 3 & 4								Maximum Deflection (mils/kip)											
			Total Strain				Norm. Strain (με/kip)				Calibration; Long LVDT = 20 volts/in., Short LVDT = 40 volts/in.											
		1	73.12	79.37	92.81	64.68	12.19	13.23	15.47	10.78	0.561	0.575	0.707	0.469	0.308	0.289	0.430	0.336	0.254	0.286	0.277	0.133
		3	64.99	65.62	72.18	55.31	10.83	10.94	12.03	9.22	0.495	0.496	0.550	0.433	0.281	0.263	0.341	0.278	0.214	0.233	0.209	0.154
		5	59.06	59.68	62.49	47.50	9.84	9.95	10.42	7.92	0.473	0.475	0.505	0.385	0.284	0.266	0.344	0.245	0.188	0.210	0.161	0.140
	9										Maximum Voltage											
		1	117.48	126.85	126.23	79.36	137.5	148.7	172.5	128.1	0.241	0.255	0.293	0.214	0.061	0.059	0.083	0.067	0.180	0.196	0.209	0.147
		3	99.36	96.24	100.61	70.62	123.7	131.9	133.7	106.9	0.213	0.230	0.237	0.177	0.055	0.068	0.066	0.054	0.158	0.162	0.171	0.123
		5	88.74	89.99	89.99	62.49	109.4	109.4	116.2	93.11	0.201	0.207	0.221	0.166	0.053	0.052	0.063	0.051	0.149	0.155	0.158	0.114
			Average Gauges 3 & 4								Maximum Deflection (mils/kip)											
			Total Strain				Norm. Strain (με/kip)				Calibration; Long LVDT = 20 volts/in., Short LVDT = 40 volts/in.											
		1	127.48	137.79	149.35	103.73	14.16	15.31	16.59	11.53	0.670	0.708	0.813	0.594	0.341	0.330	0.463	0.373	0.330	0.378	0.349	0.221
		3	111.55	114.05	117.17	88.74	12.39	12.67	13.02	9.86	0.593	0.638	0.657	0.491	0.307	0.375	0.364	0.299	0.286	0.263	0.293	0.193
		5	99.05	99.68	103.11	77.80	11.01	11.08	11.46	8.64	0.559	0.575	0.613	0.460	0.292	0.287	0.349	0.285	0.268	0.288	0.264	0.175
93.8	6										Maximum Voltage											
		1	99.36	111.86	123.1	67.49	131.2	158.1	244.9	155	0.201	0.273	0.436	0.195	0.054	0.051	0.162	0.081	0.148	0.222	0.274	0.115
		3	108.73	86.86	85.61	43.12	146.9	120.6	159.3	91.86	0.194	0.218	0.306	0.156	0.049	0.045	0.117	0.057	0.145	0.172	0.190	0.100
		5	78.74	81.86	78.74	42.49	101.9	102.5	133.1	79.36	0.184	0.213	0.273	0.143	0.050	0.048	0.101	0.050	0.134	0.165	0.173	0.093
			Average Gauges 3 & 4								Maximum Deflection (mils/kip)											
			Total Strain				Norm. Strain (με/kip)				Calibration; Long LVDT = 20 volts/in., Short LVDT = 40 volts/in.											
		1	115.30	134.98	184.02	111.23	19.22	22.50	30.67	18.54	0.839	1.138	1.815	0.814	0.448	0.428	1.349	0.672	0.390	0.710	0.466	0.142
		3	127.79	103.74	122.48	67.49	21.30	17.29	20.41	11.25	0.809	0.906	1.276	0.651	0.407	0.378	0.972	0.472	0.402	0.529	0.305	0.180
		5	90.30	92.17	105.92	60.93	15.05	15.36	17.65	10.15	0.766	0.887	1.138	0.596	0.414	0.398	0.838	0.417	0.352	0.488	0.300	0.180
	9										Maximum Voltage											
		1	178.09	177.46	180.59	94.99	228.1	272.4	376.7	240.6	0.363	0.473	0.663	0.330	0.094	0.092	0.238	0.130	0.269	0.382	0.425	0.200
		3	179.96	158.72	168.09	101.23	253.1	299.9	314.9	208.7	0.354	0.490	0.510	0.296	0.087	0.184	0.167	0.093	0.268	0.306	0.343	0.202
		5	165.59	164.97	157.47	96.86	231.2	234.3	275.5	183.1	0.339	0.374	0.464	0.273	0.083	0.081	0.153	0.085	0.256	0.293	0.311	0.188
			Average Gauges 3 & 4								Maximum Deflection (mils/kip)											
			Total Strain				Norm. Strain (με/kip)				Calibration; Long LVDT = 20 volts/in., Short LVDT = 40 volts/in.											
		1	203.08	224.94	278.66	167.78	22.56	24.99	30.96	18.64	1.009	1.315	1.841	0.916	0.521	0.509	1.321	0.722	0.488	0.806	0.520	0.194
		3	216.51	229.32	241.50	154.97	24.06	25.48	26.83	17.22	0.984	1.360	1.418	0.821	0.481	1.023	0.929	0.519	0.503	0.338	0.489	0.302
		5	198.39	199.65	216.51	139.98	22.04	22.18	24.06	15.55	0.942	1.038	1.288	0.759	0.463	0.448	0.849	0.472	0.479	0.591	0.439	0.286

Table B2 - Dynamic Response in Section A102

Dynamic Response in Section A390102																								
Temp. (°F)	Nominal Load (kips)	Wheel Speed (mph)	Maximum Strain @ Offset in inches								Maximum Voltage Output @ Offset in inches											
			Gauge No. 5 (Z = 4")				Gauge No. 6 (Z = 4")				Short LVDT No. 3 (Z = 5')				Long LVDT No. 4 (Z = 16")				Diff. between Shallow and Deep LVDTs			
			0	2	7	12	0	2	7	12	0	2	7	12	0	2	7	12	0	2	7	12
46.4	6										Maximum Voltage											
		1	73.74	73.74	92.49	50.62	68.74	66.87	81.24	45.62	0.144	0.146	0.159	0.123	0.056	0.054	0.061	0.052	0.089	0.091	0.098	0.071
		3	53.74	58.12	69.37	41.24	40.62	43.74	58.74	30.62	0.122	0.121	0.128	0.113	0.050	0.047	0.126	0.050	0.073	0.074	0.002	0.063
		5	50.62	43.74	69.37	34.99	34.99	34.37	46.87	26.87	0.125	0.107	0.122	0.094	0.049	0.040	0.155	0.042	0.076	0.067	-0.033	0.053
			Average Gauges 3 & 4								Maximum Deflection (mils/kip)											
			Total Strain				Norm. Strain (με/kip)				Calibration; Long LVDT = 20 volts/in., Short LVDT = 40 volts/in.											
		1	71.24	70.31	86.87	48.12	11.87	11.72	14.48	8.02	0.600	0.607	0.662	0.510	0.463	0.453	0.505	0.433	0.137	0.153	0.157	0.078
		3	47.18	50.93	64.06	35.93	7.86	8.49	10.68	5.99	0.509	0.504	0.535	0.473	0.414	0.391	1.049	0.419	0.095	0.113		0.053
		5	42.81	39.06	58.12	30.93	7.13	6.51	9.69	5.16	0.520	0.444	0.509	0.393	0.407	0.333	1.289	0.347	0.113	0.111		0.047
	9										Maximum Voltage											
		1	111.86	116.23	145.6	91.24	103.7	106.2	129.35	86.86	0.247	0.259	0.273	0.227	0.090	0.092	0.171	0.113	0.157	0.167	0.102	0.114
		3	101.23	125.6	130.6	83.11	90.61	106.9	106.2	73.11	0.222	0.235	0.235	0.202	0.087	0.109	0.099	0.105	0.135	0.127	0.137	0.097
		5	98.74	104.36	121.86	78.74	81.24	80.61	94.99	63.74	0.216	0.223	0.232	0.188	0.080	0.084	0.201	0.101	0.136	0.139	0.031	0.088
			Average Gauges 3 & 4								Maximum Deflection (mils/kip)											
			Total Strain				Norm. Strain (με/kip)				Calibration; Long LVDT = 20 volts/in., Short LVDT = 40 volts/in.											
		1	107.80	111.23	137.48	89.05	11.98	12.36	15.28	9.89	0.687	0.720	0.758	0.629	0.500	0.511	0.948	0.627	0.187	0.209		0.003
		3	95.92	116.23	118.42	78.11	10.66	12.91	13.16	8.68	0.616	0.654	0.654	0.560	0.481	0.604	0.549	0.582	0.134	0.049	0.105	-0.022
		5	89.99	92.49	108.43	71.24	10.00	10.28	12.05	7.92	0.600	0.620	0.644	0.523	0.444	0.467	1.118	0.559	0.155	0.153		-0.036
70	6										Maximum Voltage											
		1	46.87	184.96	241.81	121.86	48.12	172.5	206.2	109.4	0.084	0.259	0.331	0.228	0.032	0.099	0.146	0.097	0.053	0.160	0.185	0.132
		3	135.6	147.47	191.83	96.86	118.7	129.4	148.1	83.11	0.218	0.219	0.259	0.191	0.086	0.087	0.113	0.071	0.132	0.132	0.147	0.120
		5	116.86	131.85	162.47	81.86	100.6	106.2	126.9	66.24	0.199	0.207	0.231	0.174	0.075	0.076	0.096	0.065	0.124	0.131	0.135	0.109
			Average Gauges 3 & 4								Maximum Deflection (mils/kip)											
			Total Strain				Norm. Strain (με/kip)				Calibration; Long LVDT = 20 volts/in., Short LVDT = 40 volts/in.											
		1	47.50	178.72	224.01	115.61	7.92	29.79	37.33	19.27	0.352	1.078	1.379	0.950	0.266	0.826	1.219	0.805	0.086	0.253	0.160	0.145
		3	127.17	138.41	169.97	89.99	21.19	23.07	28.33	15.00	0.908	0.913	1.081	0.794	0.713	0.724	0.940	0.591	0.194	0.189	0.141	0.203
		5	108.74	119.04	144.66	74.05	18.12	19.84	24.11	12.34	0.828	0.862	0.964	0.724	0.625	0.633	0.802	0.542	0.203	0.230	0.162	0.183
	9										Maximum Voltage											
		1	239.94	269.92	328.64	184.96	211.9	243.7	279.3	168.7	0.386	0.396	0.490	0.363	0.143	0.150	0.211	0.147	0.244	0.246	0.279	0.216
		3	201.83	254.31	270.55	151.85	189.3	222.5	226.8	138.1	0.352	0.408	0.409	0.310	0.131	0.171	0.172	0.123	0.222	0.238	0.238	0.188
		5	184.34	204.95	248.06	146.85	170.6	181.8	211.2	131.2	0.328	0.326	0.374	0.288	0.125	0.128	0.152	0.115	0.203	0.198	0.222	0.173
			Average Gauges 3 & 4								Maximum Deflection (mils/kip)											
			Total Strain				Norm. Strain (με/kip)				Calibration; Long LVDT = 20 volts/in., Short LVDT = 40 volts/in.											
		1	225.90	256.81	303.97	176.84	25.10	28.53	33.77	19.65	1.073	1.101	1.361	1.008	0.792	0.835	1.172	0.814	0.281	0.266	0.189	0.193
		3	195.58	238.38	248.69	144.98	21.73	26.49	27.63	16.11	0.978	1.134	1.137	0.861	0.726	0.949	0.955	0.681	0.253	0.185	0.182	0.181
		5	177.47	193.40	229.63	139.04	19.72	21.49	25.51	15.45	0.912	0.904	1.040	0.799	0.694	0.708	0.846	0.639	0.218	0.196	0.194	0.161
93.8	6										Maximum Voltage											
		1	266.67	298.03	420.44	183.71	266.8	306.8	472.3	201.2	0.356	0.391	0.863	0.429	0.128	0.147	0.348	0.192	0.229	0.244	0.514	0.238
		3	275.54	298.66	371.11	171.22	234.9	262.4	342.4	158.7	0.334	0.329	0.652	0.349	0.129	0.130	0.275	0.147	0.205	0.199	0.377	0.203
		5	248.68	283.04	346.75	165.59	215.6	241.2	306.2	143.1	0.303	0.300	0.533	0.294	0.122	0.122	0.228	0.128	0.181	0.178	0.305	0.166
			Average Gauges 3 & 4								Maximum Deflection (mils/kip)											
			Total Strain				Norm. Strain (με/kip)				Calibration; Long LVDT = 20 volts/in., Short LVDT = 40 volts/in.											
		1	266.74	302.41	446.36	192.46	44.46	50.40	74.39	32.08	1.485	1.629	3.594	1.789	1.065	1.222	2.901	1.599	0.420	0.407	0.693	0.190
		3	255.24	280.55	356.75	164.97	42.54	46.76	59.46	27.50	1.393	1.371	2.718	1.455	1.078	1.086	2.292	1.222	0.315	0.285	0.426	0.233
		5	232.13	262.12	326.45	154.35	38.69	43.69	54.41	25.72	1.263	1.249	2.219	1.224	1.016	1.013	1.898	1.063	0.247	0.235	0.320	0.162
	9										Maximum Voltage											
		1	372.98	397.34	506.61	260.55	371.1	422.9	610.3	285.5	0.539	0.585	1.133	0.618	0.199	0.225	0.476	0.269	0.340	0.359	0.658	0.349
		3	381.72	451.67	479.76	248.06	369.2	472.9	506.6	259.9	0.516	0.929	0.844	0.531	0.186	0.415	0.380	0.217	0.330	0.514	0.464	0.313
		5	382.35	407.95	454.16	243.06	340.5	370.5	438.6	244.9	0.493	0.493	0.809	0.489	0.190	0.195	0.355	0.203	0.303	0.298	0.454	0.286
			Average Gauges 3 & 4								Maximum Deflection (mils/kip)											
			Total Strain				Norm. Strain (με/kip)				Calibration; Long LVDT = 20 volts/in., Short LVDT = 40 volts/in.											
		1	372.05	410.14	558.43	273.05	41.34	45.57	62.05	30.34	1.497	1.624	3.148	1.716	1.104	1.252	2.642	1.493	0.392	0.373	0.506	0.223
		3	375.48	462.29	493.19	254.00	41.72	51.37	54.80	28.22	1.432	2.581	2.345	1.474	1.033	2.304	2.109	1.207	0.399	0.277	0.235	0.267
		5	361.43	389.22	446.36	244.00	40.16	43.25	49.60	27.11	1.369	1.369	2.248	1.358	1.057	1.082	1.972	1.127	0.312	0.287	0.276	0.231

Table B3 - Dynamic Response in Section A105

Dynamic Response in Section A390105																								
Temp. (°F)	Nominal Load (kips)	Wheel Speed (mph)	Maximum Strain @ Offset in inches								Maximum Voltage Output @ Offset in inches													
			Gauge No. 1 (Z = 8")				Gauge No. 2 (Z = 8")				Long LVDT No. 1 (Z = 5')				Long LVDT No. 2 (Z = 12")				Diff. between Shallow and Deep LVDTs			
			0	2	7	12	0	2	7	12	0	2	7	12	0	2	7	12	0	2	7	12
46.4	6										Maximum Voltage											
		1	44.98	40.62	36.24	19.99	46.87	41.87	37.49	20.62	0.049	0.043	0.040	0.028	0.018	0.015	0.018	0.011	0.031	0.028	0.023	0.017
		3	36.87	33.12	30.62	20.62	33.74	33.74	31.24	19.37	0.037	0.036	0.036	0.028	0.014	0.014	0.017	0.012	0.023	0.022	0.020	0.016
		5	32.49	31.24	28.12	19.37	29.99	29.37	27.49	19.37	0.039	0.036	0.030	0.028	0.014	0.013	0.014	0.012	0.025	0.023	0.017	0.017
			Average Gauges 3 & 4								Maximum Deflection (mils/kip)											
			Total Strain				Norm. Strain (με/kip)				Calibration; Long LVDT = 20 volts/in											
		1	45.93	41.25	36.87	20.31	7.65	6.87	6.14	3.38	0.412	0.362	0.333	0.234	0.151	0.125	0.146	0.094	0.261	0.237	0.188	0.140
		3	35.31	33.43	30.93	20.00	5.88	5.57	5.16	3.33	0.310	0.299	0.303	0.234	0.118	0.118	0.138	0.099	0.193	0.182	0.164	0.135
		5	31.24	30.31	27.81	19.37	5.21	5.05	4.63	3.23	0.323	0.299	0.253	0.234	0.114	0.109	0.115	0.097	0.209	0.190	0.138	0.138
	9										Maximum Voltage											
		1	75.61	76.24	70.62	46.87	74.99	75.61	71.86	48.12	0.085	0.083	0.078	0.063	0.027	0.026	0.032	0.023	0.058	0.057	0.047	0.039
		3	63.74	53.12	58.74	39.99	66.24	58.74	61.24	42.49	0.072	0.068	0.070	0.057	0.024	0.028	0.027	0.021	0.048	0.041	0.043	0.036
		5	59.99	58.74	54.37	36.87	60.62	58.12	57.49	39.37	0.070	0.068	0.063	0.052	0.023	0.022	0.026	0.019	0.048	0.046	0.037	0.033
			Average Gauges 3 & 4								Maximum Deflection (mils/kip)											
			Total Strain				Norm. Strain (με/kip)				Calibration; Long LVDT = 20 volts/in											
		1	75.30	75.93	71.24	47.50	8.37	8.44	7.92	5.28	0.471	0.458	0.436	0.347	0.149	0.142	0.176	0.128	0.321	0.316	0.260	0.219
		3	64.99	55.93	59.99	41.24	7.22	6.21	6.67	4.58	0.399	0.380	0.387	0.314	0.136	0.153	0.151	0.114	0.264	0.227	0.236	0.200
		5	60.31	58.43	55.93	38.12	6.70	6.49	6.21	4.24	0.391	0.380	0.349	0.290	0.125	0.123	0.144	0.104	0.266	0.257	0.205	0.186
70	6										Maximum Voltage											
		1	99.99	100.61	94.99	58.12	83.74	84.36	85.61	56.87	0.087	0.082	0.086	0.057	0.028	0.028	0.047	0.023	0.059	0.054	0.039	0.034
		3	N/A	86.86	76.86	48.74	N/A	79.99	76.86	48.74	N/A	0.068	0.071	0.050	N/A	0.025	0.034	0.019	N/A	0.043	0.036	0.031
		5	82.49	N/A	38.74	62.49	75.61	N/A	41.24	64.99	0.065	N/A	0.040	0.061	0.023	N/A	0.018	0.031	0.042	N/A	0.022	0.029
			Average Gauges 3 & 4								Maximum Deflection (mils/kip)											
			Total Strain				Norm. Strain (με/kip)				Calibration; Long LVDT = 20 volts/in											
		1	91.87	92.49	90.30	57.50	15.31	15.41	15.05	9.58	0.724	0.683	0.716	0.477	0.237	0.237	0.388	0.193	0.488	0.446	0.328	0.284
		3	NA	83.43	76.86	48.74	NA	13.90	12.81	8.12	NA	0.565	0.588	0.417	NA	0.206	0.287	0.159	N/A	0.359	0.302	0.258
		5	79.05	NA	39.99	63.74	13.18	NA	6.67	10.62	0.539	NA	0.331	0.505	0.193	NA	0.148	0.261	0.347	N/A	0.183	0.244
	9										Maximum Voltage											
		1	175.59	184.34	173.72	111.23	145.6	152.5	158.7	105	0.143	0.145	0.157	0.112	0.046	0.052	0.080	0.047	0.097	0.093	0.076	0.065
		3	152.47	148.72		92.49	143.1	141.2	138.7	94.99	0.134	0.125	0.128	0.096	0.043	0.043	0.058	0.034	0.091	0.082	0.071	0.062
		5	138.1	135.6	128.73	86.86	132.5	135.6	131.9	94.99	0.120	0.115	0.116	0.086	0.041	0.040	0.051	0.032	0.079	0.075	0.065	0.054
			Average Gauges 3 & 4								Maximum Deflection (mils/kip)											
			Total Strain				Norm. Strain (με/kip)				Calibration; Long LVDT = 20 volts/in											
		1	160.60	168.41	166.22	108.11	17.84	18.71	18.47	12.01	0.793	0.806	0.870	0.620	0.257	0.287	0.446	0.259	0.536	0.519	0.424	0.361
		3	147.79	144.98		93.74	16.42	16.11	0.00	10.42	0.745	0.694	0.713	0.533	0.238	0.239	0.321	0.191	0.507	0.455	0.392	0.342
		5	135.29	135.60	130.29	90.93	15.03	15.07	14.48	10.10	0.667	0.641	0.646	0.477	0.226	0.222	0.285	0.176	0.441	0.418	0.361	0.302
93.8	6										Maximum Voltage											
		1	166.84	169.99	158.1	85.61	126.2	133.7	153.7	74.99	0.149	0.148	0.217	0.108	0.049	0.058	0.180	0.041	0.100	0.089	0.038	0.068
		3	163.72	158.1	147.47	87.49	127.5	128.1	131.2	73.74	0.121	0.120	0.161	0.091	0.039	0.046	0.111	0.030	0.083	0.075	0.050	0.061
		5	156.22	153.1	134.35	81.86	125.6	121.2	130	73.11	0.110	0.108	0.132	0.073	0.034	0.044	0.092	0.029	0.076	0.064	0.040	0.044
			Average Gauges 3 & 4								Maximum Deflection (mils/kip)											
			Total Strain				Norm. Strain (με/kip)				Calibration; Long LVDT = 20 volts/in											
		1	146.54	151.86	155.92	80.30	24.42	25.31	25.99	13.38	1.240	1.232	1.810	0.903	0.407	0.487	1.498	0.338	0.833	0.745	0.313	0.565
		3	NA	143.10	139.35	80.62	NA	23.85	23.23	13.44	1.011	1.003	1.344	0.758	0.323	0.380	0.928	0.248	0.688	0.623	0.417	0.510
		5	140.91	NA	132.17	77.49	23.49	NA	22.03	12.91	0.914	0.903	1.102	0.609	0.284	0.368	0.768	0.243	0.630	0.536	0.333	0.367
	9										Maximum Voltage											
		1	276.17	292.41	274.92	158.1	215	224.3	254.9	140	0.224	0.243	0.347	0.198	0.070	0.096	0.251	0.093	0.154	0.147	0.096	0.105
		3	286.79	243.06	261.18	163.72	223.7	224.9	231.2	143.1	0.208	0.260	0.263	0.169	0.063	0.171	0.154	0.068	0.145	0.089	0.109	0.101
		5	270.55	265.55	245.56	156.85	221.2	220.6	223.7	141.9	0.198	0.198	0.240	0.153	0.059	0.071	0.142	0.061	0.139	0.128	0.099	0.092
			Average Gauges 3 & 4								Maximum Deflection (mils/kip)											
			Total Strain				Norm. Strain (με/kip)				Calibration; Long LVDT = 20 volts/in											
		1	245.56	258.37	264.93	149.04	27.28	28.71	29.44	16.56	1.245	1.349	1.929	1.099	0.391	0.534	1.396	0.517	0.854	0.814	0.533	0.582
		3	255.24	234.00	246.19	153.41	28.36	26.00	27.35	17.05	1.158	1.446	1.462	0.941	0.351	0.952	0.854	0.378	0.807	0.494	0.607	0.563
		5	245.88	243.06	234.63	149.35	27.32	27.01	26.07	16.59	1.097	1.102	1.335	0.847	0.327	0.394	0.787	0.337	0.771	0.708	0.548	0.511

APPENDIX C

RUTTING PERFORMANCE ON PAD A

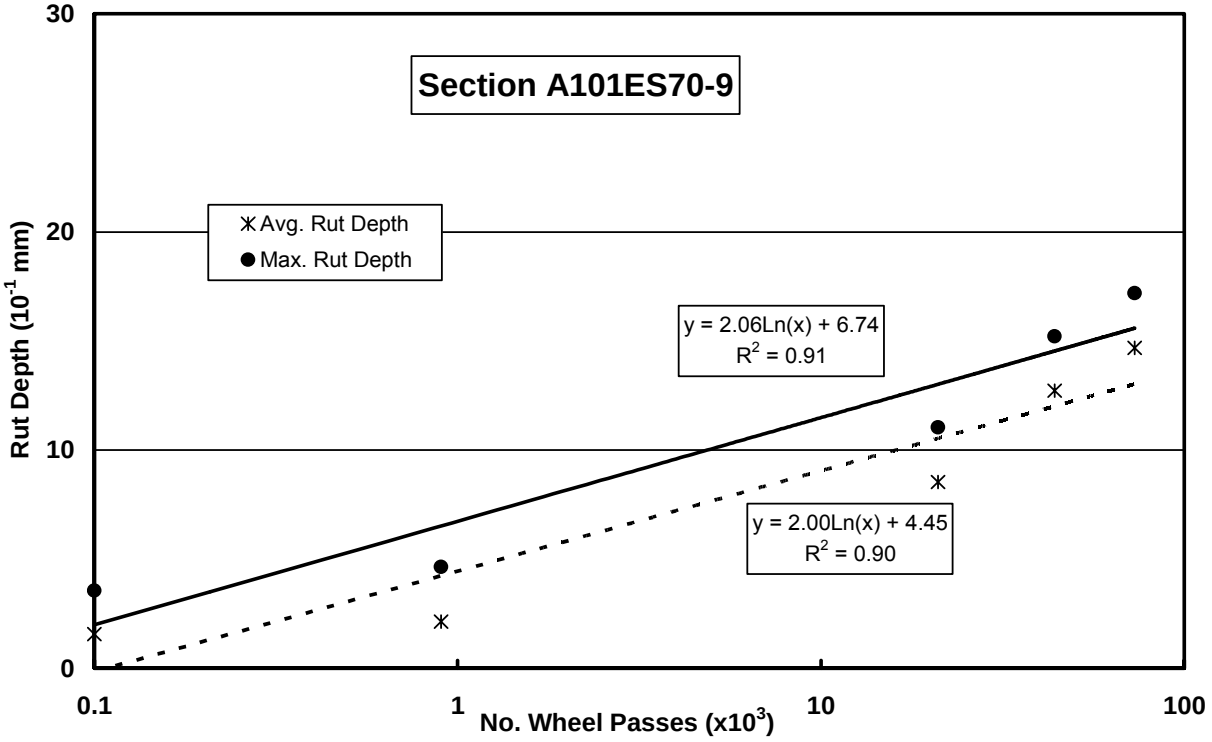

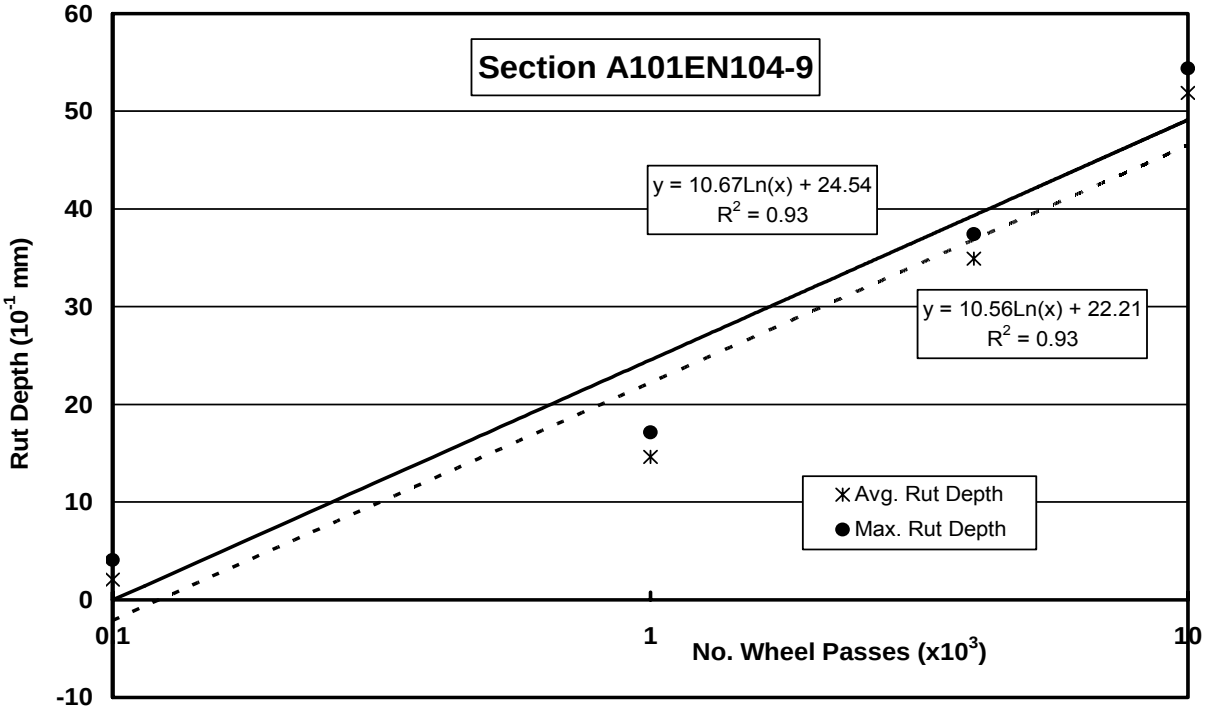

Figure C1 – Rutting Performance on Sections A101ES and A101EN

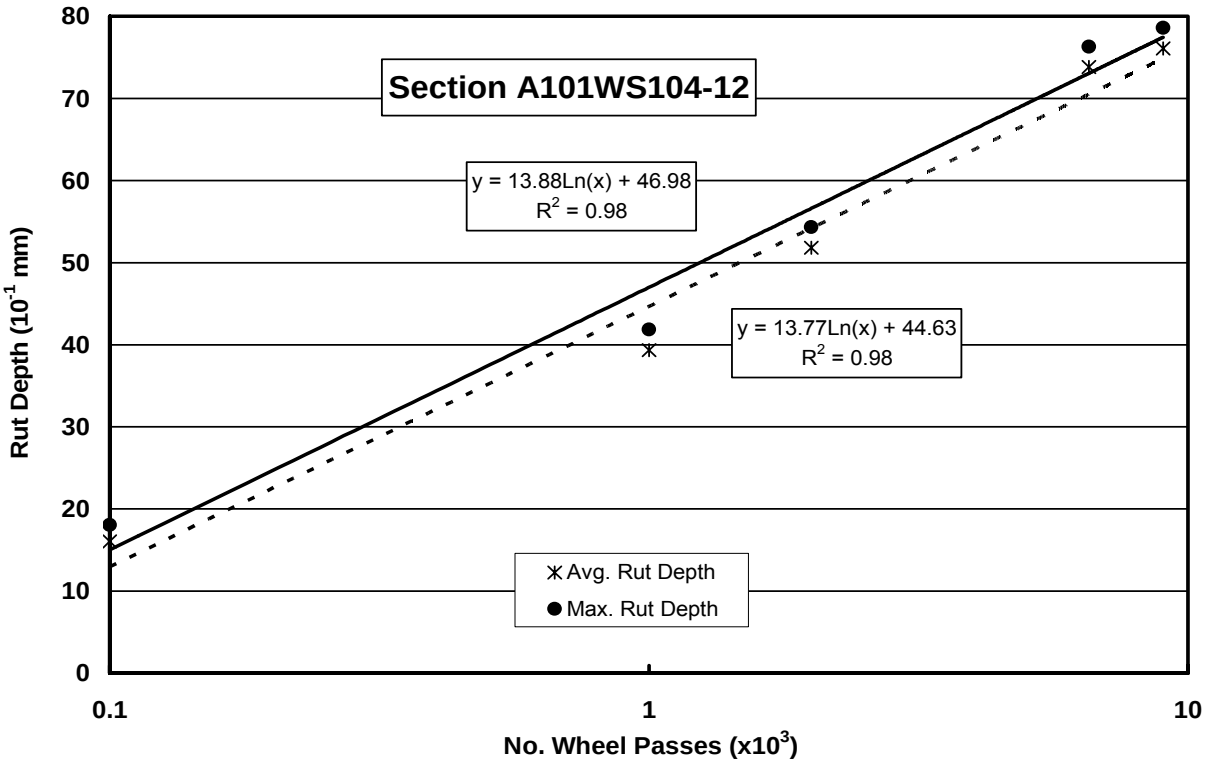

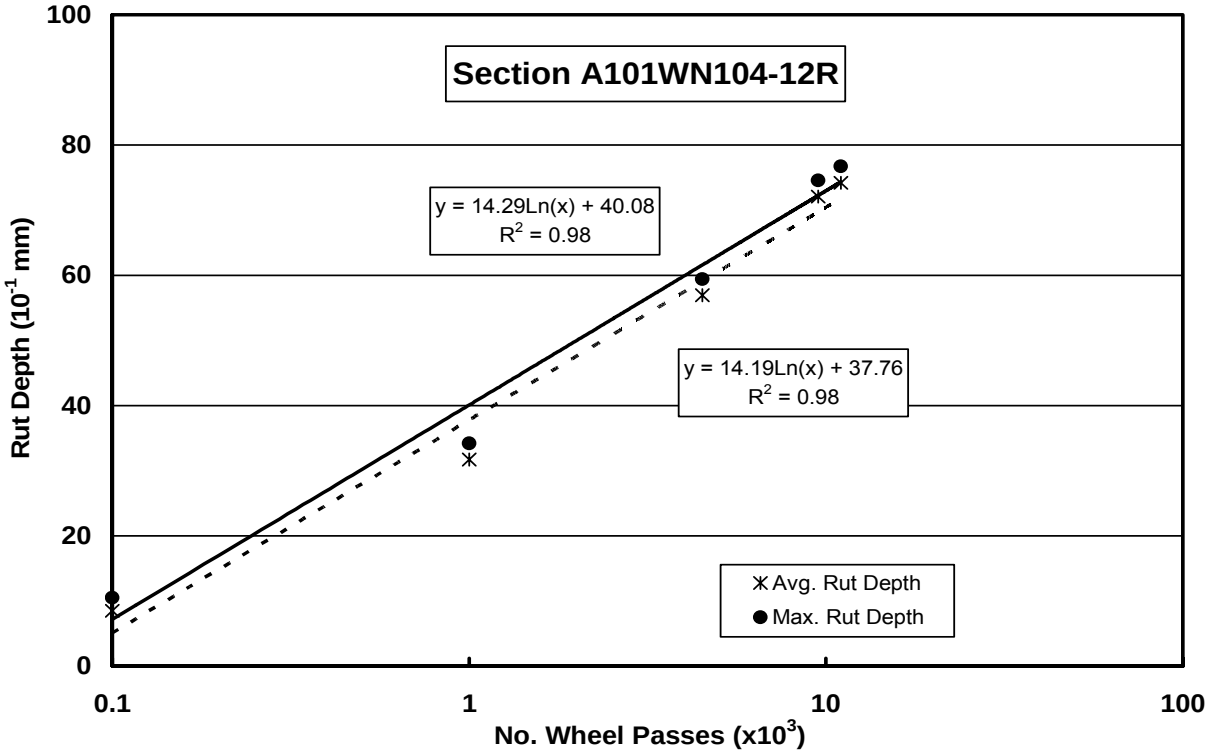

Figure C2 - Rutting Performance on Sections A101WS and A101WN

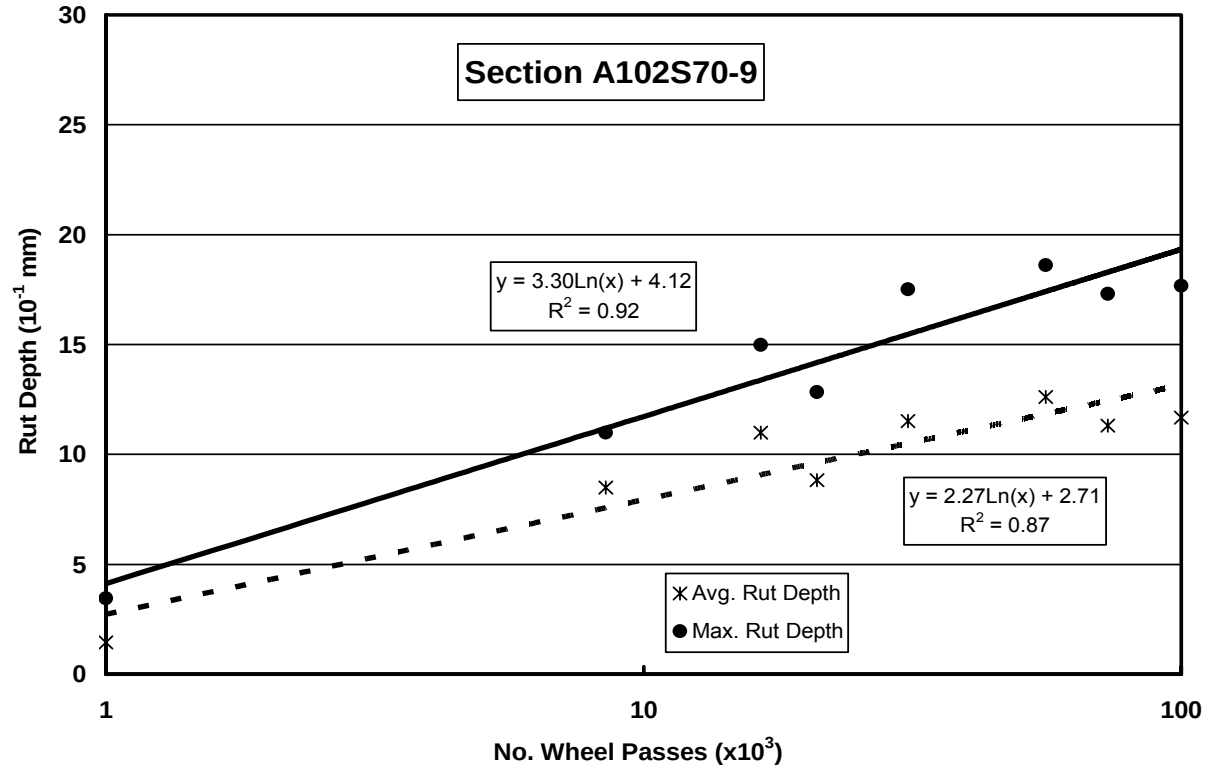

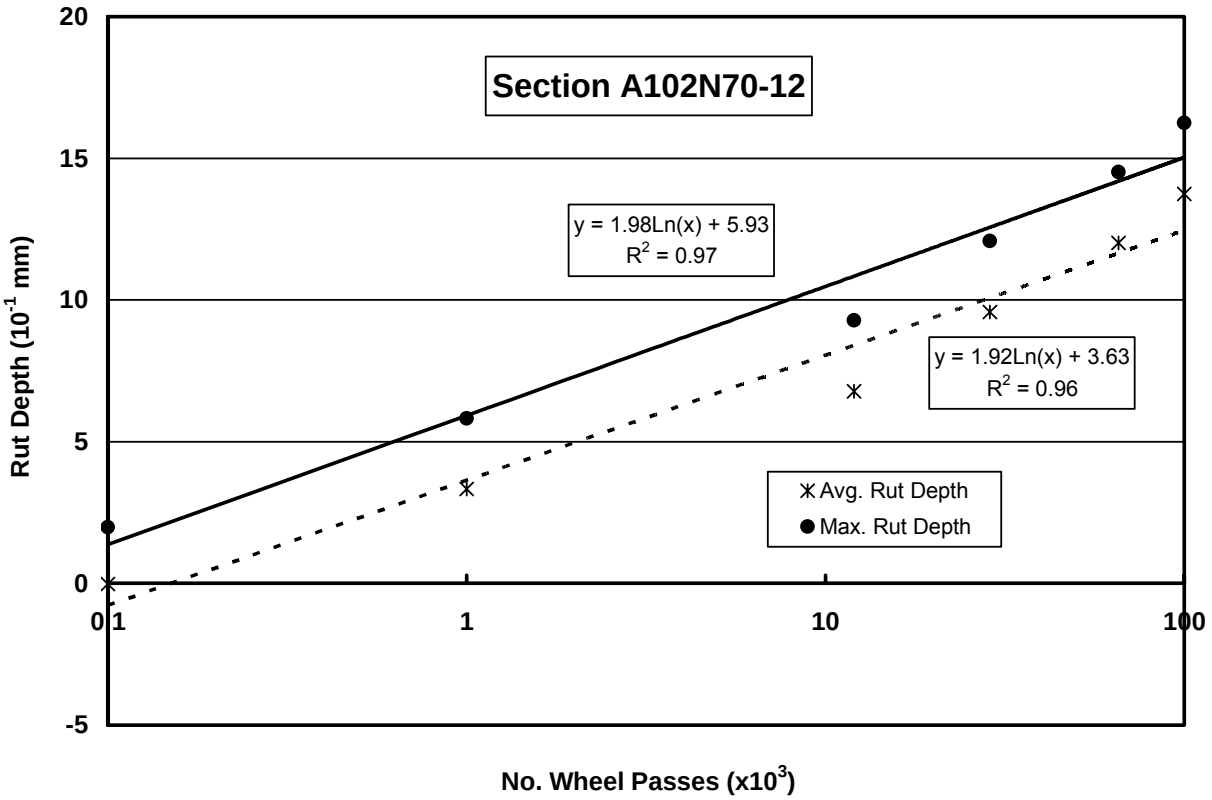

Figure C3 - Rutting Performance on Sections A102S and A102N

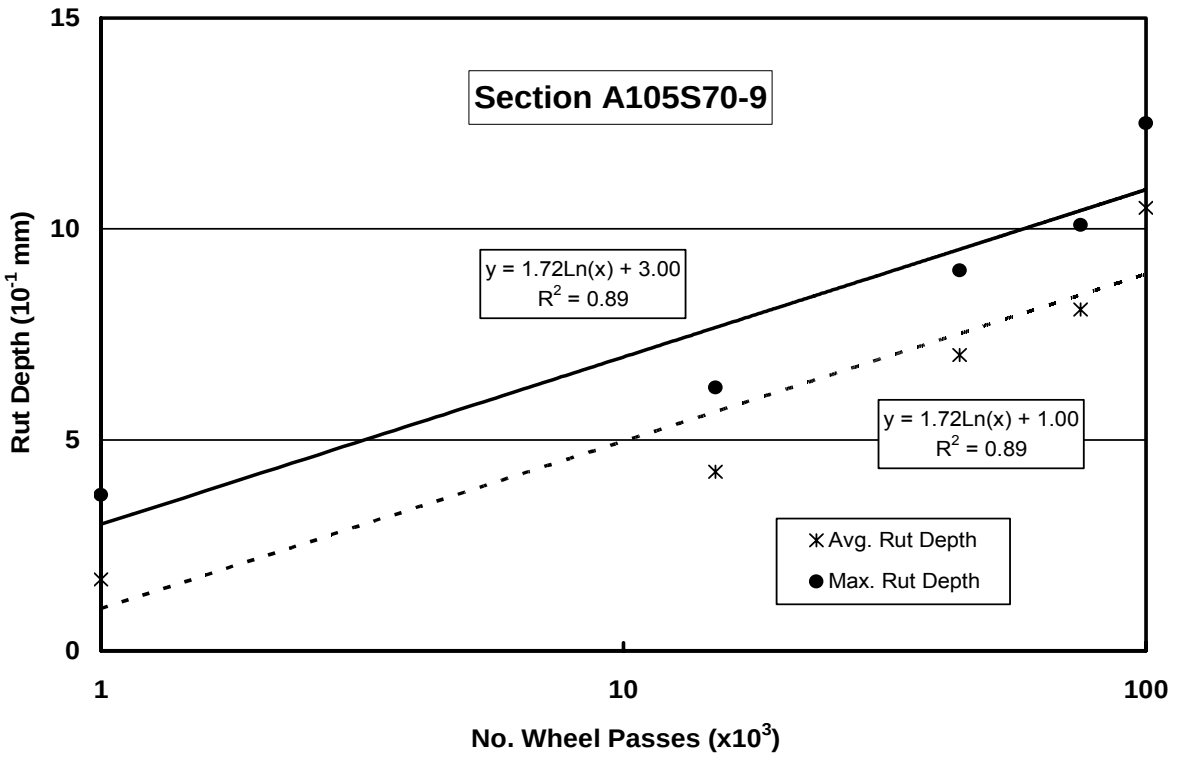

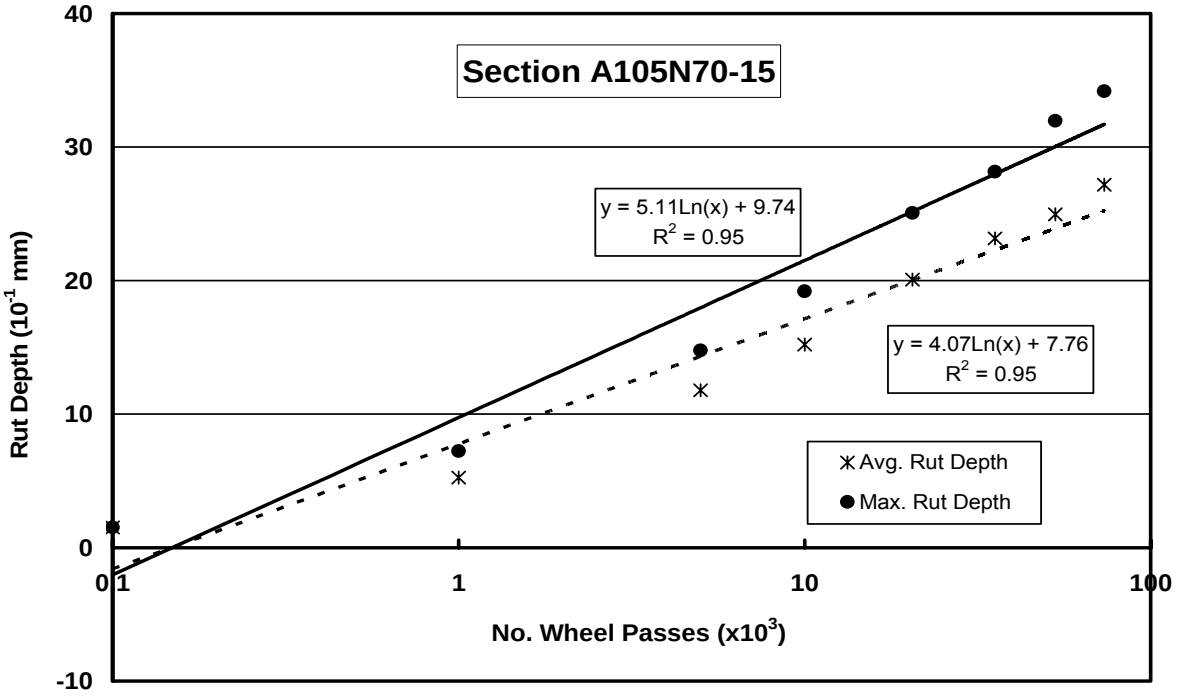

Figure C4 - Rutting Performance on Sections A105S and A105N

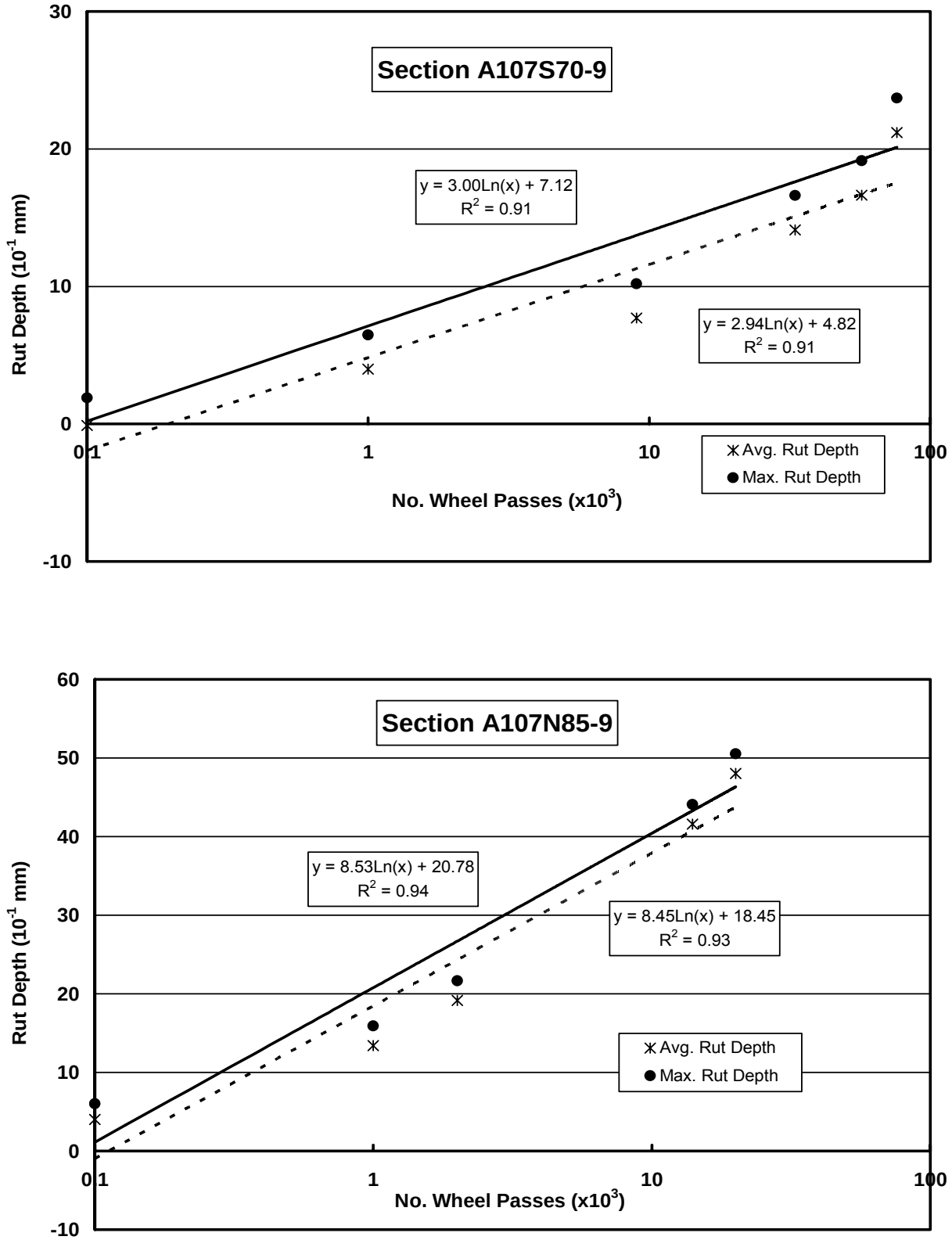

Figure C5 - Rutting Performance on Sections A107S and A107N

APPENDIX D

RERUN OF 104º F RESPONSE AT CONCLUSION OF PAD A

Table D1 – Rerun of 100º F Responses at Conclusion of Pad A

Section	Temp. (°F)	Nominal Load (kips)	Wheel Speed (mph)	Maximum Strain @ Offset in inches								Maximum Voltage Output @ Offset in inches											
				Gauge No. 3 (Z = 7")				Gauge No. 4 (Z = 7")				Short LVDT No. 5 (Z = 5')				Long LVDT No. 6 (Z = 15")				Diff. between Shallow and Deep LVDTs			
				0	2	7	12	0	2	7	12	0	2	7	12	0	2	7	12	0	2	7	12
B101W	70	6										Maximum Voltage											
			1	142.5	146.2	126.3	67.5	123.7	125.0	128.1	71.3	0.197	0.204	0.201	0.110	0.054	0.053	0.068	0.038	0.143	0.151	0.133	0.071
			3	109.4	112.5	95.0	57.5	88.8	88.1	89.4	51.3	0.159	0.162	0.164	0.097	0.044	0.047	0.053	0.032	0.114	0.115	0.112	0.065
			5	97.5	100.0	83.1	52.5	67.3	77.5	79.4	45.6	0.160	0.158	0.152	0.092	0.042	0.044	0.049	0.030	0.118	0.113	0.103	0.062
				Average Gauges 3 & 4								Maximum Deflection (mils/kip)											
				Total Strain				Norm. Strain (με/kip)				Calibration; Long LVDT = 20 volts/in., Short LVDT = 40 volts/in.											
			1	133.1	135.6	127.2	69.4	22.19	22.60	21.20	11.56	0.819	0.850	0.837	0.457	0.448	0.445	0.565	0.320	0.371	0.405	0.272	0.137
			3	99.1	100.3	92.2	54.4	16.51	16.72	15.36	9.06	0.662	0.675	0.685	0.404	0.370	0.391	0.440	0.263	0.292	0.284	0.245	0.140
			5	82.4	88.8	81.2	49.1	13.73	14.79	13.54	8.18	0.668	0.658	0.634	0.383	0.349	0.370	0.409	0.250	0.319	0.288	0.225	0.133
		9										Maximum Voltage											
			1	211.9	218.1	190.0	118.8	192.48	198.73	199.35	128.11	0.303	0.320	0.322	0.206	0.076	0.078	0.101	0.065	0.228	0.242	0.221	0.141
			3	173.7	174.4	150.0	96.9	151.86	152.49	150.61	103.74	0.268	0.275	0.266	0.171	0.063	0.068	0.076	0.050	0.204	0.208	0.190	0.121
			5	155.6	153.8	132.5	86.9	129.37	130.62	128.74	84.4	0.253	0.255	0.241	0.157	0.062	0.064	0.073	0.047	0.191	0.191	0.168	0.110
				Average Gauges 3 & 4								Maximum Deflection (mils/kip)											
				Total Strain				Norm. Strain (με/kip)				Calibration; Long LVDT = 20 volts/in., Short LVDT = 40 volts/in.											
			1	202.2	208.4	194.7	123.4	22.46	23.16	21.63	13.71	0.843	0.889	0.895	0.571	0.420	0.436	0.563	0.359	0.423	0.453	0.332	0.212
			3	162.8	163.4	150.3	100.3	18.09	18.16	16.70	11.15	0.744	0.765	0.738	0.475	0.352	0.375	0.422	0.279	0.392	0.390	0.316	0.195
			5	142.5	142.2	130.6	85.6	15.83	15.80	14.51	9.51	0.701	0.708	0.669	0.437	0.342	0.358	0.406	0.262	0.359	0.351	0.263	0.174

Section	Temp. (°F)	Nominal Load (kips)	Wheel Speed (mph)	Maximum Strain @ Offset in inches								Maximum Voltage Output @ Offset in inches											
				Gauge No. 5 (Z = 4")				Gauge No. 6 (Z = 4")				Short LVDT No. 3 (Z = 5')				Long LVDT No. 4 (Z = 16")				Diff. between Shallow and Deep LVDTs			
				0	2	7	12	0	2	7	12	0	2	7	12	0	2	7	12	0	2	7	12
B102	70	6										Maximum Voltage											
			1	188.7	223.1	262.5	122.5	193.73	216.85	241.22	121.87	0.255	0.263	0.293	0.189	0.087	0.091	0.124	0.071	0.168	0.172	0.168	0.118
			3	176.2	199.4	225.6	110.6	161.87	177.49	193.11	102.5	0.208	0.219	0.231	0.168	0.078	0.085	0.102	0.063	0.131	0.133	0.129	0.104
			5	168.7	182.5	209.5	108.1	143.74	166.24	173.74	91.9	0.212	0.205	0.207	0.154	0.070	0.075	0.089	0.053	0.142	0.130	0.117	0.102
				Average Gauges 3 & 4								Maximum Deflection (mils/kip)											
				Total Strain				Norm. Strain (με/kip)				Calibration; Long LVDT = 20 volts/in., Short LVDT = 40 volts/in.											
			1	191.2	220.0	251.8	122.2	31.87	36.66	41.97	20.36	1.063	1.095	1.220	0.787	0.722	0.758	1.037	0.591	0.341	0.338	0.183	0.196
			3	169.1	188.4	209.4	106.6	28.18	31.40	34.89	17.76	0.868	0.911	0.962	0.698	0.646	0.711	0.852	0.526	0.223	0.200	0.110	0.172
			5	156.2	174.4	191.6	100.0	26.04	29.06	31.94	16.67	0.882	0.854	0.861	0.643	0.583	0.628	0.745	0.440	0.298	0.227	0.116	0.203
		9										Maximum Voltage											
			1	286.8	332.4	371.8	191.2	273.71	301.83	320.58	183.11	0.338	0.365	0.415	0.277	0.117	0.122	0.171	0.102	0.221	0.243	0.245	0.175
			3	259.3	283.7	312.5	168.7	243.1	255.6	273.72	156.87	0.323	0.338	0.370	0.256	0.110	0.116	0.147	0.091	0.213	0.222	0.223	0.165
			5	240.0	265.0	290.6	160.0	225.0	239.35	250.6	118.75	0.303	0.309	0.331	0.238	0.109	0.112	0.138	0.088	0.194	0.197	0.193	0.150
				Average Gauges 3 & 4								Maximum Deflection (mils/kip)											
				Total Strain				Norm. Strain (με/kip)				Calibration; Long LVDT = 20 volts/in., Short LVDT = 40 volts/in.											
			1	280.3	317.1	346.2	187.2	31.14	35.24	38.47	20.80	0.938	1.015	1.154	0.770	0.648	0.677	0.948	0.568	0.290	0.338	0.206	0.202
			3	251.2	269.7	293.1	162.8	27.91	29.96	32.57	18.09	0.898	0.938	1.027	0.711	0.613	0.646	0.818	0.507	0.285	0.292	0.209	0.204
			5	232.5	252.2	270.6	139.4	25.83	28.02	30.07	15.49	0.840	0.859	0.918	0.661	0.604	0.622	0.764	0.488	0.236	0.237	0.154	0.173

Section	Temp. (°F)	Nominal Load (kips)	Wheel Speed (mph)	Maximum Strain @ Offset in inches								Maximum Voltage Output @ Offset in inches											
				Gauge No. 1 (Z = 8")				Gauge No. 2 (Z = 8")				Long LVDT No. 1 (Z = 5')				Long LVDT No. 2 (Z = 12")				Diff. between Shallow and Deep LVDTs			
				0	2	7	12	0	2	7	12	0	2	7	12	0	2	7	12	0	2	7	12
B105	70	6										Maximum Voltage											
			1	136.9	131.2	113.7	66.9	110.6	108.7	98.1	56.8	0.086	0.087	0.080	0.056	0.031	0.030	0.040	0.021	0.056	0.057	0.040	0.035
			3	108.1	110.0	91.9	56.6	93.8	93.8	82.5	49.5	0.073	0.078	0.066	0.049	0.025	0.026	0.031	0.018	0.047	0.052	0.034	0.032
			5	103.7	98.1	89.4	51.3	88.8	88.8	83.1	50.0	0.066	0.068	0.059	0.040	0.024	0.027	0.028	0.016	0.042	0.041	0.031	0.024
				Average Gauges 3 & 4								Maximum Deflection (mils/kip)											
				Total Strain				Norm. Strain (με/kip)				Calibration; Long LVDT = 20 volts/in											
			1	123.7	120.0	105.9	61.8	20.62	20.00	17.66	10.30	0.718	0.727	0.667	0.469	0.255	0.253	0.336	0.178	0.463	0.474	0.331	0.292
			3	NA	101.9	87.2	53.1	NA	16.98	14.53	8.84	N/A	0.646	0.547	0.409	N/A	0.213	0.261	0.146	N/A	0.433	0.286	0.263
			5	96.2	NA	86.2	50.6	16.04	NA	14.37	8.44	0.549	N/A	0.493	0.336	0.201	N/A	0.232	0.136	0.348	N/A	0.261	0.200
		9										Maximum Voltage											
			1	230.0	234.3	209.4	133.1	192.48	198.1	187.48	118.12	0.138	0.141	0.135	0.103	0.045	0.048	0.065	0.039	0.093	0.093	0.070	0.064
			3	195.6	190.6	167.5	NA	176.23	167.48	158.11	101.24	0.130	0.125	0.121	0.091	0.041	0.041	0.053	0.030	0.090	0.083	0.069	0.061
			5	173.1	171.2	153.7	96.3	176.86	161.61	147.49	92.5	0.118	0.112	0.105	0.083	0.039	0.039	0.045	0.028	0.079	0.072	0.060	0.055
				Average Gauges 3 & 4								Maximum Deflection (mils/kip)											
				Total Strain				Norm. Strain (με/kip)				Calibration; Long LVDT = 20 volts/in											
			1	211.2	216.2	198.4	125.6	23.47	24.02	22.05	13.96	0.767	0.781	0.749	0.571	0.250	0.266	0.361	0.216	0.517	0.516	0.388	0.356
			3	185.9	179.0	138.7	NA	20.66	19.89	15.41	NA	0.724	0.693	0.674	0.503	0.226	0.229	0.292	0.167	0.498	0.463	0.382	0.337
			5	175.0	166.4	150.6	94.4	19.44	18.49	16.74	10.49	0.654	0.620	0.583	0.462	0.216	0.219	0.250	0.154	0.439	0.401	0.333	0.307

APPENDIX E

RESPONSE MEASUREMENTS ON PAD B AT 70º F

Table E1 - Pad B Responses at 70º

Section	Nominal Load (kips)	Wheel Speed (mph)	Maximum Strain @ Offset in inches								Maximum Voltage Output @ Offset in inches											
			Gauge No. 3 (Z = 7")				Gauge No. 4 (Z = 7")				Short LVDT No. 5 (Z = 5')				Long LVDT No. 6 (Z = 15")				Diff. between Shallow and Deep LVDTs			
			0	2	7	12	0	2	7	12	0	2	7	12	0	2	7	12	0	2	7	12
B101W 70º F			Total Strain Gauge 3				Total Strain Gauge 4				Maximum Voltage											
	6	1	142	146	126	67.5	124	125	128	71.3	0.197	0.204	0.201	0.110	0.054	0.053	0.068	0.038	0.143	0.151	0.133	0.071
		3	109	113	95.0	57.5	88.8	88.1	89.4	51.3	0.159	0.162	0.164	0.097	0.044	0.047	0.053	0.032	0.114	0.115	0.112	0.065
		5	97.5	100	83.1	52.5	67.3	77.5	79.4	45.6	0.160	0.158	0.152	0.092	0.042	0.044	0.049	0.030	0.118	0.113	0.103	0.062
			Average Gauges 3 & 4								Maximum Deflection (mils/kip)											
			Total Strain				Norm. Strain (με/kip)				Calibration; Long LVDT = 20 volts/in., Short LVDT = 40 volts/in.											
		1	133	136	127	69.4	22.1	22.6	21.2	11.6	0.819	0.850	0.837	0.457	0.448	0.445	0.565	0.320	0.371	0.405	0.272	0.137
		3	98.9	100	92.2	54.4	16.5	16.7	15.4	9.1	0.662	0.675	0.685	0.404	0.370	0.391	0.440	0.263	0.292	0.284	0.245	0.140
		5	82.4	88.8	81.2	49.1	13.7	14.8	13.5	8.18	0.668	0.658	0.634	0.383	0.349	0.370	0.409	0.250	0.319	0.288	0.225	0.133
	9		Total Strain Gauge 3				Total Strain Gauge 4				Maximum Voltage											
		1	212	218	190	119	192	199	199	128	0.303	0.320	0.322	0.206	0.076	0.078	0.101	0.065	0.228	0.242	0.221	0.141
		3	174	174	150	96.9	152	152	151	104	0.268	0.275	0.266	0.171	0.063	0.068	0.076	0.050	0.204	0.208	0.190	0.121
		5	156	154	133	86.9	129	131	129	84.4	0.253	0.255	0.241	0.157	0.062	0.064	0.073	0.047	0.191	0.191	0.168	0.110
			Average Gauges 3 & 4								Maximum Deflection (mils/kip)											
			Total Strain				Norm. Strain (με/kip)				Calibration; Long LVDT = 20 volts/in., Short LVDT = 40 volts/in.											
		1	202	208	195	123	22.5	23.2	21.6	13.7	0.843	0.889	0.895	0.571	0.420	0.436	0.563	0.359	0.423	0.453	0.332	0.212
		3	163	163	150	100	18.1	18.2	16.7	11.1	0.744	0.765	0.738	0.475	0.352	0.375	0.422	0.279	0.392	0.390	0.316	0.195
		5	142	142	131	85.6	15.8	15.8	14.5	9.5	0.701	0.708	0.669	0.437	0.342	0.358	0.406	0.262	0.359	0.351	0.263	0.174
			Gauge No. 5 (Z = 4")				Gauge No. 6 (Z = 4")				Short LVDT No. 3 (Z = 5')				Long LVDT No. 4 (Z = 16")				Diff. between Shallow and Deep LVDTs			
			0	2	7	12	0	2	7	12	0	2	7	12	0	2	7	12	0	2	7	12
B102 70º F	6		Total Strain Gauge 3				Total Strain Gauge 4				Maximum Voltage											
		1	189	223	262	122	194	217	241	122	0.255	0.263	0.293	0.189	0.087	0.091	0.124	0.071	0.168	0.172	0.168	0.118
		3	176	199	226	111	162	177	193	103	0.208	0.219	0.231	0.168	0.078	0.085	0.102	0.063	0.131	0.133	0.129	0.104
		5	169	182	210	108	144	166	174	91.9	0.212	0.205	0.207	0.154	0.070	0.075	0.089	0.053	0.142	0.130	0.117	0.102
			Average Gauges 3 & 4								Maximum Deflection (mils/kip)											
			Total Strain				Norm. Strain (με/kip)				Calibration; Long LVDT = 20 volts/in., Short LVDT = 40 volts/in.											
		1	191	220	252	122	31.9	36.7	42.0	20.4	1.063	1.095	1.220	0.787	0.722	0.758	1.037	0.591	0.341	0.338	0.183	0.196
		3	169	188	209	107	28.2	31.4	34.9	17.8	0.868	0.911	0.962	0.698	0.646	0.711	0.852	0.526	0.223	0.200	0.110	0.172
		5	156	174	192	100	26.0	29.1	31.9	16.7	0.882	0.854	0.861	0.643	0.583	0.628	0.745	0.440	0.298	0.227	0.116	0.203
	9		Total Strain Gauge 3				Total Strain Gauge 4				Maximum Voltage											
		1	287	332	372	191	274	302	321	183	0.338	0.365	0.415	0.277	0.117	0.122	0.171	0.102	0.221	0.243	0.245	0.175
		3	259	284	312	169	243	256	274	157	0.323	0.338	0.370	0.256	0.110	0.116	0.147	0.091	0.213	0.222	0.223	0.165
		5	240	265	291	160	225	239	251	119	0.303	0.309	0.331	0.238	0.109	0.112	0.138	0.088	0.194	0.197	0.193	0.150
			Average Gauges 3 & 4								Maximum Deflection (mils/kip)											
			Total Strain				Norm. Strain (με/kip)				Calibration; Long LVDT = 20 volts/in., Short LVDT = 40 volts/in.											
		1	280	317	346	187	31.1	35.2	38.5	20.8	0.938	1.015	1.154	0.770	0.648	0.677	0.948	0.568	0.290	0.338	0.206	0.202
		3	251	270	293	163	27.9	30.0	32.6	18.1	0.898	0.938	1.027	0.711	0.613	0.646	0.818	0.507	0.285	0.292	0.209	0.204
		5	232	252	271	139	25.8	28.0	30.1	15.5	0.840	0.859	0.918	0.661	0.604	0.622	0.764	0.488	0.236	0.237	0.154	0.173
			Gauge No. 1 (Z = 8")				Gauge No. 2 (Z = 8")				Long LVDT No. 1 (Z = 5')				Long LVDT No. 2 (Z = 12")				Diff. between Shallow and Deep LVDTs			
			0	2	7	12	0	2	7	12	0	2	7	12	0	2	7	12	0	2	7	12
B105 70º F	6		Total Strain Gauge 3				Total Strain Gauge 4				Maximum Voltage											
		1	137	131	114	66.9	111	109	98.1	56.8	0.086	0.087	0.080	0.056	0.031	0.030	0.040	0.021	0.056	0.057	0.040	0.035
		3	108	110	91.9	56.6	93.8	93.8	82.5	49.5	0.073	0.078	0.066	0.049	0.025	0.026	0.031	0.018	0.047	0.052	0.034	0.032
		5	104	98.1	89.4	51.3	88.8	88.8	83.1	50.0	0.066	0.068	0.059	0.040	0.024	0.027	0.028	0.016	0.042	0.041	0.031	0.024
			Average Gauges 3 & 4								Maximum Deflection (mils/kip)											
			Total Strain				Norm. Strain (με/kip)				Calibration; Long LVDT = 20 volts/in											
		1	124	120	106	61.8	20.6	20.0	17.7	10.3	0.718	0.727	0.667	0.469	0.255	0.253	0.336	0.178	0.463	0.474	0.331	0.292
		3	101	102	87.2	53.1	NA	17.0	14.5	8.8	0.604	0.646	0.547	0.409	0.211	0.213	0.261	0.146	N/A	0.433	0.286	0.263
		5	96.2	93.4	86.2	50.6	16.0	NA	14.4	8.4	0.549	0.568	0.493	0.336	0.201	0.228	0.232	0.136	0.348	N/A	0.261	0.200
	9		Total Strain Gauge 3				Total Strain Gauge 4				Maximum Voltage											
		1	230	234	209	133	192	198	187	118	0.138	0.141	0.135	0.103	0.045	0.048	0.065	0.039	0.093	0.093	0.070	0.064
		3	196	191	167	110	176	167	158	101	0.130	0.125	0.121	0.091	0.041	0.041	0.053	0.030	0.090	0.083	0.069	0.061
		5	173	171	154	96.25	177	162	147	92.5	0.118	0.112	0.105	0.083	0.039	0.039	0.045	0.028	0.079	0.072	0.060	0.055
			Average Gauges 3 & 4								Maximum Deflection (mils/kip)											
			Total Strain				Norm. Strain (με/kip)				Calibration; Long LVDT = 20 volts/in											
		1	211	216	198	126	23.5	24.0	22.0	14.0	0.767	0.781	0.749	0.571	0.250	0.266	0.361	0.216	0.517	0.516	0.388	0.356
		3	186	179	163	106	20.7	19.9	18.1	11.7	0.724	0.693	0.674	0.503	0.226	0.229	0.292	0.167	0.498	0.463	0.382	0.337
		5	175	166	151	94.4	19.4	18.5	16.7	10.5	0.654	0.620	0.583	0.462	0.216	0.219	0.250	0.154	0.439	0.401	0.333	0.307

APPENDIX F

RUTTING PERFORMANCE ON PAD B

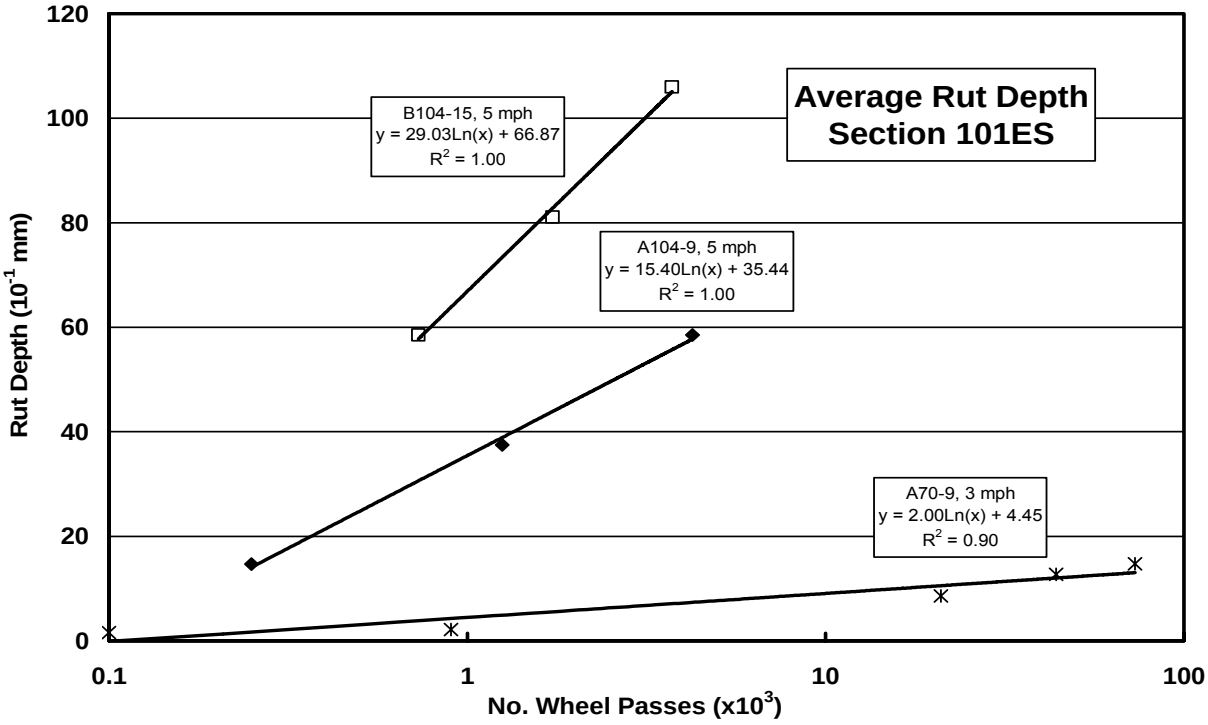

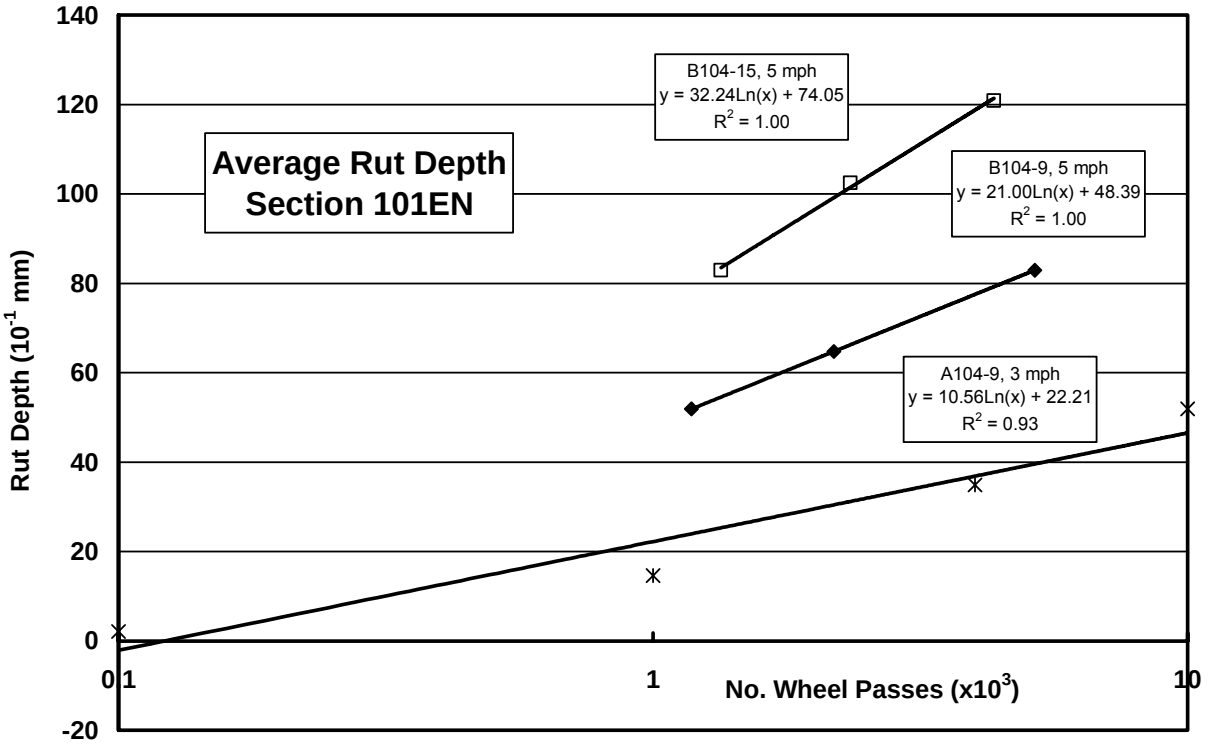

Figure F1 - Rutting Performance on Sections 101ES and 101EN

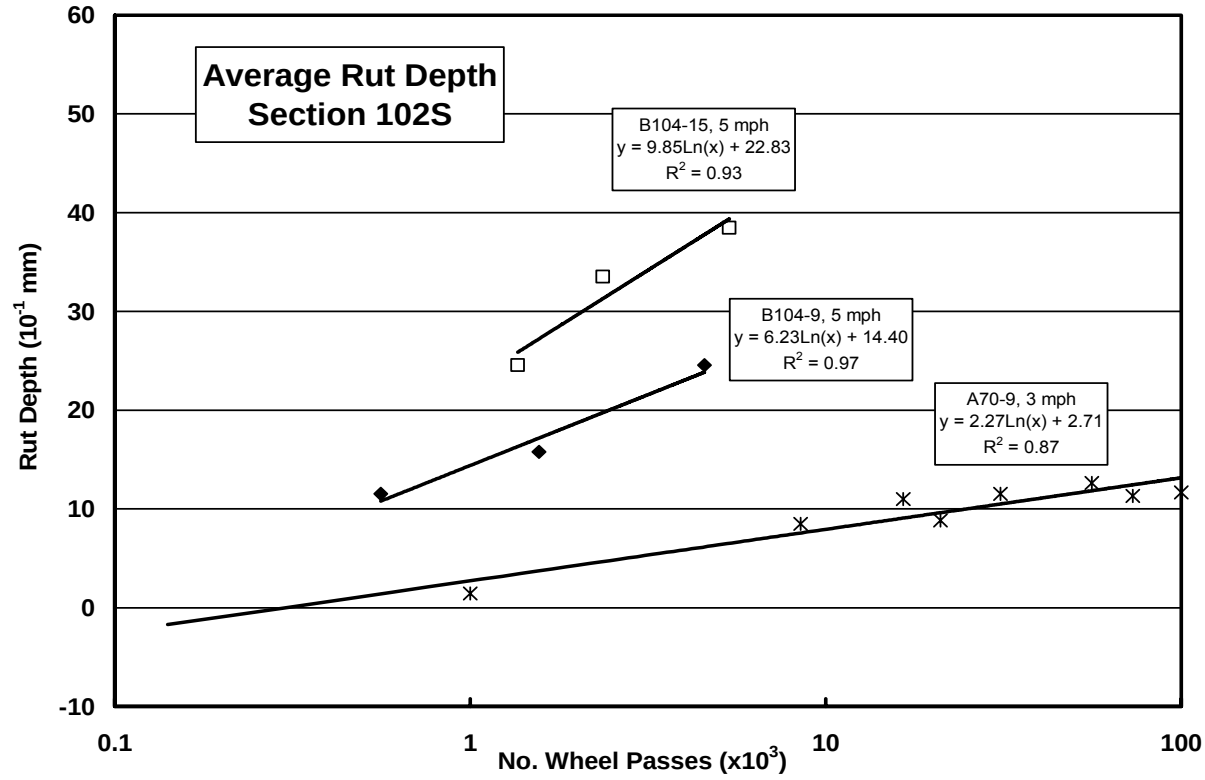

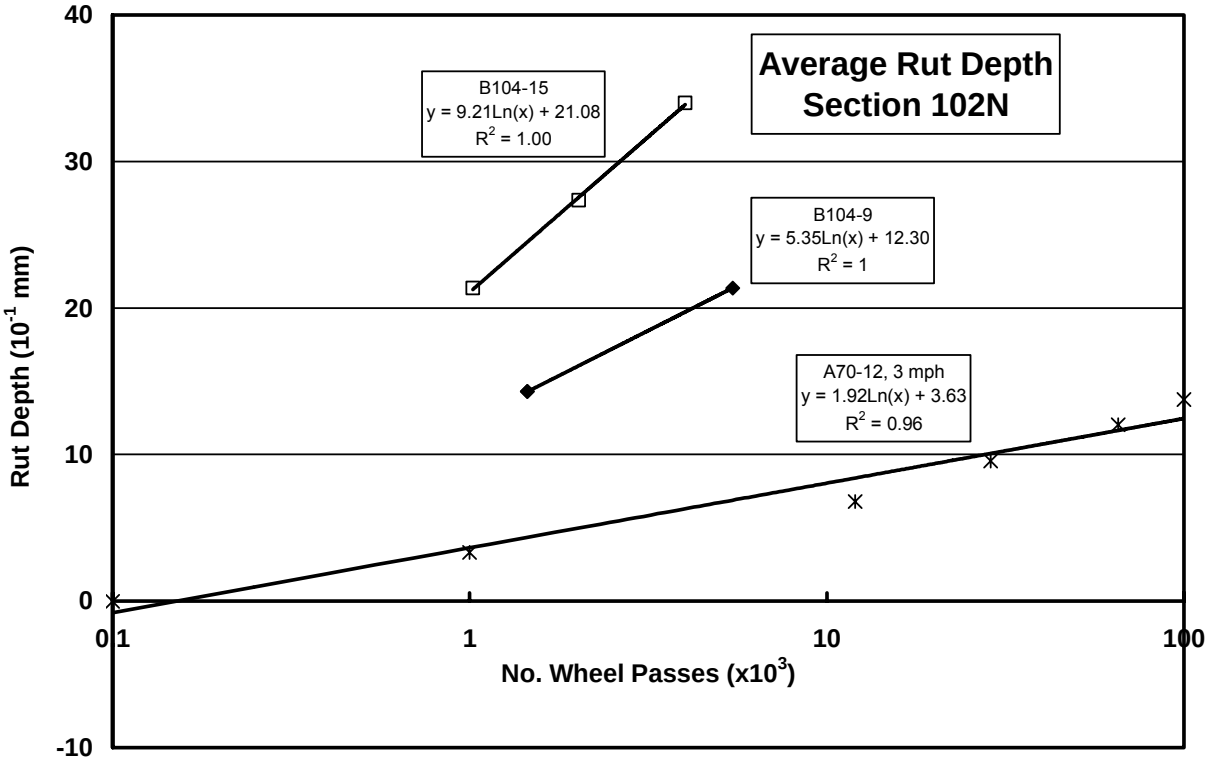

Figure F2 - Rutting Performance on Sections 102S and 102N

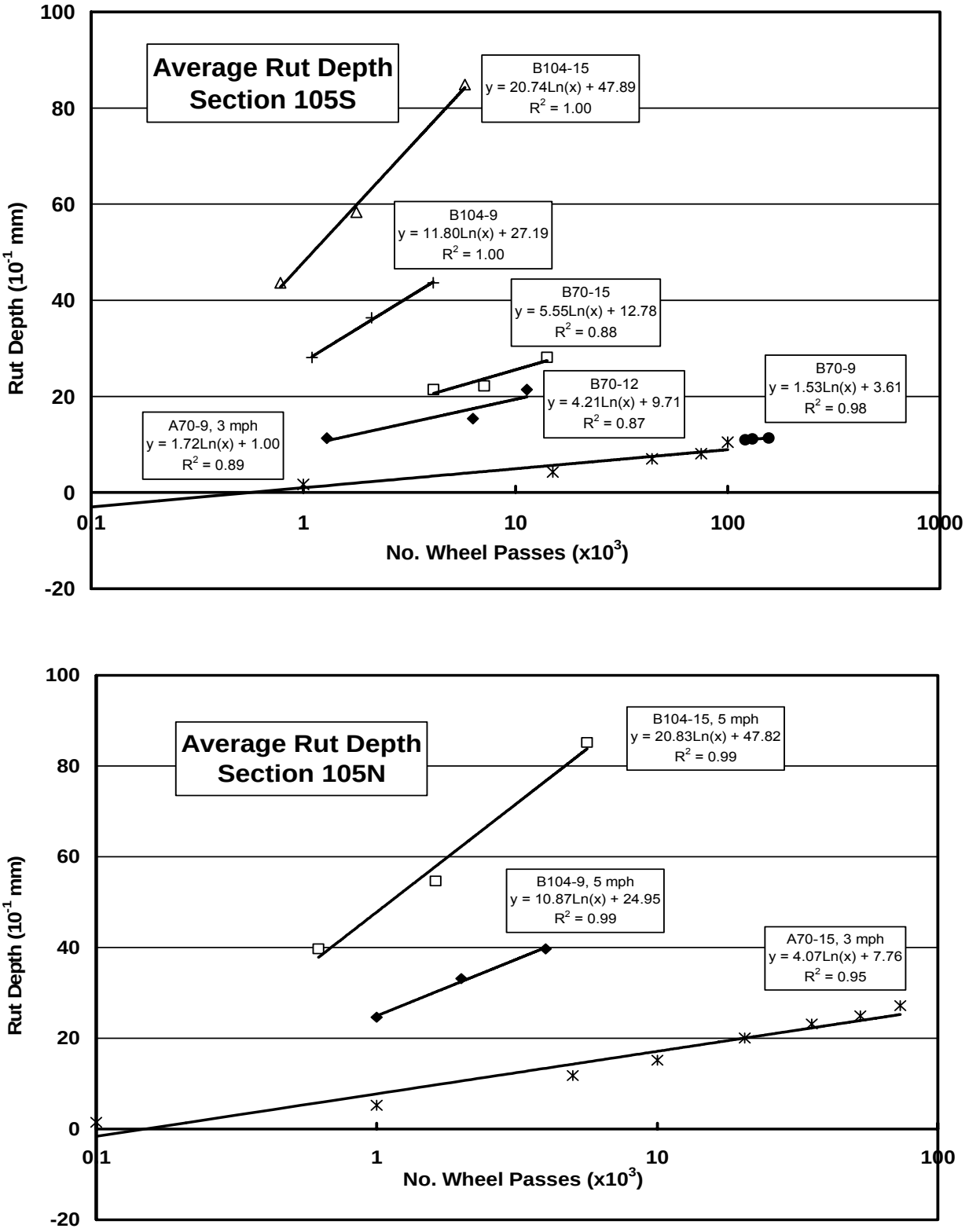

Figure F3 - Rutting Performance on Sections B105S and 105N

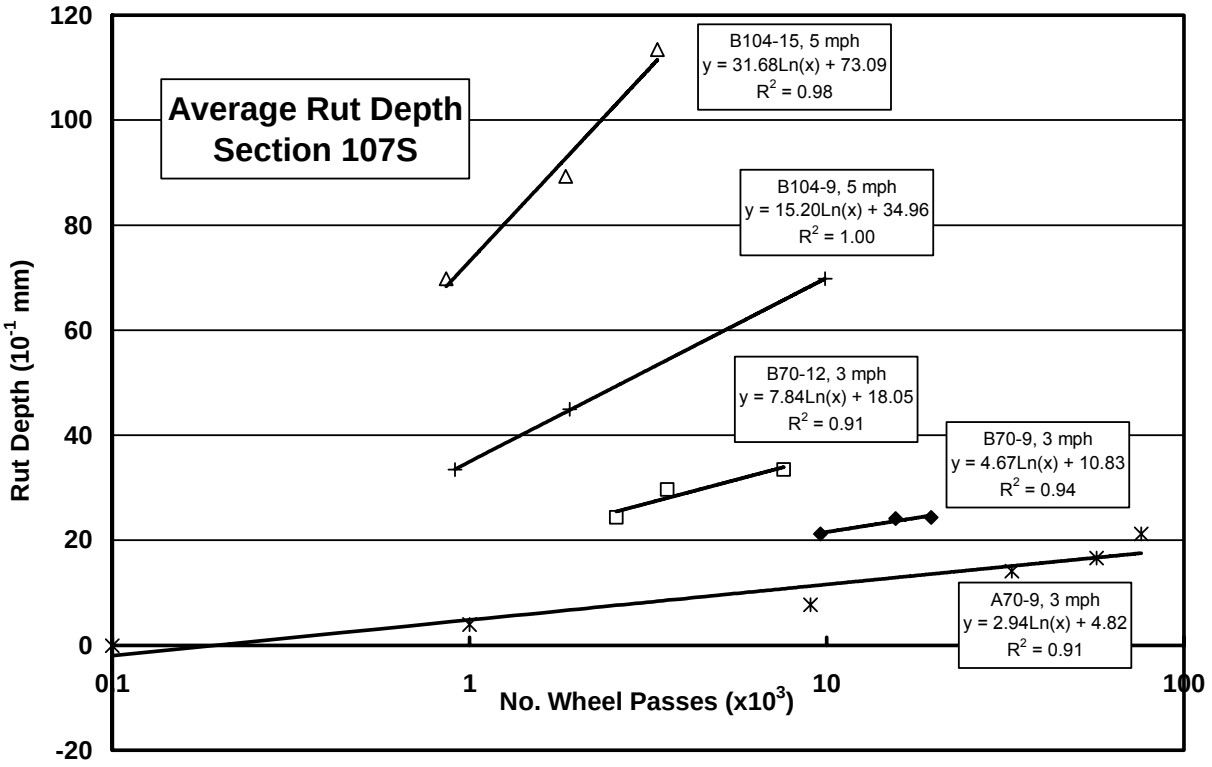

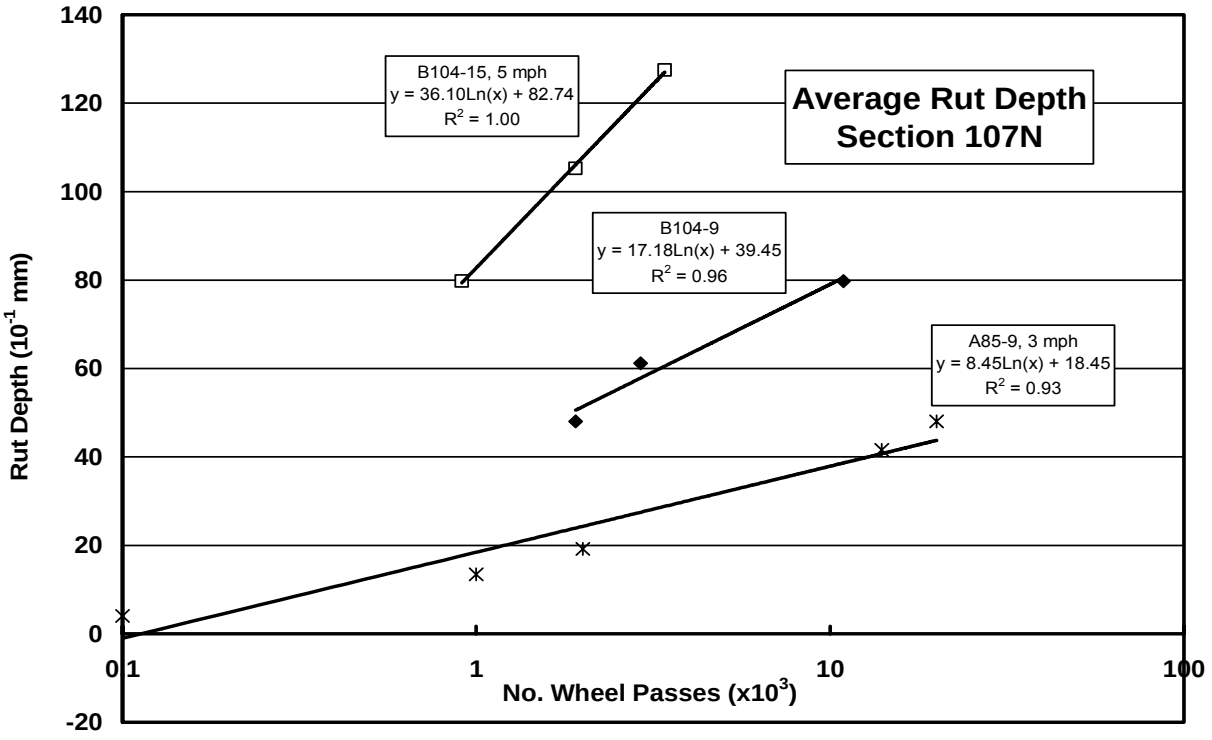

Figure F4 - Rutting Performance on Sections B107S and 107N

APPENDIX G

EFFECTS OF DGAB SLIPPAGE ON LONGITUDINAL STRAIN

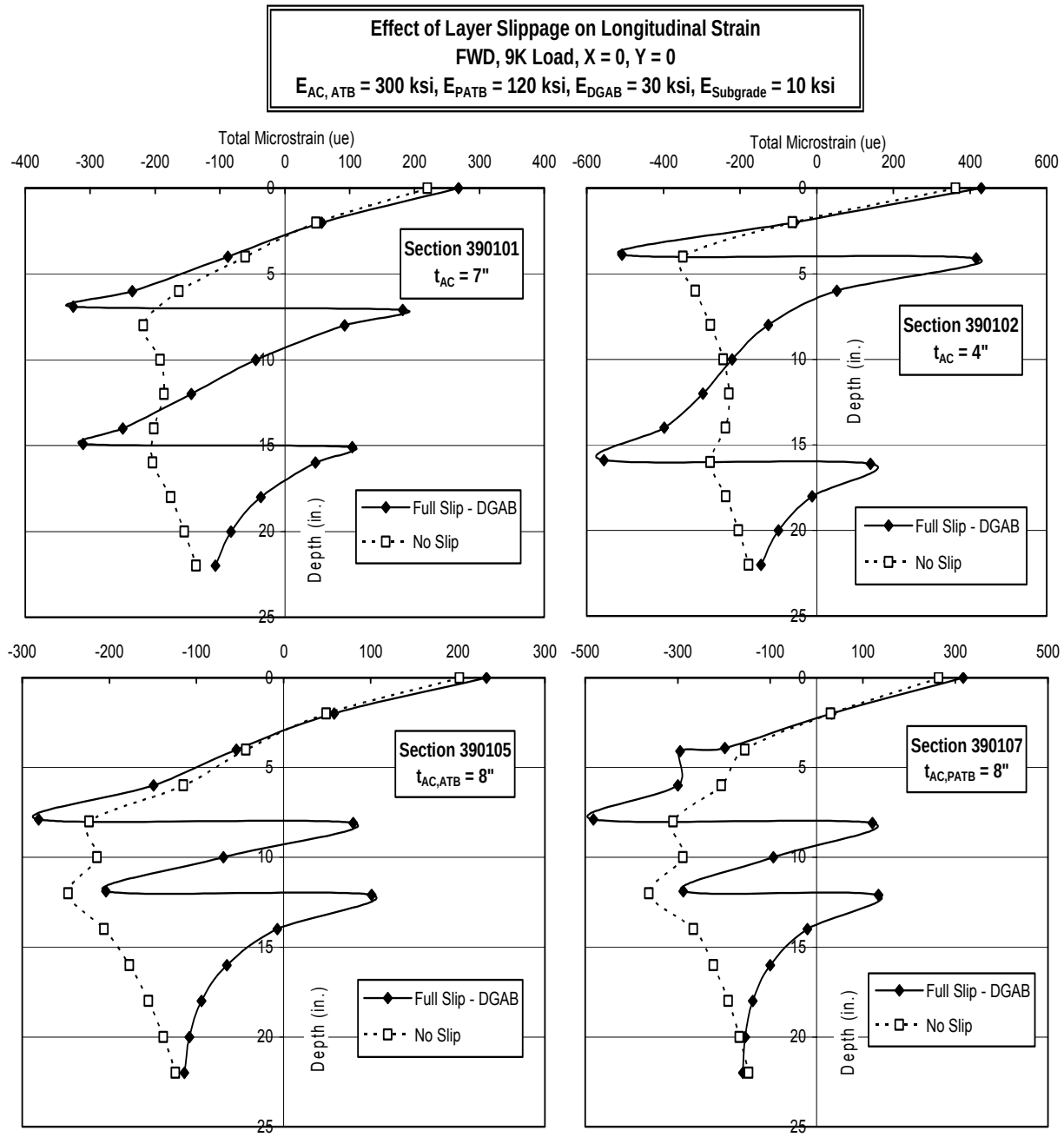

Figure G.1 – Effects of DGAB Slippage on Longitudinal Strain - FWD

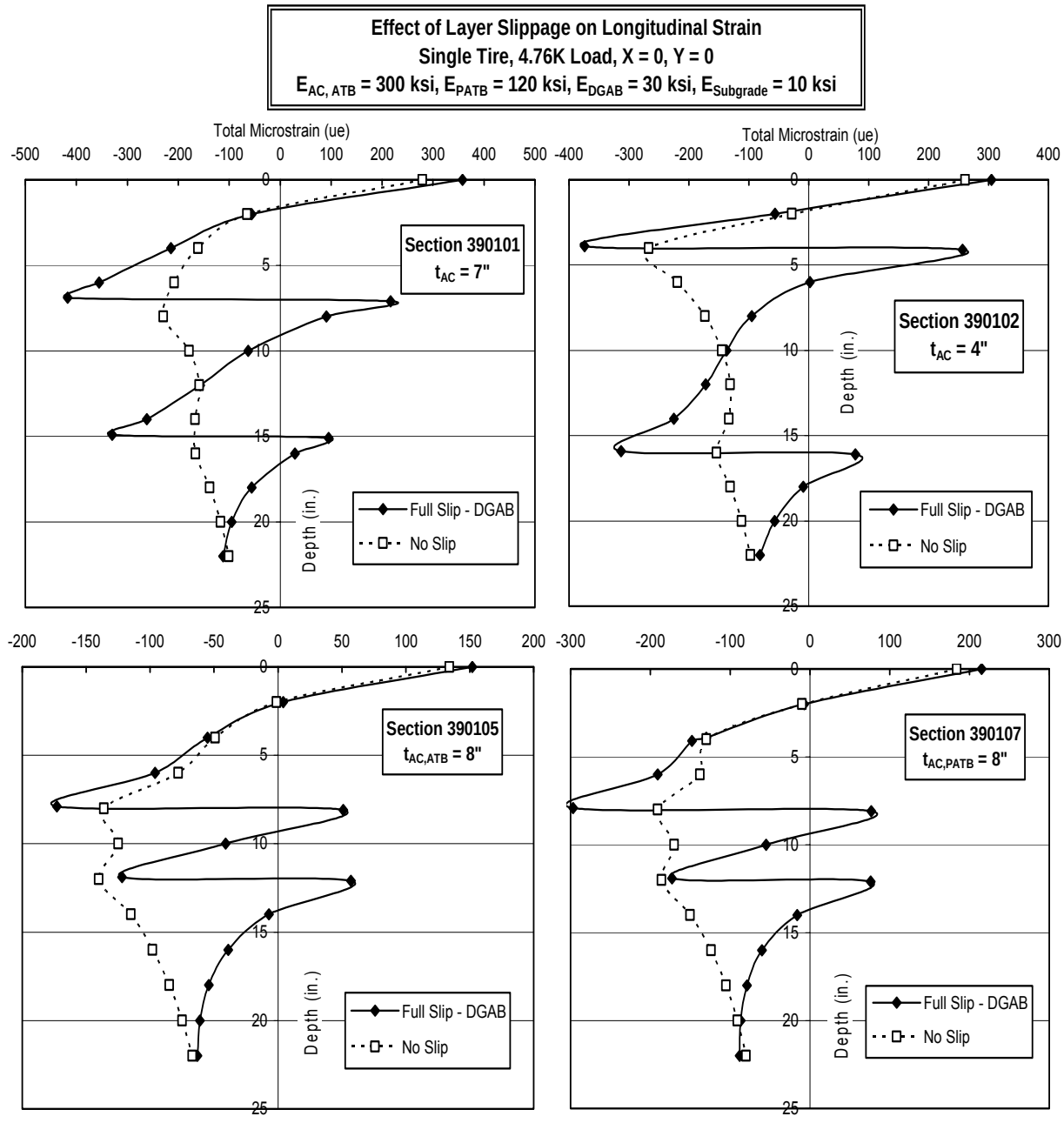

Figure G.2 – Effects of DGAB Slippage on Longitudinal Strain – Single Tire

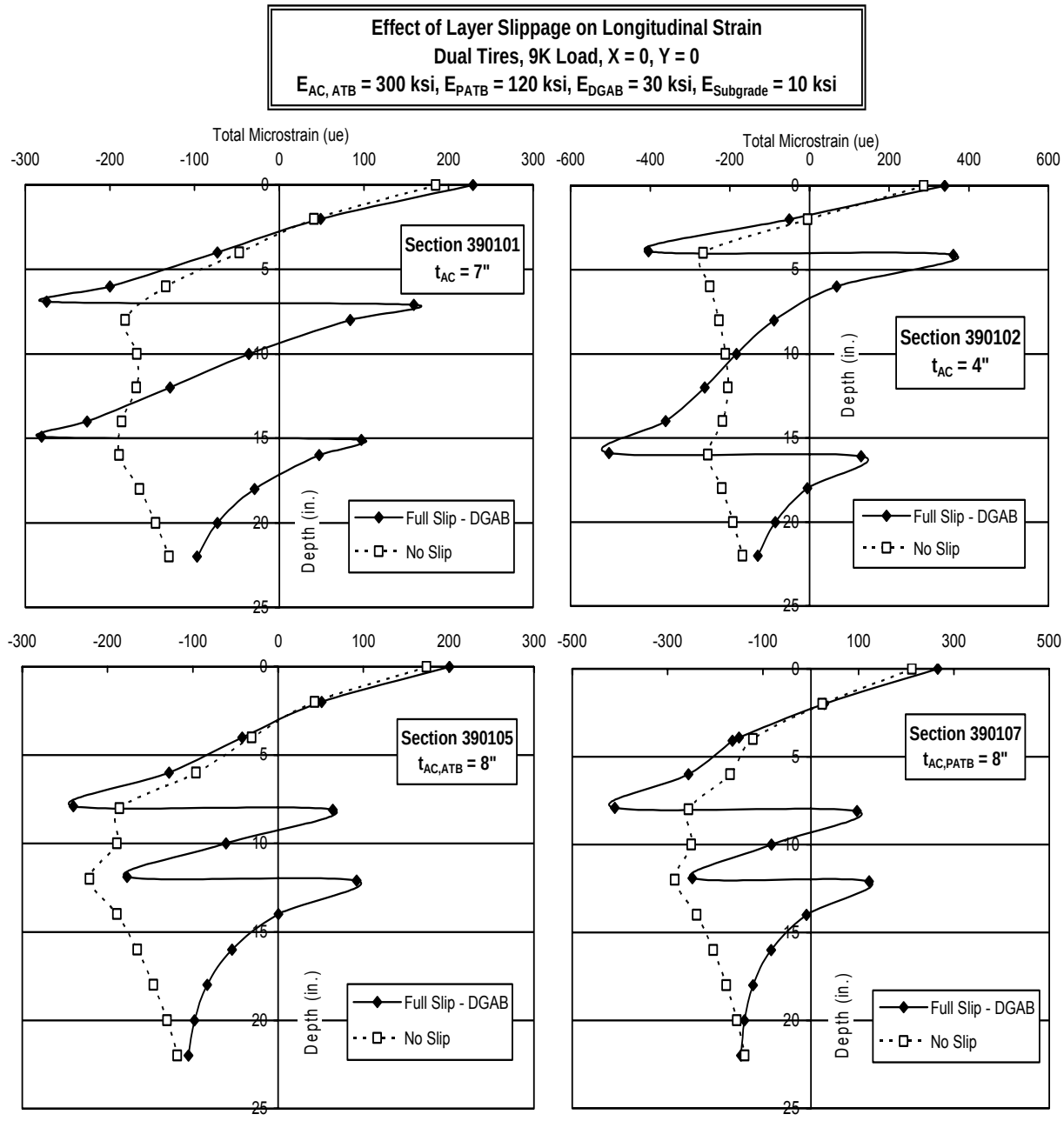

Figure G.3 – Effects of DGAB Slippage on Longitudinal Strain – Dual Tires

APPENDIX H

RELATIONSHIPS BETWEEN LAYER MODULI, STRAIN AND DEFLECTION WITH FWD GEOMETRY

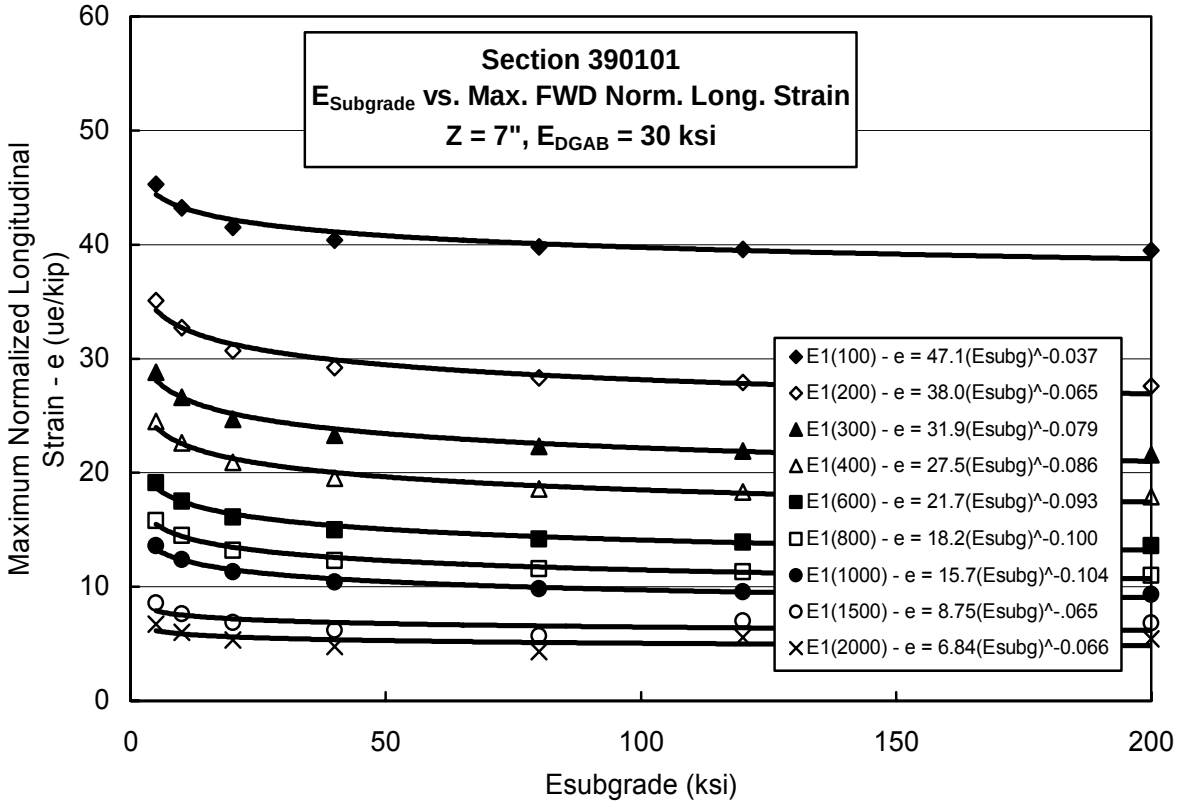

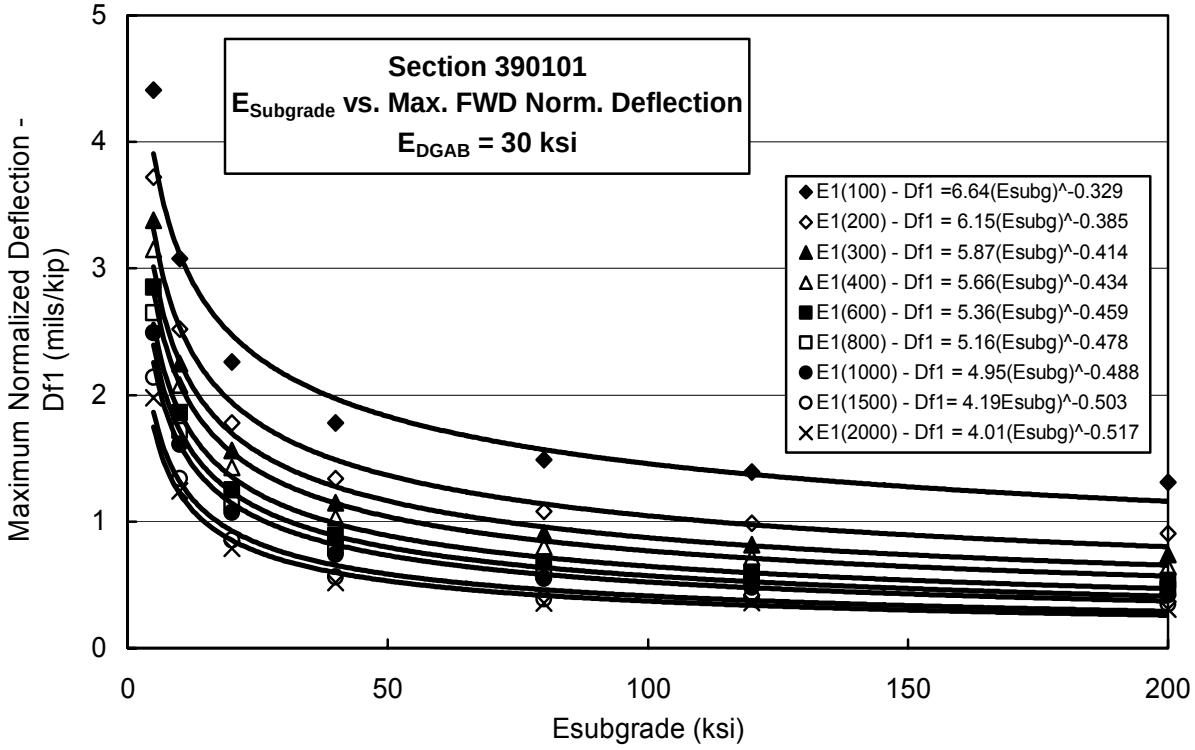

Figure H1 – Strain, Deflection vs. E_1; FWD on Section 390101

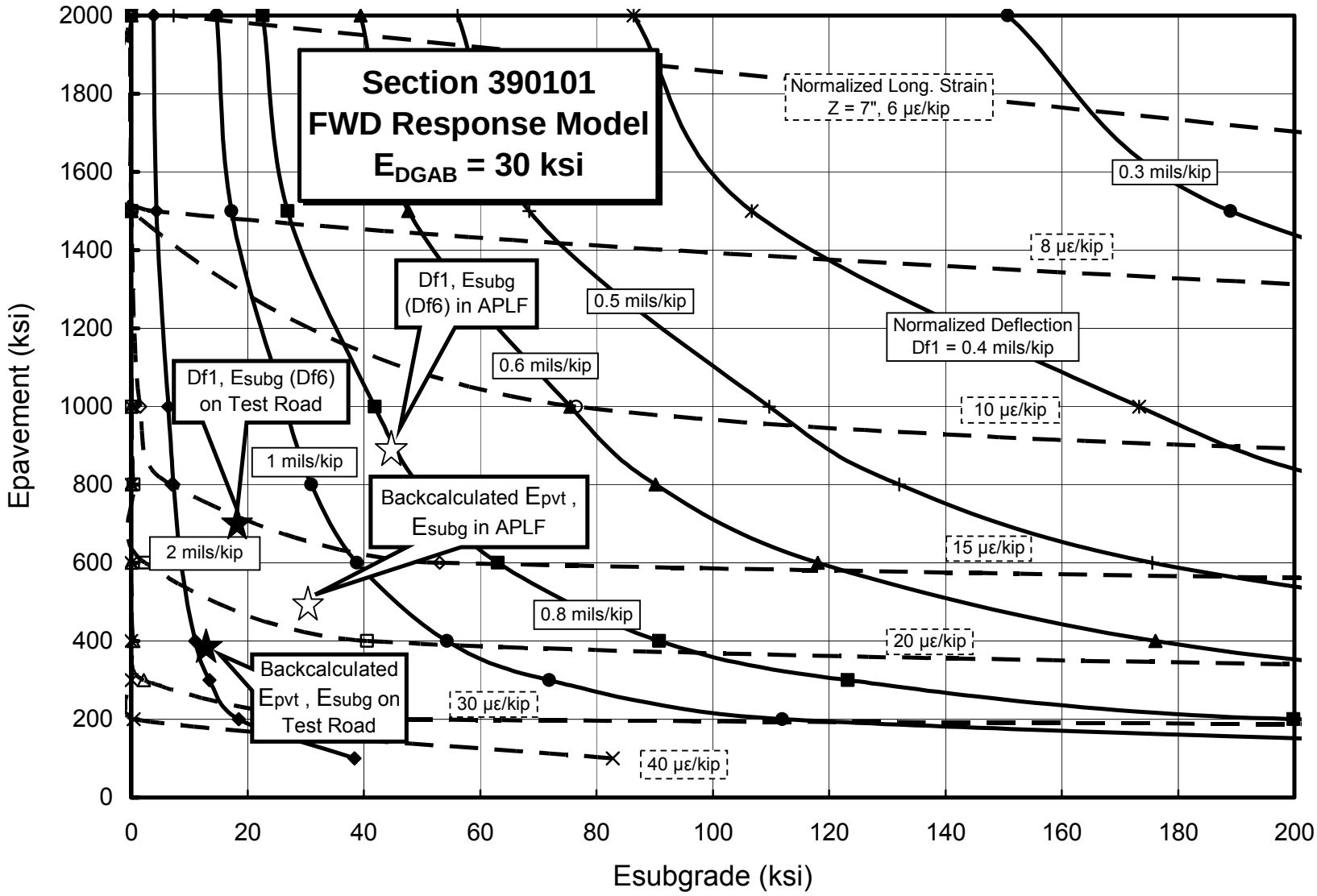

Figure H2 –Relationship between E_1, E_2, Deflection and Strain Using FWD Geometry on Section 390101

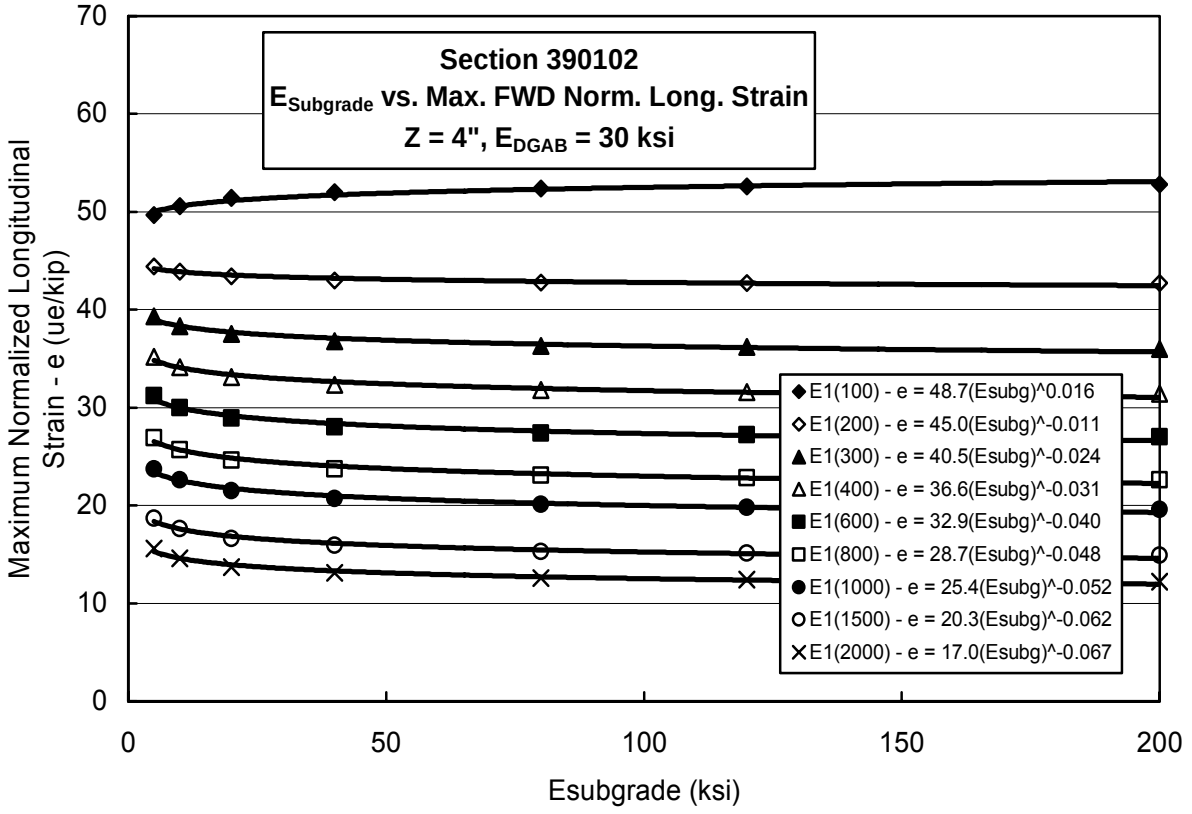

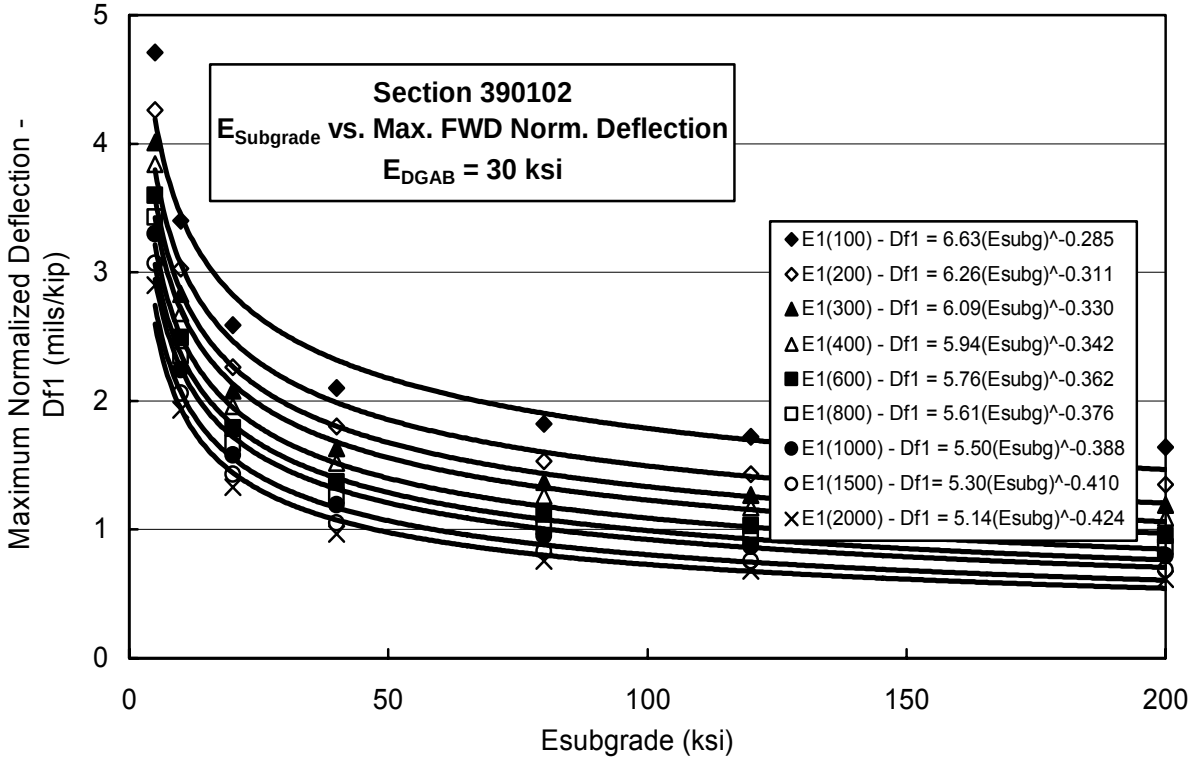

Figure H3 – Strain, Deflection vs. E_2; FWD on Section 390102

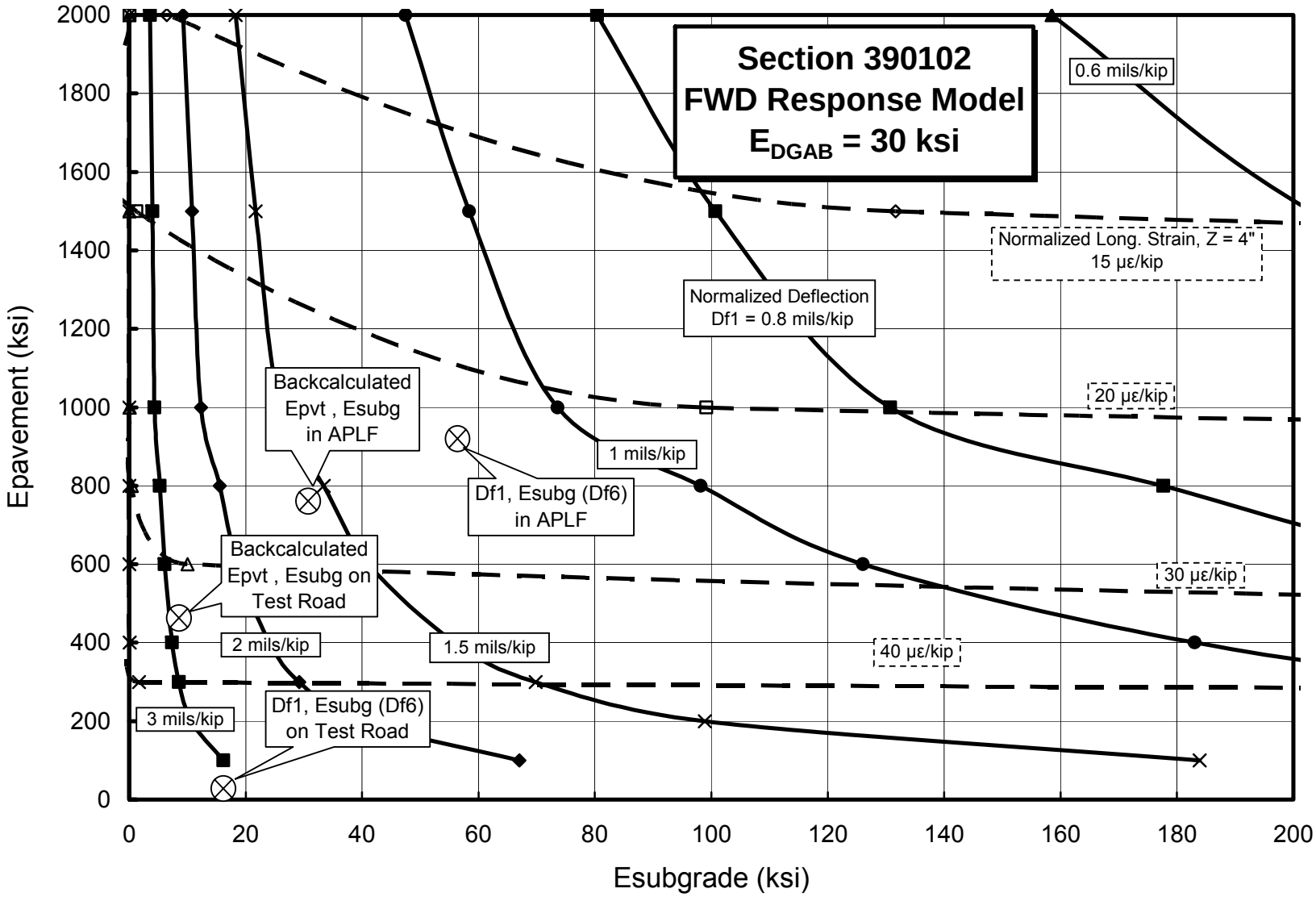

Figure H4 –Relationship between E_1, E_2, Deflection and Strain Using FWD Geometry on Section 390102

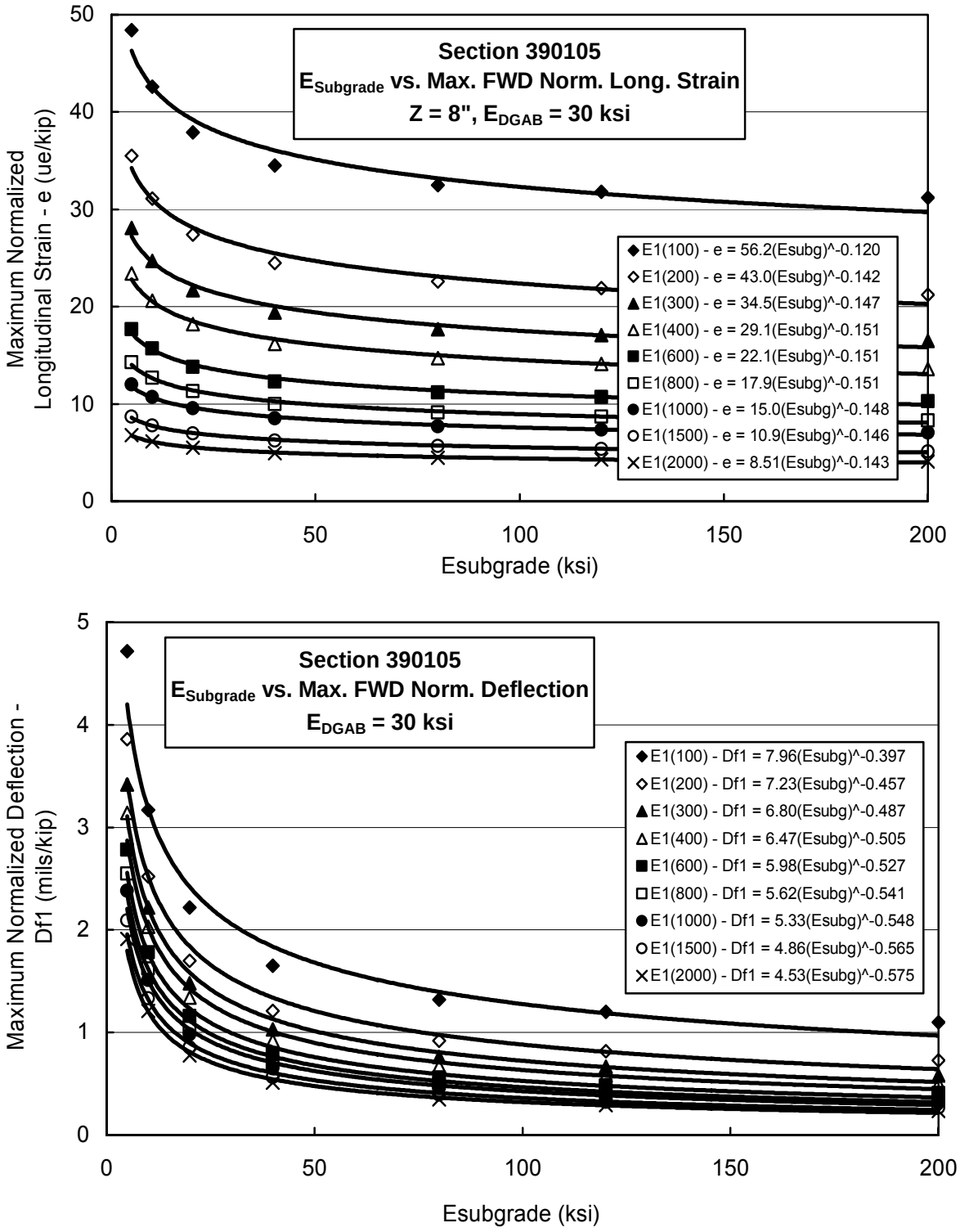

Figure H5 – Strain, Deflection vs. E_2; FWD on Section 390105

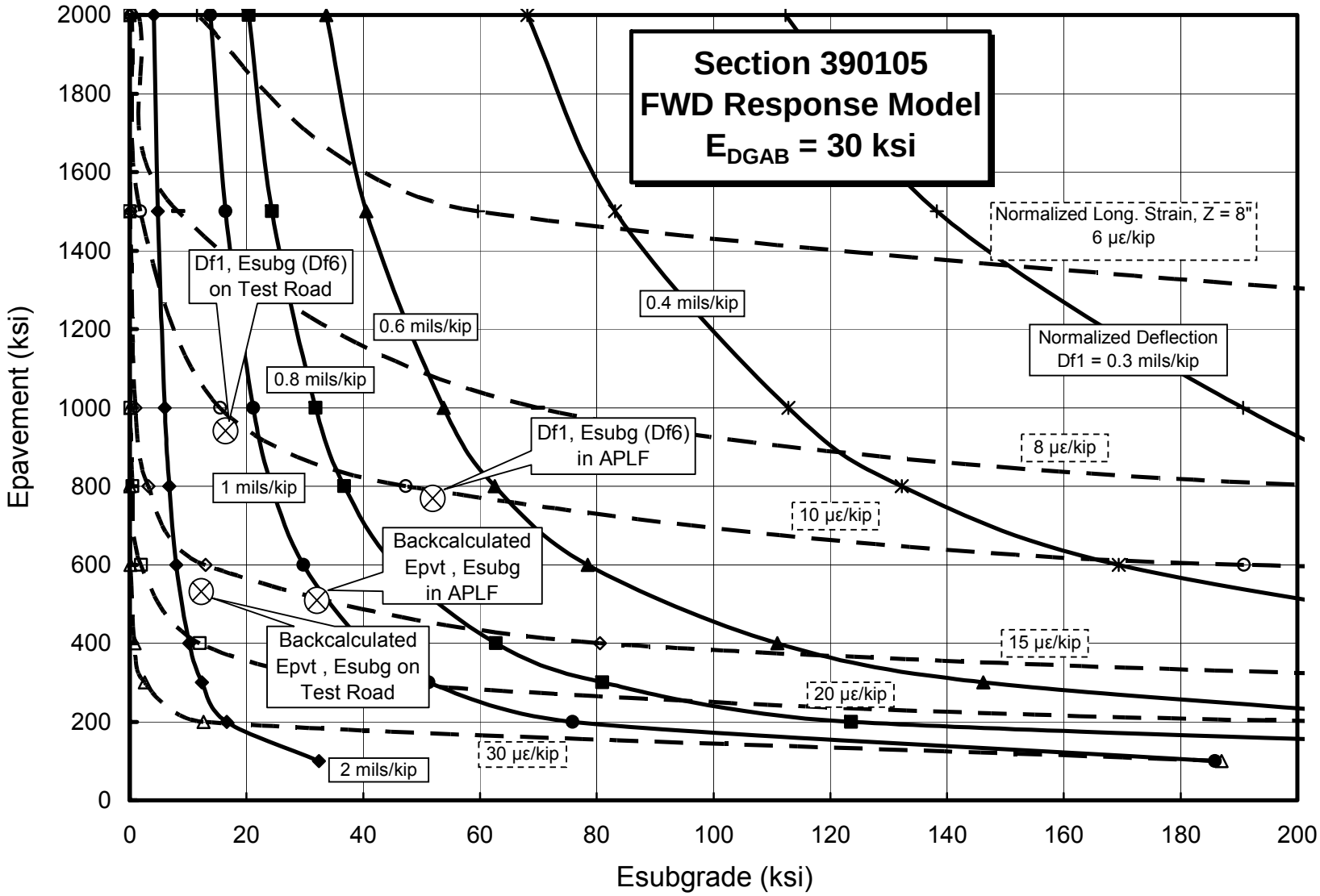

Figure H6 –Relationship between E_1, E_2, Deflection and Strain Using FWD Geometry on Section 390105

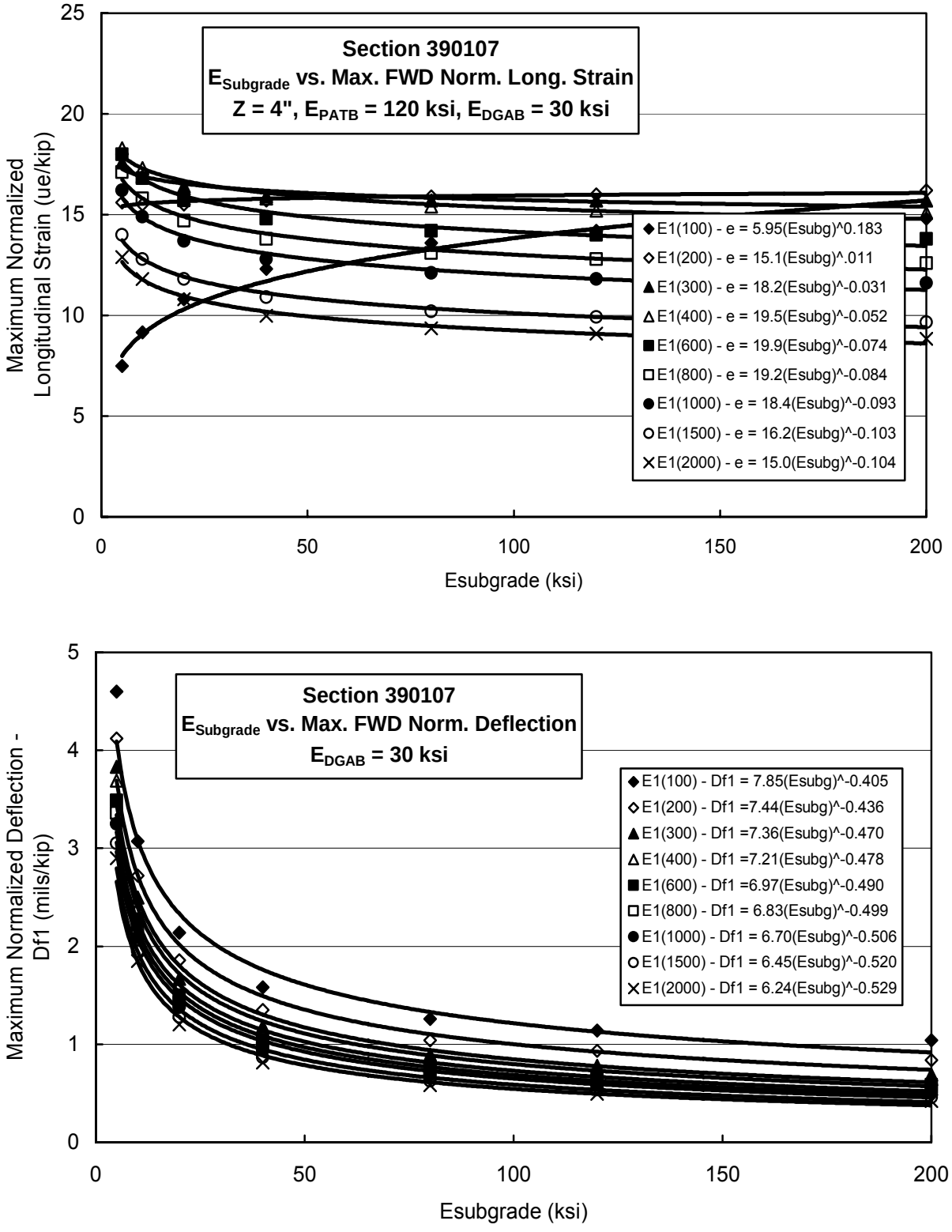

Figure H7 – Strain, Deflection vs. E_2; FWD on Section 390107

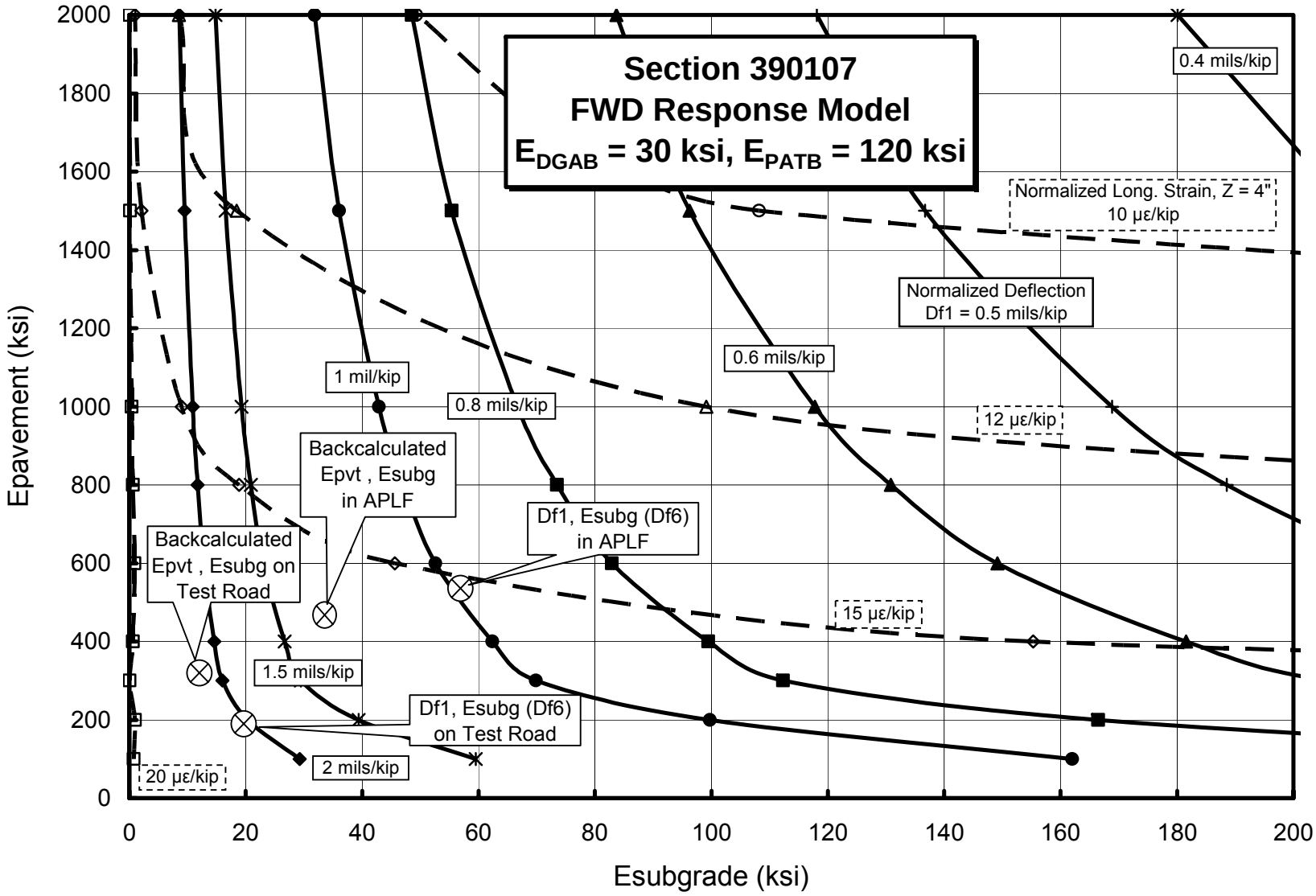

Figure H8 –Relationship between E_1, E_2, Deflection and Strain Using FWD Geometry on Section 390107

APPENDIX I

RELATIONSHIPS BETWEEN LAYER MODULI, STRAIN AND DEFLECTION WITH SINGLE TIRE GEOMETRY

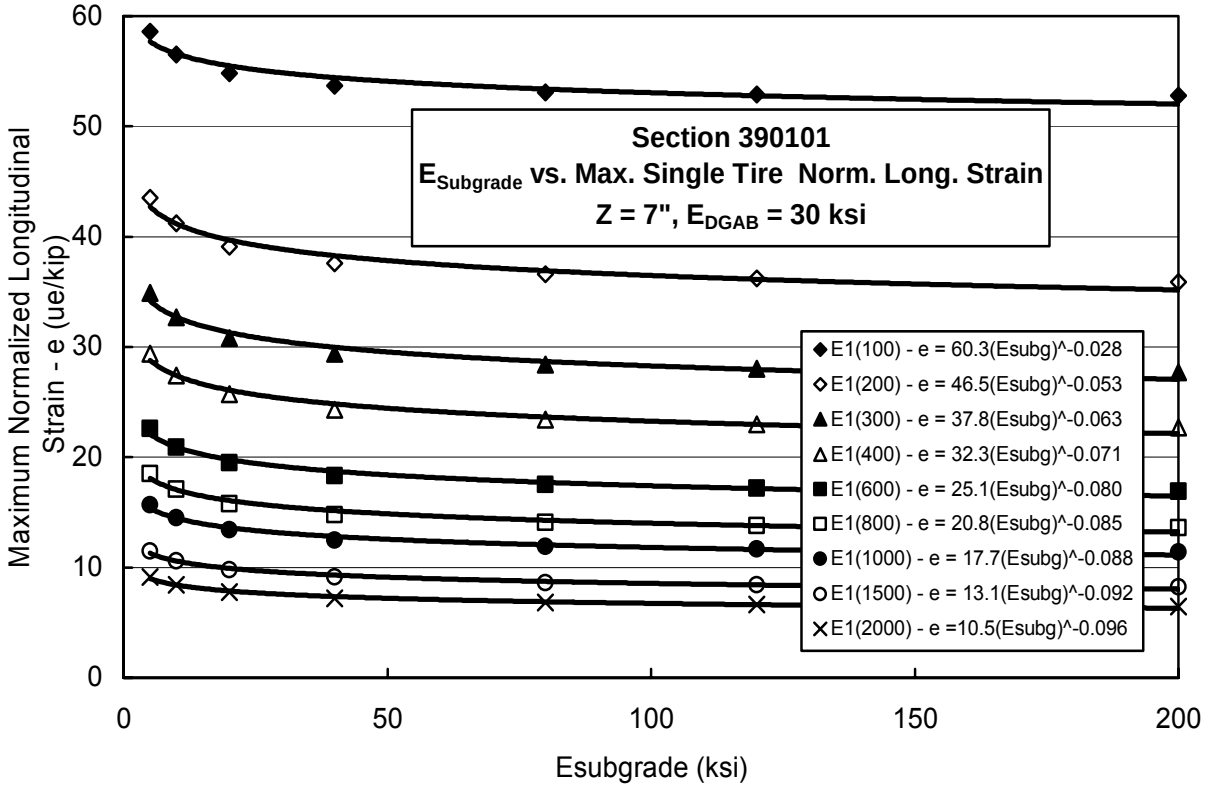

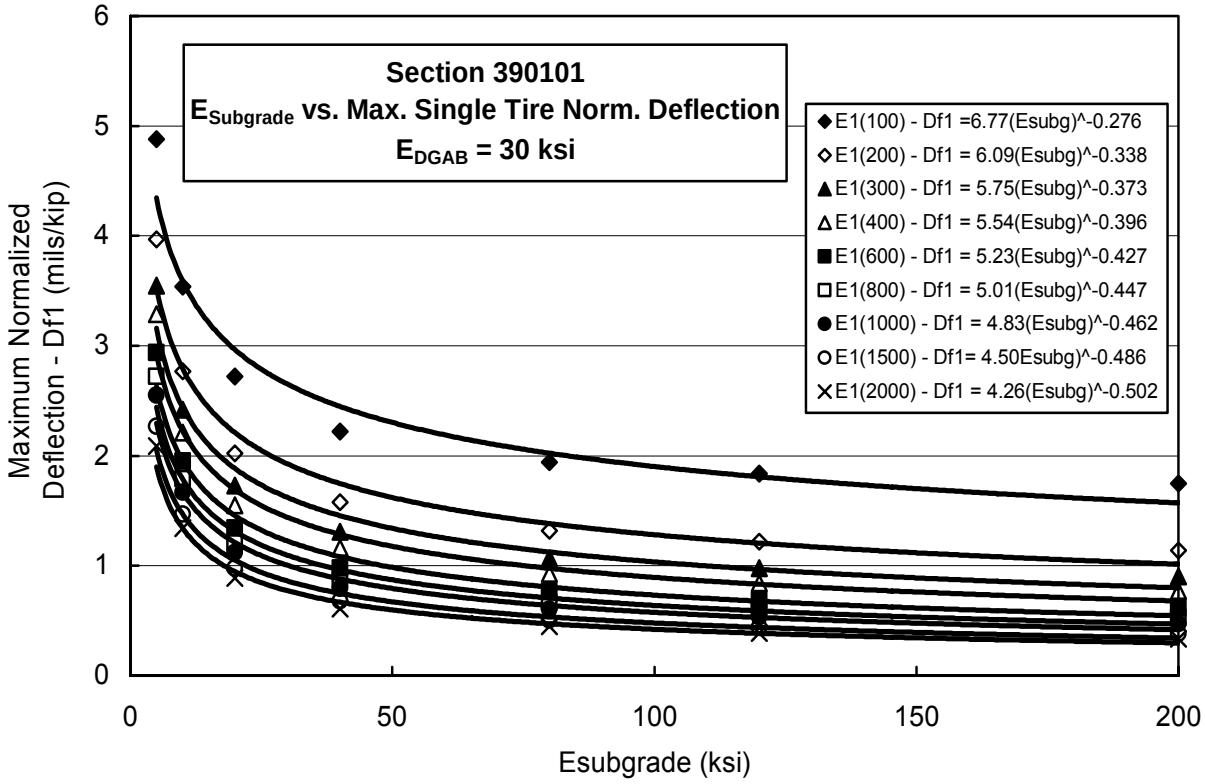

Figure I1 – Strain, Deflection vs. E_2; Single Tire on Section 390101

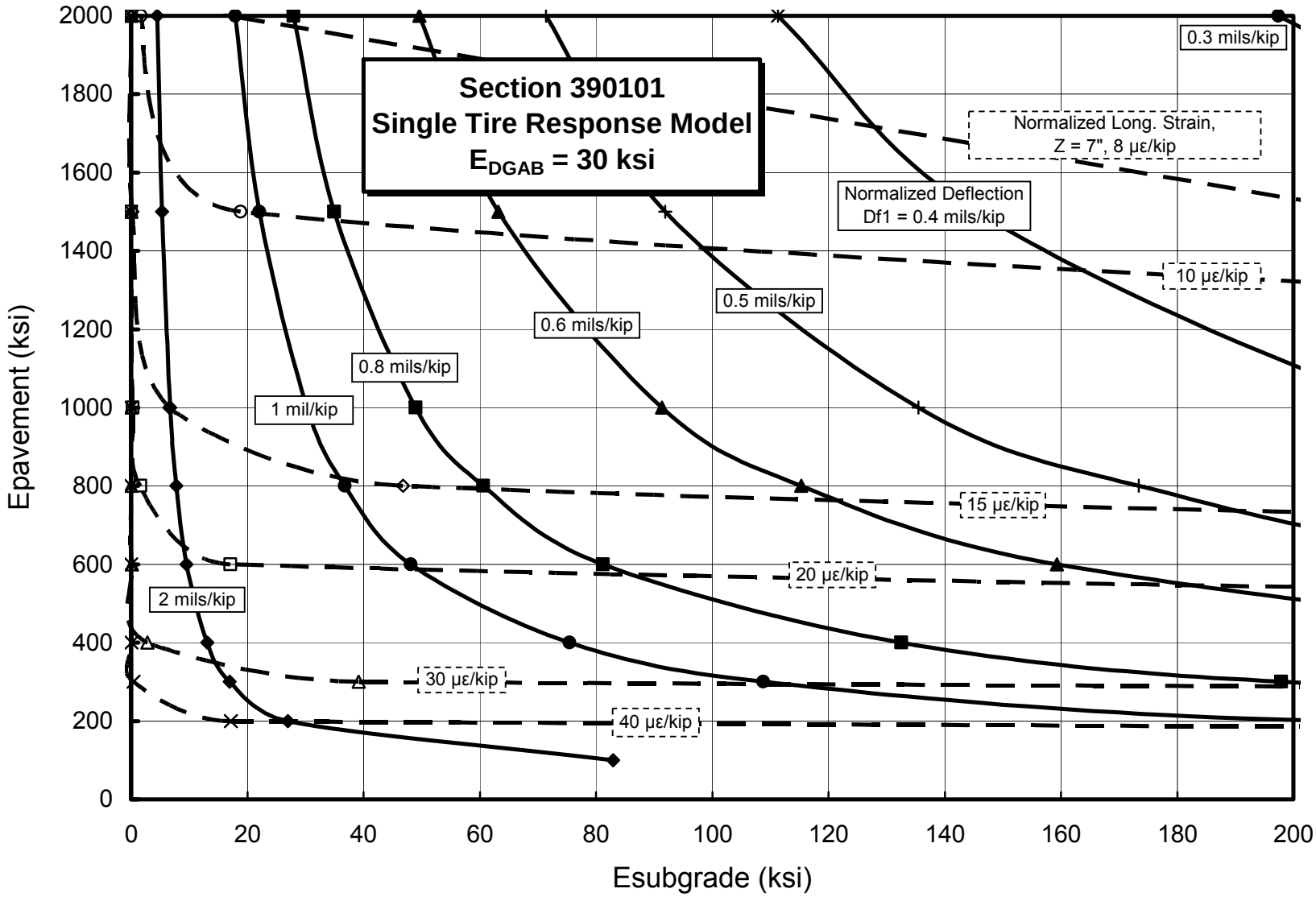

Figure I2 –Relationship between E_1, E_2, Deflection and Strain Using Single Tire Geometry on Section 390101

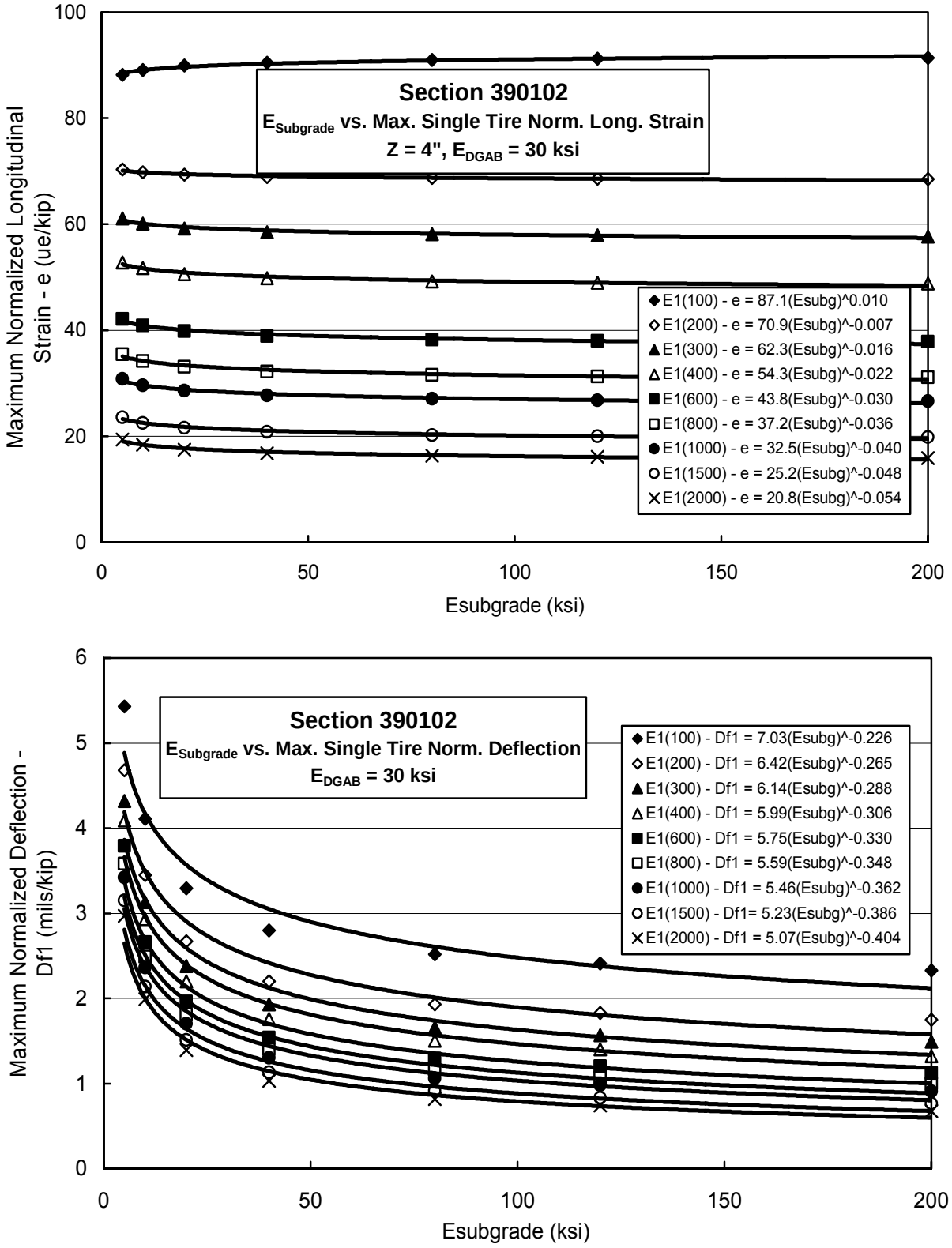

Figure I3 – Strain, Deflection vs. E_2; Single Tire on Section 390102

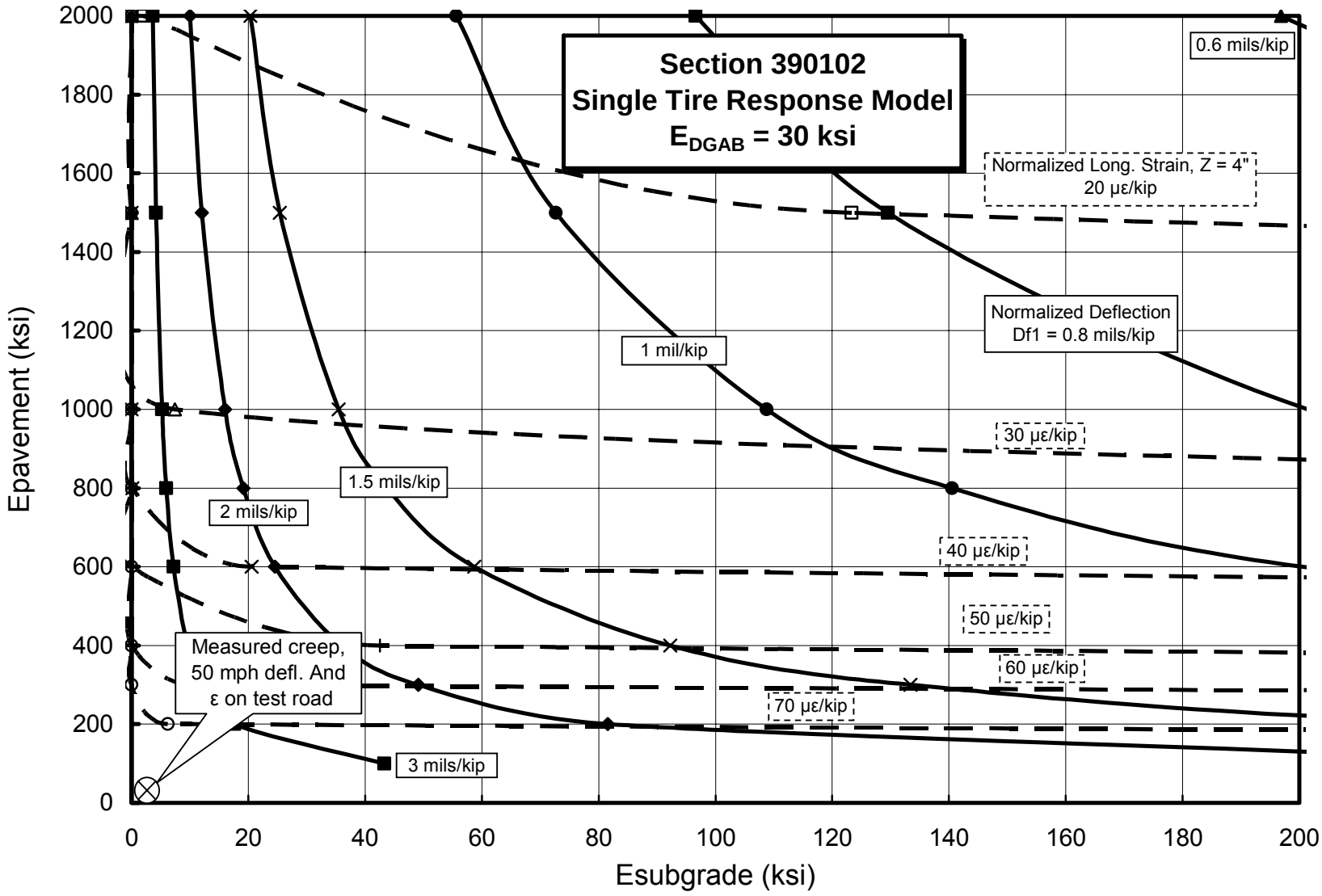

Figure I4 –Relationship between E_1, E_2, Deflection and Strain Using Single Tire Geometry on Section 390102

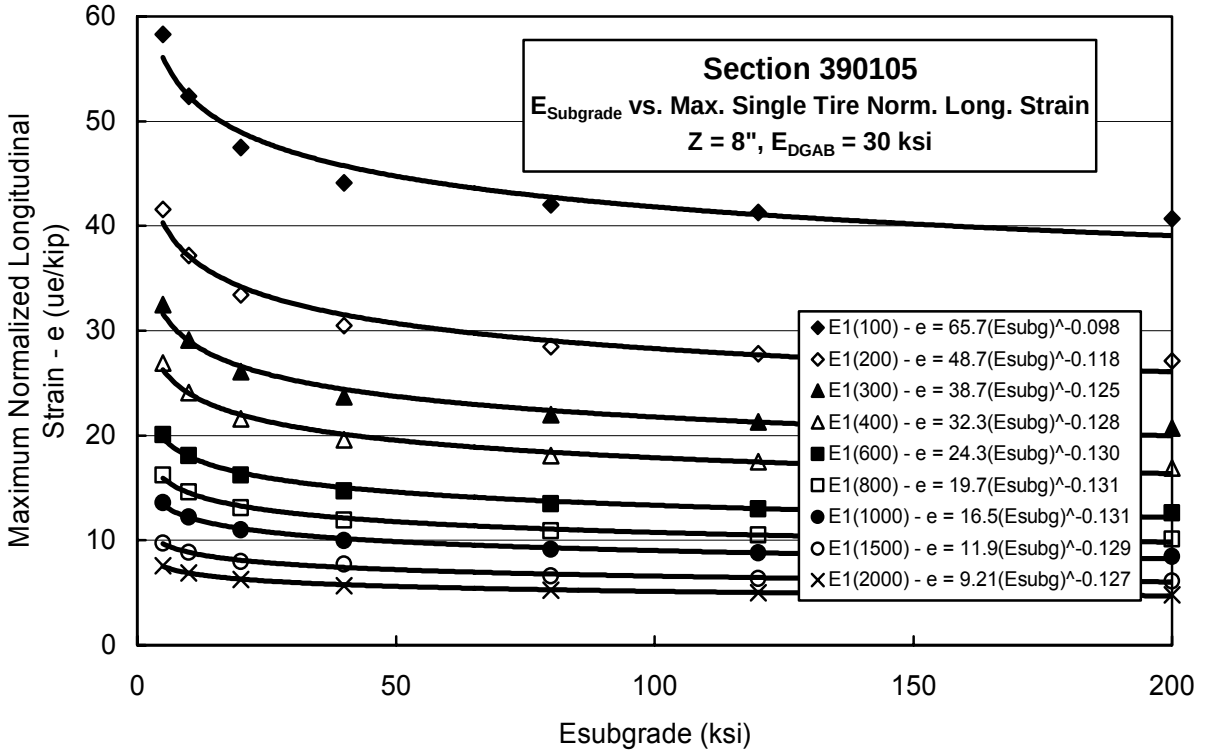

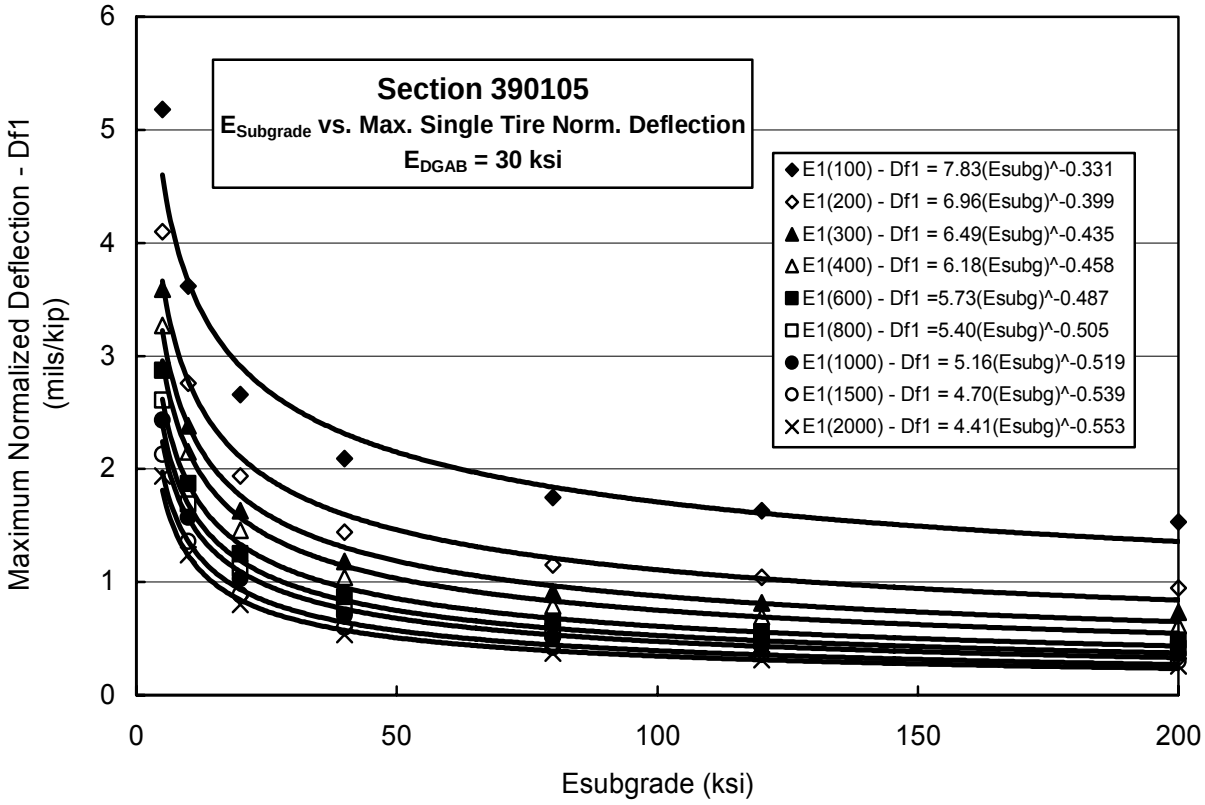

Figure I5 – Strain, Deflection vs. E_2; Single Tire on Section 390105

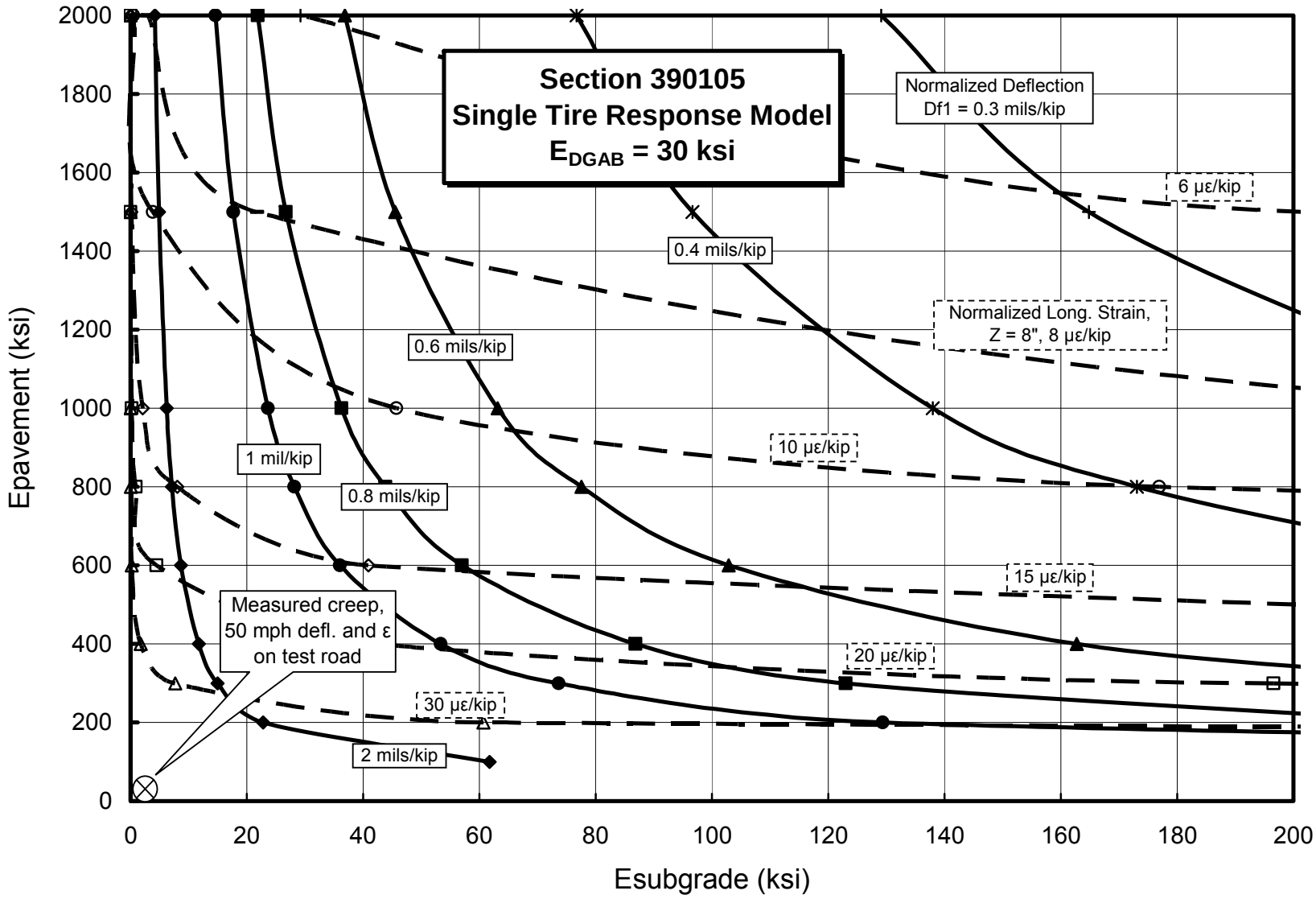

Figure I6 –Relationship between E_1, E_2, Deflection and Strain Using Single Tire Geometry on Section 390105

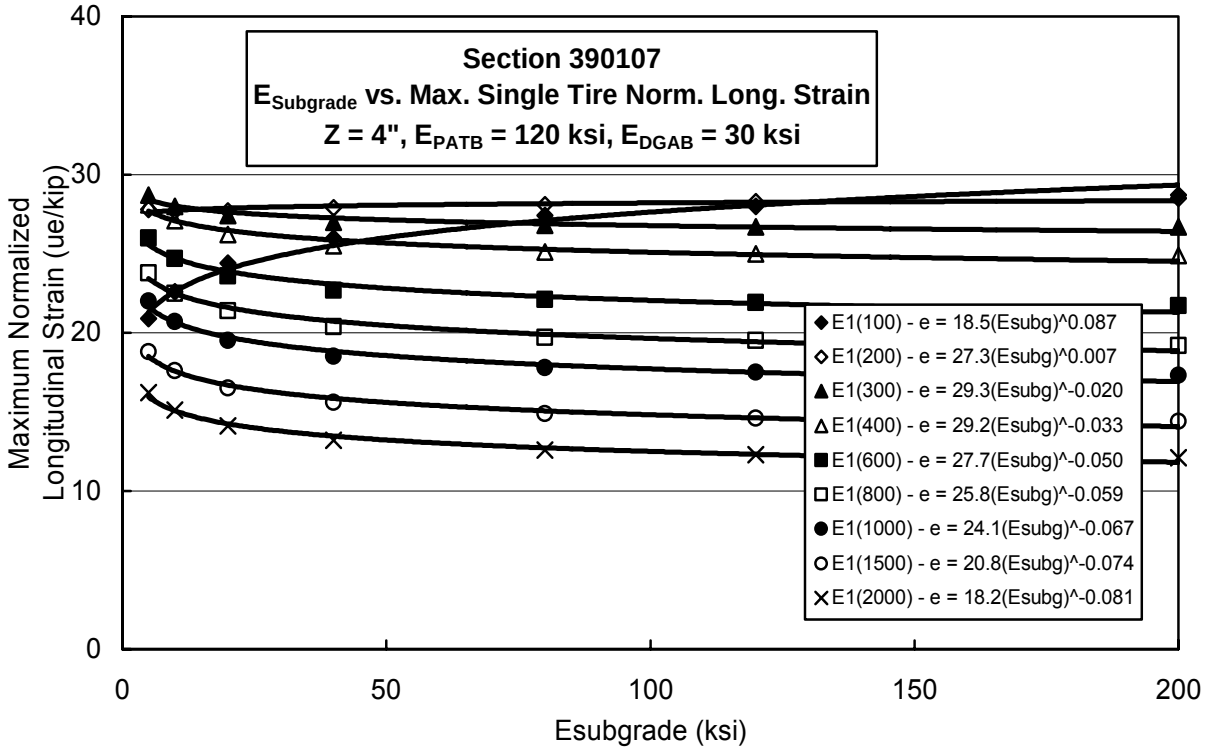

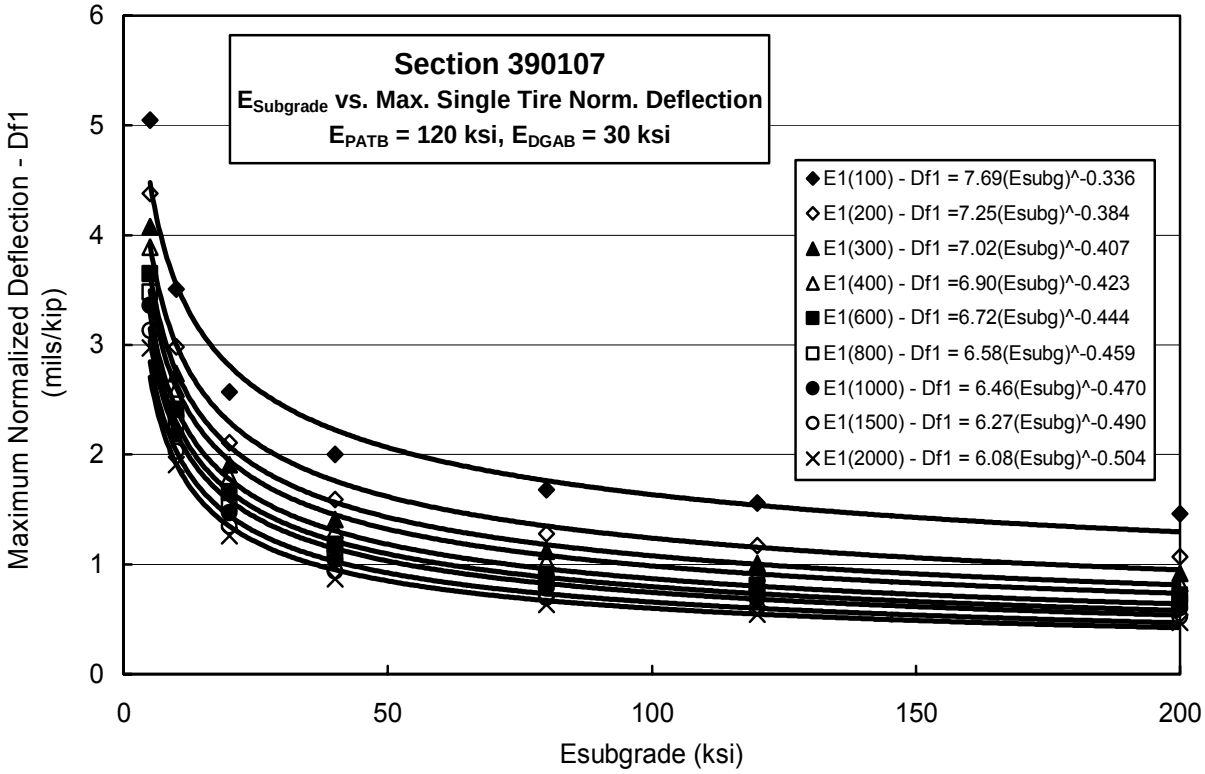

Figure I7 – Strain, Deflection vs. E_2; Single Tire on Section 390107

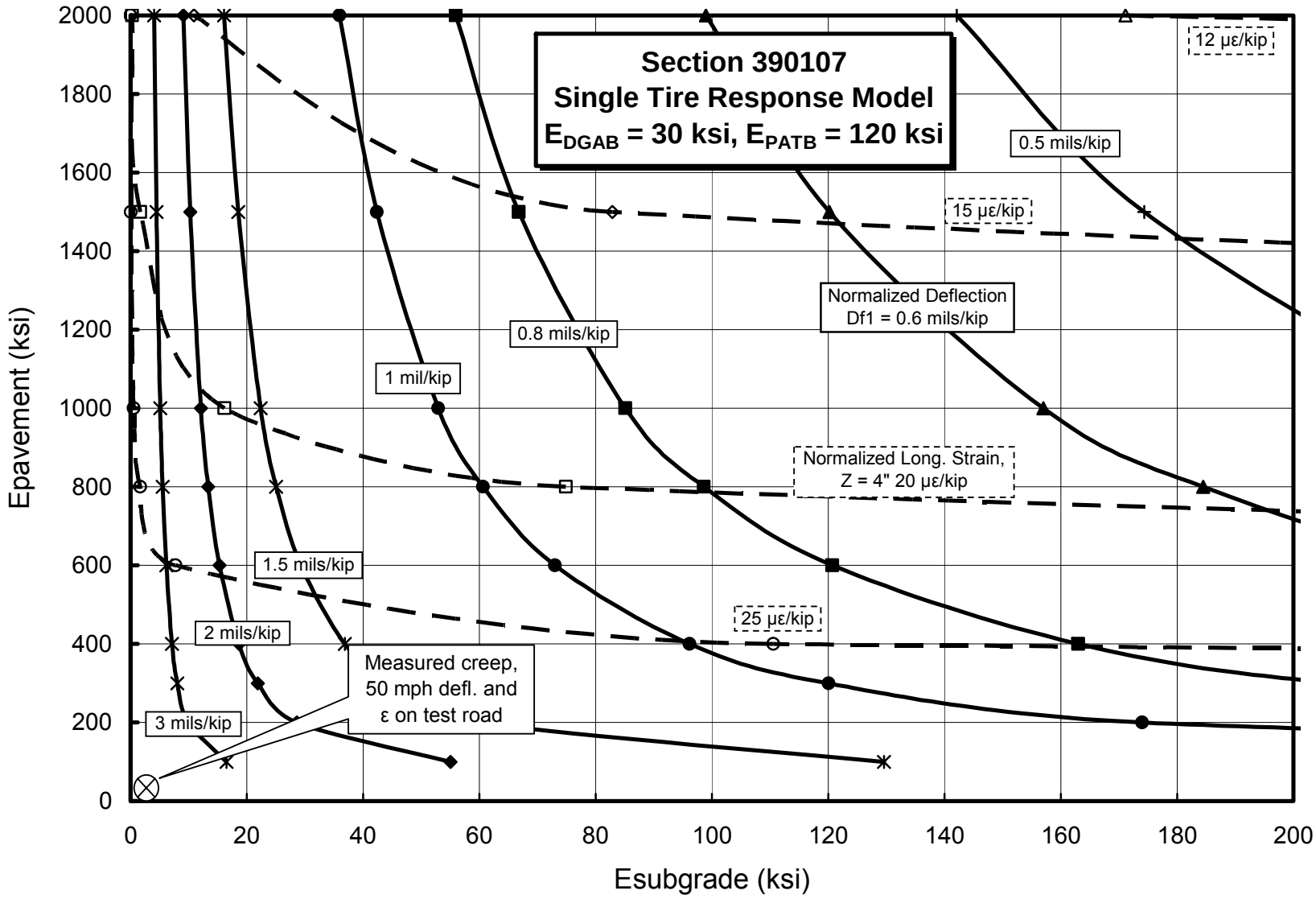

Figure I8 –Relationship between E_1, E_2, Deflection and Strain Using Single Tire Geometry on Section 390107

APPENDIX J

RELATIONSHIPS BETWEEN LAYER MODULI, STRAIN AND DEFLECTION WITH DUAL TIRE GEOMETRY

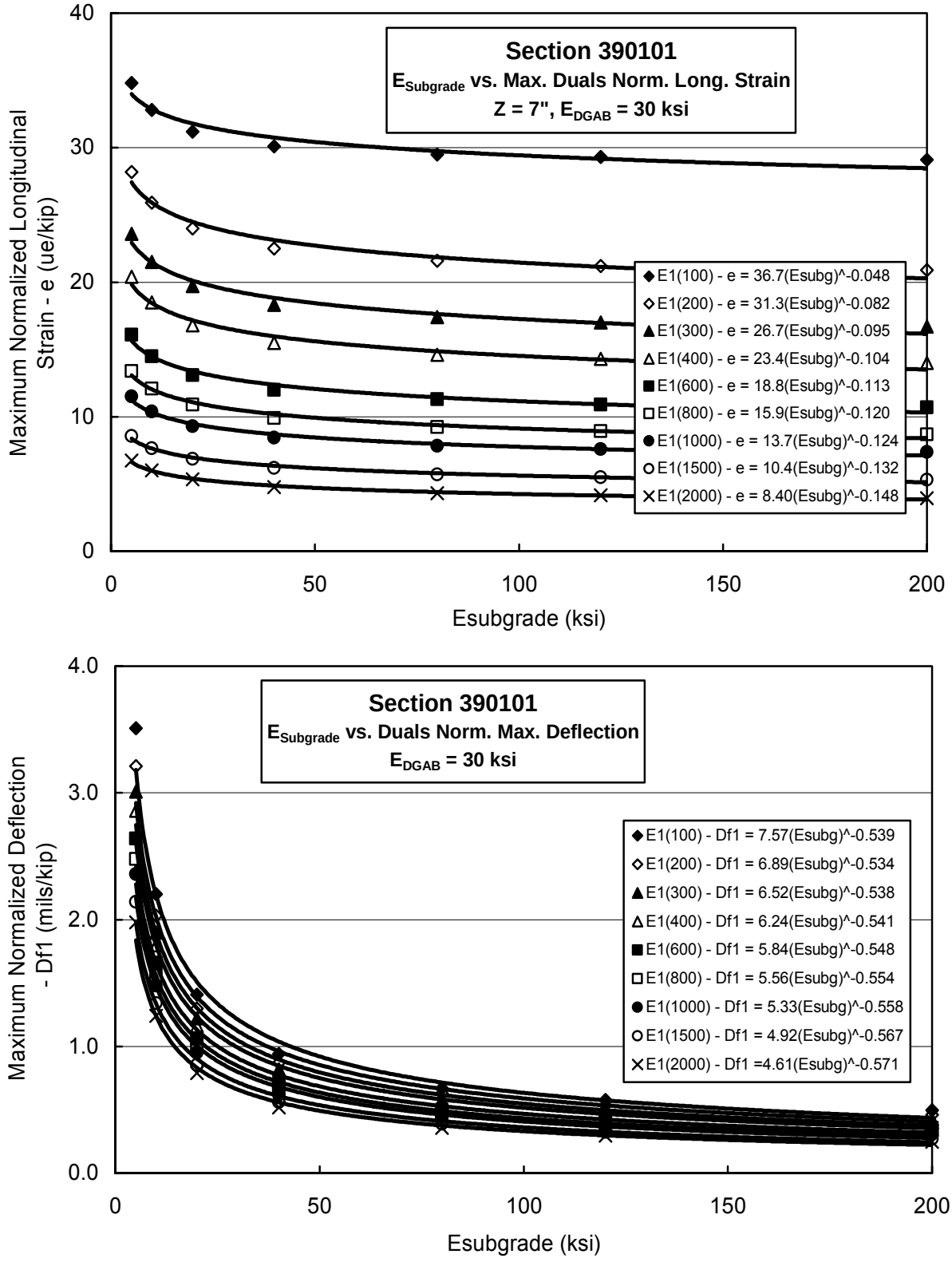

Figure J1 – Strain, Deflection vs. E_2; Dual Tires on Section 390101

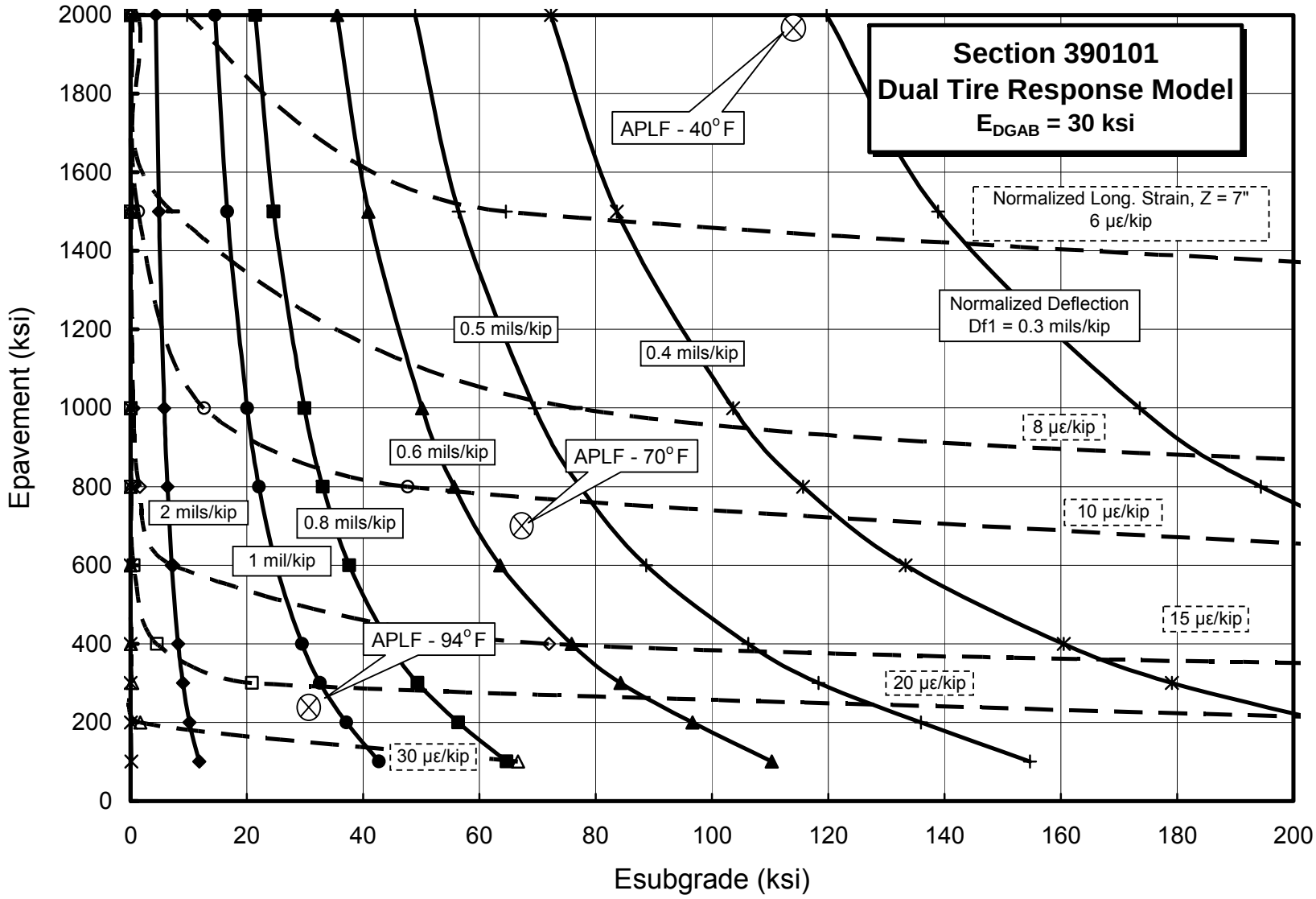

Figure J2 – Relationship between E_1, E_2, Deflection and Strain Using Dual Tire Geometry on Section 390101

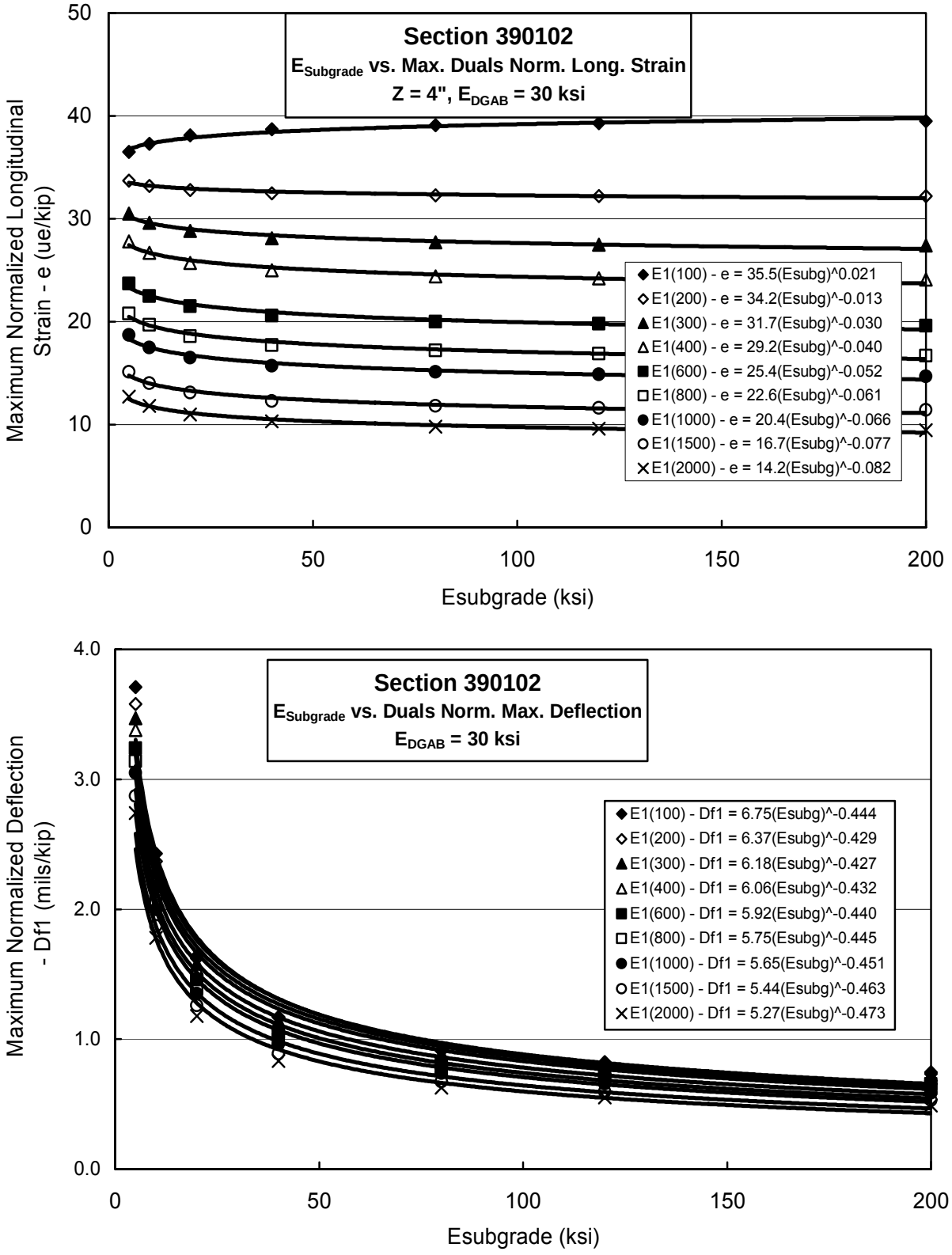

Figure J3 – Strain, Deflection vs. E_2; Dual Tires on Section 390102

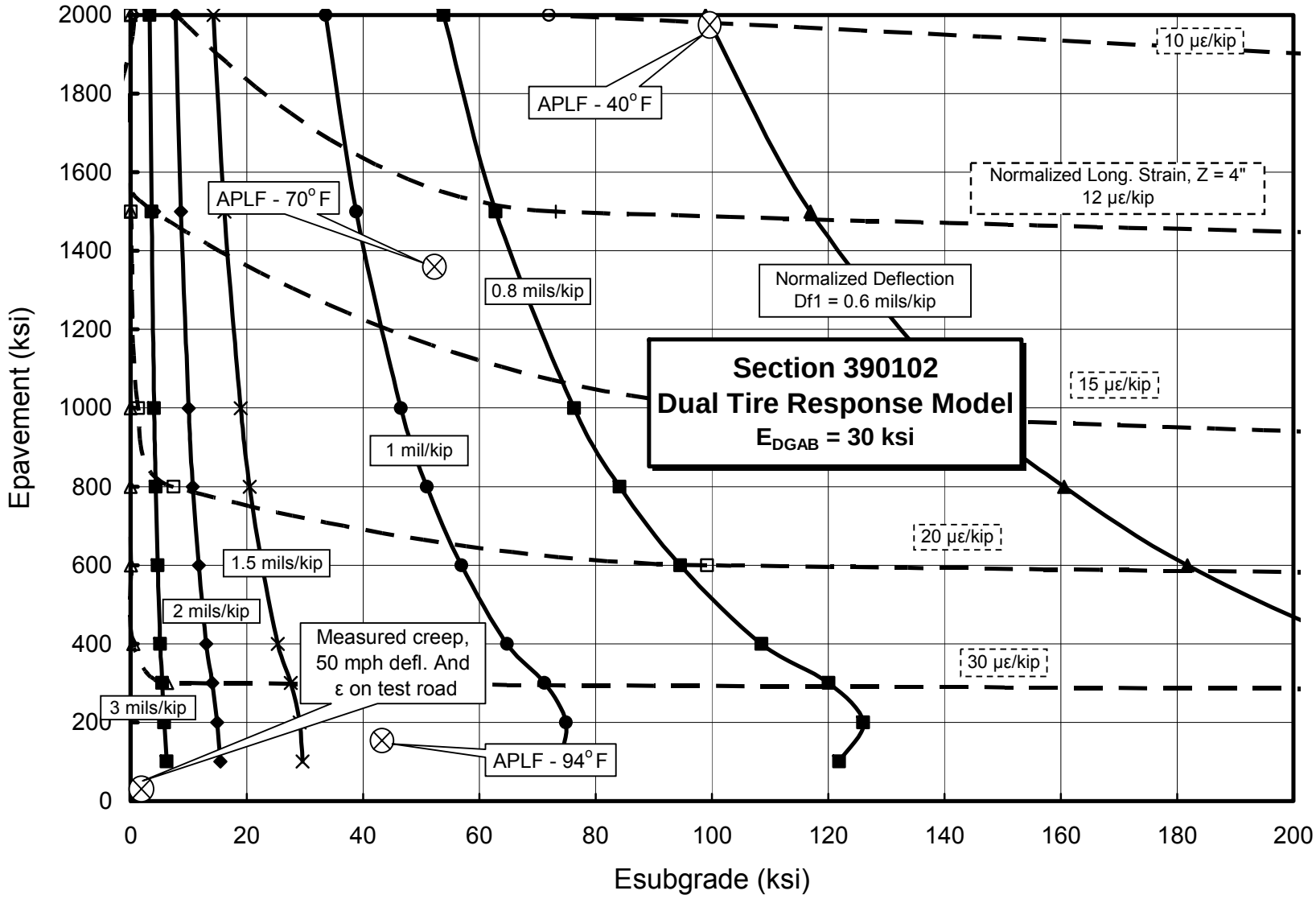

Figure J4 – Relationship between E_1, E_2, Deflection and Strain Using Dual Tire Geometry on Section 390102

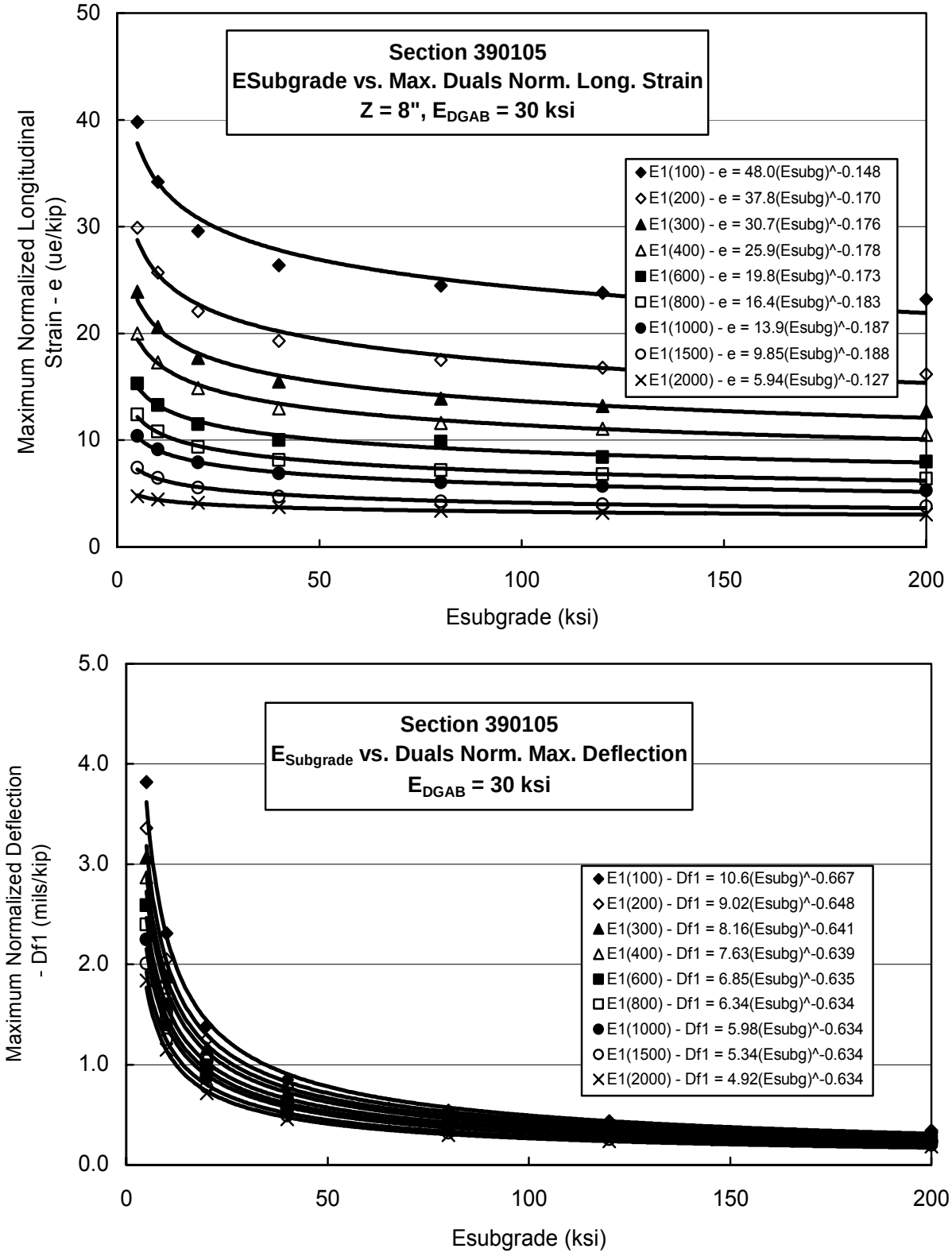

Figure J5 – Strain, Deflection vs. E_2; Dual Tires on Section 390105

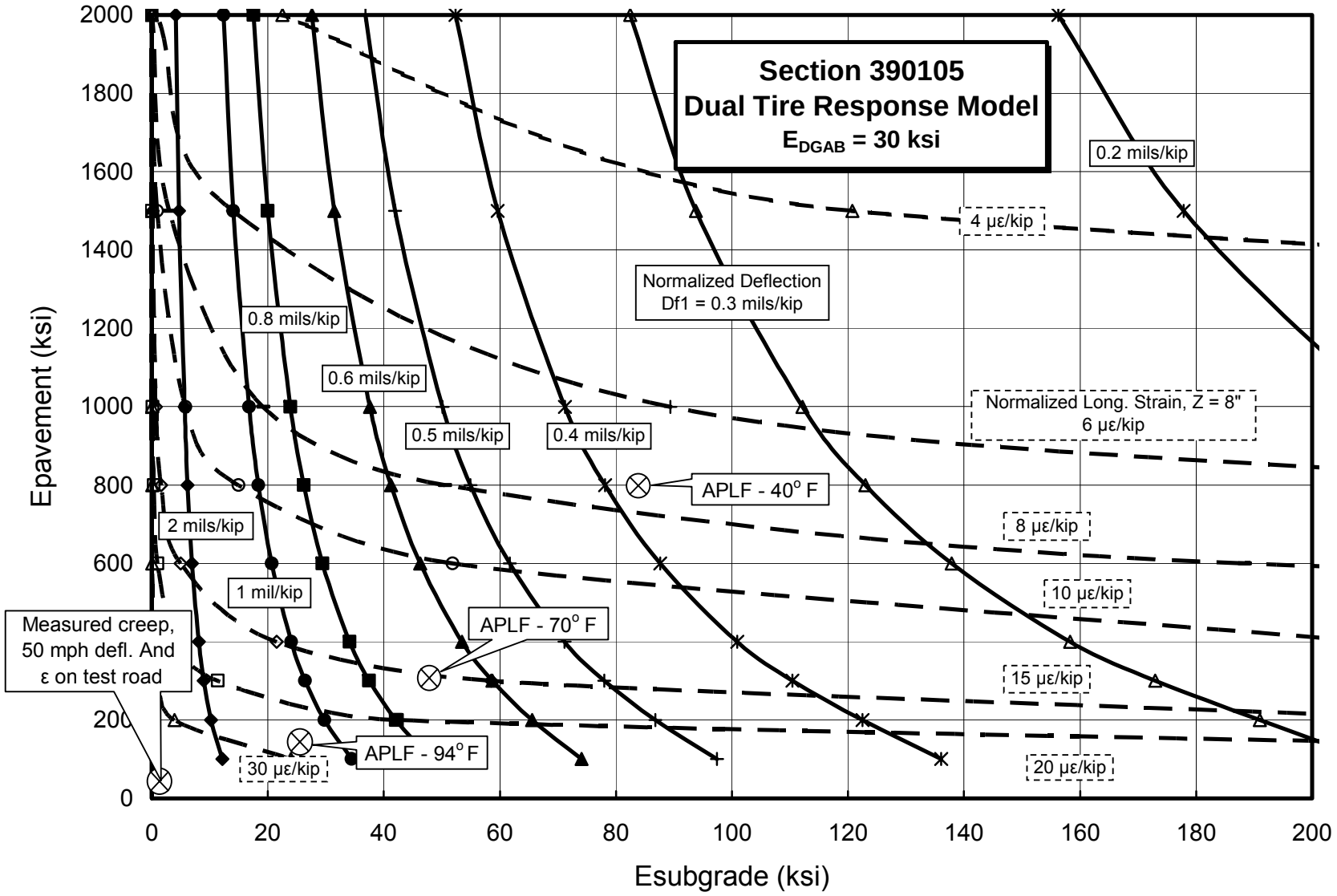

Figure J6 – Relationship between E_1, E_2, Deflection and Strain Using Dual Tire Geometry on Section 390105

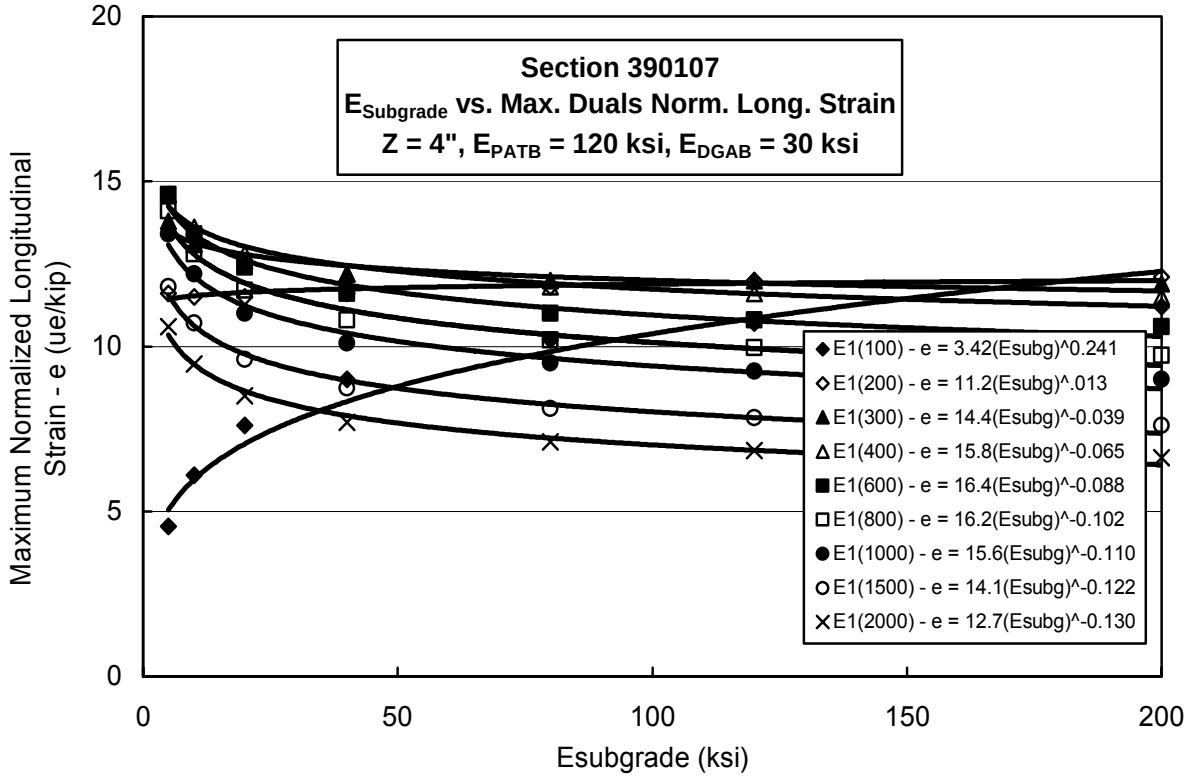

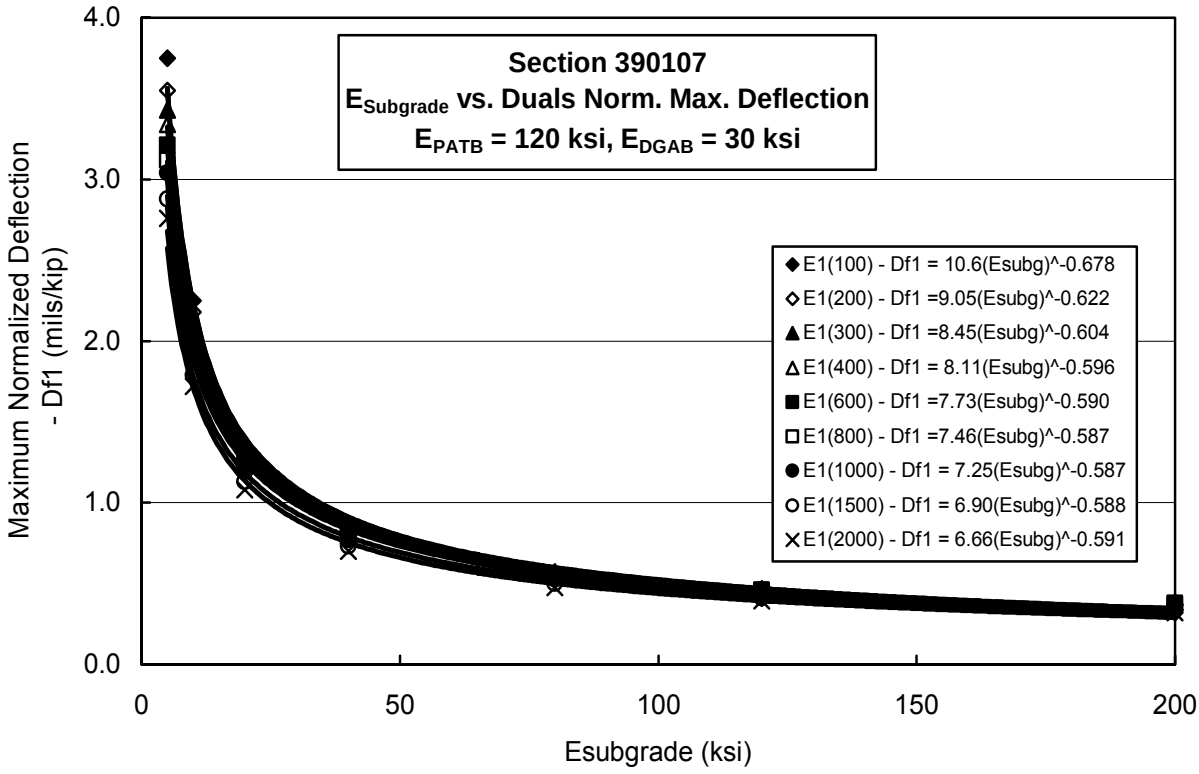

Figure J7 – Strain, Deflection vs. E_2; Dual Tires on Section 390107

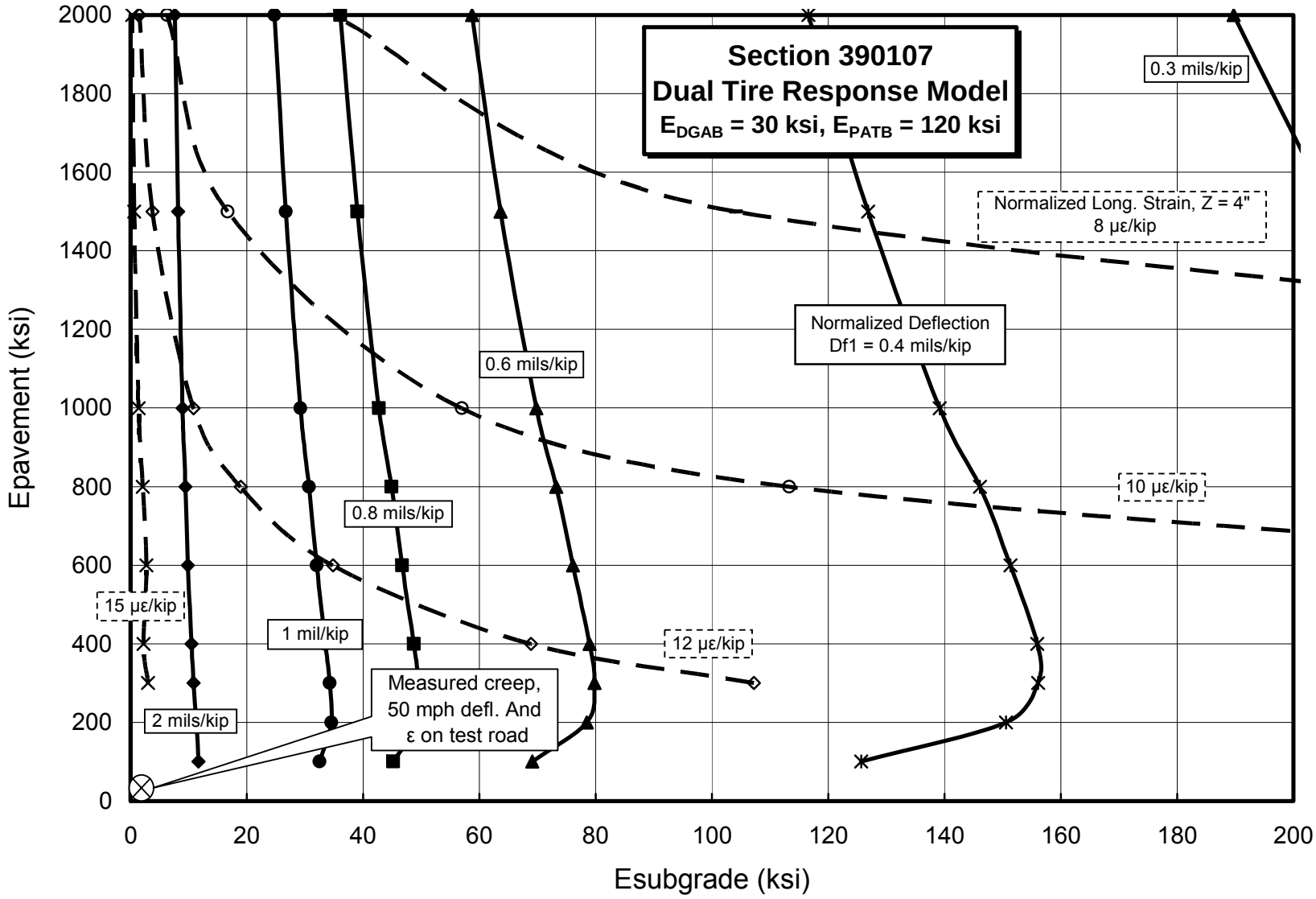

Figure J8 – Relationship between E_1, E_2, Deflection and Strain Using Dual Tire Geometry on Section 390107

APPENDIX K

DAILY WIM SUMMARIES

Table K1 – Daily WIM Summaries (1/5)

Ohio SHRP Test Road Daily WIM Summary																						
Date	Daily Volume (Classes 4-13)						Daily Weight (Kips)						Daily Loading (ESALs)					Daily Class 9 Loading (ESALs)				
	Lane					Class 9	Lane					Class 9	Lane					Lane				
	All	11	12	52	51		All	11	12	52	51		All	11	12	52	51	All	11	12	52	51
11/11/96	5019	1746	191	223	2859	3118	235617	86568	8420	8818	131811	192872	8188	2006	171	159	5852	7021	1701	153	135	5033
11/12/96	5618	2083	199	267	3069	3560	266961	104480	9134	10686	142660	219499	8713	2403	207	175	5928	7563	2027	194	146	5197
11/13/96	5790	2097	213	304	3176	3774	276906	106113	10479	11820	148494	231291	8984	2449	245	172	6117	7877	2091	223	150	5413
11/14/96	5717	2082	210	280	3145	3671	270856	104100	9113	10945	146699	224335	8615	2329	196	181	5910	7506	1994	179	160	5173
11/15/96	5440	1927	180	303	3030	3256	230402	91264	8326	10142	120670	187808	6350	1883	186	138	4143	5426	1570	171	119	3565
11/16/96	2677	769	64	99	1745	1152	90176	36410	2632	3261	47873	68052	2410	764	54	47	1544	2062	636	52	39	1335
11/17/96	2165	510	48	95	1512	989	78603	24490	2040	3323	48750	63415	2437	523	35	70	1810	2236	481	32	66	1658
Week Total	32426	11214	1105	1571	18536	19520	1449522	553425	50144	58995	786958	1187272	45697	12358	1094	941	31304	39691	10500	1004	814	27374
%	100.00	34.58	3.41	4.84	57.16	60.20	100.00	38.18	3.46	4.07	54.29	81.91	100.00	27.04	2.39	2.06	68.50	100.00	26.45	2.53	2.05	68.97
Per Vehicle							44.70	49.35	45.38	37.55	42.46	60.82	1.41	1.10	0.99	0.60	1.69	1.22	0.94	0.91	0.52	1.48
11/18/96*	4885	1778	206	251	2650	3121	215921	86121	9208	8570	112023	177785	6208	1900	199	120	3990	5327	1634	185	101	3408
11/19/96	5531	2026	240	364	2901	3567	256827	100533	10923	13200	132171	215422	7846	2257	246	185	5158	6904	1971	225	165	4542
11/20/96	5591	1984	193	295	3119	3570	260299	97996	8920	12336	141047	216710	7974	2160	199	213	5401	6995	1859	186	192	4759
11/21/96	5818	2047	252	391	3128	3744	267297	101618	11115	15665	138899	221456	7765	2272	235	255	5003	6676	1908	220	235	4314
11/22/96	5494	1956	196	259	3083	3348	245131	93620	8227	8540	134744	199186	7463	1961	160	103	5240	6416	1628	125	86	4577
11/23/96	2855	906	66	127	1756	1341	104984	43143	2374	4174	55293	80570	3002	915	42	64	1980	2572	768	34	56	1714
11/24/96	2297	577	57	108	1555	1117	85765	29608	2586	3986	49585	70585	2562	692	50	63	1757	2361	640	46	54	1621
Week Total	32471	11274	1210	1795	18192	19808	1436224	552638	53352	66472	763762	1181712	42820	12158	1131	1002	28529	37252	10407	1022	887	24936
%	100.00	34.72	3.73	5.53	56.03	61.00	100.00	38.13	3.68	4.59	52.69	81.52	100.00	26.60	2.48	2.19	62.43	100.00	26.22	2.57	2.24	62.82
Per Vehicle							44.23	49.02	44.09	37.03	41.98	59.66	1.32	1.08	0.93	0.56	1.57	1.15	0.92	0.84	0.49	1.37
12/15/97	4936	2292	253	231	2160	3648	231570	105233	9795	9971	106571	195497	4785	2274	220	186	2104	4085	1920	194	163	1808
12/16/97	5412	2458	295	238	2421	3983	258561	114077	11468	10888	122128	216103	5503	2535	237	204	2527	4620	2104	212	184	2120
12/17/97	5429	2454	285	247	2443	4047	257023	113029	11247	10703	122043	217409	5348	2498	226	211	2412	4535	2108	206	194	2028
12/18/97	5405	2463	302	258	2382	3963	259250	115049	12968	10584	120649	216313	5473	2541	299	177	2455	4621	2168	267	137	2049
12/19/97	4846	2177	240	224	2205	3460	222133	97022	9885	9805	105421	183780	4340	2013	210	173	1943	3655	1667	195	122	1671
12/20/97	1948	845	102	88	913	1275	82482	34470	3694	3326	40992	67109	1501	651	77	53	721	1240	554	67	42	577
12/21/97	1541	771	77	52	641	1151	72411	37176	3112	1679	30444	64131	1522	874	69	21	558	1394	802	57	19	516
Week Total	29517	13460	1554	1338	13165	21527	1383429	616056	62169	56957	648247	1160342	28471	13387	1339	1025	12720	24150	11322	1198	861	10768
%	100.00	45.60	5.26	4.53	44.60	72.93	100.00	42.50	4.29	3.93	44.72	80.05	100.00	29.29	2.93	2.24	27.84	100.00	28.53	3.02	2.17	27.13
Per Vehicle							46.87	45.77	40.01	42.57	49.24	53.90	0.96	0.99	0.86	0.77	0.97	0.82	0.84	0.77	0.64	0.82

* Data copied from 11/11/96 for Hours 0-8; 10% of SB trucks assumed to be in Lane 52 in Hours 9-13

Table K1 – Daily WIM Summaries (2/5)

Ohio SHRP Test Road Daily WIM Summary																						
Date	Daily Volume (Classes 4-13)						Daily Weight (Kips)						Daily Loading (ESALs)					Daily Class 9 Loading (ESALs)				
	Lane					Class 9	Lane					Class 9	Lane					Lane				
	All	11	12	52	51		All	11	12	52	51		All	11	12	52	51	All	11	12	52	51
1/19/98	4494	2057	260	204	1973	3300	212605	94189	10987	8466	98963	179664	4568	2069	249	154	2097	3935	1815	215	142	1763
1/20/98	4944	2232	235	224	2253	3624	237593	103470	9795	10316	114012	196696	4960	2254	212	219	2276	4122	1909	196	179	1837
1/21/98	5018	2358	243	221	2196	3800	244229	110136	10896	9888	113309	207467	5190	2404	271	183	2332	4490	2091	255	167	1977
1/22/98	4961	2268	291	220	2182	3612	235058	105798	10628	9635	108997	196451	4860	2314	215	161	2170	4135	1985	191	149	1810
1/23/98	4485	1999	231	223	2032	3190	203720	87988	8788	9625	97319	169751	4002	1808	183	204	1806	3404	1494	173	184	1554
1/24/98	1749	727	86	97	839	1145	76367	31666	2938	3439	38325	62446	1541	702	68	57	715	1298	599	65	44	590
1/25/98	1370	674	45	56	595	1021	65647	33453	1866	1576	28751	58983	1442	811	45	23	563	1351	776	42	22	511
Week Total	27021	12315	1391	1245	12070	19692	1275218	566701	55897	52944	599676	1071457	26563	12362	1243	1000	11959	22734	10669	1136	887	10042
%	100.00	45.58	5.15	4.61	44.67	72.88	100.00	39.10	3.86	3.65	41.37	73.92	100.00	27.05	2.72	2.19	26.17	100.00	26.88	2.86	2.23	25.30
Per Vehicle							47.19	46.02	40.18	42.53	49.68	54.41	0.98	1.00	0.89	0.80	0.99	0.84	0.87	0.82	0.71	0.83
2/16/98	4805	2180	282	216	2127	3493	222955	98870	10675	9989	103421	184390	4608	2159	187	205	2056	3794	1755	158	192	1689
2/17/98	5217	2388	282	225	2322	3740	248150	110034	11702	9793	116620	201032	5218	2321	280	186	2432	4233	1894	243	154	1942
2/18/98	5097	2333	306	261	2197	3663	242003	108464	12914	11400	109226	195312	5001	2282	276	237	2206	3991	1858	233	191	1708
2/19/98	5223	2346	281	254	2342	3733	244874	107965	12434	10939	113536	199147	4948	2264	296	217	2171	4059	1854	234	185	1786
2/20/98	4772	2140	248	265	2119	3375	219224	98052	10093	10132	100947	178170	4426	2093	228	165	1939	3610	1718	173	142	1576
2/21/98*	1784	755	77	70	882	1151	75877	31334	2537	2831	39175	61447	1444	660	49	61	674	1205	561	42	57	545
2/22/98	1371	680	72	38	581	964	62742	30878	2487	1387	27990	54114	1327	652	46	42	587	1153	615	38	20	480
Week Total	28269	12822	1548	1329	12570	20119	1315825	585597	62842	56470	610915	1073612	26972	12431	1362	1114	12064	22044	10255	1122	941	9726
%	100.00	45.36	5.48	4.70	44.47	71.17	100.00	40.40	4.34	3.90	42.15	74.07	100.00	27.20	2.98	2.44	26.40	100.00	25.84	2.83	2.37	24.50
Per Vehicle							46.55	45.67	40.60	42.49	48.60	53.36	0.95	0.97	0.88	0.84	0.96	0.78	0.80	0.72	0.71	0.77
4/4/98	1737	728	96	62	851	1222	80020	31573	3819	2414	42214	66172	1530	631	101	33	766	1307	527	82	29	669
4/5/98	1490	723	70	50	647	1136	73768	35993	3455	2032	32288	64658	1564	806	89	37	632	1407	743	81	34	550
4/6/98	4567	2075	233	184	2075	3540	227140	98123	10789	9164	109064	192765	4805	2118	241	195	2250	4114	1842	214	175	1882
4/7/98	5273	2434	279	198	2362	4067	266284	117517	12723	9628	126416	224375	5763	2656	284	197	2627	4933	2281	259	173	2219
4/8/98	5241	2416	268	248	2309	4075	262834	115296	11452	12658	123429	223914	5557	2468	219	285	2585	4785	2157	192	238	2198
4/9/98	5179	2357	273	300	2249	4005	253035	109114	11387	14491	118043	214432	5109	2227	240	280	2362	4357	1901	209	253	1994
4/10/98	3763	1593	237	179	1754	2705	177271	72806	10707	7621	86137	145286	3523	1526	238	136	1623	2929	1257	210	123	1340
Week Total	27250	12326	1456	1221	12247	20750	1340353	580421	64333	58007	637591	1131603	27851	12432	1413	1163	12844	23832	10708	1247	1025	10852
%	100.00	45.23	5.34	4.48	44.94	76.15	100.00	40.04	4.44	4.00	43.99	78.07	100.00	27.21	3.09	2.54	28.11	100.00	26.98	3.14	2.58	27.34
Per Vehicle							49.19	47.09	44.18	47.51	52.06	54.54	1.02	1.01	0.97	0.95	1.05	0.87	0.87	0.86	0.84	0.89

* Data copied from 2/14/98 for Hours 0-10

Table K1 – Daily WIM Summaries (3/5)

Ohio SHRP Test Road Daily WIM Summary																						
Date	Daily Volume (Classes 4-13)						Daily Weight (Kips)						Daily Loading (ESALs)					Daily Class 9 Loading (ESALs)				
	Lane					Class 9	Lane					Class 9	Lane					Lane				
	All	11	12	52	51		All	11	12	52	51		All	11	12	52	51	All	11	12	52	51
5/4/98*	4690	1511	852	196	2131	3649	231735	74067	39713	9194	108761	197666	4957	1685	949	160	2163	4206	1448	785	148	1824
5/5/98**	5048	2332	256	204	2256	3929	254287	114148	12361	10098	117680	215987	5321	2499	312	180	2330	4575	2183	291	151	1950
5/6/98	5019	2277	240	229	2273	3847	245248	107595	10833	10932	115889	208602	4899	2282	249	179	2189	4228	1969	226	156	1877
5/7/98	4898	2221	283	228	2166	3755	240792	107117	13178	10090	110408	203796	4952	2433	312	161	2046	4219	2072	285	141	1721
5/8/98	4815	2105	251	254	2205	3563	228112	96839	10839	11579	108854	189595	4408	2015	233	205	1954	3679	1682	194	176	1628
5/9/98	1890	762	92	85	951	1251	80592	31484	3399	3246	42464	65157	1449	657	64	53	675	1211	572	59	37	543
5/10/98	1412	672	89	60	591	979	63241	31590	3925	1965	25761	54299	1278	708	102	29	438	1131	617	98	26	390
Week Total	27772	11880	2063	1256	12573	20973	1344007	562840	94247	57103	629818	1135101	27263	12279	2221	967	11795	23250	10543	1938	835	9934
%	100.00	42.78	7.43	4.52	45.27	75.52	100.00	38.83	6.50	3.94	43.45	78.31	100.00	26.87	4.86	2.12	25.81	100.00	26.56	4.88	2.10	25.03
Per Vehicle							48.39	47.38	45.68	45.46	50.09	54.12	0.98	1.03	1.08	0.77	0.94	0.84	0.89	0.94	0.67	0.79
6/1/98	4653	2079	258	195	2121	3526	226735	98804	11581	8695	107654	191246	4687	2182	250	168	2086	3988	1855	225	150	1758
6/2/98	5008	2276	260	226	2246	3775	244525	107964	11580	10246	114734	204058	4957	2322	255	175	2205	4200	1961	226	156	1857
6/3/98	5180	2349	300	203	2328	3924	253492	112447	13904	8744	118397	212502	5247	2481	339	146	2281	4442	2092	305	124	1921
6/4/98	5248	2419	286	210	2333	3992	256318	116147	13532	9046	117593	216689	5228	2560	311	147	2210	4473	2189	286	134	1865
6/5/98	4759	2071	286	234	2168	3583	227810	97845	12559	10663	106743	192697	4578	2158	286	173	1962	3910	1873	269	152	1615
6/6/98	1986	864	98	89	935	1235	83266	34515	3932	3058	41761	65608	1558	689	113	48	708	1254	558	92	41	563
6/7/98	1543	746	85	78	634	1014	68023	34057	3603	2431	27932	58045	1408	786	91	43	489	1267	722	80	37	428
Week Total	28377	12804	1573	1235	12765	21049	1360168	601779	70693	52882	634813	1140844	27662	13178	1644	899	11941	23535	11250	1483	795	10007
%	100.00	45.12	5.54	4.35	44.98	74.18	100.00	41.52	4.88	3.65	43.79	78.70	100.00	28.84	3.60	1.97	26.13	100.00	28.34	3.74	2.00	25.21
Per Vehicle							47.93	47.00	44.94	42.82	49.73	54.20	0.97	1.03	1.05	0.73	0.94	0.83	0.88	0.94	0.64	0.78
7/11/98	1795	780	109	103	803	1008	69792	28893	3541	3201	34158	53359	1285	559	78	53	595	1048	460	70	43	475
7/12/98	1681	791	117	88	685	925	63863	30666	4072	2798	26327	51644	1235	618	81	54	482	1102	572	66	48	415
7/13/98	4358	2005	269	172	1912	3299	208810	92533	11520	8107	96650	177603	4385	1973	253	182	1978	3790	1713	210	167	1699
7/14/98	4500	2081	245	188	1986	3412	219787	98814	10996	9000	100976	185211	4674	2222	236	185	2031	3997	1930	217	153	1698
7/15/98	4823	2173	243	234	2173	3663	235357	102453	10832	11012	111060	197653	4881	2220	219	215	2227	4149	1898	188	193	1870
7/16/98	4593	2100	280	195	2018	3373	218709	96847	12406	8877	100579	179956	4450	2037	282	177	1954	3679	1729	244	152	1554
7/17/98	4329	1916	274	185	1954	3113	197571	84783	10742	7890	94155	163796	3783	1771	203	137	1672	3219	1511	180	125	1403
Week Total	26079	11846	1537	1165	11531	18793	1213890	534990	64108	50886	563905	1009222	24693	11399	1352	1003	10940	20985	9814	1175	881	9115
%	100.00	45.42	5.89	4.47	44.22	72.06	100.00	36.91	4.42	3.51	38.90	69.62	100.00	24.94	2.96	2.19	23.94	100.00	24.73	2.96	2.22	22.96
Per Vehicle							46.55	45.16	41.71	43.68	48.90	53.70	0.95	0.96	0.88	0.86	0.95	0.80	0.83	0.76	0.76	0.79

* 10% of NB traffic assumed to be in Lane 12 from Hours 8-14

** 10% of NB traffic assumed to be in Lane 12 from Hours 8-13

Table K1 – Daily WIM Summaries (4/5)

Ohio SHRP Test Road Daily WIM Summary																						
Date	Daily Volume (Classes 4-13)						Daily Weight (Kips)						Daily Loading (ESALs)					Daily Class 9 Loading (ESALs)				
	Lane					Class 9	Lane					Class 9	Lane					Lane				
	All	11	12	52	51		All	11	12	52	51		All	11	12	52	51	All	11	12	52	51
8/11/98	4901	2272	299	215	2115	3778	238173	107743	13732	10089	106609	204132	4929	2321	336	196	2076	4317	2065	302	175	1775
8/12/98	5305	2388	311	257	2349	3995	255418	112206	13993	11387	117831	214795	5153	2463	311	202	2177	4394	2097	274	181	1841
8/13/98	4863	2254	288	217	2104	3623	233944	105970	12476	9757	105741	197407	4807	2296	268	182	2061	4140	2004	244	161	1731
8/14/98	4776	2106	316	237	2117	3530	221864	93411	12462	10129	105864	187446	4249	1859	255	166	1969	3670	1626	232	132	1680
8/15/98	2013	863	122	96	932	1193	84808	35599	4345	3450	41415	64582	1688	787	92	69	740	1310	594	71	64	580
8/16/98	1776	763	104	110	799	1119	76205	34049	3654	3929	34573	63616	1641	789	77	89	685	1450	711	68	73	598
8/17/98*	3660	1714	205	201	1540	2550	167610	79621	8262	7909	71817	138746	3480	1761	157	164	1398	2965	1494	131	142	1198
Week Total	27294	12360	1645	1333	11956	19788	1278021	568598	68923	56650	583850	1070723	25947	12276	1497	1068	11107	22244	10590	1322	929	9403
%	100.00	45.28	6.03	4.88	43.80	72.50	100.00	39.23	4.75	3.91	40.28	73.87	100.00	26.86	3.28	2.34	24.31	100.00	26.68	3.33	2.34	23.69
Per Vehicle							46.82	46.00	41.90	42.50	48.83	54.11	0.95	0.99	0.91	0.80	0.93	0.81	0.86	0.80	0.70	0.79
8/31/98	4605	2084	256	184	2081	3480	223915	97902	11214	8435	106364	187566	4665	2157	267	169	2072	3979	1837	232	149	1761
9/1/98	5161	2361	270	236	2294	3904	256204	114653	12455	11128	117969	213180	5383	2578	282	214	2310	4518	2223	240	173	1882
9/2/98	5194	2368	267	236	2323	3957	258152	114866	12184	10923	120179	215812	5460	2546	282	178	2455	4611	2186	250	147	2029
9/3/98	5247	2363	332	203	2349	3952	258011	110186	15088	9640	123096	215302	5387	2325	328	212	2523	4572	2003	292	190	2088
9/4/98	4765	2049	306	224	2186	3477	222047	92037	12279	9481	108250	183690	4285	1858	223	161	2043	3599	1562	200	136	1702
9/5/98	1627	663	87	72	805	1017	66834	26864	2901	2447	34623	52245	1169	508	49	40	571	931	441	31	30	429
9/6/98	976	439	65	32	440	552	36404	15978	2071	1034	17322	29000	637	291	36	19	292	536	257	32	13	234
Week Total	27575	12327	1583	1187	12478	20339	1321567	572484	68191	53089	627803	1096796	26987	12262	1467	993	12265	22747	10510	1276	837	10124
%	100.00	44.70	5.74	4.30	45.25	73.76	100.00	39.49	4.70	3.66	43.31	75.67	100.00	26.83	3.21	2.17	26.84	100.00	26.48	3.22	2.11	25.51
Per Vehicle							47.93	46.44	43.08	44.73	50.31	53.93	0.98	0.99	0.93	0.84	0.98	0.82	0.85	0.81	0.70	0.81
11/2/98	4564	2095	226	169	2074	3501	220715	98752	9509	8124	104329	187709	4622	2187	196	169	2069	3936	1836	185	152	1762
11/3/98	4845	2219	266	183	2177	3832	239289	104469	11526	8698	114597	205391	4942	2200	234	169	2338	4284	1944	219	148	1973
11/4/98	4996	2263	270	195	2268	3933	248962	107586	12043	8836	120498	212499	5111	2270	287	158	2396	4403	1961	262	138	2043
11/5/98	4999	2326	272	196	2205	3892	247532	111625	12024	9499	114384	211006	5341	2550	250	206	2335	4576	2189	230	185	1973
11/6/98	4570	2016	241	205	2108	3478	218178	93541	10752	9069	104816	183675	4421	2011	243	158	2009	3759	1749	222	133	1655
11/7/98	1782	751	83	63	885	1231	82138	33741	3078	2418	42901	66060	1677	752	73	39	813	1342	601	68	31	642
11/8/98	1388	682	80	47	579	1027	67220	34013	3382	2073	27752	58470	1465	808	77	43	536	1328	745	67	39	477
Week Total	27144	12352	1438	1058	12296	20894	1324034	583726	62313	48719	629277	1124811	27577	12779	1360	942	12496	23628	11025	1253	826	10525
%	100.00	45.51	5.30	3.90	45.30	76.97	100.00	40.27	4.30	3.36	43.41	77.60	100.00	27.96	2.98	2.06	27.34	100.00	27.78	3.16	2.08	26.52
Per Vehicle							48.78	47.26	43.33	46.05	51.18	53.83	1.02	1.03	0.95	0.89	1.02	0.87	0.89	0.87	0.78	0.86

* Data for Hours 14-23 copied from 8/16/98

Table K1 – Daily WIM Summaries (5/5)

Ohio SHRP Test Road Daily WIM Summary																						
Date	Daily Volume (Classes 4-13)						Daily Weight (Kips)						Daily Loading (ESALs)					Daily Class 9 Loading (ESALs)				
	Lane					Class 9	Lane					Class 9	Lane					Lane				
	All	11	12	52	51		All	11	12	52	51		All	11	12	52	51	All	11	12	52	51
12/7/98	4536	2111	218	166	2041	3547	219461	99025	9945	8113	102378	188089	4411	2012	238	175	1986	3845	1761	217	157	1710
12/8/98	4950	2275	250	193	2232	3839	245601	108080	11411	9782	116327	207940	5123	2309	256	208	2349	4412	2013	231	194	1975
12/9/98	4920	2275	270	211	2164	3840	242440	108121	11413	10175	112730	205627	5030	2279	216	201	2334	4309	1995	203	177	1933
12/10/98	4875	2260	247	217	2151	3776	240894	108795	10635	11260	110204	203563	4985	2393	211	246	2135	4233	2052	193	227	1762
12/11/98	4682	2123	241	212	2106	3669	223726	98354	10642	10334	104396	191963	4286	2001	208	207	1869	3704	1731	195	180	1599
12/12/98	1687	745	75	54	813	1182	75873	32053	2814	1991	39014	60400	1359	606	42	42	668	1065	477	35	35	518
12/13/98	1357	681	75	38	563	1068	66287	32742	3671	1627	28247	59001	1325	694	99	24	507	1213	633	95	20	466
Week Total	27007	12470	1376	1091	12070	20921	1314281	587170	60532	53282	613297	1116583	26517	12294	1271	1103	11849	22781	10663	1168	989	9961
%	100.00	46.17	5.09	4.04	44.69	77.47	100.00	40.51	4.18	3.68	42.31	77.03	100.00	26.90	2.78	2.41	25.93	100.00	26.86	2.94	2.49	25.10
Per Vehicle							48.66	47.09	43.99	48.84	50.81	53.37	0.98	0.99	0.92	1.01	0.98	0.84	0.86	0.85	0.91	0.83
12/14/98	4447	2031	236	180	2000	3511	218081	94833	11122	8540	103586	187630	4300	1879	227	149	2045	3758	1633	204	132	1789
12/15/98	4976	2327	216	192	2241	3886	245230	110963	9472	9482	115313	207489	4979	2348	187	190	2254	4225	2004	166	171	1885
12/16/98	5010	2337	269	223	2181	3857	248219	112292	13100	11115	111712	207712	5118	2420	321	222	2155	4249	1968	273	205	1802
12/17/98	4956	2200	319	247	2190	3887	241434	103976	14436	11567	111456	205647	4849	2185	315	226	2123	4124	1871	285	198	1770
12/18/98	4545	1992	266	273	2014	3552	214889	90786	11818	12283	100003	184138	4063	1797	224	205	1837	3516	1585	210	184	1537
12/19/98	1694	721	76	67	830	1262	78934	33067	3139	2810	39918	66011	1437	670	58	41	668	1204	575	53	36	540
12/20/98	1299	644	76	41	538	1061	64737	32305	3438	1890	27105	58832	1284	687	78	35	484	1196	638	75	31	452
Week Total	26927	12252	1458	1223	11994	21016	1311524	578222	66524	57686	609092	1117459	26031	11987	1409	1069	11566	22271	10274	1266	956	9774
%	100.00	45.50	5.41	4.54	44.54	78.05	100.00	39.89	4.59	3.98	42.02	77.09	100.00	26.23	3.08	2.34	25.31	100.00	25.89	3.19	2.41	24.63
Per Vehicle							48.71	47.19	45.63	47.17	50.78	53.17	0.97	0.98	0.97	0.87	0.96	0.83	0.84	0.87	0.78	0.81